Novel Therapeutic strategies that interfere with senescence escape for the treatment of drug resistance in colorectal and breast cancer

Raneem Jatal

THESE DE DOCTORAT DE

L'UNIVERSITE D'ANGERS
&
UNIVERSIDADE DE SANTIAGO DE COMPOSTELA

ECOLE DOCTORALE N° 605
Biologie Santé
Spécialité : « *SCIENCES PHARMACEUTIQUES*»

Par

« Raneem JATAL »

« Novel Therapeutic strategies that interfere with senescence escape for the treatment of drug resistance in colorectal and breast cancer»

Thèse présentée et soutenue à «Angers», le « 17/12/2021 »
Unité de recherche : CRCINA Equipe 12 (INSERM U1232), Université d'Angers & Nano-oncology group, IDIS, Universidade de Santiago de Compostela.
Thèse N° :

Rapporteurs avant soutenance :

Fabrice GOUILLEUX	Directeur de Recherche Université de Tours, France
Dolores TORRES LOPEZ	Associate professor, Department of Pharmacology, Pharmacy and Pharmaceutical Technology Universidade de Santiago de Compostela, Spain.

Composition du Jury :

Fabrice GOUILLEUX	Directeur de Recherche Université de Tours, France
Dolores TORRES LOPEZ	Associate professor, Department of Pharmacology, Pharmacy and Pharmaceutical Technology Universidade de Santiago de Compostela, Spain.
Jenifer GARCIA FERNANDEZ	Senior Researcher, Nano-Oncology and Translational Therapeutics Group, Health Research Institute of Santiago de Compostela (IDIS), Spain
Président : **Frank BOURY**	Professor, Université d'Angers, France.
Dir. de thèse : **Eric Lelievre**	Maitre de Conférences, Université d'Angers, INSERM UMR 1232, France
Co-dir. de thèse : **Maria DE LA FUENTE**	Researcher of the Galician Public Health System (SERGAS), Head of the Nano-Oncology and Translational Therapeutics Group, Health Research Institute of Santiago de Compostela (IDIS), Spain

RÉSUMÉ

Les agents chimiothérapeutiques et anticancéreux ont la capacité d'induire l'entrée en sénescence des cellules en croissance mais aussi les cellules cancéreuses. Ces cellules cancéreuses sénescentes présentent des caractéristiques proches de cellules quiescentes. Plusieurs études ont montré que ces cellules sont capables de recommencer à proliférer et qu'elles possèdent des propriétés d'agressivités plus marquées que les cellules parentales, pouvant conduire chez les patients à une rechute. Les cellules sénescentes secrètent un ensemble de molécules appelé SASP, qui favorisent l'inflammation et contribue à long terme à plusieurs maladies liées à l'âge. Par conséquent, l'utilisation d'agents sénolytiques et sénostatiques ciblant les cellules sénescentes peut prévenir les rechutes du cancer, réduire les effets secondaires à court et à long terme attribués aux agents anticancéreux et améliorer la qualité de la santé avec l'âge et éventuellement la durée de vie. Dans ce travail, nous avons montré que le peptide 4N1Ks, dérivé du domaine C-terminal de la protéine TSP1, inhibe l'échappement à la sénescence dans un modèle de sénescence induite par chimiothérapie des cellules tumorales mammaires MCF7 et colorectales LS174T. Ce peptide réduit aussi les propriétés du SAPS produit par ces cellules et notamment la capacité migratoire de cellules tumorales. Nous avons également montré que 4N1Ks réduit l'activité métabolique des cellules sénescentes. L'ensemble de ces résultats nous a permis de montrer que ce peptide est capable d'induire l'autophagie de cellules tumorales sénescentes. Nous avons incorporé 4N1Ks à la surface de nanosystèmes à base de sphingomyéline après modification chimique avec du PEG-C18 afin de faciliter son association à la surface de ces nanosystèmes. Les nanosystèmes préparés par SNs-Ks ont démontré des caractéristiques appropriées en termes de taille (~ 100 nm), d'efficacité d'association (87,2 ± 6,9 %) et de stabilité dans différents milieux biopertinents. Les SNs-Ks ont montré un profil de toxicité plus élevé par rapport aux peptides modifiés et aux 4N1Ks. De plus, les SNs-Ks possédaient un bon profil d'hémocompatibilité et un taux d'internalisation cellulaire plus élevé que les nanosystèmes vierges. Les SNs-Ks ont amélioré l'activité sénolytique du peptide 4N1Ks et réduit le nombre de clones émergents dans les expériences d'échappement de la sénescence de cellules MCF7 à une dose 10 fois inférieure à celle du peptide modifié. Ces nanosystèmes représentent une approche intéressante pour réduire le nombre de cellules sénescentes accumulées après des traitements anticancéreux.

mots-clés : Sénescence cellulaire, sénescence induite par la chimiothérapie, rechute cancéreuse, protéine TSP1, peptide 4N1Ks, échappement de la sénescence, autophagie, sénolytiques, nanosystèmes à base de sphingomyéline SN.

ABSTRACT

Chemotherapeutic and anti-cancer agents have the ability to induce cellular senescence in proliferative and cancer cells. Cancer cells turning to senescent have similar characteristics to tumour dormancy. Several studies have indicated that those cells have the capacity to escape senescence state and emerge as a more aggressive form of cancer leading to cancer relapse. In addition, those accumulated senescent cells with their secretory phenotype promote local and systemic inflammation and on the long term contribute to several age-related diseases. Therefore, using senolytic and senostatic agents targeting senescent cells and their SASP can prevent cancer relapse, reduce the short- and long-term side effects attributed to anti-cancer agents, and improve the health quality over age and possibly life span. In this work, 4N1Ks peptide derived from the C-terminal domain of TSP1 protein prevented senescence escape in chemotherapy-induced senescence CIS model of MCF7 and LS174t cells. In addition, it reduced the migratory ability of the SASP and its production as well. Moreover, 4N1Ks treatment reduced the metabolic activity of senescent cells. Those results were explained by autophagy program induction triggered by 4N1Ks peptide. Later we incorporated 4N1Ks to the surface of sphingomyelin based nanosystems after chemical modification with PEG-C18 in order to facilitate its association to the surface of those nanosystems. SNs-Ks prepared nanosystems demonstrated suitable features in terms of size (~ 100 nm), association efficiency (87.2± 6.9%) and stability in different biorelevant media. SNs-Ks showed higher toxicity profile compared to both modified peptide and 4N1Ks, proved by colony forming assay on MCF7 cells. In addition, SNs-Ks possessed good hemocompatibility profile, and had higher cell internalisation rate compared to blank nanosystems. Lastly and most importantly, SNs-Ks improved the senolytic activity of 4N1Ks peptide and reduced the number of emergent clones in senescence escape experiments of CIS model of MCF7 cells at a dose 10 times smaller compared to the modified peptide. These nanosystems represent an interesting approach for reducing the burden of accumulated senescent cells caused due to anticancer treatments as chemotherapeutics, and therefore make a step forward in the management of this disease.

keywords: Cellular senescence, Chemotherapy-induced senescence, SASP, cancer relapse, TSP1 protein, 4N1Ks peptide, senescence escape, autophagy, senolytics, sphingomyelin based nanosystems SNs.

Présidence de l'université
40 rue de rennes – BP 73532
49035 Angers cedex
Tél. 02 41 96 23 23 | Fax 02 41 96 23 00

université angers

ENGAGEMENT DE NON PLAGIAT

Je, soussignée Raneem JATAL .....
déclare être pleinement conscient(e) que le plagiat de documents ou d'une partie d'un document publiée sur toutes formes de support, y compris l'internet, constitue une violation des droits d'auteur ainsi qu'une fraude caractérisée.
En conséquence, je m'engage à citer toutes les sources que j'ai utilisées pour écrire ce rapport ou mémoire.

signé par l'étudiant(e) le **08**/ **10** / **2021**

Cet engagement de non plagiat doit être signé et joint à tous les rapports, dossiers, mémoires.

Présidence de l'université
40 rue de rennes – BP 73532
49035 Angers cedex
Tél. 02 41 96 23 23 | Fax 02 41 96 23 00

Preface

This project was established through the collaborative effort between the European Commission Erasmus Mundus directive and the European Doctorate in Nanomedicine and Pharmaceutical Innovation (NanoFar) program and originated from the combined efforts of the Université d'Angers and the Universidade de Santiago de Compostela, with the research laboratories of Prof. Olivier Coqueret (Equipe 12: Senescence escape and soluble markers of cancer progression) and Dr. Maria de La FUENTE (Nano-Oncology and Translational Therapeutics group, Health Research Institute of Santiago de Compostela [IDIS]).

Dedicated to my parents and my brothers.

“If the result confirms the hypothesis, then you have made a measurement. If the result is contrary to the hypothesis, then you have made a discovery”

Enrico Fermi

Acknowledgements.

In this unique journey that I was blessed to have, I would like to extend my gratitude to many people whose support and help greatly impacted this thesis journey.

First and foremost, I would like to thank my supervisors, Eric and Maria, for giving me this fantastic opportunity and believing in my abilities to carry this work. To Eric, merci beaucoup for your guidance, support and patience through my PhD, especially through the Covid-19 times. It was a pleasure to work with you in the lab. To Maria, no words are enough to express my gratitude. You were very supportive and believed in me when I did not believe in myself. Your enthusiasm and ambition are contagious, and you are truly a role model for young female researchers. You always helped me overcome any obstacle that could impede my research. You also gave me the freedom to seek cooperation with other labs that can be helpful to the project. I genuinely enjoyed my stay in your lab and learned a lot.

I would like to thank my thesis committee members, Prof. Olivier Pluquet, Prof. Corinne Abbadie, Prof. Noemi Csaba and Prof. Marcos Garcia-Fuentes, for generously offering their expertise and guidance in evaluating my thesis.

Since it is a joint PhD programme, I had the opportunity to work at two research groups in Angers and Santiago de Compostela. In Angers, at Inserm equipe 12 group, I was super anxious as I did not have enough expertise in many of the experiments conducted over there. Therefore, I would like to thank Bertrand for explaining and helping me in many experiments. Alice and Cécile, the angels of our lab, although we had the French language barrier, your kindness and care did not need words to reach me and helped many times to overcome the stress I was experiencing. Also, thanks to Cécile for teaching me the Flow cytometry technique.

I would also like to thank Prof. Olivier Coqueret, for opening his lab doors to me. You taught me how to be a more disciplined researcher and perceive the data in molecular biology, which is totally different from pharmaceutics. Our meeting and discussion were insightful and helped me push my thesis work forward.

For my colleagues in France, Jordan, Mélanie, Amine, Coralie and Amandine, I am so grateful to all of you. You are kind and bright researchers. Thanks a lot for helping me in the lab and for all the gatherings and dinner parties; it helped break the ice of being abroad alone. For Jordan and Amandine, I was lucky to share my office with you; our conversations regarding research and life will be engraved in my memory for a long time. Amine and Coralie, you always filled our lab with joy and happiness, which helped all of us pass the good and bad days.

When I moved to Santiago de Compostela, I was fortunate to be part of the amazing Nano-Oncology Group. The year I have spent there was the best out of the 3 years of my PhD journey, and it is all because of my colleagues in Spain, Sainza, Sandra, Sandra A, Sofia, Abi, Marce, Maria, Cristina and Olaia. Your kindness has filled my heart with joy, and you all have always been there when I needed you. Sai, Sandra and Abi, your exceptional presenting skills helped improve mine greatly, and I owe that to you. To Sai and Sandra, thanks a lot for explaining to me all the experiments conducted in the lab, and Sai, I am so grateful for teaching me the HPLC technique. Also, thanks all for the coffees, dinners and parties.

Special thanks to Sofia Mendes Saraiva for the time and effort you spent in reviewing and editing my paper.

To Belen Lopez Bouzo, no words are enough to express my gratitude. At that time, you were my colleague and my housemate, but we grew to be best friends. You have helped me be a better researcher with your bright ideas and comments on my work. Also, I would like to thank your Mom and Abuela for all the supper tasty food we had. You and your family made me feel I have a second family in Spain.

Through NanoFar I had met most of the amazing and inspiring people; Chiara, Bathabile, Maruthi, Surasa, Bhanu, Shubash, Paul, Vincent, Natalija, Sohaib and Muhammad; I feel so blessed to know you all. To Janske and Baptist, no words are enough to express my gratitude. Our meetings and dinners were one of the things that let me overcome the difficulties I had in this journey. You have listened patiently to all of my complainings and cheered me up when I needed it the most. For all of that, thanks a lot. To Mathie, many many thanks for helping me in many situations and for your kindness.

To my parents, Madeline Jabbour and Moustafa Jatal, this work is dedicated to you. You are the ones who believed in my dreams and helped me make them true. Without you, I would never be here. To my brother Tamim, your kindness and silliness and your visits were the ones that helped me move forward. To my Kareem, you have been a constant source of inspiration through difficult times, and I am so grateful for that.

To my Husband, Abdo Sukari, you joined me in the most challenging times of my PhD. You endured my ugly mood swings and my stress. You are always there when I need you, so thanks a lot for being there for me in this period.

Table of Content

General introduction 1

1. Cellular Senescence. 2

1.1. Hallmarks of senescence. 3

1.1.1. Cell Cycle arrest. 3

1.1.2. DNA Damage response DDR 4

1.1.3. Senescence associated secretory phenotype SASP. 7

1.1.4. Upregulated survival pathways in senescent cells. 14

1.2. Cellular senescence in Cancer, suppressive or promoting mechanism? 20

1.2.1. Our lab findings regarding Senescence associated with chemotherapy. 22

1.2.1.1. The role of the TSP1- CD47 pathway in senescence escape. 23

2. Senescent cells to clear or not to clear? 25

3. Therapeutic approaches regarding/targeting senescent cells. 26

3.1. Senolytics/ Senolytic drugs 26

3.2. Immune modulators and immune-mediated interventions. 32

3.3. SASP modulators / senostatics (small molecules that prevent developing the SASP or ameliorate its effect) 36

3.4. Bypass/ reverse of cellular senescence. 40

3.5. Nanomedicine and drug delivery approaches. 41

4. Nanomedicine. 41

4.1. Senescence-directed nanoparticles. 43

4.1.1. Therapeutic & diagnostic senescence-directed nanoparticles. 43

5. Diagnostic probes for detecting senescent cells *in vitro* and *in vivo*. 47

6. Clinical studies and the future of Senolytic drugs 50

7. Future perspectives and important questions. 51

Background, Hypothesis and Objectives. 70

Background 71

Hypothesis 72

Objectives 72

Chapter 1: TSP1 C-terminal Derived Peptides and their Effect on Cancer and senescent cells. 75

Abstract 76

1. Introduction 76

2. Materials and Methods.

2.1. Cell lines, senescence induction, and generation of emergent cells. 77

2.2.Migration assay (Boyden chamber assay) 78

2.3.Western blotting. 78

2.4.Cell Cycle Analysis 78

2.5.Colony Forming Assay/ Clonogenic assay. 79

2.6.MTT assay 79

2.7.β-Galactosidase (β-Gal) staining. 79

2.8.RT-qPCR Analysis. 80

2.9.Statistical analysis. 80

3. Results. 80

3.1.Pilot study with TSP-1 C-terminal derived peptides. 81

3.2.TSP-1 derived peptide (4N1Ks) prevents chemotherapy induced senescence escape in breast and colon cancer models. 84

3.3. Effect of 4N1Ks peptide on p53/p21 expression in cancer and senescent cells. 86

3.4.4N1Ks peptide has an antiproliferative properties and anti-migration/anti-invasion effect. 86

3.5.4N1Ks peptide downregulates mTOR, induces autophagy (and possibly ER stress) in MCF7 cancer and senescent cells. 89

3.6. Investigating the possible effect of 4N1Ks peptide on UPR and ER stress. 92

3.7. The senolytic and senostatic possible properties of 4N1Ks peptide. 94

3.8.The effect of 4N1Ks on LS174t shCD47 and MCF7 shCD47 senescence escape. 96

4. Discussion. 98

5. Conclusions. 100

6. References 100

Chapter 2: Senolytic and Senostatic Sphingomyelin based Nanosystems. 103

Abstract: 104

1. Materials and Methods: 104

1.1. Materials 104

1.2. Methods: 105

1.2.1. Preparation of SNs 105

1.2.1.1. Preparation of SNs and association of 4N1Ks 105

1.2.1.2.Preparation of SNs loaded with ABT-737 106

1.2.1.3.Preparation of SNs loaded with Oleuropein. 107

1.2.2. Physicochemical characterisation of the nanosystems 107

1.2.3. Colloidal stability 108

1.2.4. *In vitro* toxicity. 108

1.2.4.1.Metabolic activity assay. 108

1.2.4.2.Colony forming assay (CFA). 109

1.2.4.3.Blood compatibility 109

1.2.5. Cell uptake 109

1.2.6. *In vitro* evaluation of SNs-Ks 110

1.2.6.1.Senescence escape assay 110

1.2.7. Statistical analysis 111

Part 1: Sphingomyelin nanosystems decorated with TSP-1 derived peptide targeting senescent cells 112

1. Abstract 112

2. Introduction 113

3. Results and discussion 114

3.1.Development and characterisation of SNs-Ks 115

3.2.SNs-Ks stability over time and in biorelevant media 122

3.3.*In vitro* evaluation of the nanosystems 123

3.3.1. SNs-Ks effects on MCF7 and red blood cells 123

3.3.2. Internalization by MCF7 cells. 125

3.4.Senescence escape. 126

4. Conclusions 128

Part 2: Sphingomyelin based nanosystems loaded with the senolytic drug ABT-737. 129

1. Introduction: 129
2. Results and discussion: 130

2.1.Development and characterisation of ABT-737 loaded SNs (SNs-ABT) 130

2.2.SNs-ABT stability studies. 133

2.3.*In vitro* cytotoxicity evaluation of SNs-ABT 133

2.3.1. Haemolysis assay. 133

2.3.2. *In vitro* evaluation of prepared nanosystems. (Senescence escape assay) 133

3. Conclusions. 135

Part 3: Sphingomyelin based nanosystems encapsulated with Oleuropein. 136

1. Introduction. 136

2. Results and Discussion: 136

2.1.Development and characterization of SNs-Ole nanosystems. 136

2.2.SNs-Ole stability studies. 138

2.3.*In vitro* cytotoxicity evaluation of SNs-Ole 138

2.3.1. Haemolysis assay 138

3. Conclusions 139

References 139

Overall Discussion 145

1. 4N1Ks, a TSP-1 C-terminal derived peptide and its effect on Chemotherapy-Induced Senescence. 147
2. Senolytic and Senostatic Sphingomyelin based Nanosystems. 149
3. References 157

Conclusions & Future perspectives 161

List of Abbreviations

µm	micrometer
53BP1	p-53 binding protein 1
ABT	ABT-737
ABT	ABT-737
AFM	Atomic force microscopy
ATM	ataxia-telangiectasia mutated
ATR	ataxia telangiectasia and Rad3-related
ATRIP	ATR interacting protein
ATRIP	ATR interacting protein
C/EBPβ	CCAAT/enhancer-binding protein-β
CDC25	cell-division cycle 25
CDKis	cyclin-dependent kinase inhibitors
CFA	Colony forming assay
CHK1	check point kinase 1
CHK2	check point kinase 2
CIS	Chemotherapy-induced senescence
Dasatinib	D
DDR	DNA damage response
DISC	Death-inducing signalling complex
DLS	Dynamic light scattering

Doxo	doxorubicin
DSBs	DNA double-strand break
EMT	epithelial-to-mesenchyme transition
ER	endoplasmic reticulum
FADD	Fas-associated death domain
IGFBP	insulin-like growth factor binding proteins
IGFBP	insulin-like growth factor binding proteins
MADLS	Multi-angle dynamic light scattering
MDC1	mediator of DNA damage checkpoint1
MMP-1	Matrix metalloproteases
mTORC1	mTOR complex 1
nm	nanometer
NOS	nitrogen species
NPs	nanoparticles
NTA	nano tracking analysis
Ole	Oleuropein
Ole	Oleuropein
PAI	plasminogen activator inhibitor
PI3K	phosphatidylinositol-3 kinase
Quercetin	Q
RB	retinoblastoma proteins
ROS	reactive oxygen species
RPA	the single-stranded DNA- binding replication protein A

S6K	S6 kinase
SAHF	senescence-associated heterochromatin foci
SASP	senescence-associated secretory phenotype
SA-β-gal	senescence-associated β-galactosidase
siRNA	small interference RNA
SIRPα	signal regulatory protein alpha
SN	Sphingomyelin
SNs	sphingomyelin-based nanosystems
SSBs	Single strand breaks
TIMP	tissue inhibitors of metalloproteases
TOPBP1	topoisomerase-II-binding protein 1
tPA	tissue plasminogen activator
TSP1	Thrombospondin protein 1
Tun	Tunicamycin
uPA	urokinase plasminogen activator
UPR	Unfolded protein response
VitE	Vitamin E
β-Gal	β-Galactosidase

List of Figures

General Introduction:

Figure 1: Positive and negative roles of cellular senescence based on its accumulation in the body or clearance by the immune system. The blue box represents the bright side of senescence: Cell cycle arrest in senescent cells prevents further tumour progression. Moreover, cellular senescence with its secretome SASP plays a vital role in tissue regeneration and embryonic development. An example is accelerated wound healing by attracting immune cells to the site of injury. The red box represents the dark side of cellular senescence: accumulation of non-proliferative cells (senescent cells) in the body over time impairs tissue regeneration and tissue homeostasis, leading to ageing and age-related diseases. Moreover, SASP contains several inflammatory cytokines that result in chronic inflammation. Actually, senescent cells secretome includes several factors that promote cell proliferation, cell invasion and angiogenesis; such factors are beneficial in a short term, especially for regeneration and wound healing; however, over a long-term effect, such factors can lead to tumour progression. 3

Figure 2: DNA damage response DDR pathways. Depending on the nature of DNA damage (DSB or SSB), two different pathways initiate to repair DNA damage: ATR or ATM pathway. Each pathway consists of DNA damage sensors, apical local kinases (ATM/ATR), mediators, downstream kinases, and effectors that lead in the end to cell cycle arrest in order to give the cell the time to repair the damage. In the case of persistent DDR, the cellular senescence program is activated. However, if the DNA damage is beyond repair, DDR pathways initiate apoptosis. 7

Figure 3: The bright and dark side of SASP. Senescent cells secretome (SASP) contains several factors, from inflammatory cytokines and chemokines to growth factors and proteases. Depending on the cell context and the exposure time to SASP, senescent cell secretome can either have beneficial or deleterious effects. A) SASP pro-tumour effects: the persistent exposure to SASP over a long period can lead to harmful effects. For example: long-term exposure to several growth factors such as EGF, basic fibroblast growth factor bFGF, and hepatocyte growth factor HGF leads to tumour progression. Moreover, SASP improves the tumour vasculature by inducing angiogenesis through VEGF and angiogenin, which can also promote tumour metastasis in combination with the effect of extracellular matrix remodelling proteins. In addition, prolonged exposure of immune cells to SASP cytokines result in either immunosuppressive phenotype blocking their differentiation. B) SASP anti-tumour effects: proinflammatory factors of the SASP have the capacity to promote immune response by attracting and activating immune cells. For example, activated cytotoxic T cells releases several cytotoxins and pro-apoptotic ligands (such as TNF ligand superfamily member 6 (FASL), perforin, etc.), which mediate senescent cells clearance. Moreover, reactive oxygen species ROS releases by activated macrophages and neutrophils promote cell cycle arrest. C) SASP in tissue regeneration: SASP effects on tissue regenerative potential is also time-dependent. In the case of acute tissue injury, SASP growth factors and immune modulators mediate tissue repair and remodelling by improving tissue regenerative capacity. On the contrary, the accumulation of senescent cells in the body due to immune system failure to clear them leads to tissue dysfunction due to the chronic exposure of surrounded tissue to several SASP factors especially transforming growth factor-β TGFβ, which mediate fibroblast expansion and fibrosis. GMCSF, granulocyte-macrophage colony-stimulating factor; CCL2, C-C motif chemokine 2; p16, p53, cellular tumour antigen p53; cyclin-dependent kinase inhibitor 2A. 13

Figure 4: 'Metabolic reprogramming of senescent cells. IGF-1R signalling activates PI3K leading to membrane PIP3 enrichment serving as an anchor for 3-phosphatidylinositol-dependent kinase 1 (PDK1) and Akt activation at position T308. Among its multiple functions, Akt indirectly enables the formation of mTORC1. mTORC1 positively regulates protein translation through S6K, which exerts negative feedback inhibition at the level of IGF-1R. PI3K also activates mTORC2, which further activates Akt, increasing its kinase activity. Fully activated Akt can then efficiently inhibit pro-apoptotic Bad. Akt may also inhibit pro-apoptotic FoxO transcription factors FoxO1/3, thereby preventing apoptosis. In contrast, antiapoptotic FoxO4 present in senescent cells also supports senescent cell viability. [7] 19

Figure 5: Escape from Therapy-Induced Senescence. Apoptosis is not the only fate for cancer cells treated with chemotherapy or radiation as some cells undergo cell cycle arrest and eventually cellular senescence. Several studies have pointed out the adverse effects of cellular senescence as they provide over time a survival niche through their secretome (SASP), which promote pro-tumorigenic effects in the surrounding cells. Moreover, it is suggested that those treatments activate an incomplete cellular senescence in cancer cells, providing them later with the ability of emergence and re-enter cell cycle as a

more potent form of cancer that is highly drug-resistant. Therefore, it is essential to find therapeutic strategies that eliminate those cells and prevent possible tumour relapse or other malignancies related to senescent cells accumulation. 20

Figure 6: Thrombospondin 1 structural domains and their functions: TSP1 monomer consist of N and G domain connected with a thin strand. Each domain's receptors and ligands and the activities resulted from their interaction are listed above. 24

Figure 7: USP7, MDM2 and p53 axis and the role of USP7 in regulating p53 activity. In cancer cells, senescent cells or in case of genomic stress, USP7 leads to deubiquitination of MDM2, preventing its degradation by the ubiquitination proteosome system, which in return results in p53 degradation. Therefore, inhibiting USP7 by small molecules such as P5091 or knocking it down using siRNA improve p53 activity and stability, which induce pro-apoptotic proteins expression such as PUMA and NOXA, and prevents the interaction between anti-apoptotic BCL- family proteins which result in the end in apoptosis program induction in those cells. 30

Figure 8: An example of survival pathways in senescent cells and possible senolytics that target them. 32

Figure 9: Some of the several approaches of immunotherapies targeted against cellular senescence. 36

Figure 10: Possible therapeutic interventions for modulating the SASP. 40

Figure 11: Therapeutic & diagnostic senescence-directed nanoparticles with their concept of either specific cargo release in senescent cells or the specific targeting of senescent cells. 47

Chapter1:

Figure 1: A) Following sn38 treatment (5 ng/ml) for LS174t and Doxo (25 ng/L) for MCF7, senescence induction was detected by the evaluation of p21waf1 and p-p53 expression (n=3). B) senescence was also detected after chemotherapy treatment in both LS174T and MCF7 by checking the β-galactosidase activity (n=4). 81

Figure 2: A) After CIS induction, LS174T (n=5) and MCF7 (n=3) cells emergence was induced using 10% serum in the presence or absence of 4N1K (50 µM)/ 7N3 (1 µM) peptide in comparison with the control peptide 4NGG (50/1 µM). B) SASP migratory ability in the presence of 4N1Ks peptide were also checked using boyden chamber assay, after collecting SASP from senescent lS174T and MCF7 cells, SASP were mixed with 4N1K, 7N3 or control peptide and placed in the lower chamber, (n=3). 83

Figure 3: A) After CIS induction, LS174T (n=5) and MCF7 (n=4) cells emergence was induced using 10% serum in the presence or absence of 4N1Ks in comparison with the control peptide 4NGG (50 µM), (Kolmogorov–Smirnov test, * =p < 0.05, ** =p < 0.01). B) β-galactosidase activity in LS174T and MCF7 cells after treatment with 4N1Ks 50µM and 4NGG as a control (n=3). 85

Figure 4: Effect of 4N1Ks peptide on p53/p21 expression in cancer and senescent cells. A) p53-ser15 and p21 waf-cip1 expression in MCF 7 and LS174t cells were examined by western blot after 8 and 15 h of treatment with peptides in the presence or absence of chemotherapy (Sn38 5ng/mL for LS174t cells and Doxo 25ng/ mL for MCF7 cells) (n=3). B) p53-ser15 and p21 waf-cip1 expression in MCF7 cells treated with 4N1Ks 50 µM for 48h (with 4NGG as a control) were assessed by western blot, (n=3). C) p53-ser15 and p21 waf-cip1 expression in senescent MCF7 cells treated with 4N1Ks 50 µM for 48h (EM2D) (with 4NGG as a control) were assessed by western blot, (n=3). 86

Figure 5: A) Antiproliferative effect of 4N1ks was checked using colony forming assay on LS174t (n=4) and MCF7 (n=5) for 10 days with 4NGG as a control (n=4, Kolmogorov–Smirnov test, ** =p < 0.01). B) Effect of 4N1Ks on the metabolic activity of

LS174T and MCf7 cancer cells were checked using MTT assay (n=4, Kolmogorov–Smirnov test, * =p < 0.05). C) The effect of 4N1Ks peptide on cell cycle of MCF7 cells and LS174t cells were examined by flow cytometry (n=3). 88

Figure 6: SASP migratory ability in the presence of 4N1Ks peptide were also checked using boyden chamber assay, after collecting SASP from senescent lS174T and MCF7 cells, SASP were mixed with 4N1ks or control peptide and placed in the lower chamber, (n=4). 89

Figure 7: A) protein content in both cancer and senescent MCF7 cells after treatment with 4N1Ks 50µM and 4NGG as a control (Kolmogorov–Smirnov test, * =p < 0.05, ** =p < 0.01). B) Expression of several UPR and autophagy markers by western blot in MCF7 cancer cells after 48h treatment with 4N1Ks 50µM with 4NGG as a control (n=3). C) Expression of several UPR and autophagy markers by western blot in MCF7 after two days of emergence by treating senescent cells (CIS) for two days with 4N1Ks 50µM and 4NGG as a control (n=3). D) granularity of MCF7 cells treated with 4N1Ks in comparison to non-treated and control peptide were checked by FSC/SSC using flow cytometry and supported by the microscope photos of enlarged MCF7 cells after treatment with 4N1Ks (n=3). 91

Figure 8: Investigation the possible relation between 4N1Ks peptide and UPR. A) mRNA levels of UPR markers were checked using RT-qPCR in MCF7 cell treated with peptides for 48h (n=3). B) mRNA levels of several tRNAs and LARS, CARS, and YARS ligase were assessed by RT-qPCR in MCF7 cells treated with peptides for 48h (n=3). C) The same as in C but those mRNA levels were checked in senescent cells after treatment with peptides for 2 days (EM2D) (n=3). D) After CIS induction, MCF7 (n=3) cells emergence was induced using 10% serum in the presence or absence of Tun 1µg/ 2µg/ mL (one representative image out of three experiments), (Kolmogorov–Smirnov test, * =p < 0.05) 93

Figure 9: The possible senolytic senostatic effects of 4N1Ks peptide. A) the effect of 4N1Ks on SASP production or components were assessed by collecting first SASP from senescent cells treated with 4N1Ks for 2 days and check the migration ability of this SASP using Boyden chamber assay in comparison to SASP collected form non-treated cells or cells treated with 4NGG control peptide (n=4). B) the effect of 4N1Ks on the metabolic activity of MCF7 senescent cells were checked using MTT assay after CIS (n=4). C) mRNA levels of SASP components: IL1-α, Il-6, IL-8, THSB1, TGFB1, and MMP1 was assessed by RT-qPCR in MCF7 cancer cells treated with 50 µM of peptides for 48h, (n=3). D) mRNA levels of SASP components: IL1-α, Il-6, IL-8, THSB1, TGFB1, and MMP1 was assessed by RT-qPCR in MCF7 senescent cells treated with 50 µM of peptides for 48h (EM2D), (n=3). 95

Figure 10: The effect of 4N1Ks peptide CIS emergence in MCF7 and LS174t cells expressing an shRNA directed against CD47 or a non-targeting control shRNA. Emergence was induced as described before (n=3). 97

Chapter 2:

Part1:

Figure 1: Schematic illustration of the nanosystems (SNs-blank, SNs-Ks and V-Ks) preparation by ethanol injection method. 116

Figure 2: Effect of increasing weight ratios of C18-PEG-Ks (from 0.0025 to 0.2, respective to VitE) on SNs-Ks' (composed of VitE, SM and C18-PEG-Ks) and V-Ks' (composed of VitE and) size, polydispersity index (PdI) and zeta potential, determined by DLS. 117

Figure 3: Physiochemical characterisation of dialysed vs un-dialysed SNs-blank (left), SNs-Ks (middle), and V-Ks (right) nanosystems by Dynamic light scattering (DLS) and dialysed nanosystems by Nanoparticle tracking analysis (NTA) (n≥3). 118

Figure 4: Physicochemical characterisation of dialysed nanosystems by Multi angle dynamic light scattering (MA-DLS) (n=3). The 3D plots show CONTIN-derived hydrodynamic radii distributions for different scattering angles (θ = 30 to 150º) 119

Figure 5: Physicochemical characterisation of dialysed nanosystems by Atomic force microscopy (AFM) (n=3). 121

Figure 6: Stability of SNs-blank (1:0.1) and SNs-Ks (1:0.1:0.1 and 1:0.1:0.025) upon incubation in different relevant media (PBS 5 mM, non-supplemented RPMI, RPMI supplemented with 1% FBS and plasma) up to 24 h. PBS: Phosphate Buffer Saline; FBS: Fetal Bovine Serum. **123**

Figure 7: Effect of C18-PEG-Ks and SNs-Ks on MCF7 breast cancer cells and red blood cells. A) MCF7 cells viability determined by MTT assay after treatment with the modified peptide (1 to 50 µM) for 72 h. B) Macroscopic photos of MCF7 colonies formed after C18-PEG-Ks treatment. C) Evaluation of cell proliferation activity by colony forming assay of MCF7 treated with C18-PEG-Ks (1 to 50 µM) for 10 days. D) Representative macroscopic images of MCF7 colonies. MCF7 cells after treatment for 9 days with C18-PEG-Ks, SNs-blank and SNs-Ks (peptide concentration 0.25 to 1 µM). E) Graphical representation of MCF7 colony forming capacity upon treatment with cell culture medium (NT, non-treated), C18-PEG-Ks, SNs-blank and SNs-Ks at 0.5 µM (peptide concentration). Data are presented as mean ± SD (n=6). ** $p < 0.01$. F) Human red blood cells were haemolysis (%) upon exposure to SNs-blank and SNs-Ks nanosystems up to 1 µM (peptide). Triton X-100 and PBS were used as positive and negative controls representing 100% and 0% of haemolysis, respectively (n=3). Data are presented as mean ± SD. **124**

Figure 8: Cell internalization studies of SNs-Ks and SNs-blank over time. (A) Confocal microscopy images showing the internalization of SNs-Ks and SNs-blank, labelled with TopFluor®-SM,in MCF7 cells after 30 min, 1 h and 2 h of treatment. Green channel: TopFluor®-SM labelled SNs. Blue channel: nuclei staining with DAPI. (B) Flow cytometry analysis and respective percentage of MCF7 cells internalizing TopFluor-SM SNs over time (10 min to 4 h). **126**

Figure 9: SNs-Ks effect on senescence escape. A) Ninety-six h treatment of doxorubicin (25 ng/mL) induces senescence in MCF7 breast cancer cells. Microscopic photos of the increased β-galactosidase activity (blue signal) in comparison to non-treated (NT) cells. Increased expression of senescence markers p-p53 ser15 and p21 waf-cip1, determined by western blot. B) Chemotherapy-induced senescent MCF7 cells were treated with SNs-Ks at 0.25 to 1 µM (peptide dose) and SNs-blank as negative control for 24 h and left for 14 days in culture. Non-treated (NT) cells were used as positive control. (n=1). * $p < 0.05$. C) Macroscopic images of chemotherapy-induced senescent MCF7 cells 14 days post-treatment with SNs and SNs-Ks. .. **128**

Part 2:

Figure 1: Schematic illustration of the nanosystems (SNs-blank, SNs-ABT) preparation by ethanol injection method. **130**

Figure 2: Physicochemical characterization of SNs-ABT (1:0.1:0.01) with NTA, MADLS and AFM A) before dialysis & B) after dialysis (n=3). **132**

Figure 3: A) Stability of SNs-ABT (1:0.1:0.01) upon incubation in different relevant media (PBS 5 mM, non-supplemented RPMI, and plasma) up to 24 h. PBS: Phosphate Buffer Saline. B) Human red blood cells were haemolysis (%) upon exposure to SNs-ABT nanosystems up to 1 µM (ABT-737). Triton X-100 and PBS were used as positive and negative controls representing 100% and 0% of haemolysis, respectively (n=3). Data are presented as mean ± SD. C) MCF7 cells viability determined by MTT assay after treatment with ABT-737 (1 to 15 µM) for 72 h. D) Chemotherapy-induced senescent MCF7 cells were treated with SNs-ABT at 0.25 and 0.5 µM (ABT-737) and SNs-blank as negative control for 24 h and left for 14 days in culture. Non-treated (NT) cells were used as positive control. (n=3). * $p < 0.05$. E) Macroscopic images of chemotherapy-induced senescent MCF7 cells 14 days post-treatment with SNs and SNs-ABT. **135**

Part 3:

Figure 4: Schematic illustration of the nanosystems (SNs-blank, SNs-ABT) preparation by ethanol injection method. **137**

Figure 5: A) Effect of increasing weight ratios of Oleuropein (from 0.01 to 0.5, respective to VitE) on SNs-Ole' (composed of VitE, SM and Oleuropein) size, polydispersity and zeta potential, determined by DLS. Physiochemical characterisation of SNs-Ole (1:0.1:0.05) by **B)** NTA**, C)** MADLS and **D)** AFM. (n=3). **138**

Figure 6: **A)** storage stability of SN-Ole (1:0.1:0.05) at 4 ºC over 4 months, size measurements were determined by DLS. **B)** Stability of SNs-Ole (1:0.1:0.05) upon incubation in different relevant media (PBS 5 mM, RPMI supplemented with 1% FBS, and plasma) up to 24 h. PBS: Phosphate Buffer Saline, FBS: Fetal Bovine Serum. **C)** Human red blood cells were haemolysis (%) upon exposure to SNs-Ole nanosystems up to 5 µM (Oleuropein). Triton X-100 and PBS were used as positive and negative controls representing 100% and 0% of haemolysis, respectively (n=3). Data are presented as mean ± SD. 139

List of Tables

General Introduction:

Table 1: A list of some of the diagnostic probes that detect cellular senescence or other cells (ovarian cancer cells) depending on their β-gal activity,[197]. **50**

Table 2: List of therapeutics in clinical studies against cellular senescence [197]. **51**

Chapter 2:

Part 1:

Table 1: Physicochemical properties of SNs-blank (1:0.1), SNs-Ks (1:0.1:0.1) and V-Ks (1:0.1) before and after dialysis, determined by NTA. Mean particle size (diameter), D-values (D10, D50, D90), calculated SPAN value and sample concentration in particles per millilitre (particle/mL) (mean ± SD, n= 3). **118**

Table 2: Physicochemical characterization of nanosystems (before and after dialysis) by MA-DLS and AFM. **120**

Part 2:

Table 1: SNs-blank[1] (1:0.1) [1] and SNs-ABT nanosystems physicochemical characterisation by DLS and LDA (mean ± SD, n=12). **131**

Table 2: Physicochemical characterization of nanosystems (before and after dialysis) by NTA and MA-DLS**.** **132**

Overall discussion:

Table 1: SNs-blank (1:0.1) and SNs-Ks nanosystems physicochemical characterisation by DLS and LDA (mean ± SD, n=3). **151**

Table 2: V-Ks nanosystems physicochemical characterisation by DLS and LDA (mean ± SD, n=3). **151**

Table 3: SNs-blank (1:0.1) and SNs-ABT nanosystems physicochemical characterisation by DLS and LDA (mean ± SD, n=12). **154**

General Introduction

Cellular senescence had grabbed the attention of biology researchers since it was first discovered by Leonard Hayflick and Paul Moorhead almost 70 years ago when they found that normal human fibroblasts have a definite number of divisions in culture, which is known by the 'Hayflick limit'. As from then, cellular senescence was extensively explored/ studied; however, there is a lot yet to comprehend, especially regarding the effect of senescence on overall health, in particular ageing disease and cancer. Based on that, a new platform of therapeutic agents such as senolytics or senostatics has emerged, which will be the focus of this introduction.

1. Cellular Senescence:

When the cell is subject to potential damage, there are different scenarios of the cell fate dependent on the extent of the damage; either the damage can be reversed, and the cell regains its functional integrity, or it's beyond repair, and the cell activates death mechanisms. However, there is another possibility where cells remain their viability but with permanent structural and functional changes, for instance, cellular senescence. It was first described in 1961 by Leonard Hayflick and Paul Moorhead when they discovered that normal human fibroblasts have a definite number of divisions in culture, which is known by (Hayflick limit) [1,2]. In fact, this is one type of cellular senescence, replicative senescence, that is caused by telomere shortening. Lately, several internal and external cellular insults have been identified as triggers for 'premature senescence', such as oncogenic activation, cytokines, irradiation, oxidative stress, DNA damage and chemotherapeutic agents [3,4].

Although cellular senescence is mainly characterised by the stable cell cycle arrest of old and damaged cells, senescent cells undergo phenotypic alterations such as morphology changes, chromatin remodelling, metabolic reprograming and the most important, the secretion of a vast array of proinflammatory cytokines, chemokines and growth factors all known as the senescence-associated secretory phenotype (SASP) [3].

Cellular senescence is a dynamic program that has been linked lately to cancer and age-related diseases. Here, we review the hallmarks of senescence along with the molecular mechanism governing cellular senescence with a special focus on the possible treatments/ senolytic drugs that can interfere with these molecular pathways.

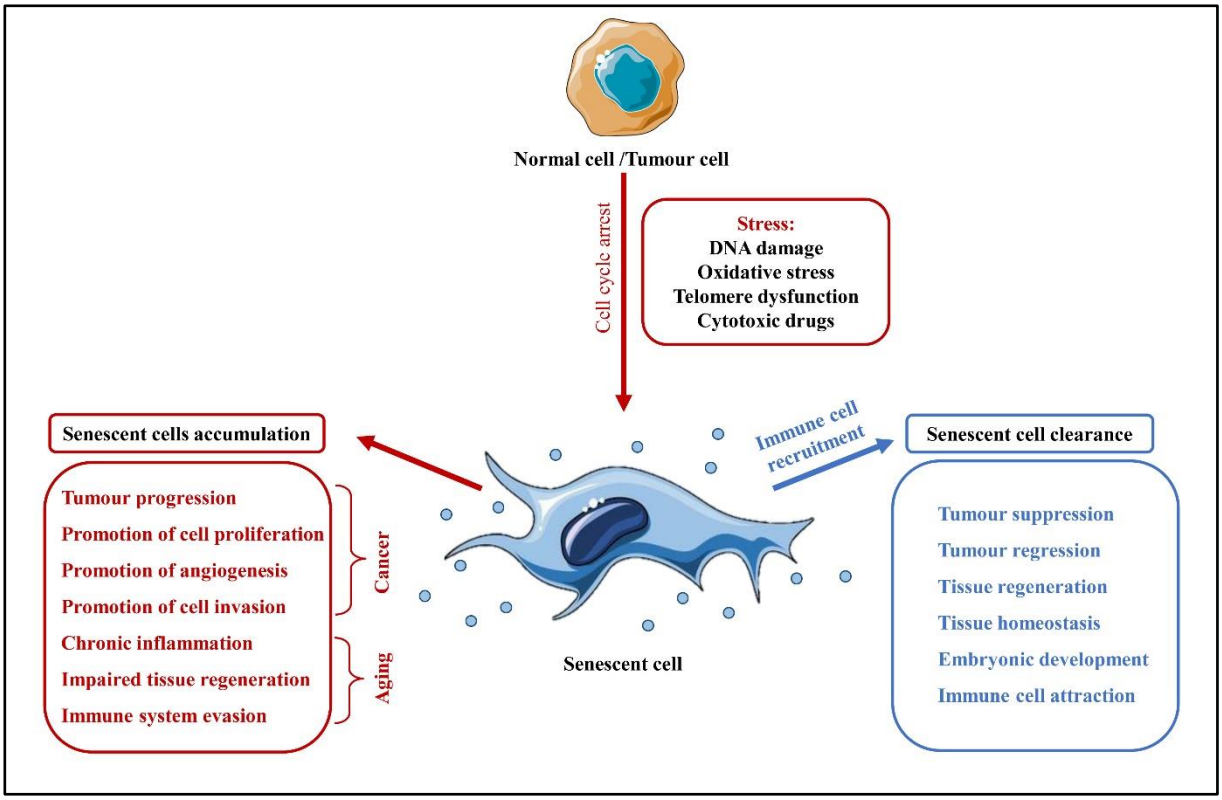

Figure 1: Positive and negative roles of cellular senescence based on its accumulation in the body or clearance by the immune system. The blue box represents the bright side of senescence: Cell cycle arrest in senescent cells prevents further tumour progression. Moreover, cellular senescence with its secretome SASP plays a vital role in tissue regeneration and embryonic development. An example is accelerated wound healing by attracting immune cells to the site of injury. The red box represents the dark side of cellular senescence: accumulation of non-proliferative cells (senescent cells) in the body over time impairs tissue regeneration and tissue homeostasis, leading to ageing and age-related diseases. Moreover, SASP contains several inflammatory cytokines that result in chronic inflammation. Actually, senescent cells secretome includes several factors that promote cell proliferation, cell invasion and angiogenesis; such factors are beneficial in a short term, especially for regeneration and wound healing; however, over a long-term effect, such factors can lead to tumour progression.

Cellular Senescence: 'Walking a Line between Life and Death' [5]

1.1. Hallmarks of senescence:

Although cellular senescence has been extensively studied in the last decade, yet there are still no specific markers that **single out** senescent cells from other types of cellular programs. Moreover, molecular pathways that **launch/ take up** in senescent cells differ depending on the type of damage/ signal that initiate senescence. Besides the permanent cell cycle arrest, senescent cells adopt morphological changes such as flat larger cells with an increase of lysosomal activity, which corresponds mainly to the senescence associated-β-galactosidase activity, accumulation of mitochondria, nuclear changes such as senescence-associated heterochromatin foci (SAHF), and most importantly the associated secretory phenotype (SASP) [6]. All these features are described in detail in this section.

1.1.1. Cell Cycle arrest:

The main feature of all types of senescent cells is the irreversible cell cycle arrest which takes place after damaging stimuli or abnormal proliferation. This cell cycle exit is mainly controlled by two main pathways: $p16^{1NK4a}$/RB and p53/$p21^{cip1}$. $p16^{1NK4a}$ and $p21^{cip1}$ are cyclin-dependent kinase inhibitors CDKis ($p16^{1NK4a}$ inhibits CDK4 and CDK6 while $p21^{cip1}$ inhibits CDK2), which in turn lead to the hypophosphorylation of RB (retinoblastoma proteins), and therefore inhibition of E2F transcription activity, which is necessary of cell cycle progression [3,6,7]. However, with time, the persistent activation of these pathways and the accumulation of $p16^{1NK4a}$ and $p21^{cip1}$ prevent the possibility to escape the cell cycle arrest even with the inactivation of RB proteins and p53 [8].

It is essential to note the difference between senescence and other forms of cell cycle arrest, in particular quiescence and terminally differentiated cells. Cell cycle arrest takes place in senescent cells in G1 or G2. However, in quiescent cells, the arrest happens in G0 and upon appropriate stimuli renter the cell cycle [9]. In the case of terminally differentiated cells, cell cycle arrest is mediated by pathways different from the ones in senescence. Moreover, terminally differentiated cells are the result of a developmental programme turning undifferentiated cells into specialised functional cells, where cellular senescence is regarded as a cellular stress response [3,5].

Also, it should be noted that senescent cells under specific circumstances can renter the cell cycle, especially in tumours [10,11], which will be addressed later extensively.

1.1.2. DNA Damage response DDR.

DNA damage is either triggered by intrinsic injuries (such as telomere shortening, oxidative stress and hyper proliferation) or by extrinsic insults like (ultraviolet, γ-irradiation, chemotherapeutic drugs), which in result activates DDR and a cascade of several pathways that lead to cell cycle arrest mentioned earlier. This gives cells the time to repair DNA damage and re-enter the cell cycle. However, in case the damage is beyond repair and persistent active DDR takes place, the cell goes either under apoptosis or senescence, depending on the cell type, nature, length and magnitude of the damage [4,12,13]. Molecular mechanisms governing the DDR and its outcome in either replicative or oncogene-induced senescence will be discussed in this section.

In brief, DDR pathways consist mainly of sensors, transduces and effectors. The sensors recognise the DNA damage and recruit transducers DDR kinases to the site of DNA damage which in turn phosphorylate and activate several mediators and effectors proteins that are

important for maintaining the genomic stability by participating in DNA repair, DNA replication and cell cycle control [14].

DNA damage takes place in two different forms, single-stranded DNA and DNA double-strand breaks (SSBs & DSBs). Both forms are strong inducers of DDR; where special complexes sense these two forms of DNA damage and recruit plus activate two types of protein kinases to the site of DNA damage; ATM (ataxia-telangiectasia mutated) and or ATR (ataxia telangiectasia and Rad3-related), which belong to phosphatidylinositol-3 kinase (PI3K) family [14,15]. Whereas ATM seems to be activated primarily by DSBs, ATR mainly responds to stalled replication forks [14]. ATM and ATR signalling pathways are quite distinct, and those differences will be explained below.

In **ATM** signalling cascade, DNA damage (DSBs) is sensed by MRN complexes which activate and recruit ATM to the site of DNA damage [13]. In return, ATM kinase locally phosphorylates the histone H2AX to its active form, ɣH2AX, which engage more ATM causing a positive feedback loop [16]. This leads to the accumulation of ATM and eventually spreading ɣH2AX along the chromatin[13]. DDR mediators: MDC1 (mediator of DNA damage checkpoint1) and 53BP1 (p-53 binding protein 1) are essential for the mentioned positive feedback loop by facilitating more ATM complexes to ɣH2AX [13].

In **ATR** signalling cascade, a single strand of DNA is exposed, which is sensed and covered by RPA (the single-stranded DNA- binding replication protein A), which in turn recruit ATR to the DNA damage site by binding to ATRIP (ATR interacting protein) [17]. In addition, ATR kinase activity is amplified by the heterotrimeric 9–1–1 complex [18] (which binds at the junction between double-strand DNA and single-strand DNA and act as a sliding clamp that is essential for repairing the DNA damage [19]. Also, the topoisomerase-II-binding protein 1 (TOPBP1) acts as a booster for the ATR kinase signal [17,20].

When ATM and ATR signals exceed a specific threshold, this leads to the phosphorylation of several substrates, spreading the DDR signal far from the DNA damage site [13]. For instance, ATM phosphorylates and activates the check point kinase CHK2, which in return diffuse freely in the nucleoplasm and spread the DDR signal by phosphorylating its substrates [13,14,21]. Similarly, CHK1 is activated by ATR. This leads us to the last part of the DDR cascade, which is the effectors' proteins; CDC25 phosphatases (cell-division cycle 25) and p53. CDC25 inactivation by ATR/CHK1 axis leads to rapid cell cycle arrest as it is crucial for proliferation [21]. On the contrary, p53 activation by DDR kinases [22] boost its ability to induce the

transcription of p21 (a cyclin-dependent kinase inhibitor), resulting in a stable and slower cell cycle arrest [13,23]. **Figure 2.**

As mentioned before, **ɣH2AX** spread along the chromatin [16], creating a **molecular 'velcro'**, as *d'Adda di Fagagna* described it in his review article [13], which attracts and engage several DDR factors creating detectable nuclear foci that contain several copies of DDR kinases and proteins, which is one of the most known markers of senescence [6]. Hence, DNA foci represent an epicentre of factors and proteins necessary for spreading the DDR signal, DNA repair and cell cycle arrest. DNA foci range in size from 0.6 to 1.6 µm, which is dependent on the time [13].

Interestingly, DDR can generate extracellular signals to spread cellular stress to neighbouring non-affected cells. This can happen through rapid and long responses. Rapid DDR extracellular signals involve transmitting cellular stress through the tight junctions between the cells; for instance, reactive oxygen or nitrogen species (ROS/NOS) can pass through those tight junctions as they are highly produced in damaged cells. Moreover, DDR regulates the expression of some surface ligands and receptors on the surface of senescent cells in order to communicate with the surrounding cells; an example is NKG2D ligands that engage near immune cells, while DR5 through receptor-ligand reaction can impact damaged cell survival. On the other hand, the secretory phenotype of senescent cells is responsible for the late DDR extracellular signals. It reinforces cellular senescence and spreads stress to the surrounding microenvironment through an autocrine and paracrine mechanism, reviewed in [24]. That will be explained in detail in the following section.

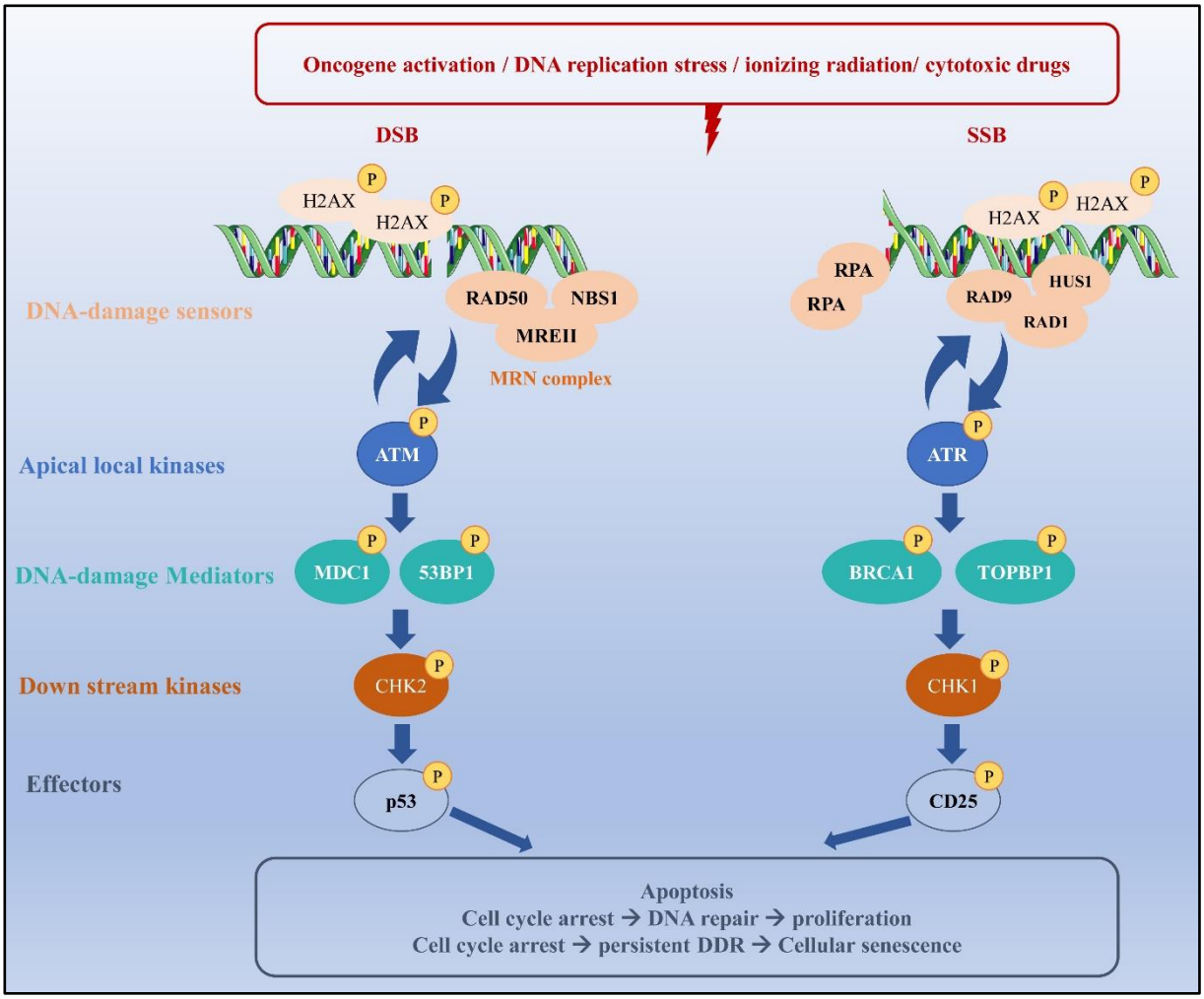

Figure 2: DNA damage response DDR pathways. Depending on the nature of DNA damage (DSB or SSB), two different pathways initiate to repair DNA damage: ATR or ATM pathway. Each pathway consists of DNA damage sensors, apical local kinases (ATM/ATR), mediators, downstream kinases, and effectors that lead in the end to cell cycle arrest in order to give the cell the time to repair the damage. In the case of persistent DDR, the cellular senescence program is activated. However, if the DNA damage is beyond repair, DDR pathways initiate apoptosis.

1.1.3. Senescence associated secretory phenotype SASP.

SASP term referring to the several factors secreted by senescent cells was first used in 2008 [25]. It is one of the most significant features of senescence, and it is what differentiate senescent cells from other types of arrested cells. Also, it is the feature that set the connection between cellular senescence and many other cellular processes such as maintaining senescence, embryogenesis, and tumorigenesis. Due to its importance, the following section will explain in detail SASP components, molecular mechanisms governing SASP production and the variant roles of SASP.

The composition and the strength of SASP vary dependent on the type of the cell, signal initiating senescence and the duration of the senescence [26,27]. However, there are two types of classification of SASP factors; the first is dependent on the chemical nature and therefore

divided into: soluble signalling factors, proteases, insoluble extracellular matrix proteins, and non-protein components. The second classification is based on the molecular mechanism of SASP factors and is divided into: factors binding to a receptor, direct-acting factors and regulatory factors [28,29]**.**

SASP factors binding to a receptor include cytokines, chemokines and growth factors. These factors achieve their functions by binding to their corresponding receptors, which sets off several intracellular signalling cascades. Interleukins such as IL-6, IL-8 and IL-1a, are the most known SASP cytokines; their role in regulating inflammatory networks in cancer and senescence is well understood [30]. SASP chemokines include GROα, GROβ, CCL-2, CCL-5, CCL-16, CCL-26 and CCL-20; these factors trigger their effect by binding to G protein-linked transmembrane receptors (which are known by chemokine receptor) [28]. Finally, increased expression of growth factors such as HGF, FGF, TGFβ, and GM-CSF have been reported in several types of senescent cells [28]. All these factors have a tremendous effect on the surrounding cells, creating a proper environment for different pathologies to emerge/ arise with time.

Direct-acting SASP factors mainly include secreted proteases whose function can be divided into three primary effects: 1) destroying membrane-associated proteins, 2) remodelling extra cellular matrix ECM and 3) degradation /cleavage of secreted signalling molecules. With the help of these factors, senescent cells can remodel and modify the surrounding microenvironment [28,29,31]. Two main groups of proteases belong to these factors, which are matrix metalloproteases MMP-1, MMP-10, MMP-3 and serine proteases: the tissue plasminogen activator (tPA) and urokinase plasminogen activator (uPA) [28,29,32]. Besides proteases, small non-protein molecules, for instance, reactive oxygen (ROS) and nitrogen species, also belong to this group of SASP factors [29,32]. These molecules are known for their ability to modulate cellular phenotype, increase cancer aggressiveness and advance age-related diseases [31].

SASP regulatory factors consist of tissue inhibitors of metalloproteases TIMP, the plasminogen activator inhibitor PAI, and insulin-like growth factor binding proteins IGFBP. These factors do not possess an enzymatic or signalling activity, but they regulate the function of the first and second group of SASP factors when they bind to them [28,29]. For instance, TIMPs regulate the activity of MMPs by mainly inhibiting most of the MMPs members [33,34]. PAI-1 also inhibits tPA and uPA proteases activity [35]; some papers also indicated the

importance of PAI-1 as it acts not only as a marker but also as a mediator for replicative senescence and ageing [35,36]. IGFBP, as it is clear from its name, behave as a carrier protein for IGF and also plays a role in mediating the half-life of IGF [31].

Exosomes or extra cellular vesicles have been the target of interest for many researchers lately, and it has been recently considered one of the components of the SASP. Depending on their composition, exosomes significantly affect the surrounding microenvironment, which can lead to maintain or suppress cellular senescence, promoting tumorigenesis or age-related diseases [37,38].

Cellular senescence is a dynamic process in which its initiation and maintenance take place in several stages; the same applies to SASP production and regulation which can be divided into three different stages: **1)** the early rapid initiation of SASP, which takes place immediately after DNA damage and lasts for 36h, **2)** the next phase consists of the secretion of the most important SASP factors in particular IL-1α which lasts for several days, and it is called the early phase of SASP, it is essential to note that the SASP factors are not secreted at high levels at this stage, and they work mainly as a self-amplifying signal which leads to the next phase **3)** mature phase of SASP [25,29,39].

Molecular mechanisms governing SASP production: Regulation of SASP production takes place at the transcriptional and post-transcriptional levels. Also, mentioned before, SASP production depends strongly on the autocrine and positive paracrine loops as they amplify the SASP signalling pathways. The most important molecular mechanism that controls the initiation and maintenance of the SASP are DDR, p38 MAPK, and cGAS/STING. All these pathways seem to intersect at the activation of NF-κB and CCAAT/enhancer-binding protein-β (C/EBPβ) [3,40].

NF-κB and C/EBPβ are transcriptional factors which are activated and enriched in senescent cells at the chromatin level leading to the production of the inflammatory factors of the SASP; such as IL-6 & IL-8, which in turn through SASP autocrine provide a feed-back loop that leads to the maintenance of activation of NF-κB and C/EBPβ, and amplification of SASP signal [3,39].

SASP is also regulated at a post-transcriptional level where DDR plays an important role. The exact mechanism by which DDR regulate SASP production is not yet fully understood. However, several DDR components were proved to have a link in activation of NF-κB; for example, the inactivated form of NF-κB is found in the cytoplasm as a complex with IκB

protein, upon DDR activation, ATM kinase forms a complex with NEMO protein that leads to its translocation from the nucleus to the cytoplasm, and later binds and activate IKK kinase. Activation of IKK kinase promotes the disassociation NF-κB complex and, therefore, its activation [39]. It is also important to note that knocking down DDR components such as ATM, Chk2, and H2AX decrease the expression and secretion of several SASP factors, especially IL-6 and IL-8 [41,42].

Other post-transcriptional pathways regulating the SASP include p38 kinase and m-TOR. The stress kinase p38 is part of the p161NK4a/Rb pathway that initiates cell cycle arrest in senescent cells [43]. Its role in the regulation of SASP production includes the activation of its targets MSK1 & MSK2 kinases, which in turn phosphorylate p65 transactivation subunit of NF-κB [39]. Other studies stated that inhibition of p38 activity leads to a remarkable reduction of secretion of most SASP components [39,44,45]. Moreover, persistent activation of p38 lead to the production of SASP even without DDR [44], which indicates the importance of p38 in SASP regulation.

m-TOR signalling pathway has been recently considered to play an essential role in SASP regulation [3]. It acts in two different ways, the first one by indirectly monitoring the stability of SASP mRNAs [3], which mechanism can be explained briefly as follows: senescent cells have high mTOR activity that mediates the phosphorylation of 4EBP protein, which is known to regulate the translation of specific SASP mRNAs, among those, is mRNA of IL-1a [46], and as we mentioned before, IL-1a is important in the positive feed-back loop that maintains the activation of NF-κB. Also, mTOR modulates positively the translation of MAPKAPK2 kinase (also known as MK2). High levels of MAPKAPK2 inhibits the activity of ZFP36L1, which is an mRNA binding protein that specifically targets and degrades SASP mRNAs [39,47]. The second mechanism in which m-TOR regulates SASP involves TOR-autophagy spatial coupling compartment (TASCC) [39] that magnify SASP production by coordinating protein synthesis and autophagy in senescent cells [3]. Although, the relation of autophagy with senescence and SASP is quite complicated since it depends on the extent of the autophagy activity that can promote or inhibit senescence and SASP production [39,48].

The regulatory mechanisms of the SASP mentioned above are the most important ones. It is essential to point out that SASP regulator mechanism and components vary dramatically depending on the type of the cell and the signal initiating senescence; however, the proinflammatory arm is preserved in most senescent cells types [3].

Variant roles of SASP: the biological effects of SASP, which state the relation between senescence and other biological processes, for instance, inflammation, cancer and age-related diseases etc., will be explained in detail in this section. However, before digging deep, we would like to state the same question in Borodkina et al. [29] review article; why do senescent cells need a vast array of secreted factors? By examining the SASP components, it is evident that SASP act as a signal in vivo to indicate the presence of senescent cells. This can be simply explained as follows: cytokines and chemokines secreted by senescent cells initiate inflammation which is needed to attract immune cells to eliminate senescent and damaged cells. On the other hand, proteins and markers that modulate the ECM; ease the entry of immune cells to senescence cite, while growth factors promote proliferation of neighbouring cells in order to replace the eliminated cells [29,49]. This represents the positive side of SASP and senescent cells in which this mechanism works perfectly in young health organisms but fails to accomplish with age, leading to the accumulation of senescent cells and prolonging secretion of SASP, promoting chronic inflammation, which represents the dark side of senescence. Therefore, the consequences of SASP effects depend mainly on two factors; on how long the SASP affects the surrounding microenvironment and how fast and effective the immune system is in eliminating senescent cells [29].

SASP and Age-related diseases, the relation between senescence and ageing will be discussed in detail later. However, accumulation of senescent cells, chronic inflammation, failure of the immune system to eliminate senescent cells with time and disruption of the surrounding tissue set the relation between age-related diseases and senescence. The autocrine and paracrine activity of senescent cells maintain senescence and promote pre-senescence in neighbouring cells. The accumulation of senescent cells with age leads to chronic inflammation, also termed “inflammaging”, due to the persistent secretion of cytokines and chemokines [50,51]. This chronic inflammation has the ability to suppress the immune system; an example of that is IL-6, which acts as a proinflammatory factor that recruits the immune cells to senescence cite to eliminate them; however, in chronic inflammation, IL-6 shifts macrophages to the immune-suppressing M2 phenotype [52].

Furthermore, chronic inflammation with the prolonged circulation of chemokines and cytokines leads to chronic stress of the immune system, resulting in immunosenescence, identified by the functional decline of the immune system along with the reduced ability to recognise new antigens [50,53]. Other SASP factors such as matrix metalloproteases significantly impact the surrounding tissue, leading to tissue disruption upon prolonged secretion [54]. All these factors

contribute to several age-related diseases such as osteoarthritis [55], atherosclerosis and cancer [51].

Most of these findings were reached by knocking down pathways that regulate the production of SASP; for example, transgenic IL-10 knock-out mice (an anti-inflammatory cytokine) have a premature ageing-like phenotype and accumulation of senescent cells and SASP factors in their tissues. Similar results were also found in Nfκb1$^{-/-}$ mouse [52].

SASP and cancer: initially, cellular senescence was considered as a tumour suppressor mechanism; however, several studies included that cellular senescence could promote tumorigenesis. The molecular mechanisms included in this will be discussed extensively later, but the role of SASP in tumour suppression and promotion will be discussed here.

SASP as a tumour suppressor: as mentioned before, several SASP components attract the immune system, which leads to the elimination of senescent, damaged and premalignant cells, which is termed by senescence immune surveillance mediated by CD4$^+$ T cells. Another immune cell recruited by SASP are neutral killer NK cells; these cells, along with T cells, can initiate cytolytic response on senescent and malignant cells [56,57]. Moreover, SASP components maintain and promote senescence and growth arrest through autocrine and paracrine activity [56].

SASP as pro-tumorigenic: SASP can promote tumour in the surrounding microenvironment by several mechanisms. One of them is related to the accumulation of senescent cells overage as the surrounding microenvironment is subjected to the prolonged secretion of the inflammatory SASP. Several SASP factors, particularly proteases, promote tissue disruption and remodelling, which facilitates the immune system cells to reach the senescence site. However, this can also promote cancer cells invasion and metastasis [56,57].

Also, SASP factors can initiate epithelial-to-mesenchyme transition (EMT) phenotype, which is an important step for cancer metastasis [56,58,59]. Moreover, SASP can promote angiogenesis directly by secreting several angiogenic factors [59] or indirectly by recruiting macrophages and shifting them to pro-angiogenic M2 phenotype [57]. Another mechanism in which SASP promote tumorigenesis is by suppressing the immune system as explained before with age-related disease; SASP cytokines engage myeloid-derived suppressor cells, which inhibit the proliferation of CD8$^+$ T cells and their ability to kill tumour cells [57,60].

SASP and tissue regeneration and development, Senescent cells have an essential role in accelerating wound healing. It has been acknowledged that senescent epithelial and fibroblasts are present at the wound site, resulting in acceleration of wound healing by inducing the differentiation of myofibroblasts through the secretion of platelet-derived growth factor AA, a SASP factor [61,62]. SASP and cellular senescence have an important role in refining the development of embryonic structures [29,63], which can be summarised by two points, the first SASP promote the vasculature structure at the early stage of pregnancy also SASP through the recruiting of immune cells that mediate cell removal is necessary of the development of embryonic structure [29,63].

Therefore SASP is a mixed blessing, which can have a beneficial or deleterious effect depending on the cell context [59,64].

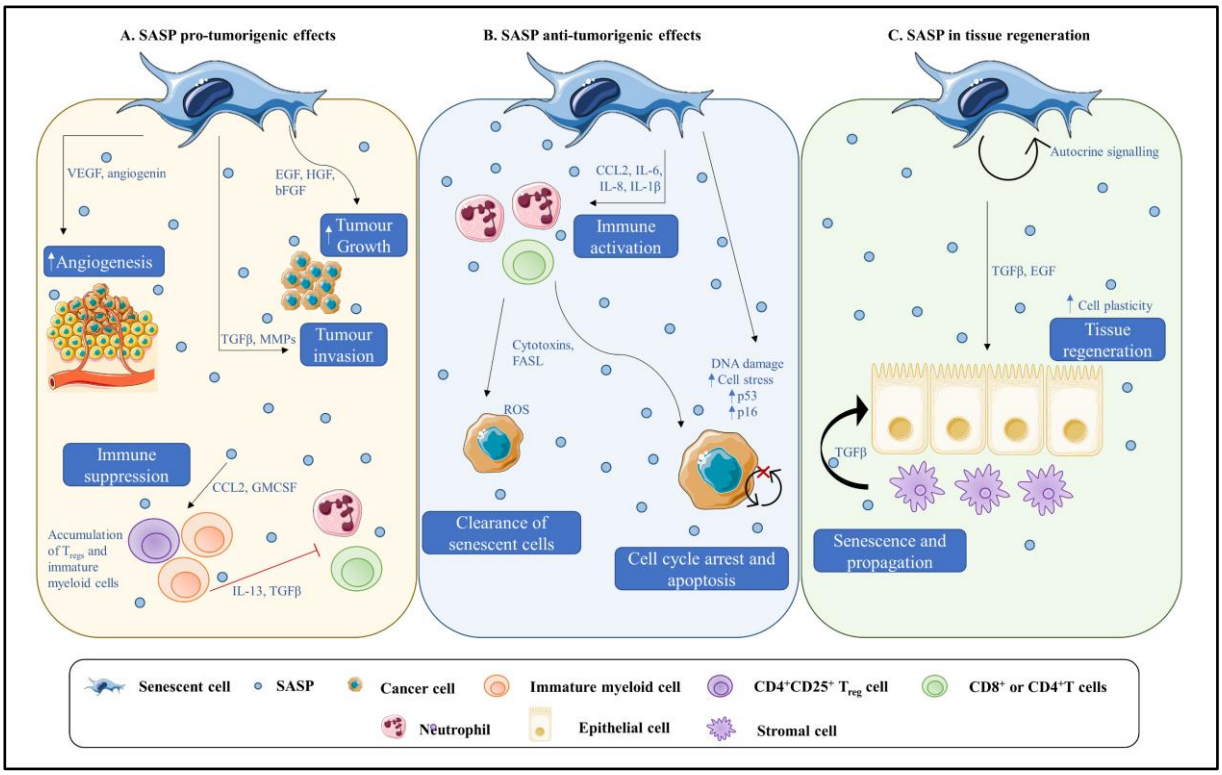

Figure 3: The bright and dark side of SASP. Senescent cells secretome (SASP) contains several factors, from inflammatory cytokines and chemokines to growth factors and proteases. Depending on the cell context and the exposure time to SASP, senescent cell secretome can either have beneficial or deleterious effects. **A) SASP pro-tumour effects:** the persistent exposure to SASP over a long period can lead to harmful effects. For example: long-term exposure to several growth factors such as EGF, basic fibroblast growth factor bFGF, and hepatocyte growth factor HGF leads to tumour progression. Moreover, SASP improves the tumour vasculature by inducing angiogenesis through VEGF and angiogenin, which can also promote tumour metastasis in combination with the effect of extracellular matrix remodelling proteins. In addition, prolonged exposure of immune cells to SASP cytokines result in either immunosuppressive phenotype blocking their differentiation. **B) SASP anti-tumour effects:** proinflammatory factors of the SASP have the capacity to promote immune response by attracting and activating immune cells. For example, activated cytotoxic T cells releases several cytotoxins and pro-apoptotic ligands (such as TNF ligand superfamily member 6 (FASL), perforin, etc.), which mediate senescent cells clearance. Moreover, reactive oxygen species ROS releases by activated macrophages and neutrophils promote cell cycle arrest. **C) SASP in tissue regeneration:** SASP effects on tissue regenerative potential is also time-dependent. In the case of acute tissue injury, SASP growth factors and immune modulators mediate tissue repair and remodelling by improving tissue regenerative capacity. On the contrary, the accumulation of senescent cells in the body due to immune system failure to clear them leads to tissue

dysfunction due to the chronic exposure of surrounded tissue to several SASP factors especially transforming growth factor-β TGFβ, which mediate fibroblast expansion and fibrosis. GMCSF, granulocyte-macrophage colony-stimulating factor; CCL2, C-C motif chemokine 2; p16, p53, cellular tumour antigen p53; cyclin-dependent kinase inhibitor 2A [65].

1.1.4. Upregulated survival pathways in senescent cells.

One of the characteristic features of cellular senescence is its resistance to apoptosis. This partially contributes to the survival and accumulation of senescent cells, which eventually affect the health span [7]. A myriad of molecular pathways are associated with senescent cells resistance to apoptosis; many have already been mentioned within the cell cycle arrest, DDR, and SASP sections. This section discusses the roles of these pathways in senescent cell survival to intrinsic and extrinsic apoptotic signals, and furthermore, the importance of these pro-survival in forming a platform for developing therapeutic agents that target senescent cells.

Intrinsic apoptotic pathway. BCL-2 protein family consist of pro-apoptotic proteins and anti-apoptotic proteins that orchestrate the mitochondria-mediated intrinsic pathway of apoptosis. Pro-apoptotic proteins consist of (PUMA, BIM, tBid, etc.) [66] that facilitate the permeabilisation of mitochondria through the activation of Bax and Bak, resulting in the release of cytochrome C. The latter, with the apoptosis protease factor 1 Apaf1, forms apoptosome, a complex protein structure that is important for activating the caspase signalling, which is responsible for the cleavage of several vital substrates in the cell. On the other hand, anti-apoptotic proteins (BCL-2, BCL-XL, BCL-W and MCL-1) prevent cell death by binding to the BH3 domain of pro-apoptotic proteins sequestering them from binding to Bax and Bak and consequently prevent the release of cytochrome C from mitochondria, reviewed in [7,66]. Thus, activating the apoptosis cascade relay majorly on the balance between the pro-apoptotic and anti-apoptotic proteins in the cell [66]. Several studies indicated the upregulation of anti-apoptotic proteins in senescent cells and associated that with their resistance to apoptosis [67,68]. Others reported an increase of pro-apoptotic proteins such as PUMA and BIM and in some types of senescent cells and related their survival to restriction of cell death program [69]. In general, disrupting the balance of the BCL-2 protein family or targeting the mentioned pathways presents an attractive strategy to eliminate senescent cells. Several studies reported promising pharmaceutical agents based on targeting intrinsic apoptotic signals described in detail later with the Senolytics section.

Extrinsic apoptotic signals. Cellular apoptosis mediated by extrinsic signals is based on activating death receptors expressed on the outer membrane of target cells, this process is actually quite complicated. To simplify it: death receptors are transmembrane proteins with intracellular domain (death domain) that, upon activation, can import the death signal to

intracellular signalling pathways. Death receptors consist of Tumour necrosis factor receptors TNFR, upon activation with ligand binding, can trimerise and, through their intracellular death domain, recruit adaptor proteins such as Fas-associated death domain (FADD). As a result, FADD engages pro-caspase 8 and forms a Death-inducing signalling complex (DISC). The latter generates by self-cleavage mature caspase 8 molecules that activate caspase 3 and, therefore, intracellular apoptotic pathways. On a side note, the negative regulator c-Flip, an upstream of caspase 8, oppose the extrinsic apoptotic signals by racing with pro-caspase 8 in binding to FADD and therefore forbidding DISC formation. In senescent cells, c-Flip has been reported to be downregulated through the activation of DDR and NF-κB. Moreover, the overexpression of decoy receptors (DcRs) in senescent cells, similar to death receptors but lack the intracellular death domain, provides an extra example of how these cells oppose extrinsic apoptotic signals. Actually, those receptors were proposed as a marker for senescent cells, reviewed in [7].

p21 important role in DDR and cell cycle arrest has already been described. A recent study linked senescent cells survival to p21, as knocking down p21 in those cells resulted in the accumulation of DNA lesions, which in turn activates ATM and NF-κB. Consequently, NF-κB induces TNF-α secretion, which leads to JNK activation, which in the end mediate senescent cell death in caspase and JNK-dependent manner [70]; this was effective in DNA damage-induced senescence but not in the case of oncogene-induced senescence. Moreover, in vivo studies on knocking p21 in mice showed efficient elimination of liver senescent stellate cells and, at the same time, improved the production of liver fibrosis and collagen [70]. Thus, targeting p21 seems to be an exciting strategy to target senescent cells and alleviate the senescent cells accumulation burden. Compatibly, in another interesting study, they showed p21 to have two opposing roles as oncosuppressive and oncopromoting, calling p21 a 'two-faced genome guardian'. p21 role is defined mainly by the cell type, p53 status, and the type and level of genotoxic stress. For example, in case of p53 deficiency and p21 consistent expression, sub-group of cells can escape the senescence state providing a more aggressive phenotype of cancer that is chemotherapy-drug resistant with increased genome instability [23].

SASP components and SASP monitoring pathways. We explained before the components of SASP and their roles in detail. However, this section will explain how some of the SASP factors can promote senescent cells survival. For instance, SASP includes several growth factors such as IGF-1, PDGF and VEGF; these factors stimulate tissue repair and regeneration of neighbouring cells. Their effect might be deleterious in case of cancer cells presence in the

surrounding tissue or the persistent activation of adjacent cells due to senescent cells accumulation, reviewed in [7]. These factors can also mediate senescent cell survival as follows: IGF-1 acute signalling through its receptor IGFR (a tyrosine kinase receptor TRK) promotes cell growth and proliferation through upregulation of PI3K/AKT pathway; however, prolonged signalling results in premature senescence [71]. Also, IGF-1 is upregulated in a p53-dependent manner as a response to chemotherapy, cell ionisation, and genome instability, providing survival of those cells in a p53-AKT-DDR manner [72]. Another proof of IGF-1 role in senescence survival is that its inhibition leads to apoptosis in senescent fibroblasts, but it delays senescence in proliferating cells [72], reviewed in [7]. Another type of TRK is the ephrin dependent receptors; **dependent receptors** are a specific type of receptors that, upon binding to its ligand, activate cellular pathways that promote cell survival, and on the contrary, facilitate caspase-dependent apoptotic pathways in case of ligand absence, reviewed in [73]. Ephrin dependent signalling has been reported to be upregulated in senescent cells and provide an attractive target for therapeutic approaches in eliminating senescent cells [68].

Another example of how some SASP components facilitate senescent cell survival: NF-κB essential role in SASP production and regulation has already been described. NF-κB can be activated by the autocrine of several inflammatory SASP factors such as IL-1, IL-6, IL-8 and TNF-α. This activation can promote senescent cell survival by initiating the transcription of anti-apoptotic BCL-2 family proteins [reviewed in [7]].

Another important regulator of SASP, mTOR signalling, is essential for establishing the senescence phenotype. As inhibiting mTOR by rapamycin drug, suppress the production of inflammatory cytokines from senescent cells [46] while prevent/delay senescence in treated cells [47,74].

UPR and autophagy. Cellular senescence is an adaptive response to stress/ different stress signals. It is characterised by an expanded endoplasmic reticulum ER to match the increased need to produce the various components of the SASP, which is usually accompanied by ER stress and proteomic toxicity due to the accumulation of misfolded and unfolded proteins in the cell [75]. In order to solve this, unfolded protein response UPR and autophagy are usually activated in senescent cells to restore the proteomic homeostatic of the cell [75]. UPR is an intracellular defence mechanism that induces several transcription and translation factors that regulates the ER-associated protein degradation system and autophagy machinery, reviewed in [7]. These two mechanisms have been linked lately in several studies to cellular senescence

establishment and maintenance. Interestingly, UPR has been found to attribute to several cellular senescence hallmarks, namely, cell cycle arrest, DNA repair capacity, morphological changes, metabolic changes, and the secretory pathway, reviewed in [76]. Treating cells with ER stress inducing drug; thapsigargin, resulted in premature senescence. Mild ER stress is necessary for senescent cells to cope with the extra need for protein synthesis specially for SASP factors production. However, persistent and unresolved ER stress promote cell death, reviewed in [75].

Moreover, senescent cells tend to accumulate damaged/ oxidised lipids, proteins, and nucleic acids due to oxidative stress and the increased levels of ROS (reactive oxygen species) [77]; this results in extra ER stress and activation of autophagy as a survival mechanism [78]. Autophagy plays a double-edged sword in senescence since it is necessary for the degradation and elimination of irreversibly oxidised biomolecules in the cell, relieving excessive oxidative stress from activating cell death, reviewed in [7]. On the other hand, high levels of dysregulated autophagy can result in crucial cellular organelle destruction leading to cell death, the case of keratinocytes senescent cells [79]. Therefore, it is necessary to achieve a balanced level of autophagy in senescent cells. This can be accomplished by upregulation of key regulators of autophagy such as BCL-2 and homolog proteins. We already explained the role of BCL-2 anti-apoptotic proteins in activating intrinsic apoptosis pathways. However, BCL-2 can regulate autophagy by interacting and inhibiting the evolutionarily conserved autophagy protein, Beclin1, from forming the autophagosome, keeping the autophagy at a level suitable for cell survival [80]. Another critical regulator of autophagy is the mTOR pathway. mTOR regulates several important metabolic programs in the cell, including protein biosynthesis, autophagy, and glucose/ lipid homoeostasis [81]. Its activity is governed by the nutritional status of the cell, growth factors and stress signals, reviewed in [81]. In the case of freely available nutrients, mTOR through its complexes block autophagy and promote protein synthesis as follows: mTOR complex 1 (mTORC1) block autophagy by inhibiting ULK 1/2 (unc-51-like autophagy activating kinase 1/2) and stimulate protein synthesis through activation of S6 kinase (S6K). On the contrary, nutrient starvation leads to mTOR complexes inactivation and degradation of several cytosolic components by autophagy machinery to overcome the nutrient shortage, reviewed in [81,82]. In conclusion, mTOR is essential for SASP production and autophagy regulation, promoting senescent cell survival.

In summary, UPR and autophagy signalling pathways are essential for senescent cell survival. In the case that the UPR pathway is not sufficient to resolve the ER stress, autophagy machinery

is activated. Also, UPR activates the transcription of several components of the autophagy signalling pathway. However, the exact mechanism in how UPR activation promotes autophagy induction, which would lead to cellular senescence establishment or maintenance, is not yet discovered, reviewed in [75]. Thus, both signalling pathways provide a promising platform for targeting senescent cells therapeutically.

Metabolic reprogramming. Even though senescent cells do not proliferate, they maintain high metabolic activity. This is to cope with the high demand for nutrients and energy accompanied with their highly active secretory phenotype. We already mentioned how autophagy and UPR signalling pathways play an important role in that. Moreover, most senescent cells tend to attain a more glycolytic state and produce more ATP by boosting oxidative phosphorylation in mitochondria in order to enhance the energy production required for several cellular mechanisms.

Higher mitochondrial biogenesis and mitochondrial dysfunction have been considered one of the senescence's hallmarks [83]. Mitochondrial dysfunction provides a high amount of mitochondrial ROS in senescent cells, which results in oxidative stress that is important for establishing and maintaining cellular senescence through a positive DDR-dependent feedback loop, [84] reviewed in [85]. This process occurs as follows: high ROS levels induce DNA damage in the cell, which in turn lead to the activation of DDR cascade, activation of ATM results in phosphorylation of AKT, which in turn activates mTORC1 complex formation, therefore promoting several mitochondrial protein syntheses through phosphorylation of S6K kinase and upregulation of transcription coactivator PGC-1β; a regulator of mitochondrial biogenesis [84,86]. Additionally, the anticancer drug Tamoxifen, which targets the mitochondria, killed cancer cells without inducing senescence *in vitro* or *in vivo* [87]. It also effectively eliminated senescent cells accumulated in ageing organs and also premature senescent cells [87]. Paradoxically, depletion of mitochondria did not result in cell death but led to the loss of several features of cellular senescence while ATP production was retrieved by increased glycolysis [84].

Besides the importance of the high metabolic activity to provide energy and nutrients for several essential cellular activities in senescent cells, the availability of nutrients is vital for cell survival as several studies pointed out how caloric restriction results in life extension and better healthspan due to delay in cellular senescence [88,89]. A very enlightening example was mentioned in the review article [7]: high glucose uptake leads to insulin production, similar to

IGF-1, has an affinity to the IGF-1R and is able to initiate a downstream signal by binding to the receptor. Active IGF-1R enlists phosphatidylinositol-3 kinase PI3K to the cell membrane, which in turn phosphorylates phosphatidylinositol-biphosphate PIP2 to phosphatidylinositol-triphosphate PIP3. The high amount of PIP3 at the cell membrane results in PDK1 recruitment, and the latter activates Akt by phosphorylation. Consequently, Akt activates the mTORC1 complex, which pro-survival mechanism has been already explained. Additionally, the other mTOR complex mTORC2 can be activated directly by IGF-1R through PI3K dependent mechanism. mTORC2 phosphorylates Akt resulting in an increase of its kinase activity by 10-fold and therefore plays an essential role in cell survival as Akt inhibits the activity of pro-apoptotic protein Bad, plus it inhibits the transcriptional activity of pro-apoptotic FOXO factors family (1/3), preventing apoptosis. On the other hand, the anti-apoptotic FOXO4 was found to be upregulated in senescent cells serving their survival [90] [reviewed in [7]], Figure (4).

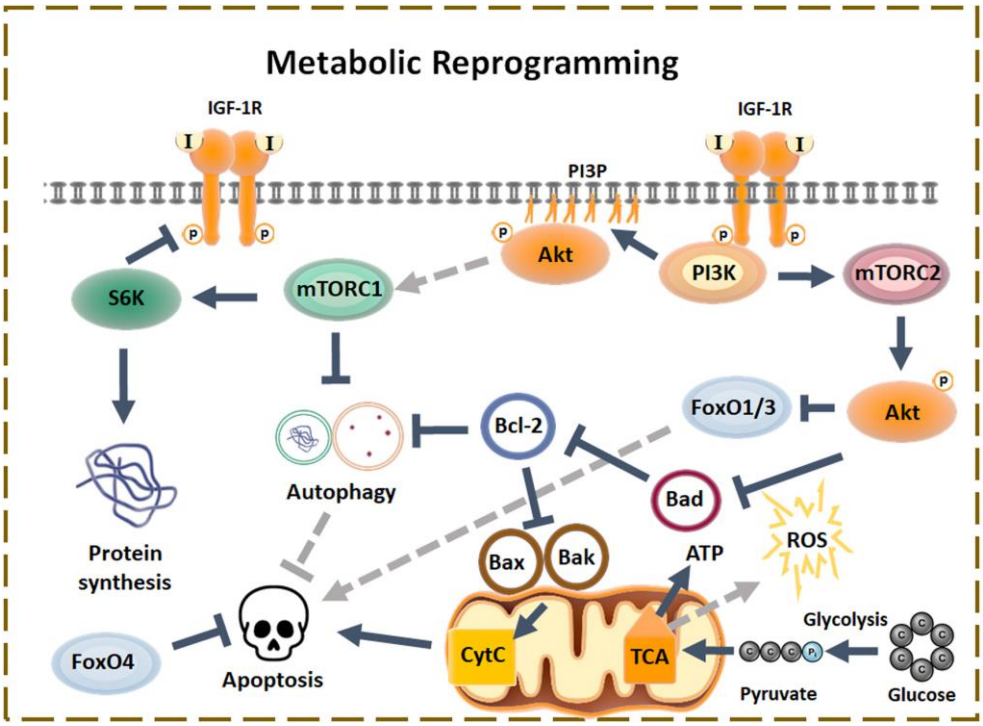

Figure 4: 'Metabolic reprogramming of senescent cells. IGF-1R signalling activates PI3K leading to membrane PIP3 enrichment serving as an anchor for 3-phosphatidylinositol-dependent kinase 1 (PDK1) and Akt activation at position T308. Among its multiple functions, Akt indirectly enables the formation of mTORC1. mTORC1 positively regulates protein translation through S6K, which exerts negative feedback inhibition at the level of IGF-1R. PI3K also activates mTORC2, which further activates Akt, increasing its kinase activity. Fully activated Akt can then efficiently inhibit pro-apoptotic Bad. Akt may also inhibit pro-apoptotic FoxO transcription factors FoxO1/3, thereby preventing apoptosis. In contrast, antiapoptotic FoxO4 present in senescent cells also supports senescent cell viability. [7]

Immune-mediated clearance. The signalling pathways implemented in how senescent cells escape immune-mediated clearance is quite complicated. We already mentioned how SASP factors play an important role in regulating the immune system and evade clearance of senescent cells. We will only focus on the upregulation of 'do not eat me' signal on senescent cells, as I

will explain the rest within the section of targeting senescent cells therapeutically later. CD47 receptor expression is found to be upregulated on the surface of senescent cells as one of 'do not eat me' signals, as it inhibits immune clearance by binding to the inhibitory receptor signal regulatory protein alpha (SIRPα) on macrophages, reviewed in [91].

1.2. Cellular senescence in Cancer, suppressive or promoting mechanism?

Cellular senescence has been considered, for a long time, as a protection mechanism against cancer and any stress that threatens the cells' genomic stability. This is true but in a time-dependent manner. As when senescent cells accumulate overage, and the immune system fails to eliminate them, senescent cells affect the neighbouring cells and promote tumour progression and cell migration. In addition, several studies have pointed out the possibility of senescent cells to escape their state, emerging as a potent form of cancer, which will be the focus of this section.

Escape from Therapy-Induced Senescence: Senescence induced-therapy represents the small portion of cells that survived the exposure to chemotherapy and radiotherapy, turning to a state of prolonged cell cycle arrest or 'tumour dormancy' where these cells maintain the ability to re-enter the cell cycle as a more invasive and aggressive type of tumour cells which lead to relapse after months or years from treatment [11], **Figure 5**. Actually, the accumulation of senescent cells associated with chemotherapy has been linked to poor outcome in cancer patients [92].

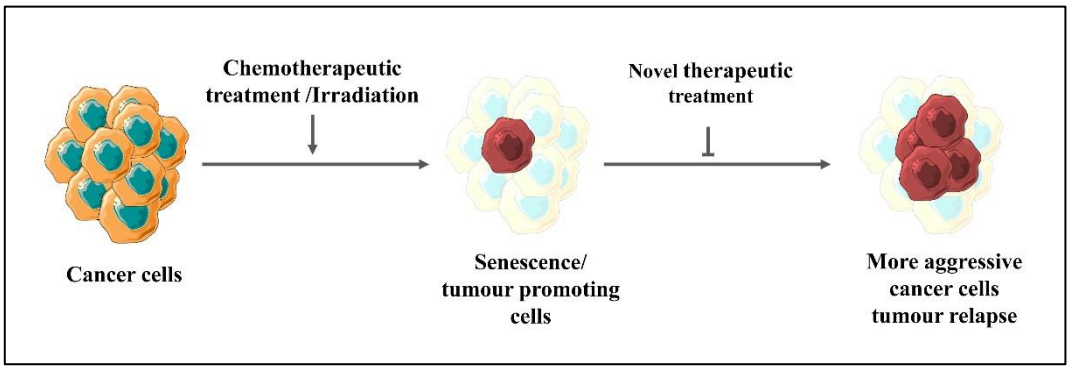

Figure 5: Escape from Therapy-Induced Senescence. Apoptosis is not the only fate for cancer cells treated with chemotherapy or radiation as some cells undergo cell cycle arrest and eventually cellular senescence. Several studies have pointed out the adverse effects of cellular senescence as they provide over time a survival niche through their secretome (SASP), which promote pro-tumorigenic effects in the surrounding cells [59]. Moreover, it is suggested that those treatments activate an incomplete cellular senescence in cancer cells, providing them later with the ability of emergence and re-enter cell cycle as a more potent form of cancer that is highly drug-resistant [93,94]. Therefore, it is essential to find therapeutic strategies that eliminate those cells and prevent possible tumour relapse or other malignancies related to senescent cells accumulation [95].

Among the early studies that described this 'biological phenomena'; Elmore and his colleagues worked on (p53 wt, $p16^{INK4a}$ null) MCF7 breast cancer cells, where they found that a small

portion of senescent cells induced by treatment with doxorubicin (Adriamycin) have the ability to escape cell cycle arrest. They described it as a way for cancer cells to resist chemotherapeutic treatment [96]. In a similar study, senescent cells from H1299 lung cancer cells (also deficient of $p16^{INK4a}$ and p53 null) after treatment with camptothecin also have the capacity to evade senescence and resume proliferation [97]. In both cases, they linked the ability of senescent cells induced by treatment to escape growth arrest to the overexpression of cyclin-dependent kinase cdc2. Moreover, using cdc2 inhibitors or knocking down the expression of cdc2 by small interfering RNA hindered the senescence escape [97]. Additionally, in the same study, they found that the frequency of senescent cells to escape is 1 to $10^{6,}$ which indicate that this biological phenomenon is quite rare.

As it has been known for ages, 'change is hard,' especially in the case of scientific beliefs; it takes a lot of research and time for a new scientific discovery to take place. Therefore, researchers were hesitant about the senescence escape since it has been well known to be an irreversible growth arrest and a tumour suppressive mechanism, and conservative researchers used the terminology 'senescence-like', 'pseudo senescence' [11] or 'accelerated senescence'[97] to describe these cells. Moreover, it was hard to prove that the emergent cells were originated from senescent cells treated with chemotherapy or that the tumour relapse could be related to SASP and not to emergent cells. Saleh and his colleagues gave the ultimate proof by isolating senescent cells induced by chemotherapy from different cancer cells, using single-cell flow cytometry-based sorting, based on their size and senescence-associated β-galactosidase (SA-β-gal) activity. These cells were able to recover proliferating capacity and form tumours when implanted *in vivo* in mouse models [98].

Senescence emerged cells from cancer therapy are associated with many features, such as polyploidy, stemness, and aggressiveness [11]. **Polyploidy** in senescent cells has been linked to the ability of those cells to resume cell division [99,100]. In addition, Wu and his colleagues found out that almost 40% of the polyploid senescent cells were able to take the EdU dye after several days of senescence induction, indicating that these cells maintained the ability of DNA replication [100]. Additionally, Wu and his colleagues reported in their studies that the overexpression of Cdc2/Cdk1 kinase and their downstream effector survivin are strongly correlated with survival and senescence escape as well the formation of polyploid in senescent cells during cancer therapy [100,101]. Interestingly, Rajaraman and colleagues suggested neosis as the mechanism of self-renewal in tumour cells and the possible mechanism of

senescence escape [102,103]. According to them, neosis is a novel form of cell division where cells are generated from senescing polyploid mother cell by budding [102,103].

Stemness and aggressiveness: Important signalling factors in senescence, such as p53/p21 and p16/Rb, also regulates stem-cell function (also known as stemness) [104]. Milanovic and his colleagues in the Schmitt group studied the link in signalling pathways between senescence and stemness. They came up with SAS 'senescence-associated stemness' as a new feature in senescent cells initiated from chemotherapy. In their study, a single treatment with Adriamycin on Eμ-Myc-Bcl2-overexpressing lymphoma resulted in senescent cells with elevated expression of stem cell-related genes. These cells have the ability to escape cell cycle arrest and form cells with cancer stem cells properties, i.e., tumour initiating cells. The latter cells have a more aggressive nature as they form colonies in vitro and more malignant tumours after implanting them in mouse models (immunosuppressant models) [10] [reviewed in [11,105]].

Interestingly, in another study, cells escaped from oncogene-induced senescence OIS after a long period of cell cycle arrest due to epigenetic changes. This senescence escape was facilitated by the derepression of *hTERT* gene expression, an enzyme that provides cellular mortality. Furthermore, cells that escaped senescence displayed high oncogene expression levels and retained functional DNA damage responses, making them targetable for DNA damage agents [106].

Senescence induced therapy is a type of Tumour dormancy? There is a scientific debate on whether to consider senescent cells initiated from cancer therapy as a tumour dormant cell or not. Saleh *et al.* review article [11] stated the similarities between senescence and tumour dormancy in comparison to quiescence. It argued that these cells would go through morphological and genetic changes plus the escaped cells are more aggressive than the cells they originated from.

In summary, therapy-induced senescence is potentially reversible through the inactivation of p53, p16(INK4A) and/or Rb, over-expression of Cdc2/cdk1 and survivin, the development of polyploidy, the survival of cancer stem cells and restoration of the nuclear landscape. This shed light on the importance of finding new cancer therapies and possible treatments that target senescent cells. Cellular senescence relation to cancer is a two-edged sword.

1.2.1. Our lab findings regarding Senescence associated with chemotherapy.

The main interest of our lab is to understand the cellular signalling pathway in senescent cells and its relation to cancer as a suppressive or promoting mechanism. We focused mainly on cellular senescence escape after chemotherapy treatment and how it can promote cancer recurrence and relapse. In our research on colorectal cells treated with irinotecan (a first-line treatment used in colorectal cancer that induced senescence), we noticed a subpopulation that was able to escape the cellular senescence state and emerge as a more aggressive cancer cells, as these cells were able to form tumour after injecting them in mice. They can also grow in low adhesion conditions. Their survival is dependent on MCL-1 signalling and, to a lesser extent, BCL-XL [107]. Inhibition of MCL-1 blocked emergence and improved treatment results with irinotecan [107]. In continuation with the previous study, we found that Akt is activated in senescent cells within the first 24 h after treatment with irinotecan. Akt pro-survival signalling pathways are well understood. Upon inhibiting Akt in treated colorectal cancer cells with irinotecan, it resulted in treatment enhancement and prevented cellular senescence emergence both *in vitro and in vivo.* This was linked to the downregulation of $p21^{waf1}$ and inhibition of MCL-1 by Noxa upregulation. We also established that the p53-p21 signalling pathway in senescent cells promote cell emergence as its downregulation resulted in treatment improvement due to apoptosis induction [108]. In addition, we were also interested in TSP-1/ CD47 signalling pathway important role in cellular senescence and emergence in both colorectal and breast cancer cells, which will be explained in detail in the following section.

1.2.1.1.The role of the TSP1- CD47 pathway in senescence escape.

TSP1 is a homotrimeric glycoprotein. Each TSP1 subunit comprises of N- and C-terminal globular domains and a thin connecting strand, **Figure** 6. TSP1 has several diverse functions depending on the interactions between its structural domains and multiple cell surface molecules. TSP1 acts as an angiogenesis inhibitor by stimulating endothelial cell apoptosis, inhibiting endothelial cell migration and proliferation, and regulating vascular endothelial growth factor bioavailability and activity. In addition to angiogenesis modulation, TSP1 also affects tumour cell adhesion, invasion, migration, proliferation, apoptosis and tumour immunity [109,110].

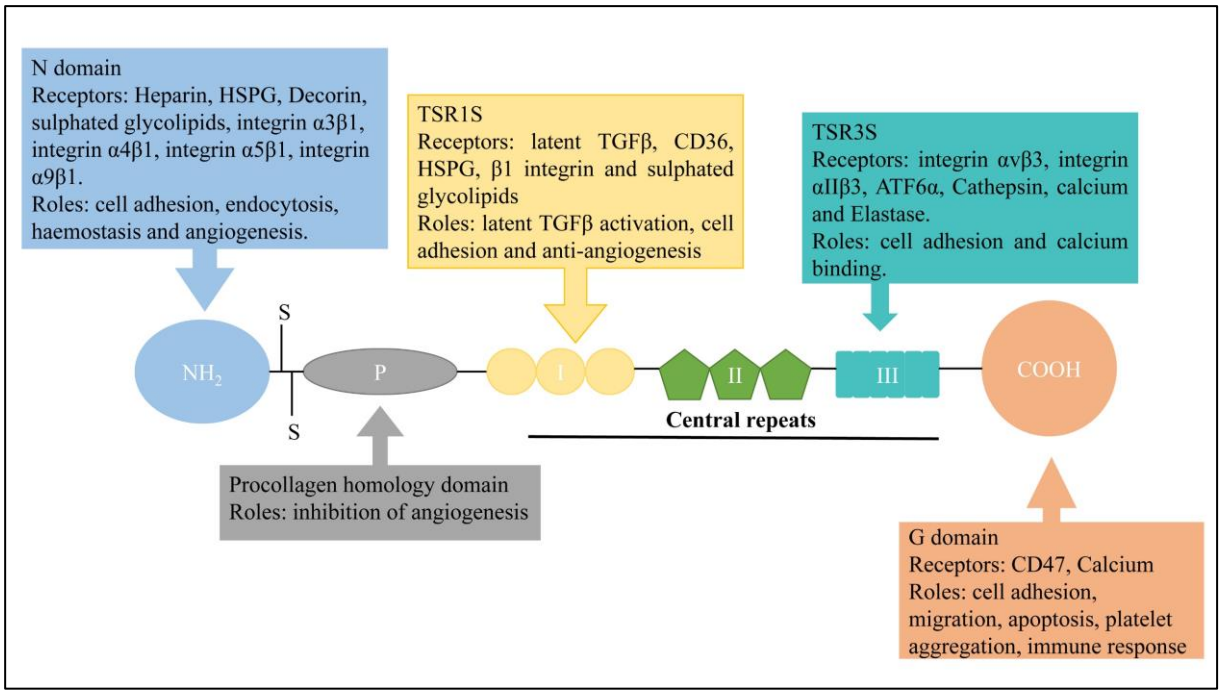

Figure 6: Thrombospondin 1 structural domains and their functions: TSP1 monomer consist of N and G domain connected with a thin strand. Each domain's receptors and ligands and the activities resulted from their interaction are listed above [109,111].

The G domain, also called the cell-binding domain (CBD), is the domain that binds to the CD47 receptor [112]. CD47 is a signalling receptor for the secreted matricellular protein thrombospondin-1 and the counterreceptor for signal-regulatory protein-α (SIRPα), which on phagocytic cells recognises CD47 engagement as a marker of self [113]. Several studies indicate two opposing roles for CD47 in cell survival. Mice lacking CD47 or TSP1 are resistant to tissue stress associated with ischemia, ischemia/reperfusion, and high dose irradiation. The survival advantage of ischemic CD47- and thrombospondin-1-null tissues is mediated in part by increased nitric oxide/cGMP signalling [114]. Radio resistance associated with CD47 blockade is cell-autonomous and independent of NO signalling, indicating that additional pro-survival signalling pathways are controlled by CD47 [115].

Engaging CD47 in some cell types triggers programmed cell death [116]. BCL2/adenovirus E1B 19 kDa protein-interacting protein 3 (BNIP3) is a pro-apoptotic BH3 domain protein that interacts with the cytoplasmic tail of CD47 and is implicated in CD47-dependent cell death. Furthermore, CD47 ligation alters localisation of the dynamin-related protein Drp1, which controls mitochondria-dependent death pathways [115], and some tissues in CD47-null and thrombospondin-1-null mice show increased mitochondrial numbers and function. Actually, mitochondrial-dependent cell death pathways involving Bcl-2 are limited by the autophagy regulator beclin-1, and it was found recently that CD47 signalling limits the induction of beclin-

1 and other autophagy-related proteins in irradiated cells. Therefore, blocking CD47 increases the protective autophagy response, which explains the radioprotective effect of CD47 blockade.

In contrast, elevated expression of CD47 confers to an indirect survival advantage in vivo. As when CD47 link to SIRPα on macrophages, it prevents phagocytic clearance [113], which explains the elevated expression of CD47 on several types of cancer cells and stem cells [117].

Therefore, our lab was interested in studying the TSP1-CD47 pathway and its effect on senescence escape. In a previous study using SWATH quantitative proteomic analysis, we found that TSP1 can be detected in the serum of patients suffering from triple-negative breast cancer and that its low expression was associated with treatment failure [118]. Moreover, in another study on breast and colorectal cancer cells, we found that TSP1 blocked senescence escape in LS174T cells after treatment with Sn38; however, this was not the case among using antibody B6H12 that blocks the CD47-TSP1 binding, this proves that TSP1 is necessary for preventing senescence escape. Also, in the same study, we found that the emergent cells have low CD47 expression and was explained by the lesser expression of p21waf1 in these cells compared to the arrested one. The low expression of p21waf1 is correlated with the upregulation of Myc, which in turn repress CD47 expression generating $CD47^{low}$ population [119], promoting their survival. As a reminder to evade confusion, we already explained how p21 has two opposing roles: oncosuppressive and oncopromoting, depending on its interaction with p53.

In conclusion, TSP1/CD47 signalling pathway represents a promising way for targeting senescent cells.

2. Senescent cells to clear or not to clear?

As discussed extensively in this introduction, cellular senescence is a physiological phenomenon that can be beneficial (tumour suppression, wound healing and embryogenesis) or deleterious (tumour progression and age-related diseases) depending on the onset nature and the accumulation of these cells with time. This led to the invention of two types of therapies, pro-senescence and anti-senescence therapies. Anti-senescence therapies grabbed the attention of several researchers investigating different strategies to target senescent cells, such as eliminating senescent cells, opposing the SASP effects and enhancing the efficiency of the immune system in eliminating senescent cells. Researchers debate that the outcome of these therapies is far more beneficial than the possible side effects. However, it is important to find therapies that solely target/ eliminate senescent cells, and this can be achieved by grasping the

molecular pathways that govern cellular senescence and find possible molecules that work on senescent cells only. Also, there is the possibility to combine these therapies with other technologies like drug delivery, for instance, using nanomedicine to achieve better results and reduce the side effects. All of this will be discussed in detail in the next point.

3. Therapeutic approaches regarding/targeting senescent cells.

There is a growing interest in targeting cellular senescence therapeutically in order to prevent age-related diseases accompanied by senescent cells accumulation and improve the health quality with age and possibly increase the life span. Indeed, this is still a growing research where there is still much to comprehend. The first to report the beneficial outcome from preventing senescent cells accumulation were Krishnamurthy and his colleagues [120] in 2004 where they found that slowing the accumulation of senescent cells in specific models of mice (Calorically restricted mice and Ames dwarf mice with pituitary hormone deficiencies) due to reduction in *Ink4a/Arf* expression, increased their healthspan and lifespan [reviewed in [121]]. Since then (2004/2005), much effort has been invested in finding new pharmaceutical drugs that eliminate and target senescent cells. These drugs are based on the biological pathways that are unique to senescent cells and therefore were divided into three categories: 1) **senolytics** that eliminate senescent cells, 2) **immune modulators** that enhance the immune system efficiency in targeting and eliminating senescent cells, 3) and lastly **SASP modulators or senostatic** that prevent the inflammation effect of SASP components. The discovery history of these therapeutic molecules with their therapeutic potential and the possible side effects will be discussed extensively in the upcoming points.

3.1. Senolytics/ Senolytic drugs

Several approaches were studied to eliminate senescent cells; the early ones suggested the concept of preventing the formation of cellular senescence by inhibiting/ inactivation the cellular pathways that lead to senescence; however, this could be disastrous as the inactivation of some of these pathways can promote cancer formation which is the case of inhibition of $p16^{INK4a}$, Rb and p53 [122,123] [reviewed in [64]]. Others worked on finding therapeutic methods for eliminating already formed senescent cells that would reduce the burden these cells cause by accumulation upon time, leading to cancer and other age-related diseases. Baker and his colleagues used $BubR1^{H/H}$ mice with a significantly shortened life span and several age-related diseases as an in vivo model for their study where they introduced these mice with a novel transgene INK-ATTAC, these mice different tissue contain a high amount of senescent

cells with high $p16^{INK4a}$ expression. Upon treating these mice with AP20187, it killed only senescent cells while normal ones were not affected, and that is due to the activation of 'suicide' protein ATTAC, which was only expressed in senescent cells expressing $p16^{INK4a}$ [124]. Treated mice showed a better healthspan.

Dr. Kirkland lab followed another therapeutic approach led by the 'hypothesis-derived discovery paradigm'[121] by answering the following question: **how senescent cells can resist apoptotic signals although living in a harsh proapoptotic surroundings caused by SASP?** [121] And by mapping and comparing normal and senescent cells pathways, they found that their survival is due to the upregulation of pro-survival pathways, and they hypothesised that by finding small molecules that can block/ interfere with these pathways, they can eliminate senescent cells. Therefore they came up with the 'senolytics' [68] idiom in 2015 to describe these therapeutic molecules. In their study, they used small interference RNA '**Senolytic siRNA'** in order to check which pro-survival pathways that upon interfering would kill senescent cells; among the 39 transcripts to knockdown, 17 were able to affect the viability of senescent cells and 6 out of those were induced senescent cell death [68]. Pro-survival pathways in senescent cells that have been identified as suitable targets for senolytics are: BCL-2 protein family, the p53/p21 axis, PI3K/AKT, receptor tyrosine kinases, and the HIF-1α and HSP90 proteins [68,125].

BCL-2 protein family are well studied at the molecular level. They consist of pro-apoptotic proteins and anti-apoptotic proteins. When the balance shift between these proteins, it can lead to survival or apoptosis. Anti-apoptotic proteins (BCL-2, BCL-XL, BCL-W) have been reported to be upregulated in several types of cancer and the reason behind chemotherapy resistance for some types of cancer [126]. Moreover, other studies also proved that anti-apoptotic proteins are also upregulated in senescent cells leading to their survival and resistance to apoptotic signals. Therefore, they represent an attractive target as blocking or silencing those proteins will initiate programmed cell death in senescent cells. Since BCL-2 proteins are well studied in cancer, there are already several pharmaceutical candidates that some of them have reached clinical studies. The most famous one is ABT-737, a small molecule that has BH3 mimetic domain with a high affinity to the anti-apoptotic proteins BCL-2, BCL-XL and BCL-W, inhibiting them from binding to pro-apoptotic proteins that have BH3 domain resulting in initiating apoptotic signal [127,128]. Yosef and his colleagues stated in their studies on mice models that ABT-737 efficiently eliminates two types of senescent cells; DNA damage-induced senescent cells in lungs due to irradiation and senescent cells accumulated in the epidermis by

p53 activation through transgenic $p14^{ARF}$ [129]. They also indicated that the treatment increased hair-follicle stem cell proliferation resulting in regrowth of hair. Important to note that in their *in vitro* studies, ABT-737 eliminates senescent cells in an efficient way comparable to siRNAs that silence both BCL-XL and BCL-W [129]. Navitoclax or ABT-263 is another well-studied inhibitor for the antiapoptotic proteins (specifically BCL-2 and BCL-XL); it is an analogue of ABT-737 and can be taken orally [130]. Similar to ABT-737, navitoclax effectively induced apoptosis in senescent bone marrow hematopoietic stem cells and senescent muscle stem cells accumulated in irradiated mice and naturally aged mice [131]. This resulted in the rejuvenation of those aged stem cells tissue leading to an increase in healthspan. In another study, several other types of senescent cells were effectively depleted by ABT-263, particularly human umbilical vein epithelial cells, IMR90 human lung fibroblasts, and murine embryonic fibroblasts but it was not the case for human primary preadipocytes [132]. Childs and his colleagues found that atherosclerosis lesion are rich with senescent foamy macrophages, and upon treating atherosclerosis prone mice with ABT-263 for 9 days, it reduced the onset of the diseases [133]. Although the mentioned BCL-2 inhibitors showed promising results in several types of senescent cell models *in vitro* and *in vivo*, they are not universal senolytics as they do not work on all types of senescent cells. Moreover, clinical studies reported that these two drugs have several side effects and some toxicity, including neutropenia and thrombocytopenia related to their effect on neutrophil and platelet viability [134,135]. Consequently, those clinical studies were impeded from going further, and there was a persistent need to find other specific inhibitors of BCL-2 anti-apoptotic proteins that can be better pharmaceutical candidates. A1331852 and A1155463 were developed as specific inhibitors for BCL-XL, they showed senolytic activity in human umbilical vein endothelial cells, IMR90 cells, but not preadipocytes, and it is expected to be less toxic [136]. In another study, genetically modified mice as a model of biliary liver fibrosis were treated with A1331852, which resulted in an 80% reduction of senescent cholangiocytes and therefore reduced liver fibrosis and liver injury [137]. In spite of that, platelets viability is dependent on BCL-XL, so these inhibitors are expected to cause thrombocytopenia, too [125]. Also, they most probably are less effective in eliminating senescent cells, whose survival is more dependent on BCL-2 and BCL-W [125,129]. It is also worth mentioning another inhibitor of the BCL-2 family, ABT-199, an orally available specific inhibitor of BCL-2, therefore not inducing thrombocytopenia [138]. ABT-199 is effective in cancer models dependent on BCL-2. However, it was not the case for the senescent cells as alone was not successfully efficient in eliminating senescent cells. Better results were achieved only upon combining ABT-199 with other inhibitors of BCL-XL or BCL-W [67]. Altogether,

these antiapoptotic inhibitors showed promising results as senolytics; however, their toxicity hinders the clinical trials from going any further. There are several other attempts to overcome the toxicity; one of them is to administrate those inhibitors locally to their site of action instead of systemically, which would reduce their side effects. An example, intra-articular injection of UBX0101, a BCL-2 inhibitor, resulted in eliminating senescent cells and consequently impaired the development of osteoarthritis, reducing pain and improving cartilage development in the aged mice model [139]. Also, drug delivery approaches might be handful in reducing the side effects of these inhibitors.

p53/p21 axis is essential in cell cycle arrest, senescence, and apoptosis. We explained before its role in cellular senescence, whether in DDR or SASP. Although it was proposed as an attractive target for senolytic candidates, there are only two molecules up to now (FOXO4 peptide and USP7 inhibitors) that interfere and target the p53/p21 axis and possess senolytic activity [69,140]. A modified FOXO4 peptide interferes in the interaction between p53 and FOXO4, leading to p53 release from the nucleus, which results in initiating cell-intrinsic apoptosis in senescent cells [69]. Additionally, in *in vivo* studies, FOXO4 peptide neutralised doxorubicin-induced chemotoxicity under conditions where the treatment was well tolerated. Furthermore, treatment with FOXO4 peptide extended the health span of fast aged and naturally aged mice as it restored their fitness, fur density, and renal function [69]. A recent study proposed USP7 as a novel target for senolytic drugs, as inhibition of USP7 result in ubiquitination of MDM2 and its degradation by the ubiquitin-proteasome system. Sequentially, p53 level increase inducing pro-apoptotic proteins (PUMA, NOXA, and FAS) and selectively killing senescent cells [140], **Figure 7**. Both USP7 inhibitors, P5091 and P22077, promoted apoptosis in senescent cells while there was no significant effect on the viability of non-senescent cells. Furthermore, *in vivo* studies on mice treated with doxorubicin to induce cellular senescence were later treated with P5091, resulting in vast elimination of senescent cells and also downregulation of several SASP components. All that while no significant effect on the body weight of the treated mice, white and red blood cells, platelets and haemoglobin [140]. As it is clear, both senolytics mentioned do not work directly on p53/p21, and actually, up until now, there are no specific senolytics that target directly p53/p21 axis. Therefore, there is much space to improve and develop novel senolytics that impact that pathway.

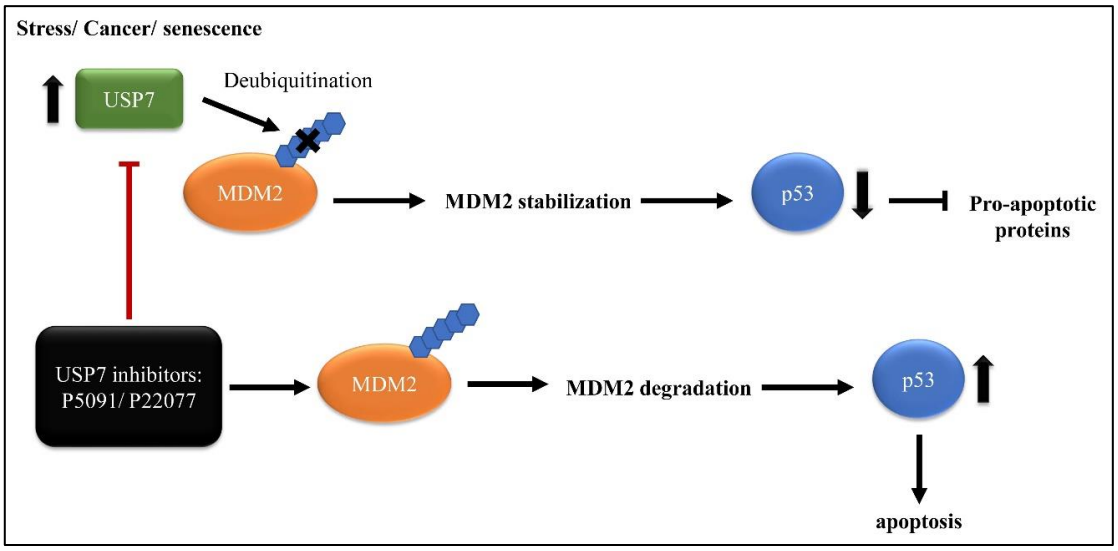

Figure 7: USP7, MDM2 and p53 axis and the role of USP7 in regulating p53 activity. In cancer cells, senescent cells or in case of genomic stress, USP7 leads to deubiquitination of MDM2, preventing its degradation by the ubiquitination proteosome system, which in return results in p53 degradation [141]. Therefore, inhibiting USP7 by small molecules such as P5091 or knocking it down using siRNA improve p53 activity and stability, which induce pro-apoptotic proteins expression such as PUMA and NOXA, and prevents the interaction between anti-apoptotic BCL- family proteins which result in the end in apoptosis program induction in those cells [140].

HSP90 is a chaperone protein, which is essential for the stabilisation and degradation of other proteins [142]. Recent studies proposed HSP90 as a novel target for developing senolytics [143], the senolytic activity will be associated with disruption of the **PI3K/AKT** pathway as follows: as we mentioned before, PI3K/AKT is one of the upregulated pathways in senescent cells that serves senescent cell survival and resistance to apoptosis. AKT kinase activity is essential to suppress apoptosis by impacting mTOR, NF-κB, FOXO3A, and other signalling pathways [7]. HSP90 is important for the stabilisation of AKT factor, and therefore HSP90 inhibitors will lead to destabilisation of AKT and eventually increase apoptosis [143,144]. 17-DMAG, an inhibitor of HSP90, was studied for cancer treatment, and when tested on senescent cells *in vitro* and *in vivo* of progeroid mice, it resulted in vast elimination of senescent cells, delayed the onset of several age-related symptoms, and increased health span of treated mice [143]. Although 17-DMAG has promising results however in this study, they recommended combining HSP90 inhibitors with other types of senolytics that affect other pathways to have even far better results [143].

Senolytic combinations Quercetin and Dasatinib Q+D. Senescent cells depend on several pathways for their survival. Therefore, a combination of senolytic drugs targeting different survival pathways might be more effective at lower doses and, consequently, with fewer possible side effects. The effect of combining quercetin and dasatinib was first published by [68]; dasatinib (D) is a tyrosine kinases inhibitor that is FDA approved for treating Leukaemia, it has been effective in eliminating senescent human preadipocytes, but it was not the case for

senescent human umbilical vein cells HUVECs. On the other hand, quercetin is a flavonoid available naturally that works through targeting BCL-2 family members, HIF-1α, PI3K, and p21-related anti-apoptotic pathways [145] and has been more effective in eliminating senescent human umbilical vein cells HUVECs. Combining Q+D selectively killed both types of senescent cells while it did not affect the proliferating capacity of non-senescent cells [68]. *In vivo* results of treating geriatric mice and other models of ageing (radiation-exposed and progeroid *Ercc1*$^{-/\Delta}$) with and Q+D revealed a decrease of the senescent cells burden in these models; moreover, it improved the cardiac function and exercise capacity in those models. Also, treating progeroid *Ercc1*$^{-/\Delta}$ mice with several doses resulted in delaying several ageing symptoms such as osteoporosis leading to extended health span [68]. Q+D combination had several promising results *in vitro* and *in vivo;* it is now being tested in several clinical studies for ageing diseases that will be mentioned later.

Another reported combination of senolytic drugs was dasatinib and A1331852 [145]. However, up to date, this combination was tested for anticancer effect only and not yet for a possible senolytic activity. Therefore, it would be interesting to study this combination in eliminating senescent cells with higher efficacy.

Natural compounds with senolytic activity. Other than quercetin, **fisetin** is a naturally available flavonoid that has been studied for its senolytic activity since it is similar in its composition to quercetin. Fisetin as a flavonoid is a potent antioxidant [146] and has been reported to have several other biological activities, for instance, antihyperglycemic, anti-inflammatory, and anti-carcinogenic effects [136,147]. Similar to quercetin, fisetin was effective in eliminating HUVECs senescent cells but not senescent human preadipocytes [136]; its senolytic activity is linked to its interaction with several cellular pathways such as PI3K/Akt/mTOR, PARP1 and NF-κB [reviewed in [148]]. **Piperlongumine** is another natural compound with senolytic activity. It has first been studied for its anticancer effects since it induces apoptosis in cancer cells by promoting ROS formation [reviewed in [148]]. However, another study revealed that its apoptotic activity is more related to its interaction with the NF-κB pathway [149]. Whether its senolytic activity is dependent on ROS formation or interfering with NF-κB is not yet fully understood [reviewed in [148]].

Metabolic targeting, we explained extensively in section **1.1.4** the unique metabolically activity of senescent cells and how they depend on UPR and autophagy for survival and maintaining homeostasis. Therefore, these cellular pathways represent an exciting approach for

targeting and eliminating senescent cells. For example, inhibition of glucose transporters by phloretin or cytochalasin B, or inhibition glycolysis by 2-deoxy-D-glucose 2DG, resulted in reduced viability of therapy-induced senescence TIS lymphomas [150]. Similar results were also obtained upon suppressing fatty acid oxidation by etomoxir or ATP depletion by antimycin, leading to TIS selective toxicity [150]. Moreover, targeting autophagy by using lysosomal V-ATPases selective inhibitors, particularly bafilomycin A1 or concanamycin A, eliminated TIS cells efficiently, which was comparable to the results obtained with knocking down p62/SQSTM1 (a protein that monitors the autophagy process) [150].

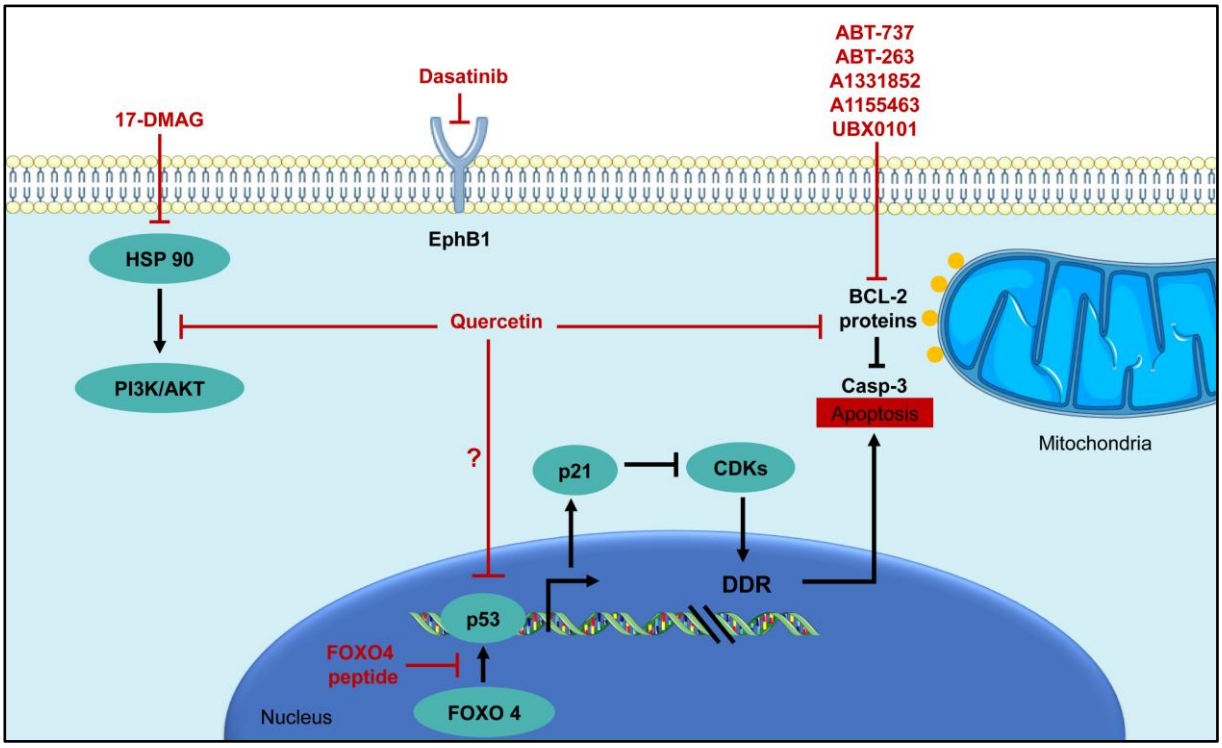

Figure 8: An example of survival pathways in senescent cells and possible senolytics that target them.

3.2. Immune modulators and immune-mediated interventions.

Senescent cells supposed to be cleared naturally by the immune system, which is called immune surveillance. We already explained (in section) how the secretory phenotype plays an important role in that, as the secreted cytokines and chemokines attract the immune cells. However, when senescent cells accumulate and become persistent, they can affect the immune system through the SASP as well and evade the clearance by the immune system. Moreover, with ageing, the immune system efficiency decline in clearing and eliminating senescent, stressed, or tumour cells, which is known by the immune senescence. So, this section is dedicated to therapeutic molecules that enhance the immune system efficiency in clearing senescent cells instead of targeting senescent cells directly.

NKG2D ligands (MICA & ULBP2). Before diving into therapeutic approaches of immune modulators, we will explain first some critical aspects in immune surveillance regarding senescence. Senescent cells upregulate specific ligands (MICA and ULBP2 proteins) on their surface, which are recognised by the NKG2D receptor on Natural Killer (NK) cells. This interaction facilitates the elimination of senescent cells by NK-mediated cytotoxicity through granule exocytosis and not through death receptors as they are suppressed by the expression of decoy receptors on senescent cells [151,152]. These ligands are upregulated on the cellular surface of senescent cells induced by several stimuli such as (replicative senescence, oncogene-induced senescence, and DNA damage-induced senescence). The upregulation of NKG2D ligands is initiated by the DDR and maintained by the ERK signalling pathway. It is important to note that those ligands are not present in normal and quiescent cells [151]. Additionally, NKG2D receptors expression on NK cells does not change with age, but the efficiency decreases. Therefore, one therapeutic approach was to boost the immune system by using immune stimulator polyinosinic-polycytidylic acid (polyI:C) that induce interferon-ɣ and improve NK efficiency in eliminating senescent fibrotic cells in the liver, and reducing liver fibrosis in treated mice [153]. However, using such a potent immune stimulator in the aged immune system might add an extra burden since it is chronically activated [125].

Senescent cells can also activate an adaptive immune system for elimination. For instance, senescent hepatocytes induced in the liver by hepatic expression of $Nras^{G12V}$ undergo immune-mediated clearance by CD4+ T cells with the help of monocytes/ macrophages as well [154].

Chimeric antigen receptor T-cells CAR-T cells. The knowledge gained in immune therapies adopted in treating cancer can be applied as well for senescent cells. For example, the approach of engineering immune cells that target specific ligands on cancer [155] cells might also be effective in the case of senescent cells. In a recently published study, chimeric antigen T-cells CAR-T cells were engineered to target plasminogen activator receptor (uPAR), a cell-surface protein that is upregulated during senescence. These cells were called ‘Senolytic CAR-T Cells’ as they were capable of eliminating senescent cells *in vitro* and *in vivo* [156]. These cells were able to alleviate some senescence-associated pathologies in treated mice; for example, mice with lung adenocarcinoma treated with a senescence-inducing combination of drugs, treatment with uPAR-specific CAR-T cells eliminated senescent cells in lungs and extended survival of treated mice. It also reduced liver fibrosis in treated mice as well [156]. In addition, a review article about cellular senescence immunotherapy [157] suggested engineering NKG2D specific CAR-T cells as a promising possible treatment.

Antibody approach. Another mechanism that boosts the immune system is by selectively blocking immune checkpoints, such as programmed death PD-1 on T-cells. These checkpoints are responsible for regulating the immune system and maintaining its haemostasis [158]. PD-1 has an inhibitory effect on T-cells, and its ligand PD-L1 has been reported to be upregulated in tumour and senescent cells as well; therefore, blocking PD-1 with a selective antibody has been effective in cancer immunotherapy. It also reduced pathologies and improved memory in mice models of Alzheimer's disease [159]. These effects are mediated by induction of interferon (IFN)-ɣ–dependent systemic immune response, leading to monocytes-derived macrophages recruitment [159]. In addition, downregulation or inhibiting of PD-L1 on the surface of senescent cells would prevent their inhibition to the immune system and improve immune system surveillance [reviewed in [157]].

Similarly, other upregulated ligands on senescent cells can be targeted using specific antibodies to facilitate immune-mediated clearance. For instance, dipeptidyl peptidase 4 DPP4 was found to be selectively expressed on the surface of senescent fibroblast but not proliferating human diploid fibroblasts. This is beneficial for senescent cells elimination by NK-cells through an antibody-dependent cell-mediated cytotoxicity (ADCC) assay [160]. In a recent study, an oxidized form of membrane-bound vimentin (MDA-vimentin) has been identified as a novel biomarker for senescent fibroblasts [161], which provides a promising target for senescence immune therapy.

Although the antibody approach was not that promising in cancer treatment as it is necessary to eliminate all malignant cells. However, this is not necessarily the case in cellular senescence [64], as a decrease in 30% of senescent cells in the body were able to alleviate age-related pathologies and extended health span in progeroid and normal chronologically aged mice [reviewed in [162]].

Decoy death receptors as a possible therapeutic target. In the extrinsic apoptotic pathways section, we already mentioned how senescent cells express decoy death receptors as a mechanism to oppose apoptosis. These receptors compete with death receptors in binding to their ligands, inhibiting downstream signalling pathways initiated by the death receptors (DR4/5). Therefore, it presents an attractive target immune therapy [reviewed in [125]].

Vaccines against senescent cells & virotherapy. In a very recent study, vaccination against specific surface markers that appears on senescent T cells has been reported as a novel mechanism to eliminate those accumulated cells from fat tissue in an obese model of mice.

Senescent T cells accumulated in fat tissue with age produce proinflammatory cytokines, resulting in metabolic disorders and cardiovascular diseases. Obese mice model treated with CD153 vaccine showed improved glucose tolerance and insulin resistance [163]. Virotherapy is another therapeutic approach that has been well studied in cancer, and some candidates even reached clinical study; therefore, such application can be adapted for cellular senescence as well. For instance, oncolytic measles vaccine viruses have been used to eliminate therapy-induced senescence TIS [164].

Immune senescence. Immune cells are also subject to senescence, known by the immune senescence, and it is responsible for the immune system impairment and senescent cells accumulation in the body. Therefore, one of the approaches to eliminating senescent cells is targeting immune senescence and retrieving its efficiency. One of those approaches is using senolytics drugs already mentioned against the senescent immune cells. Others suggested reversing the senescence state in immune cells by rejuvenating them [reviewed in [157]]. For example, blocking p38 MAPK signalling in CD8+ T senescent cells results in reversing the senescent state, and the cells resume proliferating with an increase in telomerase activity, mitochondrial biogenesis, and fitness [165]. Another study reported that novel small molecules based on resveratrol could alter mRNA splicing, which leads to reversal of cellular senescence in human primary fibroblasts [166]; such mechanism might be applicable to the senescent immune system as well [reviewed in [157]]. Another mechanism to restore the immune system efficiency was by using specific antibodies linked to magnetic beads or nanoparticles that will identify senescent immune cells and facilitate filtering them from the blood by specific devices [167,168].

Collectively, the mentioned immunotherapies seem promising; however, it is still juvenile research regarding cellular senescence, and there is much space for improvement and a lot to comprehend.

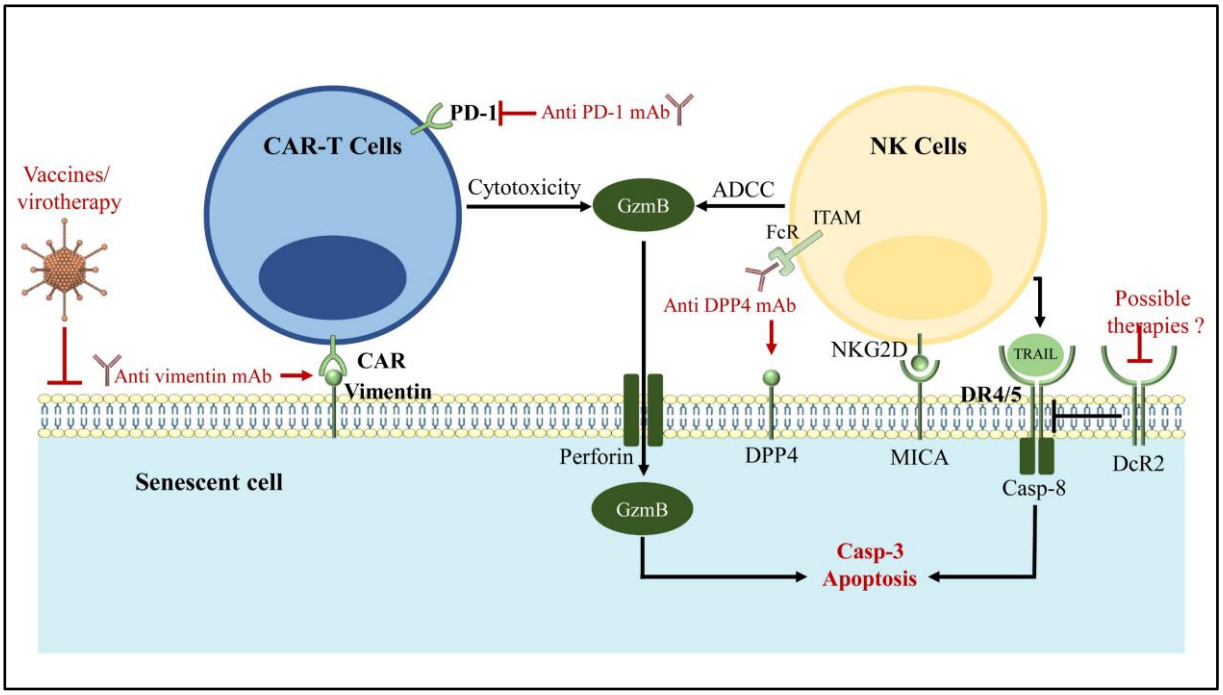

Figure 9: Some of the several approaches of immunotherapies targeted against cellular senescence.

3.3. SASP modulators / senostatics (small molecules that prevent developing the SASP or ameliorate its effect)

Senostatics or senomorphics represent drugs that suppress senescence by either blocking the development and secretion of SASP detrimental components or damping its effect. This provides an alternative therapeutic approach where eliminating senescent cells might be more harmful than beneficial, such as in the case of wound healing and tissue regeneration. Section 1.1.3 contains all necessary information about the beneficial and deleterious roles of the SASP and all the pathways that govern its development. In summary, SASP regulators, mTOR pathway, p38 MAPK signalling pathway, PI3K pathway, and GATA4/p62-mediated autophagy activate the transcription factors NF-κB and C/EBPβ at several levels and therefore control the induction of the SASP. Luckily, those pathways have been studied and understood well, and there are already several drug candidates that the FDA already approves. In a recently published review article [169], they divided therapeutic strategies targeting SASP into NF-κB dependent and NF-κB independent, which we will follow as well.

NF-κB dependent therapeutic strategies. Anti-inflammatory drugs such as glucocorticoids were suggested as a possible therapeutic approach to modulate the SASP inflammatory effect. Persistent inflammation is one of the main deleterious effects of the SASP that occurs due to the accumulation of senescent cells and has been tightly linked to many senescence-induced pathologies. Glucocorticoids are steroid hormones with potent anti-inflammatory effects and

have been FDA approved for treating several pathologies such as autoimmune diseases and asthma [170]. Regarding the SASP, glucocorticoids were found to have the ability to suppress the SASP by downregulation of the transcriptional activity of NF-κB [171], leading to reduced secretion of several SASP components [172]. The only problem is that to sustain this effect; glucocorticoids need to be taken on a long term, which is accompanied by severe side effects.

Metformin is another FDA approved drug that has been studied for its possibility to dampen the SASP. Metformin is mainly used to treat diabetes; however, in a post-trial follow up on diabetic patients who received metformin treatment, these patients had a risk reduction for microvascular diseases and myocardial infarction [173]. Moreover, cancer and mortality reduction has also been linked to metformin treatment in diabetic patients [174]. It was recently found that Metformin inhibits the transcriptional activity of NF-κB by blocking its translocation to the nucleus [175], which the previously mentioned therapeutic effect might be linked to. Since NF-κB is the master regulator of inflammatory gene expression, Moiseeva *et al.* took the initiative and proved that Metformin reduced the inflammatory phenotype of the SASP by inhibiting the production of several proinflammatory cytokines in senescent cells [176]. Interestingly, in the same study, they found that metformin treatment did not reduce the expression of anticancer cytokines such as interferon, suggesting that it only modulates the SASP inflammatory phenotype without affecting its possible anticancer effect [176]. Another study addressed Metformin as a senostatic drug reprogramming the SASP profile by inhibiting the mTOR/stat3 pathway [177]. Other studies have pointed out that combining metformin with chemotherapies resulted in prolonging tumour recurrence in mouse cancer models [178,179]. All these studies set the base for metformin clinical studies regarding its possible effect on improving health and life span in humans (NCT02432287), reviewed in [169].

IκB is a master regulator of NF-κB transcriptional activity[1]. Several natural compounds, for instance, resveratrol [180] and flavonoids (kaempferol, apigenin and wogonin), were found to attenuate the SASP, which can be attributed to their interaction with IκB kinases [181].

As we repeatedly explained before, mTOR has an important role in establishing the cellular senescence and its secretory phenotype through its interaction with several essential pathways in senescent cells, such as DDR and autophagy. Regarding SASP, mTOR regulates the expression of IL-1α, which through its receptor establish a positive feedback loop that empowers the NF-kB transcriptional activity [182]. Consequently, mTOR inhibitors, in

[1] I already explained the role of IκB in SASP section.

particular rapamycin and its analogues (rapalogs), abolish the SASP by downregulation of the IL-1 α expression, interrupting the IL-1 α positive feedback loop [182]. Moreover, rapamycin blocks MAPKAPK2/MK2 translation, which results in the degradation of several SASP components[2] [47].

Another important SASP transcriptional regulator is the p38 MAPK kinase. Downregulation or inhibition of this kinase or one of its downstream effectors significantly impacts SASP production [44]. SB203580, UR-13756 and BIRB 796 are some examples of p38 inhibitors that have been studied and showed promising results in suppressing SASP expression [45]. Actually, BIRB 769 has already reached phase III in clinical trials [45]. MK2 inhibitor PF-3644022 (MK2 is a downstream effector of p38 MAPK) has also been proven to be able to suppress the SASP [45].

NF-κB independent therapeutic strategies/ (JAK/STAT) pathway inhibitors. C/EBPβ is another critical transcription factor that is activated in senescent cells and facilitates the expression of several SASP inflammation cytokines such as IL-6 and IL-8. Through their feedback loop, those cytokines maintain the activation of the transcription factors to maintain SASP production. JAK/STAT (Janus kinase/signal transducer and activator of transcription) pathway is an important part of this mechanism, as it mediates the activation of C/EBPβ when IL-6 binds to its receptor [183], Fig (10). JAK/STAT pathway has been found to be highly activated in senescent cells [184], and its activation is not bound to IL-6 only, but other factors such as vascular endothelial growth factor (VEGF), type I/II interferons and MCP-1 were found to be activators of this pathway [169]. Therefore, inhibiting this pathway was suggested as a possible method to modulate the SASP. Several JAK inhibitors have been already tested for cancer and age-related diseases treatment. Promising results were found in both cases; for example, in age-related diseases, inhibiting the JAK/STAT pathway resulted in enhanced muscle stem cell function, muscle regeneration, improved physical function and metabolic capacity, and also reduced inflammation [185], reviewed in [169,184]. While in cancer, it improved chemotherapy treatment [186]. Some of those inhibitors are already FDA approved, in particular Ruxolitinib (JAK 1/2 inhibitor) and Tofacitinib (JAK 1/3 inhibitor), while others reached clinical studies, for instance, NVP-BSK805 a selective JAK2 inhibitor [187,188].

[2] The mechanism in which mTOR regulates MK2/MAPKAPK2 translation and its role in SASP regulation is already explained in SASP section in page 4.

Epigenetic regulators inhibitors. Senescent cells remodel their chromatin landscape in order to activate some genes while repressing others to set their senescence program [125,189]. Epigenetic regulators are the main mediators of this remodelling, the ones that are responsible for SASP expression are: mixed-lineage leukaemia protein 1 (MLL1), bromodomain-containing protein 4 (BRD4), and high-mobility group box 2 (HMGB2) [189–192]. Therefore, another treatment approach to modulate the SASP is by inhibiting specific epigenetic regulators, resulting in a permanent effect that can be preferred more than the already mentioned treatment since they needed to be taken periodically and results in several side effects. Moreover, inhibiting those epigenetic regulators 'chromatin modifiers'[125] diminishes the senescent cells' inflammatory effect without affecting their cell cycle arrest [125,190]. All of the mentioned information is based on knocking down those epigenetic regulators using shRNA; however, small molecules such as JQ1 have been identified as a selective inhibitor for BET bromodomains (BRD4) and has been used for cancer treatment [193], but it can as well be a great candidate for SASP modulation [125].

Targeting specific components of the SASP. Instead of targeting molecular mechanisms responsible for SASP production, targeting SASP components as an alternative treatment method has been suggested in the review articles [125,169]. This method is based on using neutralizing antibodies against specific SASP components such as matrix-remodelling proteases, VEGF, or inflammatory cytokines like IL-6 and IL-8. Such antibodies are already commercially available, for instance, siltuximab, an IL-6 antibody [194], tocilizumab for inhibiting IL-6 receptor [195], and Bevacizumab monoclonal antibody developed against VEGF [196]. However, the effects of these antibodies were not investigated in senescence or SASP yet and represent interesting possible research.

One drawback of targeting the SASP production or dampen its deleterious effect is that senescent cells are not cleared, and therefore the senostatics, senomorphics should be taken on a more regular basis to maintain their effect, which might be accompanied by possible side effects [162].

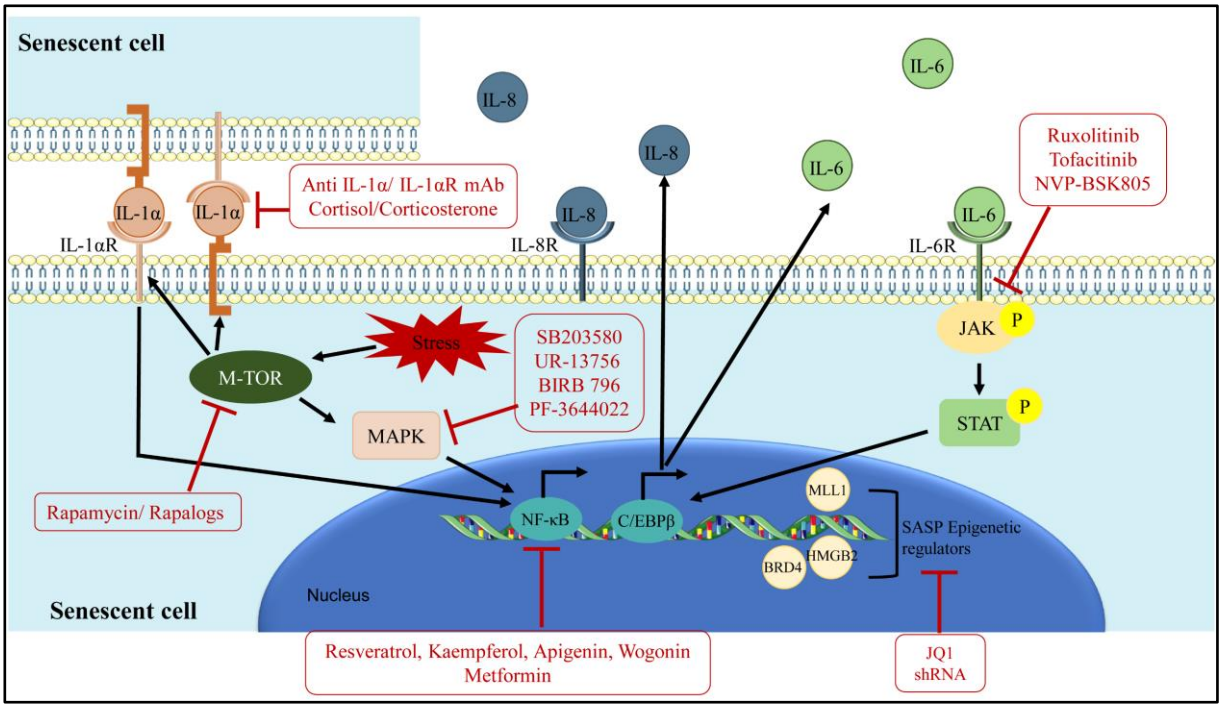

Figure 10: Possible therapeutic interventions for modulating the SASP.

3.4. Bypass/ reverse of cellular senescence.

Bypass senescence or reactivating the proliferation programme in senescence is a therapeutic method that was suggested for tissue repair and regenerative medicine. Replicative senescence in aged tissue can affect stem cells resulting in impaired or declined in their renewal capacity. This would lead to a decrease in the regenerative capacity in those tissues, which in the end results in loss of organ function. Cellular senescence is described by the irreversible cell cycle arrest; however, reactivation of the proliferation programme in senescent cells is possible in vitro using different techniques as follows [reviewed in [169,197]]: imposing the telomerase activity and reversing the telomere abrasion lead to a bypass of senescence [198]. Also, CBX8 (chromodomain-containing protein 8) ectopic overexpression leads to bypass of senescence as this protein regulates the expression of several genes that are important for proliferation and cell growth, an example: CBX8 limits the expression of INK4A-ARF locus by direct interaction [199]. In oncogene-induced senescence, IL-6 and IL-8 play an essential role in maintaining the growth arrest; therefore, inhibiting chemokine receptor CXCR2 that recognize IL-8 is one method to bypass senescence [200]. The same applies to IL-6 or its receptor IL-6R; inhibiting one of them can lead to a bypass of senescence [30]. In addition, due to the positive feedback loop between C/EBPβ and IL-6 & IL-8, inhibiting C/EBPβ could be another possible way to bypass senescence [30]. Interestingly, in vivo reactivation of the proliferation programme in aged tissue was achieved by Abad *et al.* by induction of Oct4, Sox2, Klf4 and c-Myc

transcription factors in mice, resulting in pluripotent generation stem cells *in situ*, opening new therapeutic opportunities in regenerative medicine [201]. Several genes and transcription factors have been identified as regulators for the bypass of senescence, particularly p16INK4a, p21Cip1/Waf1, p53, pRB, and PPP1CA. However, those genes and transcription factors were found to be modified in tumour cells [201]. This brings us to the next point that bypass of senescence should be pursued with caution as it can lead to the spreading of cancer cells and tumours, which has been already reported [201]. Moreover, bypassing growth arrest in cells with severely damaged DNA or oncogene-induced can result in their transition to a more aggressive form of cancer cells [169].

Lastly, it is important to note that senescent cells rely on multiple regulation levels to achieve apoptosis resistance. The traditional idea of one-drug/one-target/one-disease [121] might not be optimal in the case of pursuing treatments for senescence. Therefore, combining senolytic drugs that have different targets might be more effective and can also reduce side effects by the possibility of reducing the dose. It is even more interesting to combine senolytic drugs with SASP modulators and Immune modulators and, therefore, might achieve much better results.

3.5. Nanomedicine and drug delivery approaches.

The Nanomedicine and drug delivery systems approach has been researched extensively for treating numerous diseases. It improves the efficacy of drugs/ therapeutic molecules loaded or attached to those systems and decreases the possible side effects. However, only **nine** [202–210] research papers have investigated using nanomedicine to treat or diagnose cellular senescence up until now /this introduction has been written. The advantages of nanomedicine and combining it with therapeutic approaches for senescence will be extensively explained in the following points.

4. Nanomedicine.

So, what is nanomedicine? It is the result of the fusion between the nanotechnology field with biomedical and pharmaceutical sciences [211,212]. The term "nanomedicine" refers to all therapeutic and diagnostic products intended for innovated healthcare [212,213]. Moreover, nanomedicine represents drug delivery systems in nanometre size range (typically from 1 to 100 nm as defined by the UPAC) that possess novel characteristics in order to provide medical and pharmaceutical benefits [213,214].

There are presently more than 50 nanomedicine products in the market, and even more than 400 nanomedicine formulations are being tested in clinical trials [215–219]. Most of the nanoformulation approved for clinical use are intended for cancer treatment, iron deficiency anaemia, vaccines and imaging [216,219]. The latest additions were Patisiran /Onpattro, and COVID-19 vaccines developed by Modena and Pfizer-BioNTech [215,219]. Onpattro was approved in 2018 for the treatment of the rare disease, transthyretin amyloidosis [220]. Onpattro was the first lipid-based nanoparticles encapsulating nucleic acid (siRNA) [215,220]. Both Modena and Pfizer-BioNTech COVID-19 vaccines are lipid-based nanoformulation encapsulating mRNA [219]. In addition, both were granted an Emergency Use Authorization by the FDA in 2020 due to the urgent need for a prophylactic approach against COVID-19 disease [219,221–224]. All of this reflects the potential, and the extent of advances nanotechnology has reached in drug delivery.

Developing drugs at the nanoscale provides numerous advantages. For instance, working on the nanoscale permits the possibility of modifying the essential properties of drug carriers, such as release rate, solubility, diffusivity, biodistribution, and reduction of the dose of medication needed to achieve the therapeutic effect and immunogenicity [225]. Moreover, nanoparticles can be formulated in a way that ensures longer circulation half-lives, superior bioavailability, and lower toxicity. An example encapsulating doxorubicin in liposomes reduced significantly its cardiac and peripheral organ toxicity [225,226].

Nanoparticles represent the solution for administration problems that small therapeutic molecules, peptides, and proteins have which compromise their therapeutic efficacy. As most of the small organic molecules manifest low aqueous solubility and more than 40% of all therapeutic molecules failure are due to insufficient drug delivery [227]. On the other hand, therapeutic peptides and proteins can induce an immune response, are subject to enzymatic degradation rendering them with a short half-life, and lastly, they have poor permeability through biological membranes [228].

Nanoparticles can be classified based on their composition into polymer-based, lipid-based, protein-based, inorganic nanoparticles, viral vectors and drug conjugates. Therapeutic molecules can be either loaded in the nanosystems or attached to the surface as a conjugate [227].

Without further ado, we will move to the next section, discussing the impact of nanomedicine on anti-cellular senescence therapies.

4.1. Senescence-directed nanoparticles.

There is tremendous research for therapies targeted toward cellular senescence; however, there are only **nine** research papers until now that combined this knowledge with the nanomedicine approach [202–210]. Therefore, this is still juvenile research where there are many innovative treatment approaches to work on and investigate. Moreover, a lot of nanomedicine research targeted towards treating cancer that is loaded with therapeutic molecules/ drugs that have been found effective in eliminating senescent cells as well [229–231], represents an interesting point to be investigated towards eliminating senescent cells or age-related diseases.

There are two approaches in nanomedicine development towards cellular senescence. The first one is developing nanoparticles loaded with therapeutic molecules targeted to eliminating senescent cells. The other approach is developing nanoparticles loaded with specific probes for tracking senescent cells *in vitro* or *in vivo* (diagnostic nanoparticles), allowing direct monitoring of senescent cells accumulated after chemotherapy treatments, or in aged tissue and senescence-related disorders, Figure 11.

4.1.1. Therapeutic & diagnostic senescence-directed nanoparticles.

The first senescence-directed nanoparticles were developed by Agostini *et al.* in 2012, and their drug delivery system was based on functionalized mesoporous nanoparticles MSN [202]. Those MSN (around 100 nm in size) are coated with galacto-oligosaccharides (GOS) of different length in order to prevent the release of encapsulated rhodamine (a fluorophore) in the silica matrix, Figure 11. The idea behind developing those nanoparticles NPs is based on the high β-galactosidase activity of senescent cells as follows: after the uptake of those nanoparticles via endocytosis and the fusion with lysosomal vehicles, β-galactosidase will dissolve the coated layer facilitating the release of encapsulated rhodamine. Therefore, those NPs will only release their cargo in cells with high lysosomal activity (overexpressing β-gal) such as senescent cells. *In vitro* results of their research showed preferred release of rhodamine in SAβgal-positive human senescent fibroblasts compared to the proliferative control [202].

In another study based on the same concept of targeting senescent cells using their β-gal activity, Muñoz-Espín and his colleagues developed an improved version of those nanoparticles by coating them with a homogeneous layer of 6-mer galacto-oligosaccharide referring to them by GalNP [203]. Those GalNP were uploaded with rhodamine B, doxorubicin or navitoclax. First, they tested the efficacy of those GalNP in *in vitro* model of chemotherapy-induced senescence, where they found a preferred release of the loaded fluorophore in senescent cells

compared to control cells. Next, they developed an ***in vivo* model of chemotherapy-induced senescence** by first generating tumour using subcutaneous xenografts of melanoma cells and lung squamous carcinoma cells, then the mice carrying those xenografts were treated with Palbociclib (a selective CDK4/CDK6 inhibitor used for treating metastatic breast cancer [232]) for 7 days which resulted in intertumoral senescence. Fluorescence was highly detected in Palbociclib treated tumours after 6 h of intravenous injection of GalNP loaded with rhodamine B, while no fluorescence was detected in vital organs such as liver or spleen. The efficiency of GalNP in releasing their cargo in senescent cells was also tested in *in vivo* model of pulmonary fibrosis since it is known to be rich with senescent cells [233]. Similarly, the release of rhodamine from GalNP took place more favourably in fibrotic lungs compared to healthy lungs. Then they tested the possible therapeutic effect of GalNP loaded with senolytic compounds such as doxorubicin and navitoclax in *in vivo* model of chemotherapy-induced senescence. Besides the efficiency of releasing the cytotoxic drugs in senescent cells only, which resulted in tumour regression, encapsulating these cytotoxic drugs in GalNP reduced several serious side effects like cardiotoxicity associated with doxorubicin and thrombocytopenia with navitoclax [203]. Moreover, administrating GalNP loaded with doxorubicin in the pulmonary fibrosis model resulted in a remarkable reduction of collagen amount present, facilitating the recovery of respiratory function. In the end, this new version of GalNP proved to be versatile as their efficiency to deliver their cargo was validated in models of damage-induced and chemotherapy-induced senescence.

In another study, quercetin surface-functionalized magnetic nanoparticles (Fe_3O_4 NP) MNPQ were developed, and their senolytic activity was tested on oxidative-stress induced senescence in human fibroblast *in vitro*. MNPQ proved to have senolytic and senostatic effects as they induced non-apoptotic cell death promoted by increased AMPK activity (senolytic) and also reduced the secretion of several inflammatory cytokines such as IL-8 and IFN-β (senostatic) [204].

Ke *et al*. developed molybdenum disulfide nanoparticles MoS_2 NPs and studied their possible therapeutic effect on oxidative stress-induced cellular senescence as it is the primary cause of the ageing process in endothelial cells [205]. Pretreatment of human aortic endothelial cells with MoS_2 NPs hindered hydrogen peroxide H2O2-induced senescence and improved endothelial cells functionality. This antisenescence effect of MoS_2 NP is the conclusion/ result of autophagy activation and the reduction of cellular mitochondrial ROS levels (antioxidant activity) [205].

Thapa and his colleagues developed their nanosystems based on the idea of utilization of β-galactosidase activity in senescent cells mentioned earlier, Figure 11. However, they wanted to improve this concept by specific targeting of senescent cells [206]. They achieved that by developing porous calcium carbonate nanoparticles (CaCO3 NP) (around 130 nm in size) loaded with rapamycin (mTOR inhibitor), and CD9 monoclonal antibody conjugated to the surface of those NP for specific targeting based on the overexpression of CD9 receptor in senescence, and lastly a layer of lactose-polyethene glycol (Lac-PEG) conjugate which serves several purposes like stabilization of NP in the blood circulation, prevention of opsonization, and targeted release of loaded drug resolved by β-galactosidase activity. β-galactosidase will degrade the lactose layer facilitating the release of the loaded drug. Upon testing those nanosystems on young and old human dermal fibroblast HDF, they proved the concept of senescence specific targeting, besides these NP loaded with rapamycin possessed anti-senescence effect proved by decreased β-galactosidase activity and p53/p21/CD9/cyclin D1 expression, improved cell proliferation and migration, and inhibited cell cycle arrest in old HDF. Moreover, treatment with those NP resulted in remarkable decrease in SASP cytokines, especially IL-6 and IL-1β [206]. Similar results were also found in the chemotherapy-induced senescence model after treatment with those NP.

Another exciting study used the novel technique of molecularly imprinted nanoparticles (nanoMIPs) for detecting senescent cells and for therapeutic purposes also [207], Figure 11. The molecular imprinting technique is based on creating receptor-like binding sites in synthetic polymers [234]. In this study, they developed their nanoMIPs based on the β2 microglobulin B2M as it has been recently detected as an extracellular epitope marker in senescent cells [235] and was also suggested to be used as a tool to detect senescent cells [236]. Using Fluorescent microscopy proved that fluorescein tagged B2M nanoMIPs applied on senescent EJ bladder cancer cells specifically bind to their membrane and are preferentially accumulated in senescent cells. Then they tested the therapeutic potential of B2M-nanoMIPs by loading them with dasatinib on the same cellular senescence model, which resulted in a significant reduction of cellular viability of senescent EJp16 cells compared to proliferating control. Moreover, fluorescein tagged B2M nanoMIPs were able to recognize and accumulate in senescent cells in the *in vivo* model of old mice without showing any evident toxicity, which presents them as possible markers for future clinical studies [207].

In another very recent study, Dihydrolipoic acid-coated gold nanoclusters (DHLA-Au NCs) was developed for the protection against cellular senescence and inflammation induction in

vitro and *in vivo* [209]. Pretreatment with those nanosystems impaired JNK/c-Jun phosphorylation cascade upon treatment with lipopolysaccharide (LPS). LPS induce cellular senescence by the activation of the stress signal JNK [237]. Moreover, they found that DHLA-Au NCs interacts with mitochondria and scavenges the extra mitochondria-derived reactive oxygen species ROS, decreasing oxidative stress and provide anti-senescence effect [209].

In Pham et. al recent study [210], they developed an interesting anti-senescence nanosystems for targeting atherosclerosis as they are enriched with senescent cells. They are based on mesoporous nanoparticles loaded with the anti-senescence drug rosuvastatin and modified with CD9 antibody that were covalently bonded to the surface of those nanoparticles. CD9 antibody were chosen for the specific targeting of senescent cells and atherosclerosis lesions as they overexpress CD9 glycoprotein [238]. These NP were coated with hyaluronic acid which provides a protective coat that prevents drug leakage, in addition atherosclerosis plaques are rich with hyaluronidase enzyme which would allow a specific release in the atherosclerosis lesions. Treatment with those NP led to attenuation of senescent cells and improved the cell viability. Moreover, *in vivo* studies on *ApoE*$^{-/-}$ mice showed that treatment with those NP reduced the progression of atherosclerosis.

Lastly, in a very interesting study by Belcastro *et al.* [208], they developed theragnostic nanocarriers NC (nanoemulsions) decorated with VCAM-1 antibodies (NC-VCAM-1). VCAM-1 proteins are overexpressed on the surface of senescent endothelial cells. They first loaded those nanocarriers with fluorescent lipophilic dye to detect senescent endothelial cells after Ang II treatment. Moreover, encapsulating omega 3 polyunsaturated fatty acid in those nanocarriers improved their anti-senescence efficacy as they prevented p53 upregulation, and SA-β-galactosidase activity in coronary artery segments [208].

In conclusion, nanomedicine provides a novel strategy for targeting senescent cells *in vitro* and *in vivo* for either diagnostic, therapeutic or even theragnostic (diagnostic and therapeutic) purposes. Besides the specific targeting or specific release of cargo in senescent cells, reducing possible side effects and masking the toxicities of loaded drugs is another advantage of nanomedicine. Finally, it is important to note that there are many studies in nanomedicine intended for aged-related diseases such as Alzheimer; however, cellular senescence was not taken into consideration while developing these therapies. In the end, nanomedicine targeting cellular senescence is still juvenile research, and with the vast knowledge gained in molecular

biology in senescence and nanotechnologies, there are endless possibilities for research in this field.

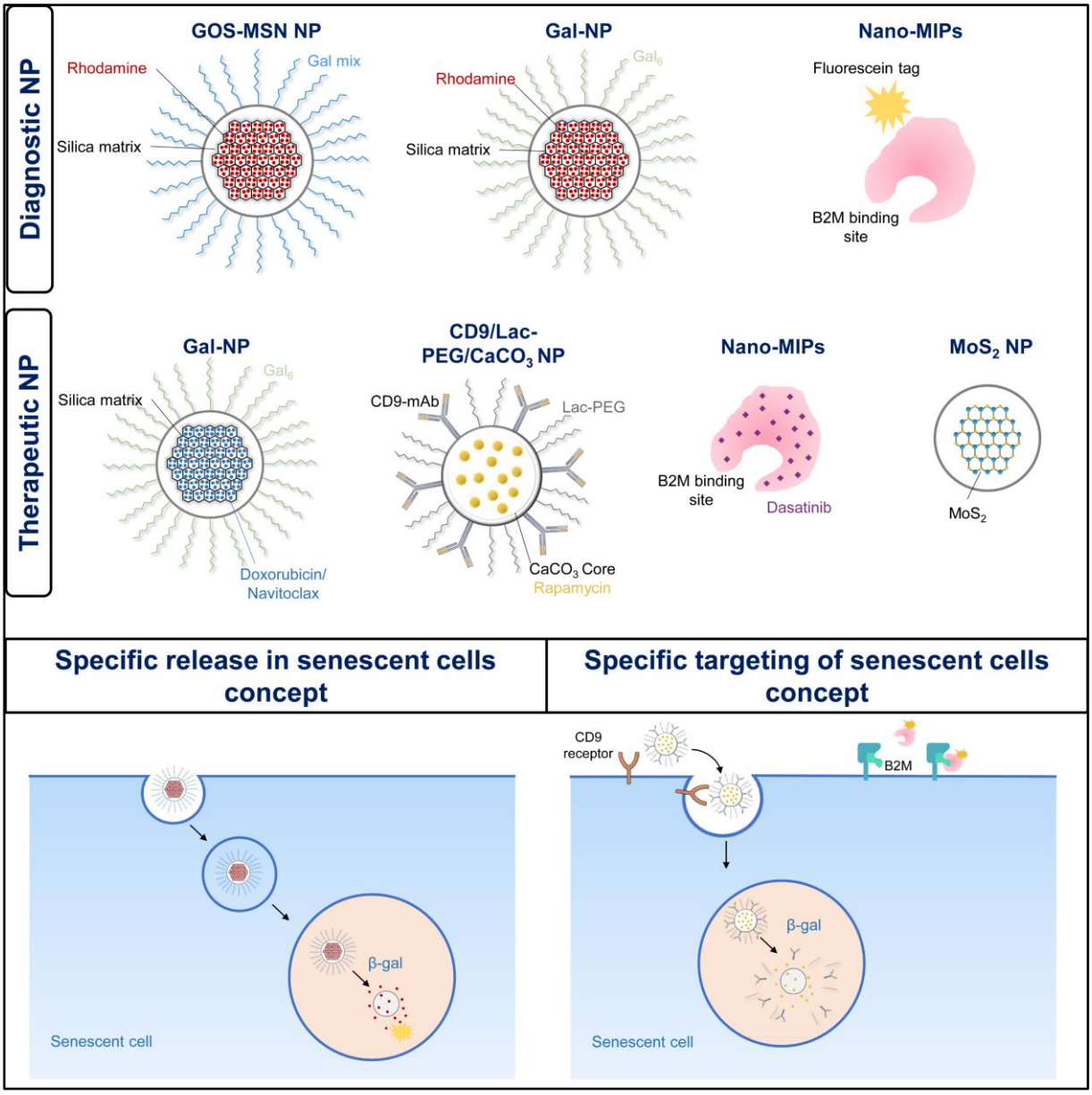

Figure 11: Therapeutic & diagnostic senescence-directed nanoparticles with their concept of either specific cargo release in senescent cells or the specific targeting of senescent cells.

5. Diagnostic probes for detecting senescent cells *in vitro* and *in vivo.*

Developing diagnostic probes that detect senescent cells *in vitro* or *in vivo* is quite essential for investigating cellular senescence in different biological conditions. Besides, it has great clinical implications, such as detecting the cellular senescence burden in the body before and after treatment [239]. Up until now, most probes that detect senescent cells are developed based on the high lysosomal (β-galactosidase) activity of these cells. Unfortunately, many of these probes efficacy were not tested in actual senescent cells but on a model of human cells transfected with

a plasmid resulting in overexpression of bacterial β-galactosidase in the cytoplasm [197]. Therefore, we will only mention diagnostic probes that their efficacy has been approved in senescent cells/ tissue, Table (1).

SG1, a naphthalene-based fluorescent probe, is the first reported for detecting senescent cells in vitro depending on their β-gal activity [240]. It is a ratiometric two-photon fluorescent probe that consists of *β-D*-galactopyranoside-derived benzyl carbamate at the β-gal hydrolytic site and a solubilizing group. Upon its reaction with β-gal, it produces a blue to yellow emission, and it is characterised by insensitivity to pH and reactive oxygen species (ROS), high photostability, and low cytotoxicity. Its efficacy has been validated in human dermal fibroblast HDFs undergoing replicative senescence and also in skin aged tissue [240].

Gal-pro is another recently developed fluorescent probe that severs as a substrate for β-galactosidase activity in senescent cells. It consists of a hemicyanine skeleton, which is conjugated with a D-galactose residue via a glycosidic bond. It was validated in an *in vitro* model of oxidative stress-induced senescence of HDFs. Gal-pro has a near-infrared emission with a rapid and sensitive fluorescent response upon its reaction with β-gal in living cells. In addition, it is characterised by high photostability and low background fluorescence [241].

Both mentioned probes are validated *in vitro*. However, developing a fluorescent probe that can selectively detect senescent cells *in vivo* with good and stable fluorescence emission is still challenging. Lozano-Torres and her colleagues developed a novel two-photon probe AHGa that can detect cellular senescence *in vivo* [242]. It is composed of a naphthalimide core, an L-histidine methyl ester linker, and an acetylated galactose bonded to one of the aromatic nitrogen atoms of the L-histidine through a hydrolysable N-glycosidic bond. Upon its reaction with β-gal, it transforms to the fluorescent AH in an OFF-ON manner/ mechanism. AHGa was first validated in human melanoma SK-MEL-103 cells treated with Palbociclib, where AHGa proved to be nontoxic for both control and treated cells. Then its efficacy was approved *in vivo;* in mice bearing tumour xenografts treated with senescence-inducing chemotherapy, in which a solid fluorescent signal only appeared in tumours treated with Palbociclib. AHGa, with its selectivity, sensitivity, and straightforward synthesis, provide a very attractive OFF-ON two-photon fluorescent probe for efficient detection of cellular senescence *in vitro* and *in vivo* [242].

NIR-BG is the first successful near-infrared probe intended for detecting cellular senescence *in vivo*, with a far-red excitation that provides better deep tissue imaging [239]. NIR-BG is synthesized by glycosylation of a hemicyanine dye and a protected galactosyl bromide, which

provides a near-infrared emission and high turn-on ratio upon SAβgal activation. Its efficacy has been tested in several human cancer lines (MCF7 & HeLa) undergoing treatment/ radiation-induced senescence. In addition, it was validated in mice with HeLa xenografted tumours undergoing chemotherapy-induced senescence [239].

In fact, several probes have been developed for detecting cells expressing β-gal naturally *in vivo,* particularly for ovarian cancer cells. However, they have never been tested in senescent cells and therefore provide an interesting approach [reviewed in [197]]. An example is the HMRef-bGal membrane-permeable fluorescent probe with strong fluorescent emission upon activation by β-gal [243]. Its high sensitivity characterises it as it can detect metastases *in vivo* as small as <1mm. HMRef-bGal development is based on a spirocyclization strategy that uses a hydroxymethyl rhodol derivative bearing a β-gal moiety [243]. Other similar probes are listed in Table 1, [reviewed in [197]].

CyBC9 is the first fluorescent probe to detect and live stain senescent mesenchymal stromal cells MSCs independently of their β-gal activity [244]. It is characterised by rapid process time (2h), nontoxicity, and high sensitivity in detecting senescent MSCs at early and late stages. CyBC9 mechanism is based on its accumulation in the mitochondria of senescent MSCs, most probably due to the loss of membrane potential [244].

Other mechanisms that detect senescent cells independently of their β-gal activity are based on targeting novel extracellular markers of senescence, that has been recently detected, using fluorescent antibodies [235,236], which is similar to B2M-nanoMIPs mentioned earlier. DEP1, NTAL, EBP50, STX4, VAMP3, ARMX3, B2MG, LANCL1, VPS26A and PLD3 represent the validated extracellular markers of senescent cells [235]. DEP1 and B2MG were used for cell sorting using flow cytometry, which is fast and provides quantification [235,236]. The researchers suggest targeting several markers at once to increase specificity [236]. This mechanism has a higher specificity and is faster than β-gal staining, which has many false positives [235].

Although there is a vast improvement in the mechanisms detecting senescent cells *in vivo*, they are still limited by their poor tissue penetration ~ 1cm, which is applicable to some tissues such as skin [197]. Therefore, the review article [197] suggested that the next generation of probes should include agents for MRI detection or PET detection for better tissue penetration. For example, Galacto-conjugation of PET radionuclides might be an interesting approach [197].

Table 1: A list of some of the diagnostic probes that detect cellular senescence or other cells (ovarian cancer cells) depending on their β-gal activity,[197]**.**

Probe	Emission nature	β-gal expression	In vitro/ in vivo	Ref.
SG1. Naphthalene conjugated with galactose	Two-photon (λ ex = 750 nm)	Endogenous (senescence)	*in vitro*	[240]
Gal-Pro. Hemicyanine skeleton conjugated with D-galactose	Single photon near-infrared (λ ex = 620 nm)	Endogenous (senescence)	*in vitro*	[241]
β-CD-CQD. β-cyclodextrin functionalized carbon quantum dots.	Single photon (λ ex = 365 nm)	Endogenous	*in vitro*	[245]
TPE-Gal. Tetra-phenylethylene conjugated with D-galactose.	Single photon (λ ex = 405 nm)	Endogenous	*in vitro*	[246]
Cyclometalated iridium (III) complex	Single photon (λ ex = 405 nm)	Endogenous	*in vitro*	[247]
Fc βgal. Naphthalimide based	Single photon (λ ex = 488 nm) Two-photon (λ ex = 750 nm)	Endogenous	*in vitro*	[248]
AHGa. Naphtalimide based, conjugated with acetylated galactose	Two-photon (λ ex = 750 nm)	Chemotherapy induced senescence	*in vitro* & *in vivo*	[242]
NIR-BG. Hemycianine dye, conjugated with galactosyl bromide	Single-photon near-infrared (λ ex = 680 nm)	Chemotherapy- and radiation-induced senescence	*in vitro* & *in vivo*	[239]
HMRef-βGal. Hydroxymethyl rhodol based	Single photon (λ ex = 498 nm)	Endogenous	*in vitro* & *in vivo*	[243]

6. Clinical studies and the future of Senolytic drugs

The first-in-human, single-arm, open-label clinical trial of senolytics was published in 2019, where Dasatinib plus Quercetin were tested in individuals idiopathic pulmonary fibrosis (IPF) [249], which resulted in statistically significant improvements in physical function in 14 subjects with this relentlessly progressive, debilitating, and ultimately fatal cellular senescence driven disease. Since then, several clinical studies established with D+Q [250] and other therapies intended against cellular senescence such as metformin and rapamycin etc., which are listed in table (2).

However, clinical trial strategies should be set for testing senolytics, senostatics and other senotherapeutic agents. Outcomes like extending life span is not feasible in humans. Therefore, possible clinical trials scenarios include the following [251].

1. Simultaneous alleviation of multiple co-morbidities.
2. Alleviation of potentially fatal diseases

3. Treatment of conditions with localized senescent cell accumulation.
4. Treatment of accelerated ageing-like states.
5. Augmenting physiological resilience. Resilience, or capacity to recover after stress such as surgery, chemotherapy, radiation, pneumonia, or myocardial infarction, declines with ageing.
6. Alleviation of frailty. Targeting senescent cells, even in late life in rodents, appears to reduce immobility, weakness, fat tissue loss, and other parameters associated with frailty.

Table 2: List of therapeutics in clinical studies against cellular senescence [197]**.**

Therapeutic agent	Disease	Clinical trial phase	Trial identification n.
Dasatinib + quercetin	Chronic kidney disease	Phase 2	NCT02848131
Dasatinib + quercetin	IPF	Phase 1	NCT02874989
Dasatinib + quercetin	Hematopoietic stem cell transplant	N/A	NCT02652052
Leniolisib	Activated PI3K Delta Syndrome (APDS)	Phase 2/3	NCT02435173 NCT02859727
Navitoclax + cancer therapies	Solid tumours Advanced EGFR-positive NSCLC	Phase 1 Phase 1/2 Phase 1b	NCT00891605 NCT02143401 NCT00887757 NCT00888108 NCT00878449 NCT01009073 NCT02079740 NCT01989585 NCT02520778 NCT02143401 NCT00887757 NCT00888108
Metformin	Old adults with increased frailty	Phase 2 Phase 3 Phase 4	NCT02325245 NCT02570672 NCT03309007 NCT03451006 NCT02432287
Rapamycin (sirolimus)	Old patients (>70)	Phase 1 Phase 2	NCT01649960 NCT02874924
Plasma transfusions	Old patients	Phase 1/2	NCT03353597

7. Future perspectives and important questions.

Strategies to prevent, replace, or remove senescent cells have become of interest. Several studies have proved that eliminating senescent cells improve health span and heal or protect from age-related diseases, especially cancer.

However, a therapeutic molecule that might prevent cellular senescence induction is not preferable since cellular senescence is essential for regeneration and wound healing and embryogenesis. Therefore, therapeutic molecules targeting senescent cells should have a temporary effect and should be taken periodically. Consequently, those therapeutic molecules should not have serious side effects. In this case, nanomedicine can provide valuable advantages such as maximizing efficacy while minimizing side effects by specific targeting and reducing the loaded dose.

Cellular senescence is a very dynamic biological phenomenon. There is still a lot to accomplish regarding therapeutic and diagnostic approaches. The best approach would be targeting senescent cells with a cocktail of agents such as senolytics and senostatics that can target several markers in cellular senescence for better therapeutic outcome. Nanomedicine can also serve this purpose by the possibility of loading several therapeutic molecules and/or diagnostic probes.

Some of the outstanding questions that have been addressed in the review article Pignolo *et al.* and yet need to be answered are listed below [162]. We found them essential to be included in this introduction as a **closing point.**

1. Do senescent cells serve any beneficial functions, such as providing an inflammatory milieu during tissue healing?
2. What are the tissue-specific thresholds for senescent cell burden that, once exceeded, promote tissue dysfunction and systemic deleterious bystander effects?
3. Does the clearance of senescent cells reduce the influence of other primary ageing processes?
4. How infrequently can senolytic agents be given to minimize senescent cell burden?
5. How can combinations of senotherapeutic agents be devised to optimize senescent cell clearance?
6. Can immune system modulation synergize with senotherapeutic agents to promote senescent cell clearance?
7. Will senolytics synergize with disease-specific treatments to yield a more than additive beneficial effect, for example, in cardiac disease?

8. Are paracrine and other bystander effects the primary mechanism for the pathophysiological consequences of senescent cell accumulation?

9. Do immune clearance mechanisms have the same accessibility to different senescent cell niches (e.g., fat versus bone versus nevi)?

References:

1. Hayflick, L.; Moorhead, P.S. The serial cultivation of human diploid cell strains. *Exp. Cell Res.* **1961**, *25*, 585–621, doi:10.1016/0014-4827(61)90192-6.
2. Hayflick, L. The limited in vitro lifetime of human diploid cell strains. *Exp. Cell Res.* **1965**, *37*, 614–636, doi:10.1016/0014-4827(65)90211-9.
3. Herranz, N.; Gil, J.; Herranz, N.; Gil, J. Mechanisms and functions of cellular senescence. *J. Clin. Invest.* **2018**, *128*, 1238–1246.
4. Kuilman, T.; Michaloglou, C.; Mooi, W.J.; Peeper, D.S. The essence of senescence. *Genes Dev.* **2010**, *24*, 2463–2479, doi:10.1101/gad.1971610.
5. Gorgoulis, V.; Adams, P.D.; Alimonti, A.; Bennett, D.C.; Bischof, O.; Bishop, C.; Campisi, J.; Collado, M.; Evangelou, K.; Ferbeyre, G.; et al. Cellular Senescence: Defining a Path Forward. *Cell* **2019**, *179*, 813–827, doi:10.1016/j.cell.2019.10.005.
6. Hernandez-Segura, A.; Nehme, J.; Demaria, M. Hallmarks of Cellular Senescence. *Trends Cell Biol.* **2018**, *28*, 436–453, doi:10.1016/j.tcb.2018.02.001.
7. Soto-Gamez, A.; Quax, W.J.; Demaria, M. Regulation of Survival Networks in Senescent Cells: From Mechanisms to Interventions. *J. Mol. Biol.* **2019**, *431*, 2629–2643, doi:10.1016/j.jmb.2019.05.036.
8. Beauséjour, C.M.; Krtolica, A.; Galimi, F.; Narita, M.; Lowe, S.W.; Yaswen, P.; Campisi, J. Reversal of human cellular senescence: Roles of the p53 and p16 pathways. *EMBO J.* **2003**, *22*, 4212–4222, doi:10.1093/emboj/cdg417.
9. Dulic, V. Senescence Regulation by mTOR. In *Cell Senescence: Methods and Protocols*; Galluzzi, L., Vitale, I., Kepp, O., Kroemer, G., Eds.; Humana Press: Totowa, NJ, 2013; pp. 15–35 ISBN 978-1-62703-239-1.
10. Milanovic, M.; Fan, D.N.Y.; Belenki, D.; Däbritz, J.H.M.; Zhao, Z.; Yu, Y.; Dörr, J.R.; Dimitrova, L.; Lenze, D.; Monteiro Barbosa, I.A.; et al. Senescence-associated reprogramming promotes cancer stemness. *Nature* **2018**, *553*, 96–100, doi:10.1038/nature25167.
11. Saleh, T.; Tyutyunyk-Massey, L.; Gewirtz, D.A. Tumor cell escape from therapy-induced senescence as a model of disease recurrence after dormancy. *Cancer Res.* **2019**, *79*, 1044–1046, doi:10.1158/0008-5472.CAN-18-3437.
12. Fumagalli, M.; Rossiello, F.; Mondello, C.; D'Adda Di Fagagna, F. Stable cellular senescence is associated with persistent DDR activation. *PLoS One* **2014**, *9*, 44–46, doi:10.1371/journal.pone.0110969.
13. D'Adda Di Fagagna, F. Living on a break: Cellular senescence as a DNA-damage response. *Nat. Rev. Cancer* **2008**, *8*, 512–522, doi:10.1038/nrc2440.
14. Maréchal, A.; Zou, L. DNA damage sensing by the ATM and ATR kinases. *Cold Spring Harb. Perspect. Biol.* **2013**, *5*, 1–17, doi:10.1101/cshperspect.a012716.

15. Zannini, L.; Delia, D.; Buscemi, G. CHK2 kinase in the DNA damage response and beyond. *J. Mol. Cell Biol.* **2014**, *6*, 442–457, doi:10.1093/jmcb/mju045.

16. Podhorecka, M.; Skladanowski, A.; Bozko, P. H2AX phosphorylation: Its role in DNA damage response and cancer therapy. *J. Nucleic Acids* **2010**, *2010*, doi:10.4061/2010/920161.

17. Awasthi, P.; Foiani, M.; Kumar, A. ATM and ATR signaling at a glance. *J. Cell Sci.* **2016**, *129*, 1285, doi:10.1242/jcs.188631.

18. Weiss, R.S.; Matsuoka, S.; Elledge, S.J.; Leder, P. Hus1 acts upstream of chk1 in a mammalian DNA damage response pathway. *Curr. Biol.* **2002**, *12*, 73–77, doi:10.1016/s0960-9822(01)00626-1.

19. Parrilla-Castellar, E.R.; Arlander, S.J.H.; Karnitz, L. Dial 9-1-1 for DNA damage: the Rad9-Hus1-Rad1 (9-1-1) clamp complex. *DNA Repair (Amst).* **2004**, *3*, 1009–1014, doi:10.1016/j.dnarep.2004.03.032.

20. Kumagai, A.; Lee, J.; Yoo, H.Y.; Dunphy, W.G. TopBP1 activates the ATR-ATRIP complex. *Cell* **2006**, *124*, 943–955, doi:10.1016/j.cell.2005.12.041.

21. Menolfi, D.; Zha, S. ATM, ATR and DNA-PKcs kinases-the lessons from the mouse models: Inhibition = deletion. *Cell Biosci.* **2020**, *10*, 1–15, doi:10.1186/s13578-020-0376-x.

22. Turenne, G.A.; Paul, P.; Laflair, L.; Price, B.D. Activation of p53 transcriptional activity requires ATM's kinase domain and multiple N-terminal serine residues of p53. *Oncogene* **2001**, *20*, 5100–5110, doi:10.1038/sj.onc.1204665.

23. Georgakilas, A.G.; Martin, O.A.; Bonner, W.M. p21: A Two-Faced Genome Guardian. *Trends Mol. Med.* **2017**, *23*, 310–319, doi:10.1016/j.molmed.2017.02.001.

24. Malaquin, N.; Carrier-Leclerc, A.; Dessureault, M.; Rodier, F. DDR-mediated crosstalk between DNA-damaged cells and their microenvironment . *Front. Genet.* 2015, *6*, 94.

25. Coppé, J.P.; Patil, C.K.; Rodier, F.; Sun, Y.; Muñoz, D.P.; Goldstein, J.; Nelson, P.S.; Desprez, P.Y.; Campisi, J. Senescence-associated secretory phenotypes reveal cell-nonautonomous functions of oncogenic RAS and the p53 tumor suppressor. *PLoS Biol.* **2008**, *6*, doi:10.1371/journal.pbio.0060301.

26. Watanabe, S.; Kawamoto, S.; Ohtani, N.; Hara, E. Impact of senescence-associated secretory phenotype and its potential as a therapeutic target for senescence-associated diseases. *Cancer Sci.* **2017**, *108*, 563–569, doi:10.1111/cas.13184.

27. Childs, B.G.; Durik, M.; Baker, D.J.; Van Deursen, J.M. Cellular senescence in aging and age-related disease: From mechanisms to therapy. *Nat. Med.* **2015**, *21*, 1424–1435, doi:10.1038/nm.4000.

28. Byun, H.O.; Lee, Y.K.; Kim, J.M.; Yoon, G. From cell senescence to age-related diseases: Differential mechanisms of action of senescence-associated secretory phenotypes. *BMB Rep.* **2015**, *48*, 549–558, doi:10.5483/BMBRep.2015.48.10.122.

29. Borodkina, A. V; Deryabin, P.I.; Giukova, A.A.; Nikolsky, N.N. "Social Life" of Senescent Cells: What Is SASP and Why Study It? *Acta Naturae* **2018**, *10*, 4–14.

30. Kuilman, T.; Michaloglou, C.; Vredeveld, L.C.W.; Douma, S.; van Doorn, R.; Desmet, C.J.; Aarden, L.A.; Mooi, W.J.; Peeper, D.S. Oncogene-Induced Senescence Relayed by an Interleukin-Dependent Inflammatory Network. *Cell* **2008**, *133*, 1019–1031, doi:10.1016/j.cell.2008.03.039.

31. Coppé, J.-P.; Desprez, P.-Y.; Krtolica, A.; Campisi, J. The Senescence-Associated Secretory Phenotype: The Dark Side of Tumor Suppression. *Annu. Rev. Pathol. Mech. Dis.* **2010**, *5*, 99–118, doi:10.1146/annurev-pathol-121808-

102144.

32. Hornebeck, W.; Maquart, F.X. Proteolyzed matrix as a template for the regulation of tumor progression. *Biomed. Pharmacother.* **2003**, *57*, 223–230, doi:10.1016/S0753-3322(03)00049-0.

33. Brew, K.; Dinakarpandian, D.; Nagase, H. Tissue inhibitors of metalloproteinases: Evolution, structure and function. *Biochim. Biophys. Acta - Protein Struct. Mol. Enzymol.* **2000**, *1477*, 267–283, doi:10.1016/S0167-4838(99)00279-4.

34. Telgenhoff, D.; Shroot, B. Cellular senescence mechanisms in chronic wound healing. *Cell Death Differ.* **2005**, *12*, 695–698, doi:10.1038/sj.cdd.4401632.

35. Vaughan, D.E.; Rai, R.; Khan, S.S.; Eren, M.; Ghosh, A.K. PAI-1 is a Marker and a Mediator of Senescence. *Arterioscler. Thromb. Vasc. Biol.* **2017**, *37*, 1446, doi:10.1161/ATVBAHA.117.309451.

36. Kortlever, R.M.; Bernards, R. Senescence, wound healing and cancer: The PAI-1 connection. *Cell Cycle* **2006**, *5*, 2697–2703, doi:10.4161/cc.5.23.3510.

37. Xu, D.; Tahara, H. The role of exosomes and microRNAs in senescence and aging. *Adv. Drug Deliv. Rev.* **2013**, *65*, 368–375, doi:10.1016/j.addr.2012.07.010.

38. Jakhar, R.; Crasta, K. Exosomes as emerging pro-tumorigenic mediators of the senescence-associated secretory phenotype. *Int. J. Mol. Sci.* **2019**, *20*, doi:10.3390/ijms20102547.

39. Malaquin, N.; Martinez, A.; Rodier, F. Keeping the senescence secretome under control: Molecular reins on the senescence-associated secretory phenotype. *Exp. Gerontol.* **2016**, *82*, 39–49, doi:10.1016/j.exger.2016.05.010.

40. Lujambio, A.; Banito, A. Functional screening to identify senescence regulators in cancer. *Curr. Opin. Genet. Dev.* **2019**, *54*, 17–24, doi:10.1016/j.gde.2019.02.001.

41. Rodier, F.; Coppé, J.-P.; Patil, C.K.; Hoeijmakers, W.A.M.; Muñoz, D.P.; Raza, S.R.; Freund, A.; Campeau, E.; Davalos, A.R.; Campisi, J. Persistent DNA damage signalling triggers senescence-associated inflammatory cytokine secretion. *Nat. Cell Biol.* **2009**, *11*, 973–979, doi:10.1038/ncb1909.

42. Rodier, F.; Muñoz, D.P.; Teachenor, R.; Chu, V.; Le, O.; Bhaumik, D.; Coppé, J.P.; Campeau, E.; Beauséjour, C.M.; Kim, S.H.; et al. DNA-SCARS: Distinct nuclear structures that sustain damage-induced senescence growth arrest and inflammatory cytokine secretion. *J. Cell Sci.* **2011**, *124*, 68–81, doi:10.1242/jcs.071340.

43. Ben-Porath, I.; Weinberg, R.A. The signals and pathways activating cellular senescence. *Int. J. Biochem. Cell Biol.* **2005**, *37*, 961–976, doi:10.1016/j.biocel.2004.10.013.

44. Freund, A.; Patil, C.K.; Campisi, J. P38MAPK is a novel DNA damage response-independent regulator of the senescence-associated secretory phenotype. *EMBO J.* **2011**, *30*, 1536–1548, doi:10.1038/emboj.2011.69.

45. Alimbetov, D.; Davis, T.; Brook, A.J.C.; Cox, L.S.; Faragher, R.G.A.; Nurgozhin, T.; Zhumadilov, Z.; Kipling, D. Suppression of the senescence-associated secretory phenotype (SASP) in human fibroblasts using small molecule inhibitors of p38 MAP kinase and MK2. *Biogerontology* **2016**, *17*, 305–315, doi:10.1007/s10522-015-9610-z.

46. Laberge, R.M.; Sun, Y.; Orjalo, A. V; Patil, C.K.; Freund, A.; Zhou, L.; Curran, S.C.; Davalos, A.R.; Wilson-Edell, K.A.; Liu, S.; et al. MTOR regulates the pro-tumorigenic senescence-associated secretory phenotype by promoting IL1A translation. *Nat. Cell Biol.* **2015**, *17*, 1049–1061, doi:10.1038/ncb3195.

47. Herranz, N.; Gallage, S.; Mellone, M.; Wuestefeld, T.; Klotz, S.; Hanley, C.J.; Raguz, S.; Acosta, J.C.; Innes, A.J.; Banito, A.; et al. mTOR regulates MAPKAPK2 translation to control the senescence-associated secretory phenotype. *Nat. Cell Biol.* **2015**, *17*, 1205–1217, doi:10.1038/ncb3225.

48. Rajendran, P.; Alzahrani, A.M.; Hanieh, H.N.; Kumar, S.A.; Ben Ammar, R.; Rengarajan, T.; Alhoot, M.A. Autophagy and senescence: A new insight in selected human diseases. *J. Cell. Physiol.* **2019**, *234*, 21485–21492, doi:10.1002/jcp.28895.

49. Rodier, F.; Campisi, J. Four faces of cellular senescence. *J. Cell Biol.* **2011**, *192*, 547–556, doi:10.1083/jcb.201009094.

50. Freund, A.; Orjalo, A. V.; Desprez, P.Y.; Campisi, J. Inflammatory networks during cellular senescence: causes and consequences. *Trends Mol. Med.* **2010**, *16*, 238–246, doi:10.1016/j.molmed.2010.03.003.

51. McHugh, D.; Gil, J. Senescence and aging: Causes, consequences, and therapeutic avenues. *J. Cell Biol.* **2018**, *217*, 65–77, doi:10.1083/jcb.201708092.

52. Prata, L.G.P.L.; Ovsyannikova, I.G.; Tchkonia, T.; Kirkland, J.L. Senescent cell clearance by the immune system: Emerging therapeutic opportunities. *Semin. Immunol.* **2018**, *40*, 101275, doi:https://doi.org/10.1016/j.smim.2019.04.003.

53. Ray, D.; Yung, R. Immune senescence, epigenetics and autoimmunity. *Clin. Immunol.* **2018**, *196*, 59–63, doi:10.1016/j.clim.2018.04.002.

54. Van Deursen, J.M. The role of senescent cells in ageing. *Nature* **2014**, *509*, 439–446, doi:10.1038/nature13193.

55. Greene, M.A.; Loeser, R.F. Aging-related inflammation in osteoarthritis. *Osteoarthr. Cartil.* **2015**, *23*, 1966–1971, doi:10.1016/j.joca.2015.01.008.

56. Velarde, M.C.; Demaria, M.; Campisi, J. Senescent cells and their secretory phenotype as targets for cancer therapy. *Interdiscip. Top. Gerontol.* **2013**, *38*, 17–27, doi:10.1159/000343572.

57. Lecot, P.; Alimirah, F.; Desprez, P.Y.; Campisi, J.; Wiley, C. Context-dependent effects of cellular senescence in cancer development. *Br. J. Cancer* **2016**, *114*, 1180–1184, doi:10.1038/bjc.2016.115.

58. Laberge, R.M.; Awad, P.; Campisi, J.; Desprez, P.Y. Epithelial-mesenchymal transition induced by senescent fibroblasts. *Cancer Microenviron.* **2012**, *5*, 39–44, doi:10.1007/s12307-011-0069-4.

59. Gonzalez-Meljem, J.M.; Apps, J.R.; Fraser, H.C.; Martinez-Barbera, J.P. Paracrine roles of cellular senescence in promoting tumourigenesis. *Br. J. Cancer* **2018**, *118*, 1283–1288, doi:10.1038/s41416-018-0066-1.

60. Toso, A.; Revandkar, A.; DiMitri, D.; Guccini, I.; Proietti, M.; Sarti, M.; Pinton, S.; Zhang, J.; Kalathur, M.; Civenni, G.; et al. Enhancing chemotherapy efficacy in pten-deficient prostate tumors by activating the senescence-associated antitumor immunity. *Cell Rep.* **2014**, *9*, 75–89, doi:10.1016/j.celrep.2014.08.044.

61. Watanabe, S.; Kawamoto, S.; Ohtani, N.; Hara, E. Impact of senescence-associated secretory phenotype and its potential as a therapeutic target for senescence-associated diseases. *Cancer Sci.* **2017**, *108*, 563–569, doi:10.1111/cas.13184.

62. Demaria, M.; Ohtani, N.; Youssef, S.A.; Rodier, F.; Toussaint, W.; Mitchell, J.R.; Laberge, R.M.; Vijg, J.; VanSteeg, H.; Dollé, M.E.T.; et al. An essential role for senescent cells in optimal wound healing through secretion of PDGF-AA. *Dev. Cell* **2014**, *31*, 722–733, doi:10.1016/j.devcel.2014.11.012.

63. Storer, M.; Mas, A.; Robert-Moreno, A.; Pecoraro, M.; Ortells, M.C.; Di Giacomo, V.; Yosef, R.; Pilpel, N.; Krizhanovsky, V.; Sharpe, J.; et al. Senescence is a developmental mechanism that contributes to embryonic growth and patterning. *Cell* **2013**, *155*, 1119, doi:10.1016/j.cell.2013.10.041.

64. Tchkonia, T.; Zhu, Y.; Deursen, J. Van; Campisi, J.; Kirkland, J.L. Cellular senescence and the senescent secretory phenotype: therapeutic opportunities. *J. Clin. Invest.* **2013**, *123*, 966–972, doi:10.1172/JCI64098.966.

65. Frey, N.; Venturelli, S.; Zender, L.; Bitzer, M. Cellular senescence in gastrointestinal diseases: From pathogenesis to therapeutics. *Nat. Rev. Gastroenterol. Hepatol.* **2018**, *15*, 81–95, doi:10.1038/nrgastro.2017.146.

66. Akl, H.; Vervloessem, T.; Kiviluoto, S.; Bittremieux, M.; Parys, J.B.; De Smedt, H.; Bultynck, G. A dual role for the anti-apoptotic Bcl-2 protein in cancer: Mitochondria versus endoplasmic reticulum. *Biochim. Biophys. Acta - Mol. Cell Res.* **2014**, *1843*, 2240–2252, doi:10.1016/j.bbamcr.2014.04.017.

67. Yosef, R.; Pilpel, N.; Tokarsky-Amiel, R.; Biran, A.; Ovadya, Y.; Cohen, S.; Vadai, E.; Dassa, L.; Shahar, E.; Condiotti, R.; et al. Directed elimination of senescent cells by inhibition of BCL-W and BCL-XL. *Nat. Commun.* **2016**, *7*, doi:10.1038/ncomms11190.

68. Zhu, Y.; Tchkonia, T.; Pirtskhalava, T.; Gower, A.C.; Ding, H.; Giorgadze, N.; Palmer, A.K.; Ikeno, Y.; Hubbard, G.B.; Lenburg, M.; et al. The Achilles' heel of senescent cells: from transcriptome to senolytic drugs. *Aging Cell* **2015**, *14*, 644–658, doi:10.1111/acel.12344.

69. Baar, M.P.; Brandt, R.M.C.; Putavet, D.A.; Klein, J.D.D.; Derks, K.W.J.; Bourgeois, B.R.M.; Stryeck, S.; Rijksen, Y.; van Willigenburg, H.; Feijtel, D.A.; et al. Targeted Apoptosis of Senescent Cells Restores Tissue Homeostasis in Response to Chemotoxicity and Aging. *Cell* **2017**, *169*, 132-147.e16, doi:10.1016/j.cell.2017.02.031.

70. Yosef, R.; Pilpel, N.; Papismadov, N.; Gal, H.; Ovadya, Y.; Vadai, E.; Miller, S.; Porat, Z.; Ben-Dor, S.; Krizhanovsky, V. p21 maintains senescent cell viability under persistent DNA damage response by restraining JNK and caspase signaling . *EMBO J.* **2017**, *36*, 2280–2295, doi:10.15252/embj.201695553.

71. Tran, D.; Bergholz, J.; Zhang, H.; He, H.; Wang, Y.; Zhang, Y.; Li, Q.; Kirkland, J.L.; Xiao, Z.X. Insulin-like growth factor-1 regulates the SIRT1-p53 pathway in cellular senescence. *Aging Cell* **2014**, *13*, 669–678, doi:10.1111/acel.12219.

72. Luo, X.; Suzuki, M.; Ghandhi, S.A.; Amundson, S.A.; Boothman, D.A. ATM regulates insulin-like growth factor 1-secretory clusterin (IGF-1-sCLU) expression that protects cells against senescence. *PLoS One* **2014**, *9*, doi:10.1371/journal.pone.0099983.

73. Negulescu, A.M.; Mehlen, P. Dependence receptors – the dark side awakens. *FEBS J.* **2018**, *285*, 3909–3924, doi:10.1111/febs.14507.

74. Houssaini, A.; Breau, M.; Kebe, K.; Abid, S.; Marcos, E.; Lipskaia, L.; Rideau, D.; Parpaleix, A.; Huang, J.; Amsellem, V.; et al. mTOR pathway activation drives lung cell senescence and emphysema. *JCI insight* **2018**, *3*, doi:10.1172/jci.insight.93203.

75. Pluquet, O.; Pourtier, A.; Abbadie, C. The unfolded protein response and cellular senescence. A Review in the Theme: Cellular Mechanisms of Endoplasmic Reticulum Stress Signaling in Health and Disease. *Am. J. Physiol. - Cell Physiol.* **2015**, *308*, C415–C425, doi:10.1152/ajpcell.00334.2014.

76. Abbadie, C.; Pluquet, O. Unfolded Protein Response (UPR) Controls Major Senescence Hallmarks. *Trends Biochem. Sci.* **2020**, *45*, 371–374, doi:10.1016/j.tibs.2020.02.005.

77. Pole, A.; Dimri, M.; P. Dimri, G. Oxidative stress, cellular senescence and ageing. *AIMS Mol. Sci.* **2016**, *3*, 300–324, doi:10.3934/molsci.2016.3.300.

78. Ogata, M.; Hino, S.; Saito, A.; Morikawa, K.; Kondo, S.; Kanemoto, S.; Murakami, T.; Taniguchi, M.; Tanii, I.; Yoshinaga, K.; et al. Autophagy Is Activated for Cell Survival after Endoplasmic ReticulumStress. *Mol. Cell. Biol.* **2006**, *26*, 9220–9231, doi:10.1128/mcb.01453-06.

79. Gosselin, K.; Deruy, E.; Martien, S.; Vercamer, C.; Bouali, F.; Dujardin, T.; Slomianny, C.; Houel-Renault, L.; Chelli, F.; De Launoit, Y.; et al. Senescent keratinocytes die by autophagic programmed cell death. *Am. J. Pathol.*

2009, *174*, 423–435, doi:10.2353/ajpath.2009.080332.

80. Pattingre, S.; Tassa, A.; Qu, X.; Garuti, R.; Xiao, H.L.; Mizushima, N.; Packer, M.; Schneider, M.D.; Levine, B. Bcl-2 antiapoptotic proteins inhibit Beclin 1-dependent autophagy. *Cell* **2005**, *122*, 927–939, doi:10.1016/j.cell.2005.07.002.

81. Navas, P.R.; Thedieck, K. Differential control of ageing and lifespan by isoforms and splice variants across the mTOR network. *Essays Biochem.* **2017**, *61*, 349–368, doi:10.1042/EBC20160086.

82. Jung, C.H.; Ro, S.-H.; Cao, J.; Otto, N.M.; Kim, D.-H. mTOR and autophagy. *NIH Public Access* **2010**, *584*, 1287–1295, doi:10.1016/j.febslet.2010.01.017.mTOR.

83. Vasileiou, P.; Evangelou, K.; Vlasis, K.; Fildisis, G.; Panayiotidis, M.; Chronopoulos, E.; Passias, P.-G.; Kouloukoussa, M.; Gorgoulis, V.; Havaki, S. Mitochondrial Homeostasis and Cellular Senescence. *Cells* **2019**, *8*, 686, doi:10.3390/cells8070686.

84. Correia-Melo, C.; Marques, F.D.; Anderson, R.; Hewitt, G.; Hewitt, R.; Cole, J.; Carroll, B.M.; Miwa, S.; Birch, J.; Merz, A.; et al. Mitochondria are required for pro-ageing features of the senescent phenotype. *EMBO J.* **2016**, *35*, 724–742, doi:10.15252/embj.201592862.

85. Birch, J.; Passos, J.F. Targeting the SASP to combat ageing: Mitochondria as possible intracellular allies? *BioEssays* **2017**, *39*, 1–7, doi:10.1002/bies.201600235.

86. Summer, R.; Shaghaghi, H.; Schriner, D.L.; Roque, W.; Sales, D.; Cuevas-Mora, K.; Desai, V.; Bhushan, A.; Ramirez, M.I.; Romero, F. Activation of the mTORC1/PGC-1 axis promotes mitochondrial biogenesis and induces cellular senescence in the lung epithelium. *Am. J. Physiol. - Lung Cell. Mol. Physiol.* **2019**, *316*, L1049–L1060, doi:10.1152/ajplung.00244.2018.

87. Hubackova, S.; Davidova, E.; Rohlenova, K.; Stursa, J.; Werner, L.; Andera, L.; Dong, L.F.; Terp, M.G.; Hodny, Z.; Ditzel, H.J.; et al. Selective elimination of senescent cells by mitochondrial targeting is regulated by ANT2. *Cell Death Differ.* **2019**, *26*, 276–290, doi:10.1038/s41418-018-0118-3.

88. EVERITT, A. V; Le COUTEUR, D.G. Life Extension by Calorie Restriction in Humans. *Ann. N. Y. Acad. Sci.* **2007**, *1114*, 428–433, doi:10.1196/annals.1396.005.

89. Fontana, L.; Nehme, J.; Demaria, M. Caloric restriction and cellular senescence. *Mech. Ageing Dev.* **2018**, *176*, 19–23, doi:https://doi.org/10.1016/j.mad.2018.10.005.

90. Zhang, X.; Tang, N.; Hadden, T.J.; Rishi, A.K. Akt, FoxO and regulation of apoptosis. *Biochim. Biophys. Acta - Mol. Cell Res.* **2011**, *1813*, 1978–1986, doi:https://doi.org/10.1016/j.bbamcr.2011.03.010.

91. Song, P.; An, J.; Zou, M.-H. Immune Clearance of Senescent Cells to Combat Ageing and Chronic Diseases. *Cells* **2020**, *9*, 671, doi:10.3390/cells9030671.

92. Haugstetter, A.M.; Loddenkemper, C.; Lenze, D.; Gröne, J.; Standfu, C.; Petersen, I.; Dörken, B.; Schmitt, C.A. Cellular senescence predicts treatment outcome in metastasised colorectal cancer. *Br. J. Cancer* **2010**, *103*, 505–509, doi:10.1038/sj.bjc.6605784.

93. Guillon, J.; Petit, C.; Toutain, B.; Guette, C.; Lelièvre, E.; Coqueret, O. Chemotherapy-induced senescence, an adaptive mechanism driving resistance and tumor heterogeneity. *Cell Cycle* **2019**, *18*, 2385–2397, doi:10.1080/15384101.2019.1652047.

94. Cellular senescence and cancer chemotherapy resistance | Enhanced Reader.

95. Demaria, M.; O'Leary, M.N.; Chang, J.; Shao, L.; Liu, S.; Alimirah, F.; Koenig, K.; Le, C.; Mitin, N.; Deal, A.M.;

et al. Cellular senescence promotes adverse effects of chemotherapy and cancer relapse. *Cancer Discov.* **2017**, *7*, 165–176, doi:10.1158/2159-8290.CD-16-0241.

96. Elmore, L.W.; Di, X.; Dumur, C.; Holt, S.E.; Gewirtz, D.A. Evasion of a single-step, chemotherapy-induced senescence in breast cancer cells: Implications for treatment response. *Clin. Cancer Res.* **2005**, *11*, 2637–2643, doi:10.1158/1078-0432.CCR-04-1462.

97. Roberson, R.S.; Kussick, S.J.; Vallieres, E.; Chen, S.Y.J.; Wu, D.Y. Escape from therapy-induced accelerated cellular senescence in p53-null lung cancer cells and in human lung cancers. *Cancer Res.* **2005**, *65*, 2795–2803, doi:10.1158/0008-5472.CAN-04-1270.

98. Saleh, T.; Tyutyunyk-Massey, L.; Murray, G.F.; Alotaibi, M.R.; Kawale, A.S.; Elsayed, Z.; Henderson, S.C.; Yakovlev, V.; Elmore, L.W.; Toor, A.; et al. Tumor cell escape from therapy-induced senescence. *Biochem. Pharmacol.* **2019**, *162*, 202–212, doi:10.1016/j.bcp.2018.12.013.

99. Erenpreisa, J.; Cragg, M.S. Three steps to the immortality of cancer cells: Senescence, polyploidy and self-renewal. *Cancer Cell Int.* **2013**, *13*, 1, doi:10.1186/1475-2867-13-92.

100. Wang, Q.; Wu, P.C.; Dong, D.Z.; Ivanova, I.; Chu, E.; Zeliadt, S.; Vesselle, H.; Wu, D.Y. Polyploidy road to therapy-induced cellular senescence and escape. *Int. J. Cancer* **2013**, *132*, 1505–1515, doi:10.1002/ijc.27810.

101. Wang, Q.; Wu, P.C.; Roberson, R.S.; Luk, B. V.; Ivanova, I.; Chu, E.; Wu, D.Y. Survivin and escaping in therapy-induced cellular senescence. *Int. J. Cancer* **2011**, *128*, 1546–1558, doi:10.1002/ijc.25482.

102. Rajaraman, R.; Guernsey, D.L.; Rajaraman, M.M.; Rajaraman, S.R. Stem cells, senescence, neosis and self-renewal in cancer. *Cancer Cell Int.* **2006**, *6*, 1–26, doi:10.1186/1475-2867-6-25.

103. Sundaram, M.; Guernsey, D.L.; Rajaraman, M.M.; Rajaraman, R. Neosis: A Novel Type of Cell Division in Cancer. *Cancer Biol. Ther.* **2004**, *3*, 207–218, doi:10.4161/cbt.3.2.663.

104. Zon, L.I. Intrinsic and extrinsic control of haematopoietic stem-cell self-renewal. *Nature 453*, 306–313, doi:10.1038/nature07038.

105. Dou, Z.; Berger, S.L. Senescence Elicits Stemness: A Surprising Mechanism for Cancer Relapse. *Cell Metab.* **2018**, *27*, 710–711, doi:10.1016/j.cmet.2018.03.009.

106. Patel, P.L.; Suram, A.; Mirani, N.; Bischof, O.; Herbig, U. Derepression of hTERT gene expression promotes escape from oncogene-induced cellular senescence. *Proc. Natl. Acad. Sci. U. S. A.* **2016**, *113*, E5024–E5033, doi:10.1073/pnas.1602379113.

107. Jonchère, B.; Vétillard, A.; Toutain, B.; Lam, D.; Bernard, A.C.; Henry, C.; Carné Trécesson, S. De; Gamelin, E.; Juin, P.; Guette, C.; et al. Irinotecan treatment and senescence failure promote the emergence of more transformed and invasive cells that depend on anti-apoptotic Mcl-1. *Oncotarget* **2015**, *6*, 409–426, doi:10.18632/oncotarget.2774.

108. Vétillard, A.; Jonchère, B.; Moreau, M.; Toutain, B.; Henry, C.; Fontanel, S.; Bernard, A.C.; Campone, M.; Guette, C.; Coqueret, O. Akt inhibition improves irinotecan treatment and prevents cell emergence by switching the senescence response to apoptosis. *Oncotarget* **2015**, *6*, 43342–43362, doi:10.18632/oncotarget.6126.

109. Huang, T.; Sun, L.; Yuan, X.; Qiu, H. Thrombospondin-1 is a multifaceted player in tumor progression. *Oncotarget* **2017**, *8*, 84546–84558, doi:10.18632/oncotarget.19165.

110. Kazerounian, S.; Yee, K.O.; Lawler, J. Thrombospondins in cancer. *Cell. Mol. Life Sci.* **2008**, *65*, 700–12, doi:10.1007/s00018-007-7486-z.

111. Resovi, A.; Pinessi, D.; Chiorino, G.; Taraboletti, G. Current understanding of the thrombospondin-1 interactome. *Matrix Biol.* **2014**, *37*, 83–91, doi:https://doi.org/10.1016/j.matbio.2014.01.012.

112. Huang, T.; Sun, L.; Yuan, X.; Qiu, H. Thrombospondin-1 is a multifaceted player in tumor progression. **2017**, *8*, 84546–84558.

113. Matozaki, T.; Murata, Y.; Okazawa, H.; Ohnishi, H. Functions and molecular mechanisms of the CD47-SIRPα signalling pathway. *Trends Cell Biol.* **2009**, *19*, 72–80, doi:10.1016/j.tcb.2008.12.001.

114. Roberts, D.D.; Miller, T.W.; Rogers, N.M.; Yao, M.; Isenberg, J.S. The matricellular protein thrombospondin-1 globally regulates cardiovascular function and responses to stress via CD47. *Matrix Biol.* **2012**, *31*, 162–169, doi:10.1016/j.matbio.2012.01.005.

115. Kaur, S.; Soto-Pantoja, D.R.; Stein, E. V.; Liu, C.; Elkahloun, A.G.; Pendrak, M.L.; Nicolae, A.; Singh, S.P.; Nie, Z.; Levens, D.; et al. Thrombospondin-1 Signaling through CD47 Inhibits Self-renewal by Regulating c-Myc and Other Stem Cell Transcription Factors. *Sci. Rep.* **2013**, *3*, 1673, doi:10.1038/srep01673.

116. Bras, M.; Yuste, V.J.; Roue, G.; Barbier, S.; Sancho, P.; Virely, C.; Rubio, M.; Baudet, S.; Esquerda, J.E.; Merle-Beral, H.; et al. Drp1 Mediates Caspase-Independent Type III Cell Death in Normal and Leukemic Cells. *Mol. Cell. Biol.* **2007**, *27*, 7073–7088, doi:10.1128/MCB.02116-06.

117. Jaiswal, S.; Jamieson, C.H.M.; Pang, W.W.; Park, C.Y.; Chao, M.P.; Majeti, R.; Traver, D.; van Rooijen, N.; Weissman, I.L. CD47 Is Upregulated on Circulating Hematopoietic Stem Cells and Leukemia Cells to Avoid Phagocytosis. *Cell* **2009**, *138*, 271–285, doi:10.1016/J.CELL.2009.05.046.

118. Campone, M.; Valo, I.; Jézéquel, P.; Moreau, M.; Boissard, A.; Campion, L.; Loussouarn, D.; Verriele, V.; Coqueret, O.; Guette, C. Prediction of recurrence and survival for triple-negative breast cancer (TNBC) by a protein signature in tissue samples. *Mol. Cell. Proteomics* **2015**, *14*, 2936–2946, doi:10.1074/mcp.M115.048967.

119. Guillon, J.; Petit, C.; Moreau, M.; Toutain, B.; Henry, C.; Roché, H.; Bonichon-Lamichhane, N.; Salmon, J.P.; Lemonnier, J.; Campone, M.; et al. Regulation of senescence escape by TSP1 and CD47 following chemotherapy treatment. *Cell Death Dis.* **2019**, *10*, doi:10.1038/s41419-019-1406-7.

120. Krishnamurthy, J.; Torrice, C.; Ramsey, M.R.; Kovalev, G.I.; Al-Regaiey, K.; Su, L.; Sharpless, N.E. Ink4a/Arf expression is a biomarker of aging. *J. Clin. Invest.* **2004**, *114*, 1299–1307, doi:10.1172/jci200422475.

121. Wissler Gerdes, E.O.; Zhu, Y.; Tchkonia, T.; Kirkland, J.L. Discovery, development, and future application of senolytics: theories and predictions. *FEBS J.* **2020**, *287*, 2418–2427, doi:10.1111/febs.15264.

122. Krimpenfort, P.; Quon, K.C.; Mooi, W.J.; Loonstra, A.; Berns, A. Loss of p16Ink4a confers susceptibility to metastatic melanoma in mice. *Nature* **2001**, *413*, 83–86, doi:10.1038/35092584.

123. Xue, W.; Zender, L.; Miething, C.; Dickins, R.A.; Hernando, E.; Krizhanovsky, V.; Cordon-Cardo, C.; Lowe, S.W. Senescence and tumour clearance is triggered by p53 restoration in murine liver carcinomas. *Nature* **2007**, *445*, 656–660, doi:10.1038/nature05529.

124. Baker, D.J.; Wijshake, T.; Tchkonia, T.; Lebrasseur, N.K.; Childs, B.G.; Van De Sluis, B.; Kirkland, J.L.; Van Deursen, J.M. Clearance of p16 Ink4a-positive senescent cells delays ageing-associated disorders. *Nature* **2011**, *479*, 232–236, doi:10.1038/nature10600.

125. Ovadya, Y.; Krizhanovsky, V. Strategies targeting cellular senescence. *J. Clin. Invest.* 2018, *128*, 1247–1254.

126. Carné Trécesson, S. De; Souazé, F.; Basseville, A.; Bernard, A.C.; Pécot, J.; Lopez, J.; Bessou, M.; Sarosiek, K.A.; Letai, A.; Barillé-Nion, S.; et al. BCL-XL directly modulates RAS signalling to favour cancer cell stemness. *Nat.*

Commun. **2017**, *8*, doi:10.1038/s41467-017-01079-1.

127. Oltersdorf, T.; Elmore, S.W.; Shoemaker, A.R.; Armstrong, R.C.; Augeri, D.J.; Belli, B.A.; Bruncko, M.; Deckwerth, T.L.; Dinges, J.; Hajduk, P.J.; et al. An inhibitor of Bcl-2 family proteins induces regression of solid tumours. *Nature* **2005**, *435*, 677–681, doi:10.1038/nature03579.

128. Hennessy, E.J. Selective inhibitors of Bcl-2 and Bcl-xL: Balancing antitumor activity with on-target toxicity. *Bioorganic Med. Chem. Lett.* **2016**, *26*, 2105–2114, doi:10.1016/j.bmcl.2016.03.032.

129. Yosef, R.; Pilpel, N.; Tokarsky-Amiel, R.; Biran, A.; Ovadya, Y.; Cohen, S.; Vadai, E.; Dassa, L.; Shahar, E.; Condiotti, R.; et al. Directed elimination of senescent cells by inhibition of BCL-W and BCL-XL. *Nat. Commun.* **2016**, *7*, 1–11, doi:10.1038/ncomms11190.

130. Tse, C.; Shoemaker, A.R.; Adickes, J.; Anderson, M.G.; Chen, J.; Jin, S.; Johnson, E.F.; Marsh, K.C.; Mitten, M.J.; Nimmer, P.; et al. ABT-263: A potent and orally bioavailable Bcl-2 family inhibitor. *Cancer Res.* **2008**, *68*, 3421–3428, doi:10.1158/0008-5472.CAN-07-5836.

131. Chang, J.; Wang, Y.; Shao, L.; Laberge, R.M.; Demaria, M.; Campisi, J.; Janakiraman, K.; Sharpless, N.E.; Ding, S.; Feng, W.; et al. Clearance of senescent cells by ABT263 rejuvenates aged hematopoietic stem cells in mice. *Nat. Med.* **2016**, *22*, 78–83, doi:10.1038/nm.4010.

132. Zhu, Y.; Tchkonia, T.; Fuhrmann-Stroissnigg, H.; Dai, H.M.; Ling, Y.Y.; Stout, M.B.; Pirtskhalava, T.; Giorgadze, N.; Johnson, K.O.; Giles, C.B.; et al. Identification of a novel senolytic agent, navitoclax, targeting the Bcl-2 family of anti-apoptotic factors. *Aging Cell* **2016**, *15*, 428–435, doi:10.1111/acel.12445.

133. Childs, B.G.; Baker, D.J.; Wijshake, T.; Conover, C.A.; Campisi, J.; Van Deursen, J.M. Senescent intimal foam cells are deleterious at all stages of atherosclerosis. *Science (80-.).* **2016**, *354*, 472–477, doi:10.1126/science.aaf6659.

134. Zhang, H.; Nimmer, P.M.; Tahir, S.K.; Chen, J.; Fryer, R.M.; Hahn, K.R.; Iciek, L.A.; Morgan, S.J.; Nasarre, M.C.; Nelson, R.; et al. Bcl-2 family proteins are essential for platelet survival. *Cell Death Differ.* **2007**, *14*, 943–951, doi:10.1038/sj.cdd.4402081.

135. Wilson, W.H.; O'Connor, O.A.; Czuczman, M.S.; LaCasce, A.S.; Gerecitano, J.F.; Leonard, J.P.; Tulpule, A.; Dunleavy, K.; Xiong, H.; Chiu, Y.L.; et al. Navitoclax, a targeted high-affinity inhibitor of BCL-2, in lymphoid malignancies: A phase 1 dose-escalation study of safety, pharmacokinetics, pharmacodynamics, and antitumour activity. *Lancet Oncol.* **2010**, *11*, 1149–1159, doi:10.1016/S1470-2045(10)70261-8.

136. Zhu, Y.; Doornebal, E.J.; Pirtskhalava, T.; Giorgadze, N.; Wentworth, M.; Fuhrmann-Stroissnigg, H.; Niedernhofer, L.J.; Robbins, P.D.; Tchkonia, T.; Kirkland, J.L. New agents that target senescent cells: The flavone, fisetin, and the BCL-XL inhibitors, A1331852 and A1155463. *Aging (Albany. NY).* **2017**, *9*, 1–9, doi:10.18632/aging.101202.

137. Moncsek, A.; Al-Suraih, M.S.; Trussoni, C.E.; O'Hara, S.P.; Splinter, P.L.; Zuber, C.; Patsenker, E.; Valli, P. V.; Fingas, C.D.; Weber, A.; et al. Targeting senescent cholangiocytes and activated fibroblasts with B-cell lymphoma-extra large inhibitors ameliorates fibrosis in multidrug resistance 2 gene knockout (Mdr2−/−) mice. *Hepatology* **2018**, *67*, 247–259, doi:10.1002/hep.29464.

138. Souers, A.J.; Leverson, J.D.; Boghaert, E.R.; Ackler, S.L.; Catron, N.D.; Chen, J.; Dayton, B.D.; Ding, H.; Enschede, S.H.; Fairbrother, W.J.; et al. ABT-199, a potent and selective BCL-2 inhibitor, achieves antitumor activity while sparing platelets. *Nat. Med.* **2013**, *19*, 202–208, doi:10.1038/nm.3048.

139. Jeon, O.H.; Kim, C.; Laberge, R.M.; Demaria, M.; Rathod, S.; Vasserot, A.P.; Chung, J.W.; Kim, D.H.; Poon, Y.; David, N.; et al. Local clearance of senescent cells attenuates the development of post-traumatic osteoarthritis and creates a pro-regenerative environment. *Nat. Med.* **2017**, *23*, 775–781, doi:10.1038/nm.4324.

140. He, Y.; Li, W.; Lv, D.; Zhang, X.; Zhang, X.; Ortiz, Y.T.; Budamagunta, V.; Campisi, J.; Zheng, G.; Zhou, D. Inhibition of USP7 activity selectively eliminates senescent cells in part via restoration of p53 activity. *Aging Cell* **2020**, *19*, 1–11, doi:10.1111/acel.13117.

141. Wang, Z.; Kang, W.; You, Y.; Pang, J.; Ren, H.; Suo, Z.; Liu, H.; Zheng, Y. USP7: Novel drug target in cancer therapy. *Front. Pharmacol.* **2019**, *10*, 1–15, doi:10.3389/fphar.2019.00427.

142. Taipale, M.; Jarosz, D.F.; Lindquist, S. HSP90 at the hub of protein homeostasis: emerging mechanistic insights. *Nat. Rev. Mol. Cell Biol.* **2010**, *11*, 515–528, doi:10.1038/nrm2918.

143. Fuhrmann-Stroissnigg, H.; Ling, Y.Y.; Zhao, J.; McGowan, S.J.; Zhu, Y.; Brooks, R.W.; Grassi, D.; Gregg, S.Q.; Stripay, J.L.; Dorronsoro, A.; et al. Identification of HSP90 inhibitors as a novel class of senolytics. *Nat. Commun.* **2017**, *8*, doi:10.1038/s41467-017-00314-z.

144. Karkoulis, P.K.; Stravopodis, D.J.; Konstantakou, E.G.; Voutsinas, G.E. Targeted inhibition of heat shock protein 90 disrupts multiple oncogenic signaling pathways, thus inducing cell cycle arrest and programmed cell death in human urinary bladder cancer cell lines. *Cancer Cell Int.* **2013**, *13*, 1, doi:10.1186/1475-2867-13-11.

145. Lucas, C.M.; Milani, M.; Butterworth, M.; Carmell, N.; Scott, L.J.; Clark, R.E.; Cohen, G.M.; Varadarajan, S. High CIP2A levels correlate with an antiapoptotic phenotype that can be overcome by targeting BCL-X L in chronic myeloid leukemia. *Leukemia* **2016**, *30*, 1273–1281, doi:10.1038/leu.2016.42.

146. Naeimi, A.F.; Alizadeh, M. Antioxidant properties of the flavonoid fisetin: An updated review of in vivo and in vitro studies. *Trends Food Sci. Technol.* **2017**, *70*, 34–44, doi:https://doi.org/10.1016/j.tifs.2017.10.003.

147. Youns, M.; Abdel Halim Hegazy, W. The Natural Flavonoid Fisetin Inhibits Cellular Proliferation of Hepatic, Colorectal, and Pancreatic Cancer Cells through Modulation of Multiple Signaling Pathways. *PLoS One* **2017**, *12*, e0169335, doi:10.1371/journal.pone.0169335.

148. Myrianthopoulos, V.; Evangelou, K.; Vasileiou, P.V.S.; Cooks, T.; Vassilakopoulos, T.P.; Pangalis, G.A.; Kouloukoussa, M.; Kittas, C.; Georgakilas, A.G.; Gorgoulis, V.G. Senescence and senotherapeutics: a new field in cancer therapy. *Pharmacol. Ther.* 2019, *193*, 31–49.

149. Zheng, J.; Son, D.J.; Gu, S.M.; Woo, J.R.; Ham, Y.W.; Lee, H.P.; Kim, W.J.; Jung, J.K.; Hong, J.T. Piperlongumine inhibits lung tumor growth via inhibition of nuclear factor kappa B signaling pathway. *Sci. Rep.* **2016**, *6*, doi:10.1038/srep26357.

150. Dörr, J.R.; Yu, Y.; Milanovic, M.; Beuster, G.; Zasada, C.; Däbritz, J.H.M.; Lisec, J.; Lenze, D.; Gerhardt, A.; Schleicher, K.; et al. Synthetic lethal metabolic targeting of cellular senescence in cancer therapy. *Nature* **2013**, *501*, 421–425, doi:10.1038/nature12437.

151. Sagiv, A.; Burton, D.G.A.; Moshayev, Z.; Vadai, E.; Wensveen, F.; Ben-Dor, S.; Golani, O.; Polic, B.; Krizhanovsky, V. NKG2D ligands mediate immunosurveillance of senescent cells. *Aging (Albany. NY).* **2016**, *8*, 328–344, doi:10.18632/aging.100897.

152. Sagiv, A.; Biran, A.; Yon, M.; Simon, J.; Lowe, S.W.; Krizhanovsky, V. Granule exocytosis mediates immune surveillance of senescent cells. *Oncogene* **2013**, *32*, 1971–1977, doi:10.1038/onc.2012.206.

153. Krizhanovsky, V.; Yon, M.; Dickins, R.A.; Hearn, S.; Simon, J.; Miething, C.; Yee, H.; Zender, L.; Lowe, S.W. Senescence of Activated Stellate Cells Limits Liver Fibrosis. *Cell* **2008**, *134*, 657–667, doi:10.1016/j.cell.2008.06.049.

154. Kang, T.W.; Yevsa, T.; Woller, N.; Hoenicke, L.; Wuestefeld, T.; Dauch, D.; Hohmeyer, A.; Gereke, M.; Rudalska, R.; Potapova, A.; et al. Senescence surveillance of pre-malignant hepatocytes limits liver cancer development.

Nature **2011**, *479*, 547–551, doi:10.1038/nature10599.

155. Grupp, S.A.; Kalos, M.; Barrett, D.; Aplenc, R.; Porter, D.L.; Rheingold, S.R.; Teachey, D.T.; Chew, A.; Hauck, B.; Wright, J.F.; et al. Chimeric Antigen Receptor–Modified T Cells for Acute Lymphoid Leukemia. *N. Engl. J. Med.* **2013**, *368*, 1509–1518, doi:10.1056/NEJMoa1215134.

156. Amor, C.; Feucht, J.; Leibold, J.; Ho, Y.J.; Zhu, C.; Alonso-Curbelo, D.; Mansilla-Soto, J.; Boyer, J.A.; Li, X.; Giavridis, T.; et al. Senolytic CAR T cells reverse senescence-associated pathologies. *Nature* **2020**, doi:10.1038/s41586-020-2403-9.

157. Burton, D.G.A.; Stolzing, A. Cellular senescence: Immunosurveillance and future immunotherapy. *Ageing Res. Rev.* **2018**, *43*, 17–25, doi:10.1016/j.arr.2018.02.001.

158. Pardoll, D.M. The blockade of immune checkpoints in cancer immunotherapy. *Nat. Rev. Cancer* **2012**, *12*, 252–264, doi:10.1038/nrc3239.

159. Baruch, K.; Deczkowska, A.; Rosenzweig, N.; Tsitsou-Kampeli, A.; Sharif, A.M.; Matcovitch-Natan, O.; Kertser, A.; David, E.; Amit, I.; Schwartz, M. PD-1 immune checkpoint blockade reduces pathology and improves memory in mouse models of Alzheimer's disease. *Nat. Med.* **2016**, *22*, 135–137, doi:10.1038/nm.4022.

160. Kim, K.M.; Noh, J.H.; Bodogai, M.; Martindale, J.L.; Yang, X.; Indig, F.E.; Basu, S.K.; Ohnuma, K.; Morimoto, C.; Johnson, P.F.; et al. Identification of senescent cell surface targetable protein DPP4. *Genes Dev.* **2017**, *31*, 1529–1534, doi:10.1101/gad.302570.117.

161. Frescas, D.; Roux, C.M.; Aygun-Sunar, S.; Gleiberman, A.S.; Krasnov, P.; Kurnasov, O. V.; Strom, E.; Virtuoso, L.P.; Wrobel, M.; Osterman, A.L.; et al. Senescent cells expose and secrete an oxidized form of membrane-bound vimentin as revealed by a natural polyreactive antibody. *Proc. Natl. Acad. Sci. U. S. A.* **2017**, *114*, E1668–E1677, doi:10.1073/pnas.1614661114.

162. Pignolo, R.J.; Passos, J.F.; Khosla, S.; Tchkonia, T.; Kirkland, J.L. Reducing Senescent Cell Burden in Aging and Disease. *Trends Mol. Med.* **2020**, *26*, 630–638, doi:10.1016/j.molmed.2020.03.005.

163. Yoshida, S.; Nakagami, H.; Hayashi, H.; Ikeda, Y.; Sun, J.; Tenma, A.; Tomioka, H.; Kawano, T.; Shimamura, M.; Morishita, R.; et al. The CD153 vaccine is a senotherapeutic option for preventing the accumulation of senescent T cells in mice. *Nat. Commun.* **2020**, *11*, 1–10, doi:10.1038/s41467-020-16347-w.

164. Weiland, T.; Lampe, J.; Essmann, F.; Venturelli, S.; Berger, A.; Bossow, S.; Berchtold, S.; Schulze-Osthoff, K.; Lauer, U.M.; Bitzer, M. Enhanced killing of therapy-induced senescent tumor cells by oncolytic measles vaccine viruses. *Int. J. Cancer* **2014**, *134*, 235–243, doi:10.1002/ijc.28350.

165. Henson, S.M.; Lanna, A.; Riddel, N.E.; Franzese, O.; Macaulay, R.; Griffiths, S.J.; Puleston, D.J.; Watson, A.S.; Simon, A.K.; Tooze, S.A.; et al. P38 signaling inhibits mTORC1-independent autophagy in senescent human CD8+ T cells. *J. Clin. Invest.* **2014**, *124*, 4004–4016, doi:10.1172/JCI75051.

166. Latorre, E.; Birar, V.C.; Sheerin, A.N.; Jeynes, J.C.C.; Hooper, A.; Dawe, H.R.; Melzer, D.; Cox, L.S.; Faragher, R.G.A.; Ostler, E.L.; et al. Small molecule modulation of splicing factor expression is associated with rescue from cellular senescence. *BMC Cell Biol.* **2017**, *18*, 1–15, doi:10.1186/s12860-017-0147-7.

167. Chen, J.; Chen, K.H.; Fu, B.Q.; Zhang, W.; Dai, H.; Lin, L.R.; Wang, L.M.; He, Y.N. Isolation and identification of senescent renal tubular epithelial cells using immunomagnetic beads based on DcR2. *Exp. Gerontol.* **2017**, *95*, 116–127, doi:10.1016/j.exger.2017.04.008.

168. Rebo, J.; Causey, K.; Zealley, B.; Webb, T.; Hamalainen, M.; Cook, B.; Schloendorn, J. Whole-animal senescent cytotoxic T cell removal using antibodies linked to magnetic nanoparticles. *Rejuvenation Res.* **2010**, *13*, 298–300,

doi:10.1089/rej.2009.0964.

169. Soto-Gamez, A.; Demaria, M. Therapeutic interventions for aging: the case of cellular senescence. *Drug Discov. Today* **2017**, *22*, 786–795, doi:10.1016/j.drudis.2017.01.004.

170. Chrousos, G.P.; Kino, T. Glucocorticoid Signaling in the Cell. *Ann. N. Y. Acad. Sci.* **2009**, *1179*, 153–166, doi:10.1111/j.1749-6632.2009.04988.x.

171. Zanchi, N.E.; De Siqueira Filho, M.A.; Felitti, V.; Nicastro, H.; Lorenzeti, F.M.; Lancha, A.H. Glucocorticoids: Extensive physiological actions modulated through multiple mechanisms of gene regulation. *J. Cell. Physiol.* **2010**, *224*, 311–315, doi:10.1002/jcp.22141.

172. Laberge, R.M.; Zhou, L.; Sarantos, M.R.; Rodier, F.; Freund, A.; de Keizer, P.L.J.; Liu, S.; Demaria, M.; Cong, Y.S.; Kapahi, P.; et al. Glucocorticoids suppress selected components of the senescence-associated secretory phenotype. *Aging Cell* 2012, *11*, 569–578.

173. Holman, R.R.; Paul, S.K.; Bethel, M.A.; Matthews, D.R.; Neil, H.A.W. 10-Year Follow-up of Intensive Glucose Control in Type 2 Diabetes. *N. Engl. J. Med.* 2008, *359*, 1577–1589.

174. Gandini, S.; Puntoni, M.; Heckman-Stoddard, B.M.; Dunn, B.K.; Ford, L.; DeCensi, A.; Szabo, E. Metformin and cancer risk and mortality: A systematic review and meta-analysis taking into account biases and confounders. *Cancer Prev. Res.* **2014**, *7*, 867–885, doi:10.1158/1940-6207.CAPR-13-0424.

175. Stavri, S.; Trusca, V.G.; Simionescu, M.; Gafencu, A. V. Metformin reduces the endotoxin-induced down-regulation of apolipoprotein e gene expression in macrophages. *Biochem. Biophys. Res. Commun.* **2015**, *461*, 435–440, doi:10.1016/j.bbrc.2015.04.057.

176. Moiseeva, O.; Deschênes-Simard, X.; St-Germain, E.; Igelmann, S.; Huot, G.; Cadar, A.E.; Bourdeau, V.; Pollak, M.N.; Ferbeyre, G. Metformin inhibits the senescence-associated secretory phenotype by interfering with IKK/NF-κB activation. *Aging Cell* **2013**, *12*, 489–498, doi:10.1111/acel.12075.

177. Hu, Q.; Peng, J.; Jiang, L.; Li, W.; Su, Q.; Zhang, J.; Li, H.; Song, M.; Cheng, B.; Xia, J.; et al. Metformin as a senostatic drug enhances the anticancer efficacy of CDK4/6 inhibitor in head and neck squamous cell carcinoma. *Cell Death Dis.* 2020, *11*.

178. Iliopoulos, D.; Hirsch, H.A.; Struhl, K. Metformin Decreases the Dose of Chemotherapy for Prolonging Tumor Remission in Mouse Xenografts Involving Multiple Cancer Cell Types. **2011**, doi:10.1158/0008-5472.CAN-10-3471.

179. Hirsch, H.A.; Iliopoulos, D.; Tsichlis, P.N.; Struhl, K. Metformin Selectively Targets Cancer Stem Cells, and Acts Together with Chemotherapy to Block Tumor Growth and Prolong Remission. *Cancer Res* **2009**, *69*, 7507–7518, doi:10.1158/0008-5472.CAN-09-2994.

180. Pitozzi, V.; Mocali, A.; Laurenzana, A.; Giannoni, E.; Cifola, I.; Battaglia, C.; Chiarugi, P.; Dolara, P.; Giovannelli, L. Chronic resveratrol treatment ameliorates cell adhesion and mitigates the inflammatory phenotype in senescent human fibroblasts. *Journals Gerontol. - Ser. A Biol. Sci. Med. Sci.* **2013**, *68*, 371–381, doi:10.1093/gerona/gls183.

181. Lim, H.; Park, H.; Kim, H.P. Effects of flavonoids on senescence-associated secretory phenotype formation from bleomycin-induced senescence in BJ fibroblasts. *Biochem. Pharmacol.* **2015**, *96*, 337–348, doi:10.1016/j.bcp.2015.06.013.

182. Laberge, R.M.; Sun, Y.; Orjalo, A. V.; Patil, C.K.; Freund, A.; Zhou, L.; Curran, S.C.; Davalos, A.R.; Wilson-Edell, K.A.; Liu, S.; et al. MTOR regulates the pro-tumorigenic senescence-associated secretory phenotype by promoting IL1A translation. *Nat. Cell Biol.* **2015**, *17*, 1049–1061, doi:10.1038/ncb3195.

183. Luo, Y.; Zheng, S.G. Hall of fame among pro-inflammatory cytokines: Interleukin-6 gene and its transcriptional regulation mechanisms. *Front. Immunol.* **2016**, *7*, 1–7, doi:10.3389/fimmu.2016.00604.

184. Xu, M.; Tchkonia, T.; Kirkland, J.L. Perspective: Targeting the JAK/STAT pathway to fight age-related dysfunction. *Pharmacol. Res.* **2016**, *111*, 152–154, doi:10.1016/j.phrs.2016.05.015.

185. Xu, M.; Tchkonia, T.; Ding, H.; Ogrodnik, M.; Lubbers, E.R.; Pirtskhalava, T.; White, T.A.; Johnson, K.O.; Stout, M.B.; Mezera, V.; et al. JAK inhibition alleviates the cellular senescence-associated secretory phenotype and frailty in old age. *Proc. Natl. Acad. Sci. U. S. A.* **2015**, *112*, E6301–E6310, doi:10.1073/pnas.1515386112.

186. Toso, A.; Di Mitri, D.; Alimonti, A. Enhancing chemotherapy efficacy by reprogramming the senescence-associated secretory phenotype of prostate tumors: A way to reactivate the antitumor immunity. *Oncoimmunology* **2015**, *4*, 1–3, doi:10.4161/2162402X.2014.994380.

187. Meyer, S.C.; Levine, R.L. Molecular pathways: Molecular basis for sensitivity and resistance to JAK kinase inhibitors. *Clin. Cancer Res.* **2014**, *20*, 2051–2059, doi:10.1158/1078-0432.CCR-13-0279.

188. Vainchenker, W.; Leroy, E.; Gilles, L.; Marty, C.; Plo, I.; Constantinescu, S.N. JAK inhibitors for the treatment of myeloproliferative neoplasms and other disorders. *F1000Research* **2018**, *7*, 1–19, doi:10.12688/f1000research.13167.1.

189. Nacarelli, T.; Liu, P.; Zhang, R. Epigenetic basis of cellular senescence and its implications in aging. *Genes (Basel).* **2017**, *8*, doi:10.3390/genes8120343.

190. Capell, B.C.; Drake, A.M.; Zhu, J.; Shah, P.P.; Dou, Z.; Dorsey, J.; Simola, D.F.; Donahue, G.; Sammons, M.; Rai, T.S.; et al. Mll1 is essential for the senescenceassociated secretory phenotype. *Genes Dev.* **2016**, *30*, 321–336, doi:10.1101/gad.271882.115.

191. Vizioli, M.G.; Adams, P.D. Senescence can Be BETter without the SASP? *Cancer Discov.* **2016**, *6*, 576–578, doi:10.1158/2159-8290.CD-16-0485.

192. Tasdemir, N.; Banito, A.; Roe, J.S.; Alonso-Curbelo, D.; Camiolo, M.; Tschaharganeh, D.F.; Huang, C.H.; Aksoy, O.; Bolden, J.E.; Chen, C.C.; et al. BRD4 connects enhancer remodeling to senescence immune surveillance. *Cancer Discov.* **2016**, *6*, 613–629, doi:10.1158/2159-8290.CD-16-0217.

193. Filippakopoulos, P.; Qi, J.; Picaud, S.; Shen, Y.; Smith, W.B.; Fedorov, O.; Morse, E.M.; Keates, T.; Hickman, T.T.; Felletar, I.; et al. Selective inhibition of BET bromodomains. *Nature* **2010**, *468*, 1067–1073, doi:10.1038/nature09504.

194. Karkera, J.; Steiner, H.; Li, W.; Skradski, V.; Moser, P.L.; Riethdorf, S.; Reddy, M.; Puchalski, T.; Safer, K.; Prabhakar, U.; et al. The anti-interleukin-6 antibody siltuximab down-regulates genes implicated in tumorigenesis in prostate cancer patients from a phase i study. *Prostate* **2011**, *71*, 1455–1465, doi:10.1002/pros.21362.

195. Emery, P.; Keystone, E.; Tony, H.P.; Cantagrel, A.; Van Vollenhoven, R.; Sanchez, A.; Alecock, E.; Lee, J.; Kremer, J. IL-6 receptor inhibition with tocilizumab improves treatment outcomes in patients with rheumatoid arthritis refractory to anti-tumour necrosis factor biologicals: Results from a 24-week multicentre randomised placebo-controlled trial. *Ann. Rheum. Dis.* **2008**, *67*, 1516–1523, doi:10.1136/ard.2008.092932.

196. Shih, T.; Lindley, C. Bevacizumab: An angiogenesis inhibitor for the treatment of solid malignancies. *Clin. Ther.* **2006**, *28*, 1779–1802, doi:https://doi.org/10.1016/j.clinthera.2006.11.015.

197. Paez-Ribes, M.; González-Gualda, E.; Doherty, G.J.; Muñoz-Espín, D. Targeting senescent cells in translational medicine. *EMBO Mol. Med.* **2019**, e10234, doi:10.15252/emmm.201810234.

198. Pellegrini, G.; Dellambra, E.; Paterna, P.; Golisano, O.; Traverso, C.E.; Rama, P.; Lacal, P.; De Luca, M. Telomerase activity is sufficient to bypass replicative senescence in human limbal and conjunctival but not corneal keratinocytes. *Eur. J. Cell Biol.* **2004**, *83*, 691–700, doi:10.1078/0171-9335-00424.

199. Dietrich, N.; Bracken, A.P.; Trinh, E.; Schjerling, C.K.; Koseki, H.; Rappsilber, J.; Helin, K.; Hansen, K.H. Bypass of senescence by the polycomb group protein CBX8 through direct binding to the INK4A-ARF locus. *EMBO J.* **2007**, *26*, 1637–1648, doi:10.1038/sj.emboj.7601632.

200. Acosta, J.C.; O'Loghlen, A.; Banito, A.; Guijarro, M. V.; Augert, A.; Raguz, S.; Fumagalli, M.; Da Costa, M.; Brown, C.; Popov, N.; et al. Chemokine Signaling via the CXCR2 Receptor Reinforces Senescence. *Cell* **2008**, *133*, 1006–1018, doi:10.1016/j.cell.2008.03.038.

201. Abad, M.; Mosteiro, L.; Pantoja, C.; Cañamero, M.; Rayon, T.; Ors, I.; Graña, O.; Megías, D.; Domínguez, O.; Martínez, D.; et al. Reprogramming in vivo produces teratomas and iPS cells with totipotency features. *Nature* **2013**, *502*, 340–345, doi:10.1038/nature12586.

202. Agostini, A.; Mondragõn, L.; Bernardos, A.; Martínez-Máñez, R.; Dolores Marcos, M.; Sancenõn, F.; Soto, J.; Costero, A.; Manguan-García, C.; Perona, R.; et al. Targeted cargo delivery in senescent cells using capped mesoporous silica nanoparticles. *Angew. Chemie - Int. Ed.* **2012**, *51*, 10556–10560, doi:10.1002/anie.201204663.

203. Muñoz-Espín, D.; Rovira, M.; Galiana, I.; Giménez, C.; Lozano-Torres, B.; Paez-Ribes, M.; Llanos, S.; Chaib, S.; Muñoz-Martín, M.; Ucero, A.C.; et al. A versatile drug delivery system targeting senescent cells. *EMBO Mol. Med.* **2018**, *10*, 1–18, doi:10.15252/emmm.201809355.

204. Lewinska, A.; Adamczyk-Grochala, J.; Bloniarz, D.; Olszowka, J.; Kulpa-Greszta, M.; Litwinienko, G.; Tomaszewska, A.; Wnuk, M.; Pazik, R. AMPK-mediated senolytic and senostatic activity of quercetin surface functionalized Fe3O4 nanoparticles during oxidant-induced senescence in human fibroblasts. *Redox Biol.* **2020**, *28*, 101337, doi:10.1016/j.redox.2019.101337.

205. Ke, S.; Lai, Y.; Zhou, T.; Li, L.; Wang, Y.; Ren, L.; Ye, S. Molybdenum Disulfide Nanoparticles Resist Oxidative Stress-Mediated Impairment of Autophagic Flux and Mitigate Endothelial Cell Senescence and Angiogenic Dysfunctions. *ACS Biomater. Sci. Eng.* **2018**, *4*, 663–674, doi:10.1021/acsbiomaterials.7b00714.

206. Thapa, R.K.; Nguyen, H.T.; Jeong, J.H.; Kim, J.R.; Choi, H.G.; Yong, C.S.; Kim, J.O. Progressive slowdown/prevention of cellular senescence by CD9-targeted delivery of rapamycin using lactose-wrapped calcium carbonate nanoparticles. *Sci. Rep.* **2017**, *7*, 1–11, doi:10.1038/srep43299.

207. Ekpenyong-Akiba, A.E.; Canfarotta, F.; Abd, B.; Poblocka, M.; Casulleras, M.; Castilla-Vallmanya, L.; Kocsis-Fodor, G.; Kelly, M.E.; Janus, J.; Althubiti, M.; et al. Detecting and targeting senescent cells using molecularly imprinted nanoparticles. *Nanoscale Horizons* **2019**, *4*, 757–768, doi:10.1039/c8nh00473k.

208. Belcastro, E.; Rehman, A.U.; Remila, L.; Park, S.H.; Gong, D.S.; Anton, N.; Auger, C.; Lefebvre, O.; Goetz, J.G.; Collot, M.; et al. Fluorescent nanocarriers targeting VCAM-1 for early detection of senescent endothelial cells. *Nanomedicine Nanotechnology, Biol. Med.* **2021**, *34*, 102379, doi:10.1016/j.nano.2021.102379.

209. Wang, H.H.; Lin, C.A.J.; Tseng, Y.M.; Lee, H.I.; Lee, Y.N.; Yeh, H.I.; Yang, P.S.; Peng, H.Y.; Wu, Y.J. Dihydrolipoic acid-coated gold nanocluster bioactivity against senescence and inflammation through the mitochondria-mediated JNK/AP-1 pathway. *Nanomedicine Nanotechnology, Biol. Med.* **2021**, *36*, 102427, doi:10.1016/j.nano.2021.102427.

210. Pham, L.M.; Kim, E.C.; Ou, W.; Phung, C.D.; Nguyen, T.T.; Pham, T.T.; Poudel, K.; Gautam, M.; Nguyen, H.T.; Jeong, J.H.; et al. Targeting and clearance of senescent foamy macrophages and senescent endothelial cells by

antibody-functionalized mesoporous silica nanoparticles for alleviating aorta atherosclerosis. *Biomaterials* **2021**, *269*, 120677, doi:10.1016/j.biomaterials.2021.120677.

211. Lee Ventola, C. *Progress in Nanomedicine: Approved and Investigational Nanodrugs*; 2017; Vol. 42;.

212. What is nanomedicine? | ETPN Available online: https://etp-nanomedicine.eu/about-nanomedicine/what-is-nanomedicine/ (accessed on Jun 15, 2021).

213. *The Nanomedicine Revolution, Part 2*;

214. European Commission On the definition of nanomaterial Text with EEA relevance. *Off. J. Eur. Union* **2011**, *275*, 38–40.

215. Germain, M.; Caputo, F.; Metcalfe, S.; Tosi, G.; Spring, K.; Åslund, A.K.O.; Pottier, A.; Schiffelers, R.; Ceccaldi, A.; Schmid, R. Delivering the power of nanomedicine to patients today. *J. Control. Release* **2020**, *326*, 164–171, doi:10.1016/j.jconrel.2020.07.007.

216. Anselmo, A.C.; Mitragotri, | Samir; Mitragotri, S.; Paulson, J.A. Nanoparticles in the clinic: An update. *Bioeng Transl Med* **2019**, *4*, doi:10.1002/btm2.10143.

217. Marques, M.R.C.; Choo, Q.; Ashtikar, M.; Rocha, T.C.; Bremer-Hoffmann, S.; Wacker, M.G. Nanomedicines - Tiny particles and big challenges. *Adv. Drug Deliv. Rev.* **2019**, *151–152*, 23–43, doi:10.1016/j.addr.2019.06.003.

218. Weissig, V.; Pettinger, T.K.; Murdock, N. Nanopharmaceuticals (part 1): products on the market. *Int. J. Nanomedicine* **2014**, *9*, 4357–4373, doi:10.2147/IJN.S46900.

219. Anselmo, A.C.; Mitragotri, S. Nanoparticles in the clinic: An update post COVID-19 vaccines. *Bioeng. Transl. Med.* 2021, *6*.

220. Adams, D.; Gonzalez-Duarte, A.; O'Riordan, W.D.; Yang, C.-C.; Ueda, M.; Kristen, A. V.; Tournev, I.; Schmidt, H.H.; Coelho, T.; Berk, J.L.; et al. Patisiran, an RNAi Therapeutic, for Hereditary Transthyretin Amyloidosis. *N. Engl. J. Med.* **2018**, *379*, 11–21, doi:10.1056/nejmoa1716153.

221. Haynes, B.F. A New Vaccine to Battle Covid-19. *N. Engl. J. Med.* 2021, *384*, 470–471.

222. Udugama, B.; Kadhiresan, P.; Kozlowski, H.N.; Malekjahani, A.; Osborne, M.; Li, V.Y.C.; Chen, H.; Mubareka, S.; Gubbay, J.B.; Chan, W.C.W. Diagnosing COVID-19: The Disease and Tools for Detection. *ACS Nano* **2020**, *14*, 3822–3835, doi:10.1021/acsnano.0c02624.

223. Le, T.T.; Cramer, J.P.; Chen, R.; Mayhew, S. Evolution of the COVID-19 vaccine development landscape. *Nat. Rev. Drug Discov.* 2020, *19*, 667–668.

224. Liu, C.; Zhou, Q.; Li, Y.; Garner, L. V; Watkins, S.P.; Carter, L.J.; Smoot, J.; Gregg, A.C.; Daniels, A.D.; Jervey, S.; et al. Research and Development on Therapeutic Agents and Vaccines for COVID-19 and Related Human Coronavirus Diseases. *ACS Cent. Sci.* 2020, *6*, 315–331.

225. Saboktakin, M. The biological and biomedical nanoparticles - synthesis and applications. *Adv. Mater. Sci.* **2017**, *2*, 1–14, doi:10.15761/ams.1000127.

226. Emerich, D.F.; Thanos, C.G. Targeted nanoparticle-based drug delivery and diagnosis. *J. Drug Target.* **2007**, *15*, 163–183, doi:10.1080/10611860701231810.

227. Jahangirian, H.; Kalantari, K.; Izadiyan, Z.; Rafiee-Moghaddam, R.; Shameli, K.; Webster, T.J. A review of small molecules and drug delivery applications using gold and iron nanoparticles. *Int. J. Nanomedicine* 2019, *14*, 1633–1657.

228. Pudlarz, A.; Szemraj, J. Nanoparticles as carriers of proteins, peptides and other therapeutic molecules. *Open Life Sci.* 2018, *13*, 285–298.

229. Adamczyk-Grochala, J.; Lewinska, A. Nano-Based Theranostic Tools for the Detection and Elimination of Senescent Cells. *Cells* 2020, *9*.

230. Bala Tannan, N.; Manzari, M.T.; Herviou, L.; Da Silva Ferreira, M.; Hagen, C.; Kiguchi, H.; Manova-Todorova, K.; Seshan, V.; de Stanchina, E.; Heller, D.A.; et al. Tumor-targeted nanoparticles improve the therapeutic index of BCL2 and MCL1 dual inhibition. *Blood* **2021**, *137*, 2057–2069, doi:10.1182/blood.2020008017.

231. Yoon, M.S. Nanotechnology-based targeting of mTOR signaling in cancer. *Int. J. Nanomedicine* **2020**, *15*, 5767–5781, doi:10.2147/IJN.S254574.

232. Kwapisz, D. Cyclin-dependent kinase 4/6 inhibitors in breast cancer: palbociclib, ribociclib, and abemaciclib. *Breast Cancer Res. Treat.* **2017**, *166*, 41–54, doi:10.1007/s10549-017-4385-3.

233. Schafer, M.J.; White, T.A.; Iijima, K.; Haak, A.J.; Ligresti, G.; Atkinson, E.J.; Oberg, A.L.; Birch, J.; Salmonowicz, H.; Zhu, Y.; et al. Cellular senescence mediates fibrotic pulmonary disease. *Nat. Commun.* **2017**, *8*, doi:10.1038/ncomms14532.

234. Rostamizadeh, K.; Abdollahi, H.; Parsajoo, C. Synthesis, optimization, and characterization of molecularly imprinted nanoparticles. *Int. Nano Lett.* **2013**, *3*, 1–9, doi:10.1186/2228-5326-3-20.

235. Althubiti, M.; Lezina, L.; Carrera, S.; Jukes-Jones, R.; Giblett, S.M.; Antonov, A.; Barlev, N.; Saldanha, G.S.; Pritchard, C.A.; Cain, K.; et al. Characterization of novel markers of senescence and their prognostic potential in cancer. *Cell Death Dis.* **2014**, *5*, e1528-10, doi:10.1038/cddis.2014.489.

236. Althubiti, M.; Macip, S. Detection of senescent cells by extracellular markers using a flow cytometry-based approach. *Methods Mol. Biol.* **2017**, *1534*, 147–153, doi:10.1007/978-1-4939-6670-7_14.

237. Kim, C.O.; Huh, A.J.; Han, S.H.; Kim, J.M. Analysis of cellular senescence induced by lipopolysaccharide in pulmonary alveolar epithelial cells. *Arch. Gerontol. Geriatr.* **2012**, *54*, e35-41, doi:10.1016/j.archger.2011.07.016.

238. Cho, J.H.; Kim, E.-C.; Son, Y.; Lee, D.-W.; Park, Y.S.; Choi, J.H.; Cho, K.-H.; Kwon, K.-S.; Kim, J.-R. CD9 induces cellular senescence and aggravates atherosclerotic plaque formation. *Cell Death Differ.* **2020**, *27*, 2681–2696, doi:10.1038/s41418-020-0537-9.

239. Wang, Y.; Liu, J.; Ma, X.; Cui, C.; Deenik, P.R.; Henderson, P.K.P.; Sigler, A.L.; Cui, L. Real-time imaging of senescence in tumors with DNA damage. *Sci. Rep.* **2019**, *9*, 2102, doi:10.1038/s41598-019-38511-z.

240. Lee, H.W.; Heo, C.H.; Sen, D.; Byun, H.O.; Kwak, I.H.; Yoon, G.; Kim, H.M. Ratiometric two-photon fluorescent probe for quantitative detection of β-galactosidase activity in senescent cells. *Anal. Chem.* **2014**, *86*, 10001–10005, doi:10.1021/ac5031013.

241. Zhang, J.; Li, C.; Dutta, C.; Fang, M.; Zhang, S.; Tiwari, A.; Werner, T.; Luo, F.T.; Liu, H. A novel near-infrared fluorescent probe for sensitive detection of β-galactosidase in living cells. *Anal. Chim. Acta* **2017**, *968*, 97–104, doi:10.1016/j.aca.2017.02.039.

242. Lozano-Torres, B.; Galiana, I.; Rovira, M.; Garrido, E.; Chaib, S.; Bernardos, A.; Muñoz-Espín, D.; Serrano, M.; Martínez-Máñez, R.; Sancenón, F. An OFF-ON Two-Photon Fluorescent Probe for Tracking Cell Senescence in Vivo. *J. Am. Chem. Soc.* **2017**, *139*, 8808–8811, doi:10.1021/jacs.7b04985.

243. Asanuma, D.; Sakabe, M.; Kamiya, M.; Yamamoto, K.; Hiratake, J.; Ogawa, M.; Kosaka, N.; Choyke, P.L.; Nagano, T.; Kobayashi, H.; et al. Sensitive β-galactosidase-targeting fluorescence probe for visualizing small

peritoneal metastatic tumours in vivo. *Nat. Commun.* **2015**, *6*, doi:10.1038/ncomms7463.

244. Ang, J.; Lee, Y.A.; Raghothaman, D.; Jayaraman, P.; Teo, K.L.; Khan, F.J.; Reuveny, S.; Chang, Y.T.; Kang, N.Y.; Oh, S. Rapid Detection of Senescent Mesenchymal Stromal Cells by a Fluorescent Probe. *Biotechnol. J.* **2019**, *14*, 1–10, doi:10.1002/biot.201800691.

245. Tang, C.; Zhou, J.; Qian, Z.; Ma, Y.; Huang, Y.; Feng, H. A universal fluorometric assay strategy for glycosidases based on functional carbon quantum dots: β-galactosidase activity detection in vitro and in living cells. *J. Mater. Chem. B* **2017**, *5*, 1971–1979, doi:10.1039/C6TB03361J.

246. Jiang, G.; Zeng, G.; Zhu, W.; Li, Y.; Dong, X.; Zhang, G.; Fan, X.; Wang, J.; Wu, Y.; Tang, B.Z. A selective and light-up fluorescent probe for β-galactosidase activity detection and imaging in living cells based on an AIE tetraphenylethylene derivative. *Chem. Commun.* **2017**, *53*, 4505–4508, doi:10.1039/C7CC00249A.

247. Wang, W.; Vellaisamy, K.; Li, G.; Wu, C.; Ko, C.-N.; Leung, C.-H.; Ma, D.-L. Development of a Long-Lived Luminescence Probe for Visualizing β-Galactosidase in Ovarian Carcinoma Cells. *Anal. Chem.* **2017**, *89*, 11679–11684, doi:10.1021/acs.analchem.7b03114.

248. Huang, J.; Li, N.; Wang, Q.; Gu, Y.; Wang, P. A lysosome-targetable and two-photon fluorescent probe for imaging endogenous β-galactosidase in living ovarian cancer cells. *Sensors Actuators B Chem.* **2017**, *246*, 833–839, doi:https://doi.org/10.1016/j.snb.2017.02.158.

249. Justice, J.N.; Nambiar, A.M.; Tchkonia, T.; LeBrasseur, N.K.; Pascual, R.; Hashmi, S.K.; Prata, L.; Masternak, M.M.; Kritchevsky, S.B.; Musi, N.; et al. Senolytics in idiopathic pulmonary fibrosis: Results from a first-in-human, open-label, pilot study. *EBioMedicine* **2019**, *40*, 554–563, doi:10.1016/j.ebiom.2018.12.052.

250. Hickson, L.T.J.; Langhi Prata, L.G.P.; Bobart, S.A.; Evans, T.K.; Giorgadze, N.; Hashmi, S.K.; Herrmann, S.M.; Jensen, M.D.; Jia, Q.; Jordan, K.L.; et al. Senolytics decrease senescent cells in humans: Preliminary report from a clinical trial of Dasatinib plus Quercetin in individuals with diabetic kidney disease. *EBioMedicine* **2019**, *47*, 446–456, doi:10.1016/j.ebiom.2019.08.069.

251. Kirkland, J.L.; Tchkonia, T.; Zhu, Y.; Niedernhofer, L.J.; Robbins, P.D. The Clinical Potential of Senolytic Drugs. *J. Am. Geriatr. Soc.* **2017**, *65*, 2297–2301, doi:10.1111/jgs.14969.

Background, Hypothesis and Objectives.

Background.

Cellular senescence is a dynamic biological phenomenon that impacts several physiological and pathological processes ranging from tissue regeneration and development, wound healing, age-related diseases, and cancer [1]. Plenty of research is guided towards understanding the molecular biological aspects governing cellular senescence in order to find the best therapeutic approaches and strategies targeted towards eliminating senescent cells and the side effects/ pathologies caused by their accumulation. This thesis work is divided into two chapters and is based on the following backgrounds:

Chapter 1: *"TSP1 C-terminal Derived Peptides and their Effect on Cancer and senescent cells through CD47 Receptor".*

The main feature of cellular senescence is the irreversible cell cycle arrest [2,3]. Controversially, recently published papers indicated that when cancer cells are treated with chemotherapy or radiotherapy, a small portion of the cell enters the senescence state and maintains the possibility to re-enter the cell cycle, which is called senescence escape /emergence [4–16]. The emerged cells express higher tumour-initiation capacity compared to the cancer cells that have not entered cellular senescence [1] and thought to be the reason behind cancer relapse after months or years from treatment [12].

Our lab is mainly interested in molecular biological aspects that govern cellular senescence; especially molecular pathways responsible for emergence from chemotherapy-induced senescence CIS. Our lab recently investigated the role of TSP-1 and CD47 receptor in the emergence from CIS, and they found the following:

- TSP1 can be detected in the serum of patients suffering from triple-negative breast cancer and that its low expression was associated with treatment failure [7].
- TSP1 blocked senescence escape in LS174T cells after treatment with Sn38; however, this was not the case among using antibody B6H12 that blocks the CD47-TSP1 binding, this proves that TSP1 is necessary for preventing senescence escape [8].
- emergent cells have low CD47 expression [8].

TSP1 is a homotrimeric glycoprotein, has several functions depending on the cell surface molecules it interacts with [17]. 4N1Ks and 7N3 are small peptides derived from the C-terminal domain of TSP1 that binds to CD47 receptor [18][19]. These peptides have been used in

research instead of TSP1 due to their small size and possible higher selectivity towards CD47 receptor.

Chapter 2: *"Senolytic/ Senostatic Sphingomyelin based Nanosystems targeting MCF7 senescent cells".* Sphingomyelin based nanosystem SNs is a novel drug delivery system developed in Nano-oncology research Group of Dr. Maria De la Fuente. SNs are characterized by their biodegradability, biocompatibility, and the versatility for association and encapsulation of variety of therapeutic molecules [20–22]. It has been the base for formulating several nanosystems loaded or associated with peptides, antibodies, therapeutic RNAs, and small molecules.

Hypothesis.

H1. Peptides derived from the C-terminal domain of the TSP1, might be more selective in the interaction with CD47 since TSP1 interacts with several cell surface receptors. Moreover, 4N1K peptide is found to induce apoptosis in different cancer cell lines [23,24] and it will be interesting to check its effect on senescent cells.

H2. SNs nanosystems loaded/ associated with TSP-1 derived peptides, or senolytic senostatic molecules might improve their efficacy, decrease the effective dose, protect them from possible enzymatic degradation and overall provide therapeutics with improved properties.

Objectives.

O1. Investigate the effect of several TSP-1 derived peptides on the emergence from chemotherapy-induced senescence model of MCF7 and LS174T cells.

O2. Associate the most promising peptide to SNs to improve its efficacy and deliver innovative nano-pharmaceuticals to control senescence escape from a chemotherapy-induced senescence model.

O3. Develop additional nano-pharmaceuticals to target senescence by loading SNs with other senolytic, senostatic molecules, and check their effect on chemotherapy-induced senescence model.

References:

1. S, L.; CA, S. The dynamic nature of senescence in cancer. *Nat. Cell Biol.* **2019**, *21*.

2. Hayflick, L. The limited in vitro lifetime of human diploid cell strains. *Exp. Cell Res.* **1965**, *37*, 614–636, doi:10.1016/0014-4827(65)90211-9.

3. Herranz, N.; Gil, J.; Herranz, N.; Gil, J. Mechanisms and functions of cellular senescence. *J. Clin. Invest.* **2018**, *128*, 1238–1246.

4. Saleh, T.; Tyutyunyk-Massey, L.; Gewirtz, D.A. Tumor cell escape from therapy-induced senescence as a model of disease recurrence after dormancy. *Cancer Res.* **2019**, *79*, 1044–1046, doi:10.1158/0008-5472.CAN-18-3437.

5. Georgakilas, A.G.; Martin, O.A.; Bonner, W.M. p21: A Two-Faced Genome Guardian. *Trends Mol. Med.* **2017**, *23*, 310–319, doi:10.1016/j.molmed.2017.02.001.

6. Vétillard, A.; Jonchère, B.; Moreau, M.; Toutain, B.; Henry, C.; Fontanel, S.; Bernard, A.C.; Campone, M.; Guette, C.; Coqueret, O. Akt inhibition improves irinotecan treatment and prevents cell emergence by switching the senescence response to apoptosis. *Oncotarget* **2015**, *6*, 43342–43362, doi:10.18632/oncotarget.6126.

7. Campone, M.; Valo, I.; Jézéquel, P.; Moreau, M.; Boissard, A.; Campion, L.; Loussouarn, D.; Verriele, V.; Coqueret, O.; Guette, C. Prediction of recurrence and survival for triple-negative breast cancer (TNBC) by a protein signature in tissue samples. *Mol. Cell. Proteomics* **2015**, *14*, 2936–2946, doi:10.1074/mcp.M115.048967.

8. Guillon, J.; Petit, C.; Moreau, M.; Toutain, B.; Henry, C.; Roché, H.; Bonichon-Lamichhane, N.; Salmon, J.P.; Lemonnier, J.; Campone, M.; et al. Regulation of senescence escape by TSP1 and CD47 following chemotherapy treatment. *Cell Death Dis.* **2019**, *10*, doi:10.1038/s41419-019-1406-7.

9. Haugstetter, A.M.; Loddenkemper, C.; Lenze, D.; Gröne, J.; Standfu, C.; Petersen, I.; Dörken, B.; Schmitt, C.A. Cellular senescence predicts treatment outcome in metastasised colorectal cancer. *Br. J. Cancer* **2010**, *103*, 505–509, doi:10.1038/sj.bjc.6605784.

10. Elmore, L.W.; Di, X.; Dumur, C.; Holt, S.E.; Gewirtz, D.A. Evasion of a single-step, chemotherapy-induced senescence in breast cancer cells: Implications for treatment response. *Clin. Cancer Res.* **2005**, *11*, 2637–2643, doi:10.1158/1078-0432.CCR-04-1462.

11. Roberson, R.S.; Kussick, S.J.; Vallieres, E.; Chen, S.Y.J.; Wu, D.Y. Escape from therapy-induced accelerated cellular senescence in p53-null lung cancer cells and in human lung cancers. *Cancer Res.* **2005**, *65*, 2795–2803, doi:10.1158/0008-5472.CAN-04-1270.

12. Saleh, T.; Tyutyunyk-Massey, L.; Murray, G.F.; Alotaibi, M.R.; Kawale, A.S.; Elsayed, Z.; Henderson, S.C.; Yakovlev, V.; Elmore, L.W.; Toor, A.; et al. Tumor cell escape from therapy-induced senescence. *Biochem. Pharmacol.* **2019**, *162*, 202–212, doi:10.1016/j.bcp.2018.12.013.

13. Dou, Z.; Berger, S.L. Senescence Elicits Stemness: A Surprising Mechanism for Cancer Relapse. *Cell Metab.* **2018**, *27*, 710–711, doi:10.1016/j.cmet.2018.03.009.

14. Milanovic, M.; Fan, D.N.Y.; Belenki, D.; Däbritz, J.H.M.; Zhao, Z.; Yu, Y.; Dörr, J.R.; Dimitrova, L.; Lenze, D.; Monteiro Barbosa, I.A.; et al. Senescence-associated reprogramming promotes cancer stemness. *Nature* **2017**, *553*, 96.

15. Patel, P.L.; Suram, A.; Mirani, N.; Bischof, O.; Herbig, U. Derepression of hTERT gene expression promotes escape from oncogene-induced cellular senescence. *Proc. Natl. Acad. Sci. U. S. A.* **2016**, *113*, E5024–E5033, doi:10.1073/pnas.1602379113.

16. Jonchère, B.; Vétillard, A.; Toutain, B.; Lam, D.; Bernard, A.C.; Henry, C.; Carné Trécesson, S. De; Gamelin, E.; Juin, P.; Guette, C.; et al. Irinotecan treatment and senescence failure promote the emergence of more transformed and invasive cells that depend on anti-apoptotic Mcl-1. *Oncotarget* **2015**, *6*, 409–426, doi:10.18632/oncotarget.2774.

17. Huang, T.; Sun, L.; Yuan, X.; Qiu, H. Thrombospondin-1 is a multifaceted player in tumor progression. *Oncotarget* 2017, *8*, 84546–84558.

18. Kalas, W.; Swiderek, E.; Świtalska, M.; Wietrzyk, J.; Rak, J.; Strządała, L. Thrombospondin-1 receptor mediates autophagy of RAS-expressing cancer cells and triggers tumour growth inhibition. *Anticancer Res.* **2013**, *33*, 1429–1438.

19. Soto-pantoja, D.R.; Kaur, S.; Roberts, D.D. CD47 signaling pathways controlling cellular differentiation and Responses To Stress. **2016**, *50*, 212–230, doi:10.3109/10409238.2015.1014024.CD47.

20. Bouzo, B.L.; Calvelo, M.; Martín-Pastor, M.; García-Fandiño, R.; de la Fuente, M. In Vitro–In Silico Modeling Approach to Rationally Designed Simple and Versatile Drug Delivery Systems. *J. Phys. Chem. B* **2020**, *124*, 5788–5800,

doi:10.1021/acs.jpcb.0c02731.

21. Bouzo, B.; Lores, S.; Jatal, R.; Alijas, S.; Alonso, M.J.; Conejos-Sánchez, I.; Fuente, M. de la Uroguanylin-decorated Nanosystems Containing Etoposide, a Potential Targeted Combination Therapy for Colorectal Cancer 2020.

22. Nagachinta, S.; Bouzo, B.L.; Vazquez-Rios, A.J.; Lopez, R.; de la Fuente, M. Sphingomyelin-based nanosystems (SNs) for the development of anticancer miRNA therapeutics. *Pharmaceutics* **2020**, *12*, 1–16, doi:10.3390/pharmaceutics12020189.

23. Leclair, P.; Kim, M.J.; Lim, C.J. Peptide analogues PKHB1 and 4N1K induce cell death through CD47-independent mechanisms. *Cancer Sci.* **2020**, *111*, 1028–1030, doi:10.1111/cas.14310.

24. Denèfle, T.; Boullet, H.; Herbi, L.; Newton, C.; Martinez-Torres, A.C.; Guez, A.; Pramil, E.; Quiney, C.; Pourcelot, M.; Levasseur, M.D.; et al. Thrombospondin-1 Mimetic Agonist Peptides Induce Selective Death in Tumor Cells: Design, Synthesis, and Structure-Activity Relationship Studies. *J. Med. Chem.* **2016**, *59*, 8412–8421, doi:10.1021/acs.jmedchem.6b00781.

Chapter 1:

TSP1 C-terminal Derived Peptides and their Effect on Cancer and senescent cells.

1. Abstract.

Cellular senescence is mainly identified by its irreversible cell cycle arrest as a result to mitogenic signals or cytotoxic agents such as chemotherapy. However, recent investigations indicated the possibility of those cells to escape cell cycle arrest into a more persistent form of cancer. These cells are thought to be the reason behind tumour relapse and chemotherapeutic failure. Our lab has recently showed that Thrombospondin 1 protein prevents senescence escape, and its low serum level is associated with tumour relapse. In this study, we investigated the effect of 4N1Ks peptide, a 10 amino acids peptide derived from the C-terminal domain of TSP1 on a chemotherapy-induced senescence model of MCF7 and LS174t cancer cells. We found that 4N1Ks prevented senescence escape at concentration 50µM. It also has antiproliferative effects proved by MTT and colony forming assays. Moreover, we found that 4N1Ks induces autophagy by downregulating each of pS6, LC3B and p62 in both treated cancer and senescent cells, which can explain previous results. In addition, we proved through Boyden chamber assay that 4N1Ks reduce the migratory ability of senescent cells secretome (SASP). All these results indicate that 4N1Ks possess senolytic & senostatic effects and can be used for future investigations as a possible senotherapeutic agent specially for patients received chemotherapy to improve their health and life span.

1. Introduction.

In the general introduction we have already covered all the molecular pathways that govern the cellular senescence and possible inducers. In this chapter, our main focus is the relation between cellular senescence and cancer.

Cellular senescence is concluded as tumour suppressive [1] mechanism besides that it has other beneficial roles such as in wound healing, tissue regeneration and tissue development (embryogenesis) [1,2] when it happens in transient mode [3]. However, when senescent cells accumulate in the body as immune system fails to eliminate them, this leads to detrimental consequences caused by the chronic effects of the SASP on the surrounding tissue resulting in chronic inflammation, disrupting tissue homeostasis and eventually promoting age-related disorders as well as tumour progression [3]. Additionally, in a recent paper published by Milanovic *et al.* they reported that senescent cells induced by chemotherapy treatment can escape cell cycle arrest and acquire stem cell features resulting in a more aggressive form of cancer with enhanced growth potential where relapsed tumours are enriched with [4]. In consonance with these findings, our lab has also developed and studied models of senescence

escape in response to oncogene inducers [5,6] and chemotherapy [7–10], where we found subpopulation of senescent cells re-enter cell cycle and emerge as a more persistent and transformed form of cells. Several papers have reported similar observations [11,12] which provides additional evidence that cellular senescence induction in tumour cells in response to chemotherapy/ radiation is incomplete and represents more of an adaptive mechanism. This shed the light on the importance to find new therapies for cancer and possible treatments that target senescent cells and reduce their burden.

In this work, we wanted to find a therapeutic biological compound that can interfere in one of the important pathways in senescent cells, and therefore preventing them from cell cycle arrest escape. In a recent study, our lab investigated the role of TSP1 on cellular senescence and emergence [13], and found the following observations: **I)** Thrombospondin-1 is overexpressed in the emergent population and suppresses proliferation, **II)** TSP1 prevents senescence escape and a low serum level is associated with tumour relapse [13]. In fact, TSP1 protein plays an essential role in various cellular processes/functions such as proliferation, apoptosis, inflammation, and angiogenesis [14–16]. However, TSP1 interacts with several cell surface molecules [17,18]. Therefore, we wanted to investigate the effect of 4N1K peptide; a 10 amino acid peptide derived from the C-terminal domain of TSP1 and study its effect on chemotherapy-induced senescence and senescence emergence. This will provide a better understanding of TSP1 role in cellular senescence. The effect of 4N1K peptide has already been investigated in several cancer cells and epithelial cells [19–22]. To our knowledge up until now its effect on senescent cells has not been identified yet. A scramble peptide 4NGG with 10 amino acids too is used as a control.

2. Materials and Methods.

2.1. Cell lines, senescence induction, and generation of emergent cells.

All cells were obtained from the American Type Culture Collection. Cell lines were authenticated by STR profiling and were regularly tested to exclude mycoplasma contamination. To induce senescence, all cells were treated for 96 h with sn38 (5 ng/ml, LS174T) or doxorubicin (25 ng/ml for, MCF7). Senescence was validated by expression of cell cycle inhibitors and β-galactosidase staining. For generation of emergent cells, LS174T & MCF7 cells were treated for 4 days with sn38 (5 ng/ml) and doxorubicin (25 ng/ml for MCF7) in 3% FBS, washed with PBS, and then restimulated with fresh 10% FBS for 7 days.

Sn38 (Tocris Bioscience 2684), the active metabolite of irinotecan which is a hemisynthetic analogue of camptothecin. Doxorubicin (Tocris Bioscience 2252), a biosynthetic analogue of daunorubicin. As topoisomerase I and II inhibitors, respectively, these drugs prevent the DNA religation and are responsible for DNA single- or double-strand breaks. These DNA damages lead to senescence in our conditions.

2.2. Migration assay (Boyden chamber assay)

Cells were harvested and resuspended in serum-free culture medium. Cell suspension of 200,000 cells/ml was prepared, of which 200 µL were deposited in each insert. Below the inserts, 800 µL of (RPMI or SASP) supplemented with 3% FBS were placed, and cells were incubated for 72 h. Then, cells were fixed, washed with PBS, and stained with crystal violet. Cells in the inner compartment were removed and cells on the outside were counted with ImageJ software.

2.3. Western blotting.

Following cell lysis with FASP Buffer (0.1 M Tris-HCL, 4% SDS, pH=7.6) containing a cocktail of inhibitors (10 µg/ml aprotinin, 10 µg/ml leupeptin, 10 µg/ml pepstatin, 1 mM Na3VO4, 50 mM NaF), lysates were sonicated and then boiled for 10 minutes. Proteins were separated on a SDS polyacrylamide gel and transferred to a PVDF membrane. Following one-hour incubation in 5% milk, Tris-buffered saline (TBS), and 0.1% Tween 20, the membranes were incubated overnight at 4°C with the following primary antibodies: p21Waf1 (Cell Signaling, 2947S), p-p53ser15 (Cell Signaling, 9211), p-S6 ribosomal (S235/236), Bip (Cell Signaling, 3177), IRE1-α (Cell Signaling, 3294), LC3B (Cell Signaling, 2775), TBP (Cell Signaling, 44059), and hsc-70 (Santa Cruz, sc-7298).

Membranes were then washed three times with TBS with 0.1% Tween 20 and incubated for 45 minutes with the secondary antibodies listed below (1/3,000): anti-rabbit IgG, HRP-linked antibody (Cell Signaling, 7074), anti-mouse IgG, and HRP-linked antibody (Cell Signaling, 7076). Visualization was performed by chemiluminescence with a Bio-Rad ChemiDoc XRS imaging device (Bio-Rad) and Fusion Solo (Vilber).

2.4. Cell Cycle Analysis

250 000 cells were incubated with 150 µL of solution A (trypsin 30 µg/mL, Sigma) for 10 min at room temperature in the dark. Then, 125µL of solution B (trypsin inhibitor 0,5 mg/mL, RNAse A 0,1 mg/mL, Sigma) was added for 10 min in the dark. Finally, cells were incubated

with 125 µL of solution C (propidium iodide 0,6 mM, spermine tetrahydrochloride 3,3 mM, Sigma) for 10 min at 4°C. All the solutions were prepared in a storage buffer pH 7,6 containing 3,4 mM sodium citrate 2H20 (Sigma), 0,1% Igepal CA-630 (Sigma), 3 mM spermine tetrahydrochloride and 1mM de tris-aminomethane.

2.5. Colony Forming Assay/ Clonogenic assay.

Assays were performed to evaluate proliferation and survival. In total, 286 LS174T and 180 MCF7 cells were seeded into 24-well cell culture plates with 3% FBS, in the presence or absence of peptides (4N1Ks/ 4NGG); note that peptides was added on floating cells, the first day. Cells were then incubated at 37 °C in a 5% CO2 atmosphere for 7 days, then washed twice with PBS, and stained with 0.4% crystal violet. The colonies were then washed twice with water, visualized with a Bio-Rad Chemi Doc XRS Imaging device, and counted using Quantity One imaging software (Bio-Rad).

2.6. MTT assay

Cell viability was also measured by the MTT (3-4,5-dimethylthiazol 2,5-diphenyltetrazolium bromide) assay. Cells were seeded in 96-well clear-bottomed plates at a density of 1500 cells per well in 200 µL medium, incubated for 24 hrs, and treated with doxorubicin (25 ng/ml), 4N1Ks (50 µM) and 4NGG (50 µM) as a control. Four replicates per concentration, per treatment were done. After 72 hrs, 40 µL of 5 mg/ mL MTT solution was added to each well and incubated in a humidified 5% CO2 atmosphere at 37°C for 3 hrs.

After incubation, the cells were pelleted and dried. Subsequently, 100 µL of DMSO (dimethylsulfoxyde) was added to each well, and the cells were incubated at room temperature for 2-3 hrs. Absorbance was measured by a microtiter plate reader at 562 nm.

2.7. β-Galactosidase (β-Gal) staining.

Cells were fixed for 15 min (room temperature) in 1% formaldehyde, washed with PBS and incubated at 37°C (no CO2) with fresh staining solution: 0.3 mg/mL of 5-bromo4-chloro-3 indolyl β-D-galactoside (X-Gal, Fermentas), 40 mM citric acid (Sigma), 40 mM sodium phosphate (Sigma) (stock solution (400 mM citric acid, 400 mM sodium phosphate) must be at pH6), 5 mM potassium ferrocyanide (Sigma), 5 mM potassium ferricyanide (Sigma), 150 mM NaCl (Sigma), 150 mM MgCl2 (Sigma). SA-β-GAL-positive cells were quantified after 16-20 h as compared to unstained cells.

2.8. RT-qPCR Analysis.

Analysis was performed using the comparative CT method (2^(ΔCt)), according to the expression of three endogenous housekeeping gene TBP, PPIA and EEF1A1 (for tRNA). TRFC, B2M, and β-Actin were the housekeeping genes for detecting UPR markers. Lastly G3PDH and rplpo for detecting SASP markers.

2.9. Statistical analysis.

All values were expressed as mean +/− standard deviation (SD). Differences were analyzed using nonparametric tests (t test, Mann–Whitney, Kolmogorov– Smirnov, and one-way Anova). *$p < 0.05$, **$p < 0.01$, and ***$p < 0.001$. NS on the figure means that the result was not significant.

3. Results.

In our previous inspections we found that in chemotherapy-induced senescence of colon and breast cancer, senescent cells have the ability to escape cell cycle arrest and emerge as a more persistent form of cancer [7,8,13,23]. So first we replicated those results by inducing CIS in MCF7 & LS174T cells. Higher expression of p21waf and p-p53 in MCF7 and LS174t after treatment with Doxo and Sn38 for 24 h lead the cancer cells to enter senescent state, Figure 1-A. Moreover, β-galactosidase activity in those cells after 4 days of chemotherapy treatment is an extra proof of their senescent state, Figure 1-B.

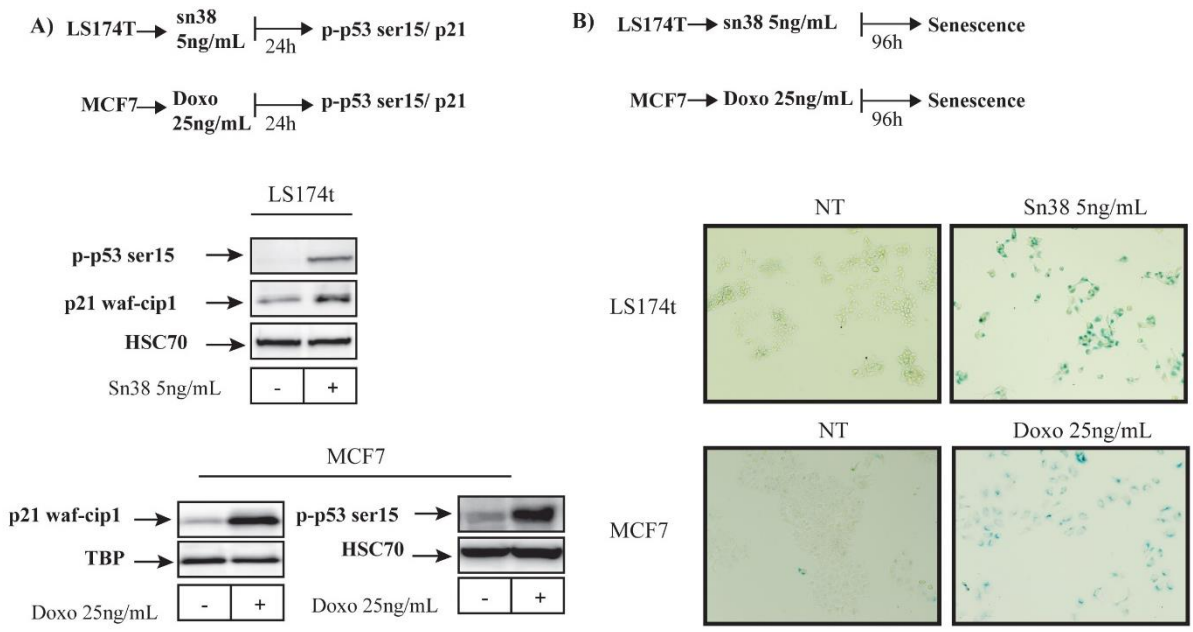

Figure 1: A) Following sn38 treatment (5 ng/ml) for LS174t and Doxo (25 ng/L) for MCF7, senescence induction was detected by the evaluation of p21waf1 and p-p53 expression (n=3). **B)** senescence was also detected after chemotherapy treatment in both LS174T and MCF7 by checking the β-galactosidase activity (n=4).

3.1. Pilot study with TSP-1 C-terminal derived peptides.

7N3 (FIRVVMYEGKK) and 4N1K (KRFYVVMWKK) are two different peptides derived from the C-terminal domain of the TSP-1 protein. The effect of both peptides has been investigated on several cell lines and considered as a representative of TSP-1 interaction with the CD47 receptor. Both peptides contain the VVM sequence, which is regarded as the pharmacophore for binding to the CD47 receptor [20,22].

Since we wanted to check if we can replicate the results we had in a previous study [13] with TSP-1 using TSP-1 derived peptides. Two experiments were chosen as a pilot study, the first one is the senescence escape while the second was Boyden chamber assay with SASP. The first experiment would investigate the effect of the peptides on the senescent cells while the second will check the effect of those peptides on SASP migratory ability.

Therefore, we investigated the effect of both peptides on the emergence from the chemotherapy-induced senescence model of LS174T colon cancer cells and MCF7 breast cancer cells. Peptides' concentrations of 1µM for 7N3 and 50µM for 4N1K, have been chosen based on previous studies [15,21]. 4NGG (KRFYGGMWKK) is a control peptide similar in composition to 4N1K, but the VVM sequence is replaced by GGM. As it is clear from Figure

2-A, both peptides at the earlier mentioned concentrations did not have significant effect on senescence escape for both LS174t and MCF7 cells.

On the contrary, Boyden chamber assay on MCF7 cells and LS174T with the peptides showed different results. Results presented in Figure 2-B shows significant reduction in cell migration for both cell lines in wells containing 4N1K 50 µM. However, in the case of 7N3, promising results were only feasible at a concentration of 5 µM.

Several research papers pointed out that the substitution of amino acids with their D-form on the N- and C- terminal of the peptide will have great impact on the overall stability of the peptide without affecting its activity [24]. Consequently, we aimed to adjust the 4N1K peptide by changing the Lysing amino acid on the N- and C- terminals to the D-form. The effect of the new peptide (4N1Ks) on senescent and cancer cells will be investigated in the next part. 4N1K peptide was chosen instead of 7N3 for this modification as 4N1K showed more promising results.

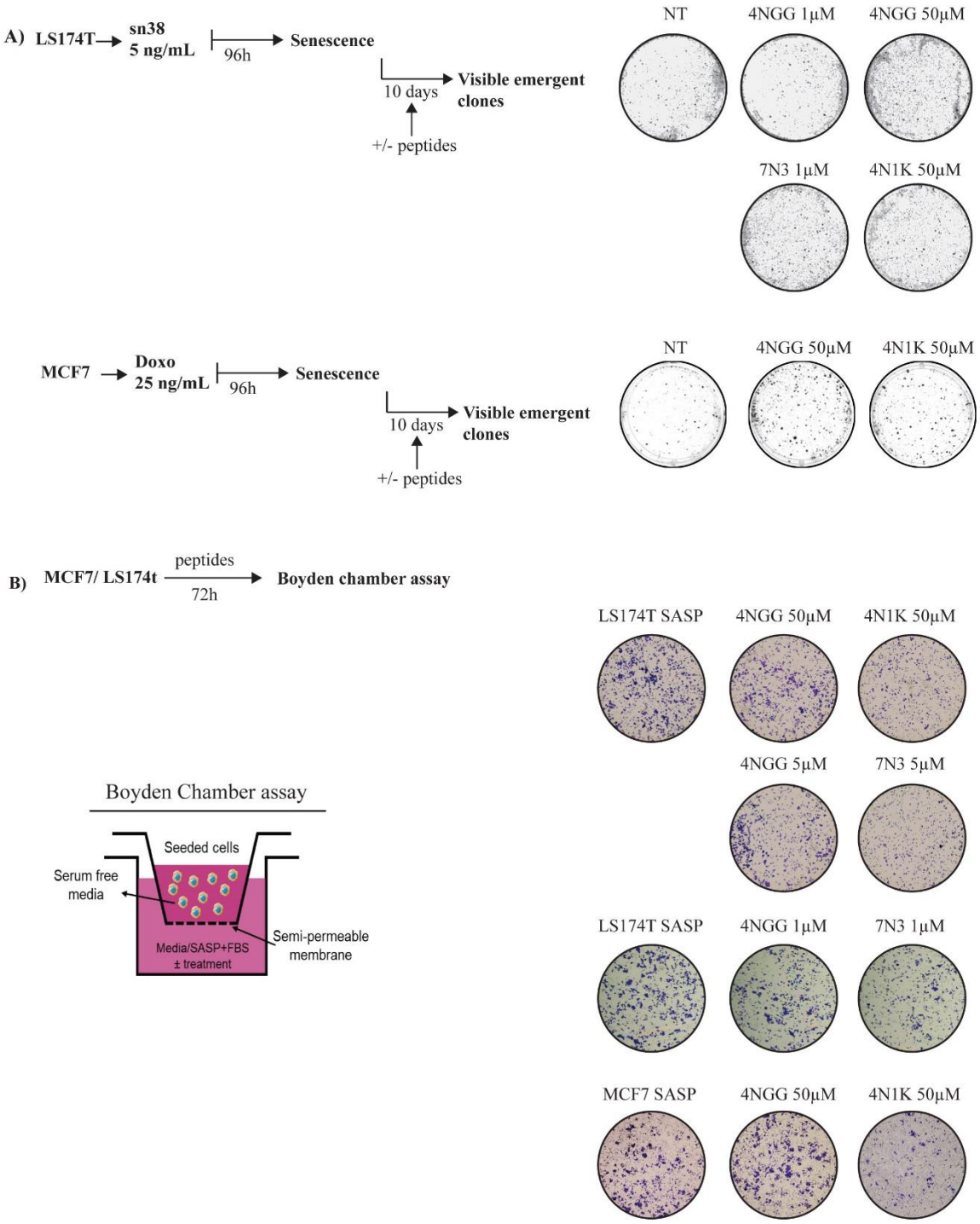

Figure 2: A) After CIS induction, LS174T (n=5) and MCF7 (n=3) cells emergence was induced using 10% serum in the presence or absence of 4N1K (50 µM)/ 7N3 (1 µM) peptide in comparison with the control peptide 4NGG (50/1 µM). **B)** SASP migratory ability in the presence of 4N1Ks peptide were also checked using boyden chamber assay, after collecting SASP from senescent lS174T and MCF7 cells, SASP were mixed with 4N1K, 7N3 or control peptide and placed in the lower chamber, (n=3).

3.2. TSP-1 derived peptide (4N1Ks) prevents chemotherapy induced senescence escape in breast and colon cancer models.

The modified peptide 4N1Ks efficacy were examined first in senescence escape experiment of CIS of MCF7 and LS174t cells. After senescence induction with chemotherapy treatment Sn38 5ng/mL (for LS174T) and doxorubicin 25ng/mL (for MCF7), a fresh cultural media was introduced to senescent cells and 4N1Ks 50µM was added, with 4NGG peptide as a positive control. What we found was that 4N1Ks was able to reduce emergent clones by almost 58% in MCF7 cells and 51% in LS174T cells, Figure 3-A.

Since β-galactosidase is one of the representative features of cellular senescence, we detected 4N1Ks effect on β-galactosidase activity, where we found an increase in β-galactosidase activity in 33% of MCF7 cancer cells and 22% in LS174T cancer cells in comparison to chemotherapeutic treatment, while the control peptide plates were similar to the non-treated ones, Figure 3-B.

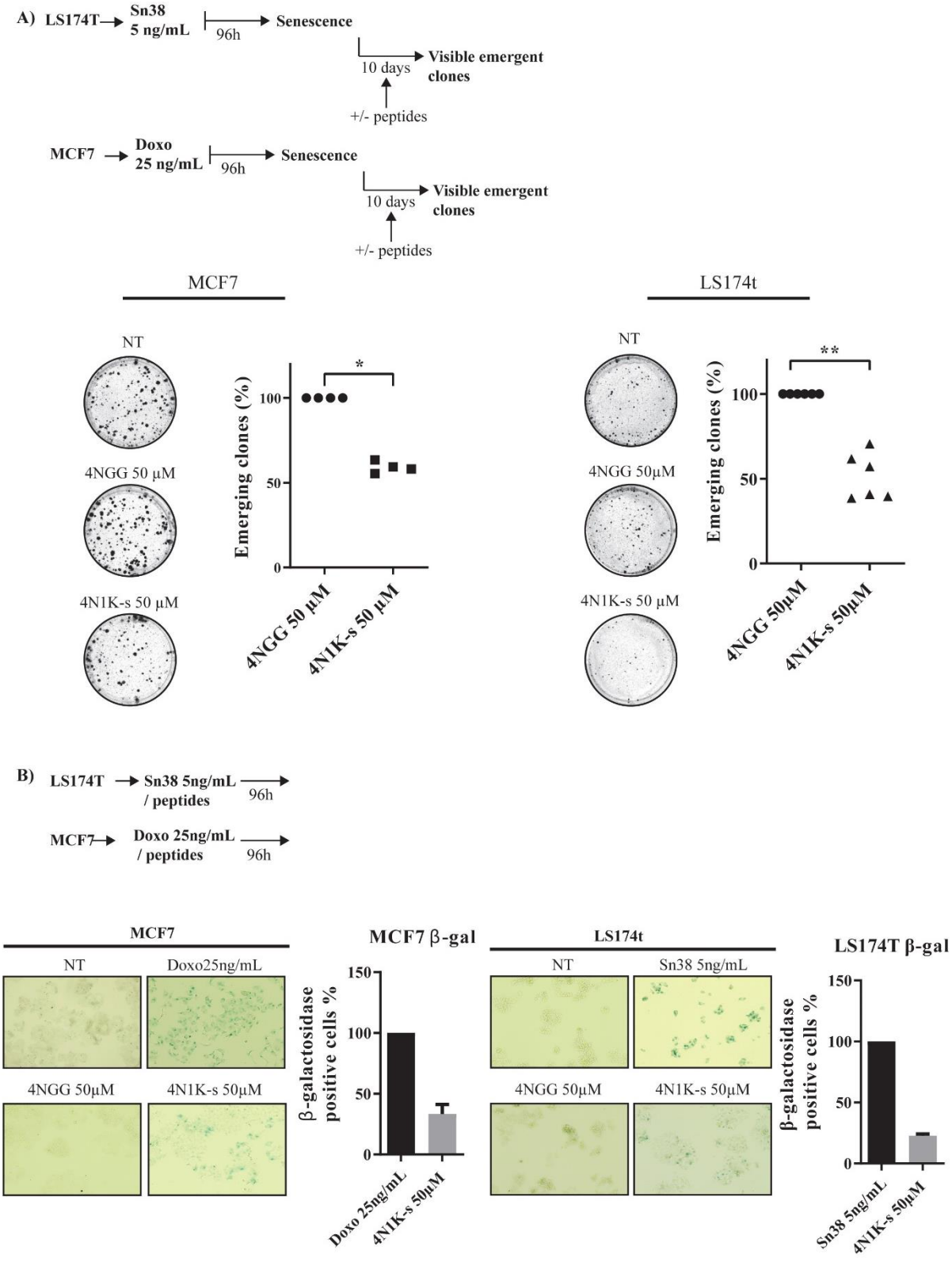

Figure 3: A) After CIS induction, LS174T (n=5) and MCF7 (n=4) cells emergence was induced using 10% serum in the presence or absence of 4N1Ks in comparison with the control peptide 4NGG (50 µM), (Kolmogorov–Smirnov test, * =p < 0.05, ** =p < 0.01). **B)** β-galactosidase activity in LS174T and MCF7 cells after treatment with 4N1Ks 50µM and 4NGG as a control (n=3).

3.3. Effect of 4N1Ks peptide on p53/p21 expression in cancer and senescent cells.

Since 4N1Ks has an effect on senescent cells emergence, we wanted to check the expression of p-p53^{ser15} and p21$^{waf\text{-}cip1}$ upon treatment with 4N1Ks, due the importance of those two proteins in establishing the cellular senescence [25–27]. Therefore, their expression was detected in LS174t cells after 8h and 15 h of treatment with the peptides accompanied or not with Sn38 5 ng/mL. Results displayed in Figure-4A, show that treated LS174t cells showed no change in the expression of p-p53.

We also checked p-p53^{ser15} and p21$^{waf\text{-}cip1}$ expression in MCF7 cancer cells after 48h of treatment with peptides (4N1Ks and 4NGG at 50 µM) and after two days of emergence (EM2D). In both cases, 4N1Ks at 50 µM did not have any effect on the both proteins expression, Figure 4-B, C.

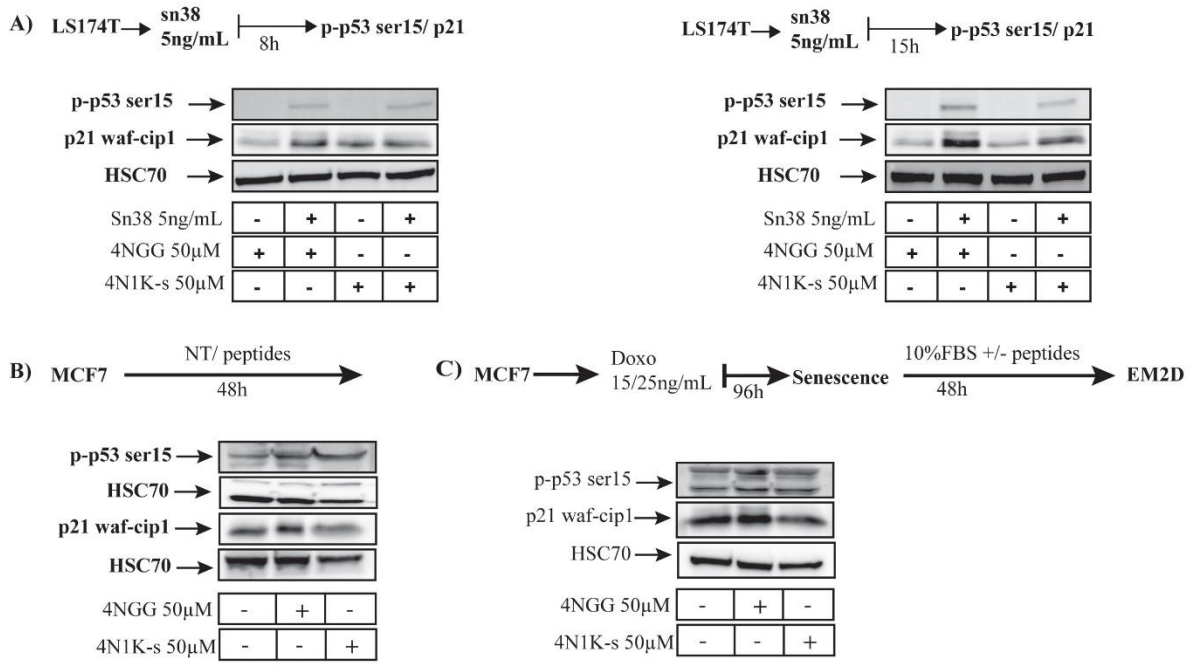

Figure 4: Effect of 4N1Ks peptide on p53/p21 expression in cancer and senescent cells. A) p53-ser15 and p21 waf-cip1 expression in MCF 7 and LS174t cells were examined by western blot after 8 and 15 h of treatment with peptides in the presence or absence of chemotherapy (Sn38 5ng/mL for LS174t cells and Doxo 25ng/ mL for MCF7 cells) (n=3). **B)** p53-ser15 and p21 waf-cip1 expression in MCF7 cells treated with 4N1Ks 50 µM for 48h (with 4NGG as a control) were assessed by western blot, (n=3). **C)** p53-ser15 and p21 waf-cip1 expression in senescent MCF7 cells treated with 4N1Ks 50 µM for 48h (EM2D) (with 4NGG as a control) were assessed by western blot, (n=3).

3.4. 4N1Ks peptide has an antiproliferative properties and anti-migration/anti-invasion effect.

Since previous studies [14,17,29] have shown that TSP1 protein plays an important role in cell proliferation. Therefore, we detected the effect of 4N1Ks on the proliferative capacity of

MCF7 and LS174T cancer cells through MTT and colony forming assay. In case of MCF7 cells, 4N1Ks significantly decreased the number of colonies formed by almost 60%. However, it was not the case for LS174T, as 4N1Ks did not have any effect on the ability of cells to form colonies, Figure 5-A. Contrarily, MTT results showed that 4N1Ks led to decrease in the proliferation capacity of both cell lines, MCF7 and LS174T, by 86% and 44% respectively, Figure 5-B.

Based on the previous results we were intrigued to know if 4N1Ks has any effect on the cell cycle through Flow cytometry. Consequently, we checked the effect of the 4N1Ks on both cell lines after 48h of treatment. Results presented in Figure 5-C indicate an increase in the number of cells in G2M phase by 7% ±2.5 in MCF7 cells and 3.2% ±1.2 in LS174t cells upon treatment with 4N1Ks.

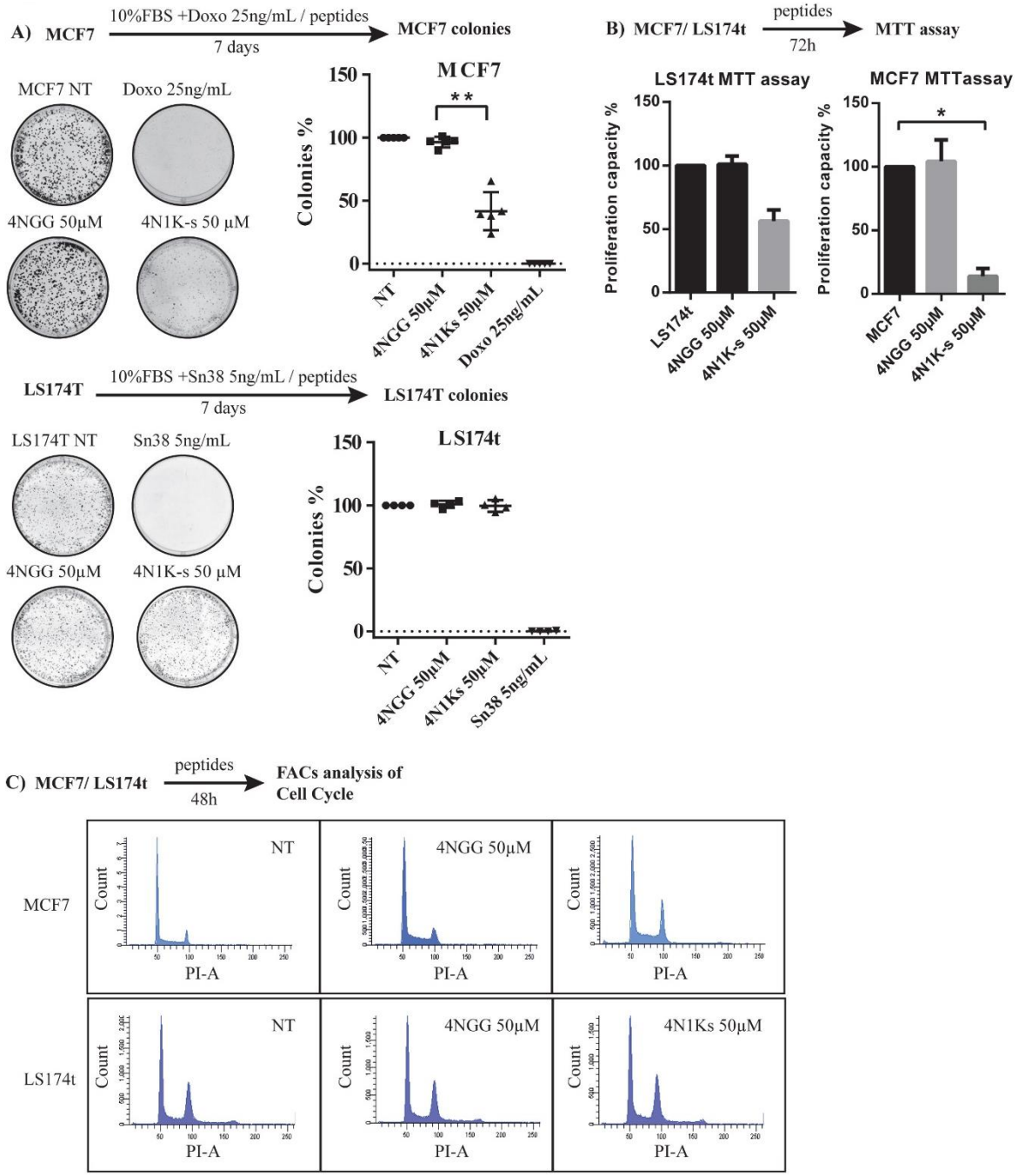

Figure 5: A) Antiproliferative effect of 4N1ks was checked using colony forming assay on LS174t (n=4) and MCF7 (n=5) for 10 days with 4NGG as a control (n=4, Kolmogorov–Smirnov test, ** =p < 0.01). **B)** Effect of 4N1Ks on the metabolic activity of LS174T and MCf7 cancer cells were checked using MTT assay (n=4, Kolmogorov–Smirnov test, * =p < 0.05). **C)** The effect of 4N1Ks peptide on cell cycle of MCF7 cells and LS174t cells were examined by flow cytometry (n=3).

SASP factors' ability to promote invasion and migration of cells have been well explored and studied [30–32]. Therefore, we wanted to check if 4N1Ks peptide ability to prevent senescence escape were linked to its effect on SASP factors, the cells directly, or it could be a mixture of both. Hence, a Boyden chamber assay were performed on both cell lines with SASP collected from the senescent cells of MCF7/ LS174t and the peptides were mixed or not with the SASP. What we found that 4N1Ks were able to prevent the migration of cancer cells

in both lines but to a higher extent in MCF7 cells, Figure 6, and its effect was greater than the one obtained with 4N1K peptide.

Taking all these results in consideration, it confirms that 4N1Ks has antiproliferative effect, and can block cancer cell migration by altering the deleterious effect of senescent cells secretome/ SASP.

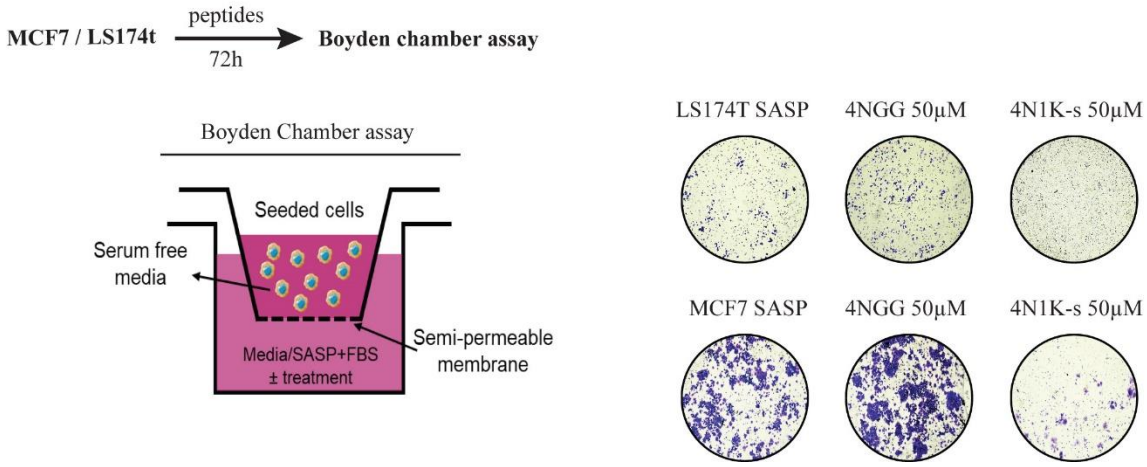

Figure 6: SASP migratory ability in the presence of 4N1Ks peptide were also checked using boyden chamber assay, after collecting SASP from senescent lS174T and MCF7 cells, SASP were mixed with 4N1ks or control peptide and placed in the lower chamber, (n=4).

3.5. 4N1Ks peptide downregulates mTOR, induces autophagy (and possibly ER stress) in MCF7 cancer and senescent cells.

Towards understanding what is exactly happening inside cancer and senescent cells treated with 4N1Ks. We collected the protein extracts for MCF7 cancer and senescent cells treated with 4N1Ks for further investigation, and we found that protein content in cells treated with 4N1Ks was much lower than the non-treated or the ones treated with control peptide, Figure 7-A. Since ER stress and autophagy is highly correlated with protein content in the cell [33,34] , we wanted to check the expression of several UPR and autophagy markers in MCF7 cancer and senescent cells treated with 4N1Ks. Western blot results showed that the expression of PERK, IRE1-α were decreased in MCF7 cancer and senescent cells, while Bip protein were higher with cells treated with 4N1Ks. For the autophagy markers, we checked the expression of the p62 and LC3B, p62 expression was much lower in both cancer and senescent cells treated with 4N1Ks, also the light band of LC3B totally disappeared in cells treated with 4N1Ks too. Moreover, the phosphorylated form of ribosomal protein S6 (p-S6), a downstream of m-TOR pathway, its expression was much lower in cells treated with 4N1Ks, Figure 7-B&C.

UPR stress and autophagy are intertwined at several levels, and all the results mentioned above indicated that 4N1Ks induce autophagy, might activate UPR stress which can explain the lower protein levels in cells treated with 4N1Ks and its ability to prevent senescence escape.

In addition to what mentioned above, cells treated with 4N1Ks possess higher granularity compared to non-treated ones as we observed in the FSC/SSC scattering with follow cytometer. This increase in granularity is also an indicator of larger cell compartments and organelles which can be linked to UPR and autophagy as well, Figure 7-D.

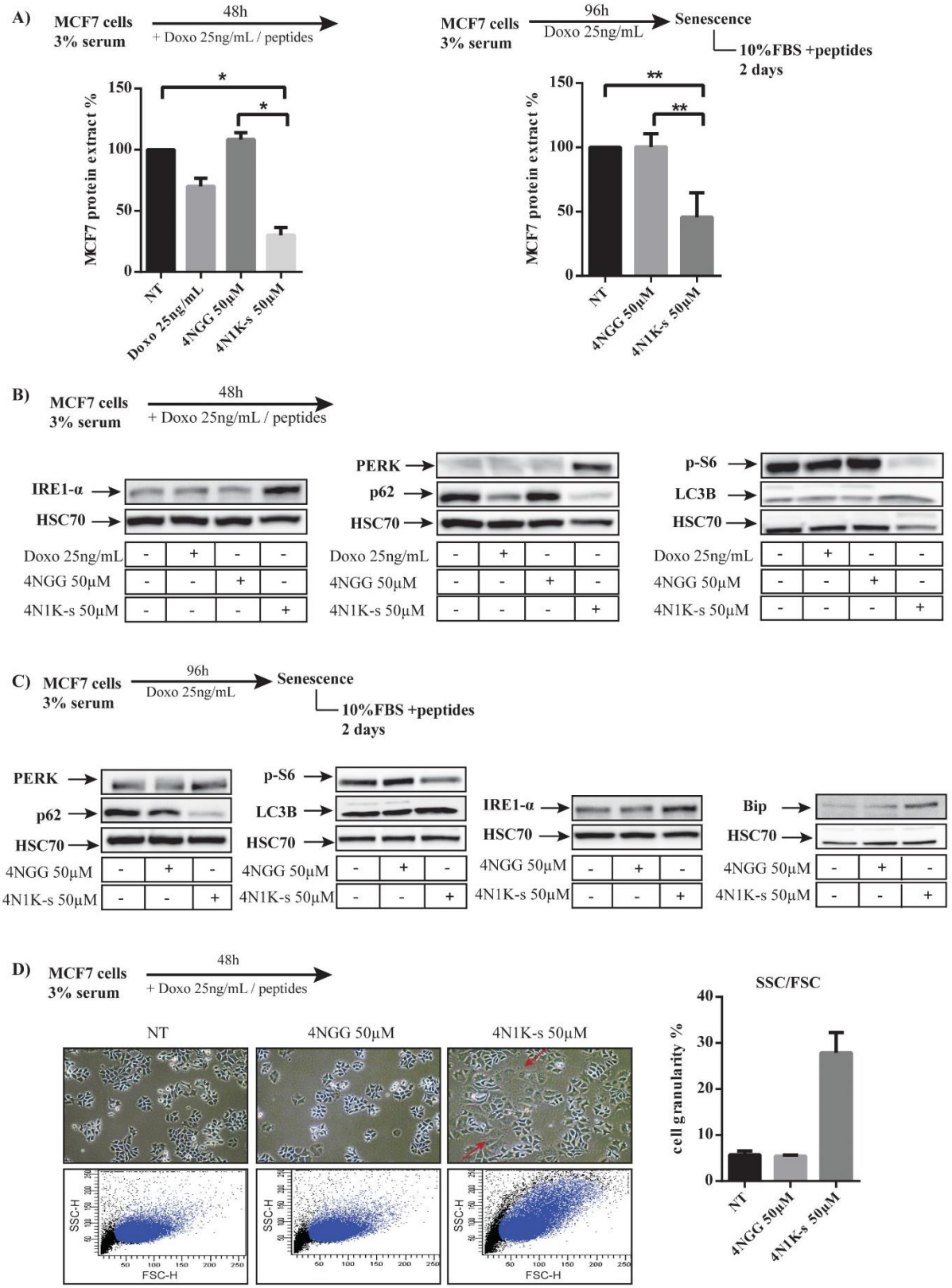

Figure 7: A) protein content in both cancer and senescent MCF7 cells after treatment with 4N1Ks 50µM and 4NGG as a control (Kolmogorov–Smirnov test, * =p < 0.05, ** =p < 0.01). **B)** Expression of several UPR and autophagy markers by western blot in MCF7 cancer cells after 48h treatment with 4N1Ks 50µM with 4NGG as a control (n=3). **C)** Expression of several UPR and autophagy markers by western blot in MCF7 after two days of emergence by treating senescent cells (CIS) for two days with 4N1Ks 50µM and 4NGG as a control (n=3). **D)** granularity of MCF7 cells treated with 4N1Ks in comparison to non-treated and control peptide were checked by FSC/SSC using flow cytometry and supported by the microscope photos of enlarged MCF7 cells after treatment with 4N1Ks (n=3).

3.6. Investigating the possible effect of 4N1Ks peptide on UPR and ER stress.

In order to investigate if 4N1Ks effects on cancer and senescent cells are related to UPR stress or not, we had to do more experiments to confirm this, such as detecting UPR genes expression. We also compared results obtained with Tunicamycin effect on cancer and senescent cells.

The mRNA levels of UPR genes were detected in MCF7 cells after 48h of treatment with 4N1Ks 50 µM. Total RNA was collected from treated and non-treated cells and the expression of the following UPR genes: ERO1Lb, Chop, GADD34, Herpud, GRP78, GRP94, XBP1s, ERDJ4, and ATF6, was detected by RT-qPCR. Results presented in Figure 8-B indicate to significance difference in all mentioned UPR genes, as the effect of 4N1Ks on their expression was not steady.

In a previous work in our lab, where it indicated the role of tRNA in regulating cellular senescence [35]. Also, it was found that mTOR regulates tRNA biogenesis during CIS escape. Based on that, we wanted to check the expression of several tRNA in MCF7 cancer or senescent cells after 48h of treatment using RT-qPCR, Figure 8-C&D.

Tunicamycin (Tun) is a drug known to induce Er stress by inhibition N-glycosylation of proteins leading to the accumulation of unfolded glycoproteins and ER stress eventually [36]. So, the next step was to compare the effect of 4N1Ks with Tun on MCF7 cancer and senescent cells, as well emergence. In colony forming assay experiment, Tun at 1 and 2 µM did not reduce the number of colonies formed, however they were much smaller compared to NT wells. While wells treated with 5 and 10 µM of Tun were totally empty Figure 8-E. Additionally Tun blocked emergence in CIS model MCF7 cells by 38% 1µM at concentration, and by 86% at 2 µM of Tun. We also checked the expression of the same UPR and autophagy markers that expression already investigated with 4N1Ks treatment (section 4.5.). Tun reduced the expression of IRE1-α, PERK, p-S6, p62, and the light chain of LC3B, Figure 1S (supplementary data).

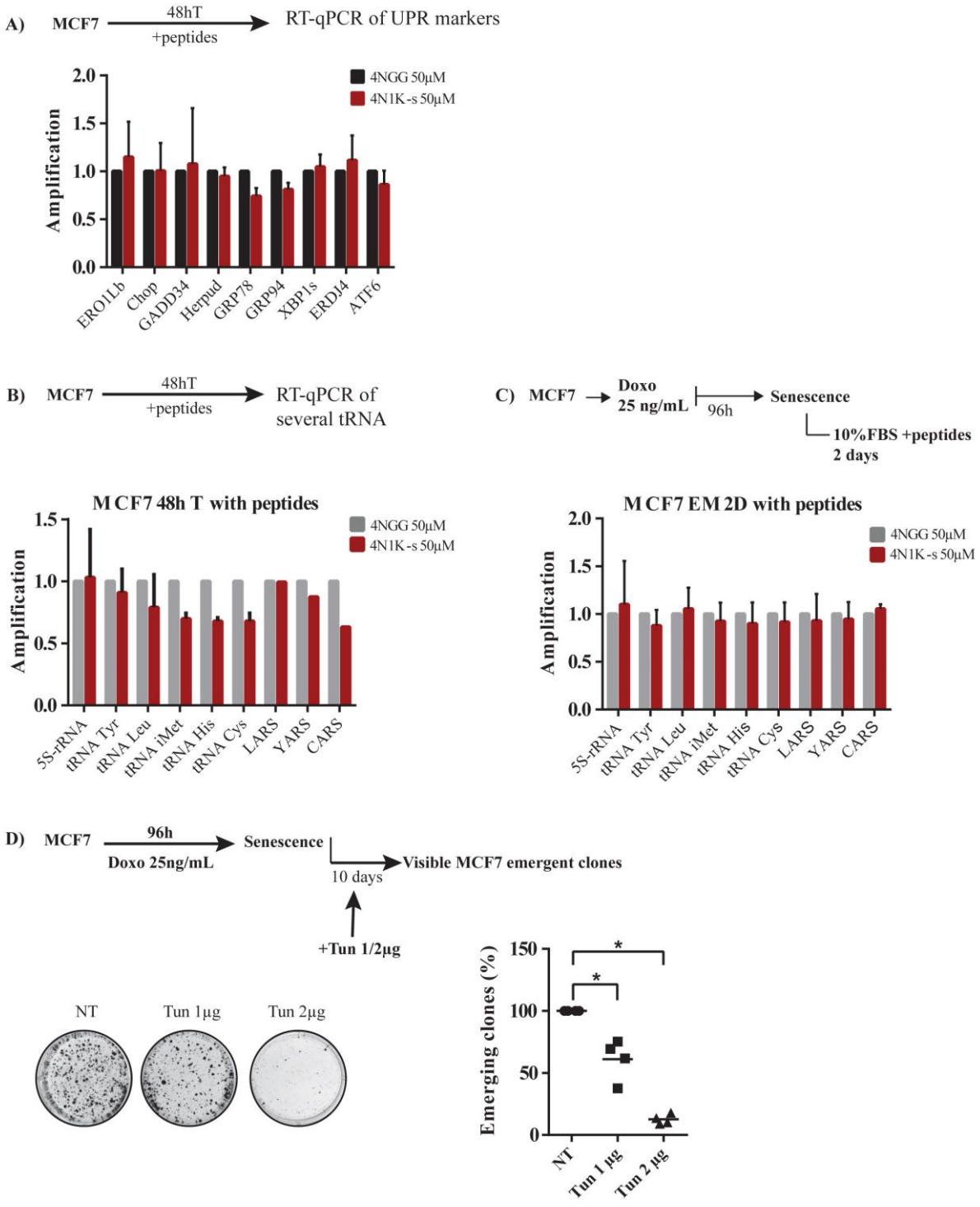

Figure 8: Investigation the possible relation between 4N1Ks peptide and UPR. **A)** mRNA levels of UPR markers were checked using RT-qPCR in MCF7 cell treated with peptides for 48h (n=3). **B)** mRNA levels of several tRNAs and LARS, CARS, and YARS ligase were assessed by RT-qPCR in MCF7 cells treated with peptides for 48h (n=3). **C)** The same as in C but those mRNA levels were checked in senescent cells after treatment with peptides for 2 days (EM2D) (n=3). **D)** After CIS induction, MCF7 (n=3) cells emergence was induced using 10% serum in the presence or absence of Tun 1µg/ 2µg/ mL (one representative image out of three experiments), (Kolmogorov–Smirnov test, * =$p < 0.05$)

3.7. The senolytic and senostatic possible properties of 4N1Ks peptide.

In relation to the previous results, we speculated the possibility that 4N1Ks could affect SASP production or components due to autophagy/ER stress and downregulation of mTOR. Therefore, we collected SASP from MCF7 senescent cells after treatment with 4N1Ks (4N1Ks-T-SASP) and compared it with SASP collected from untreated cells or cells treated with control peptide (4NGG-T-SASP), then we checked the migration/invasion ability of the collected SASP using Boyden chamber assay. As it is clear in Figure 9-A, 4N1Ks-T-SASP has much less migratory ability than the other two samples. To support our findings, we did a RT-qPCR on MCF7 senescent cells treated or not with 4N1Ks and check the mRNA expression of several SASP components, however there were no significant difference between the non-treated cells and the treated ones, Figure-8B.

In addition, we checked the effect of 4N1Ks peptide on the metabolic activity of MCF7 senescent cells through an MTT assay. 4N1Ks was able to significantly reduce the metabolic activity of MCF7 senescent cells, Figure 9-C.

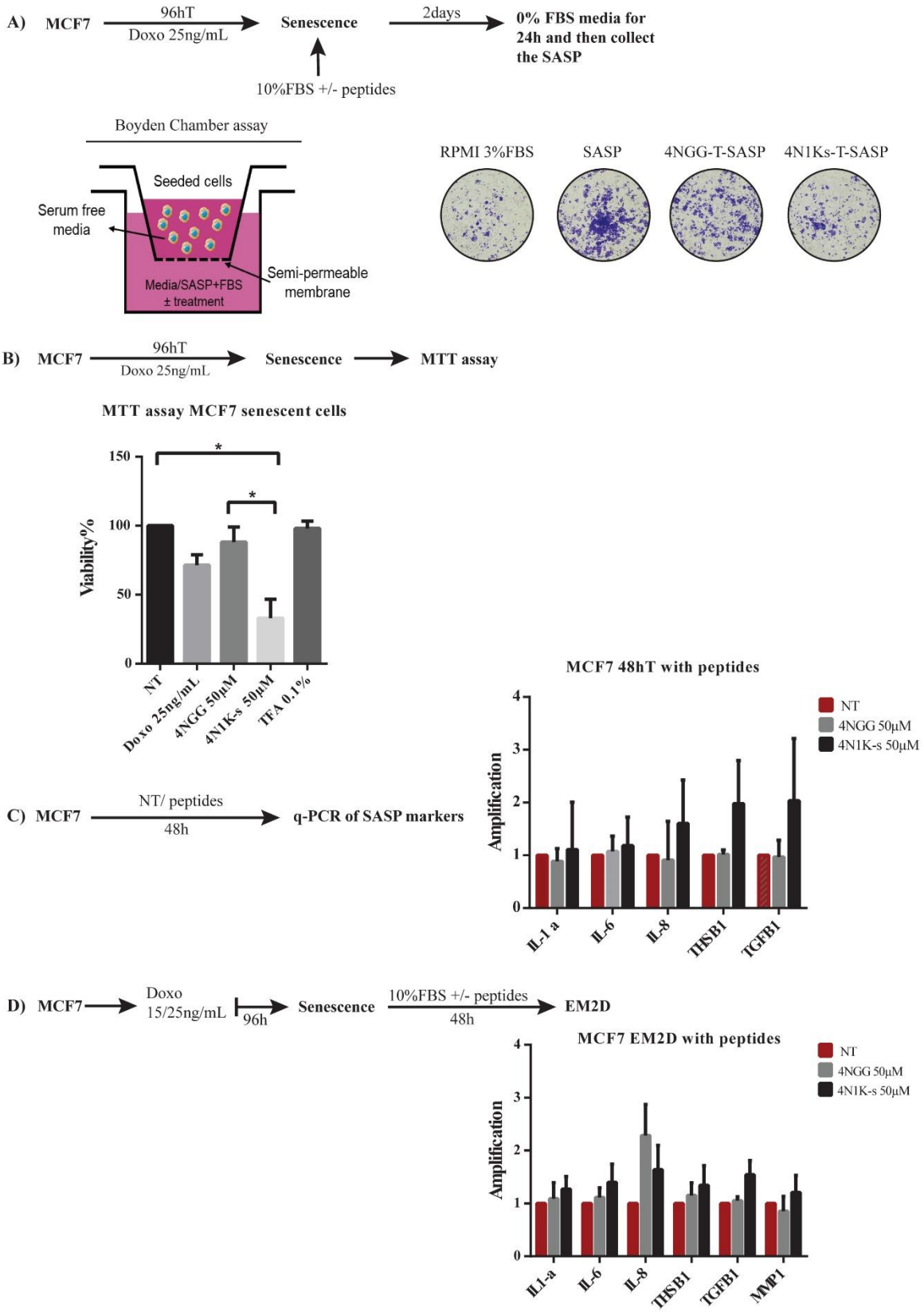

Figure 9: The possible senolytic senostatic effects of 4N1Ks peptide. A) the effect of 4N1Ks on SASP production or components were assessed by collecting first SASP from senescent cells treated with 4N1Ks for 2 days and check the migration ability of this SASP using Boyden chamber assay in comparison to SASP collected form non-treated cells or cells treated with 4NGG control peptide (n=4). **B)** the effect of 4N1Ks on the metabolic activity of MCF7 senescent cells were checked using MTT assay after CIS (n=4). **C)** mRNA levels of SASP components: IL1-α, Il-6, IL-8, THSB1, TGFB1, and MMP1 was assessed by RT-qPCR in MCF7 cancer cells treated

with 50 µM of peptides for 48h, (n=3). **D)** mRNA levels of SASP components: IL1-α, Il-6, IL-8, THSB1, TGFB1, and MMP1 was assessed by RT-qPCR in MCF7 senescent cells treated with 50 µM of peptides for 48h (EM2D), (n=3).

3.8. The effect of 4N1Ks on LS174t shCD47 and MCF7 shCD47 senescence escape.

In order to proof if 4N1Ks previously mentioned effects on cancer and senescent cells are related to its interaction with CD47 receptor or not, we investigated the effect of 4N1Ks peptide on MCF7 and LS174t cells where CD47 expression is reduced using shRNA. Silencing CD47 expression using siRNA was not possible as cells did not survive it. There was no difference in the effect of 4N1Ks on shCD47 cells compared to the control, Figure 10.

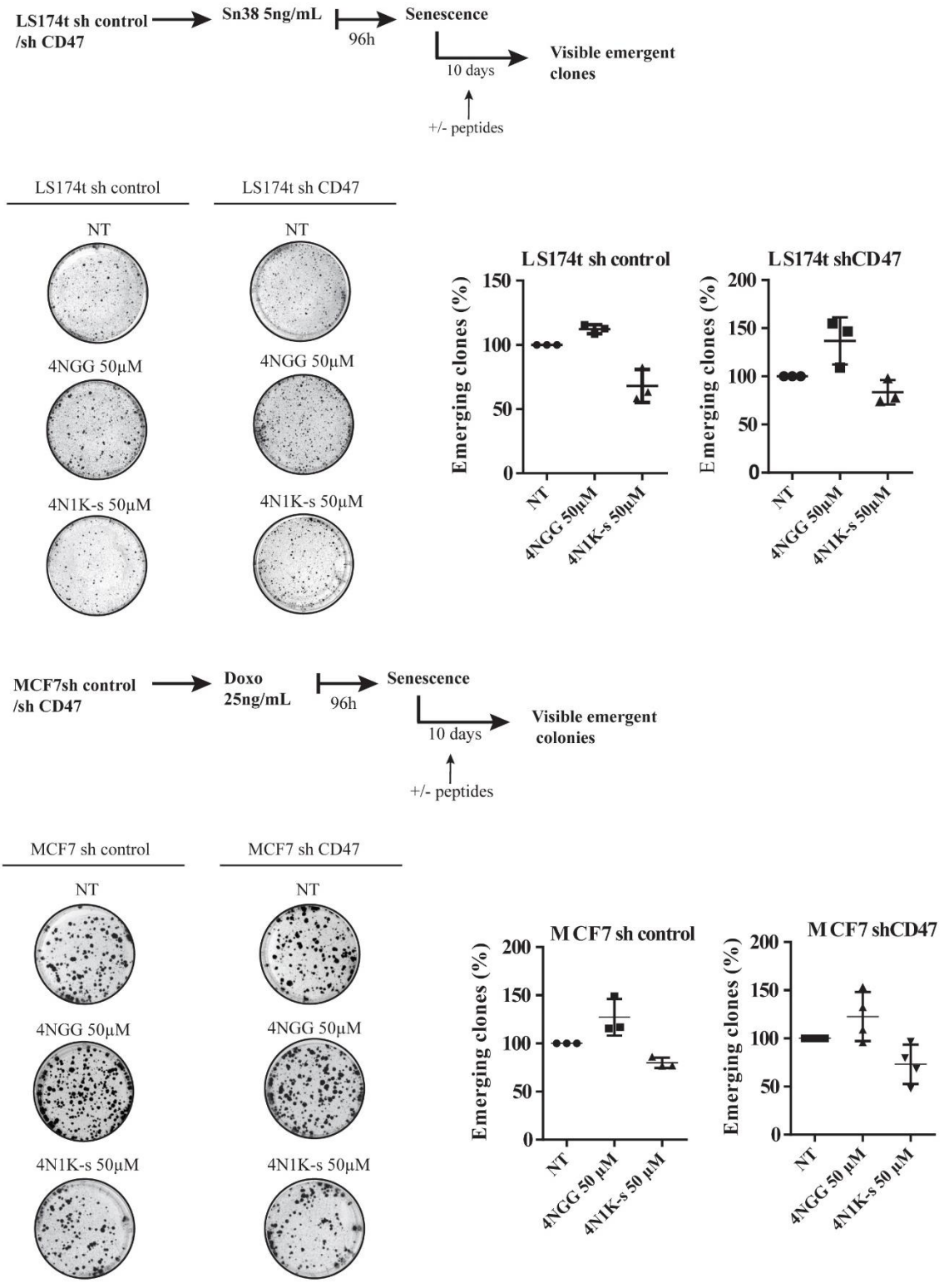

Figure 10: The effect of 4N1Ks peptide CIS emergence in MCF7 and LS174t cells expressing an shRNA directed against CD47 or a non-targeting control shRNA. Emergence was induced as described before (n=3).

4. Discussion.

The main purpose of cellular senescence is to hinder the progression and proliferation of damaged cells as well as facilitate/promote tissue repair mediated by secreted cytokines of senescent cells (SASP). However, when this biological phenomenon is induced in cancer cells due to chemotherapy or radiation treatment, the suppression might be incomplete leading to senescent cells that favours cell cycle arrest escape to more aggressive form of cancer cells with enhanced proliferation capacity. This has a detrimental effect on the health span and life span of cancer patients who received either chemotherapy or radiotherapy treatment, since the emergent cells might lead to cancer relapse or age-related diseases. Accordingly, finding pharmacological agents that eliminate senescent cells or oppose the harmful effects of SASP, is becoming a critical therapeutic need.

Based on a previous study conducted in our lab, where it was concluded that TSP1 protein prevent senescence escape in CIS model of MCF7 and LS174t cells, we first did a pilot study with two candidate peptides that are both derived from the C-terminal domain of TSP1; 7N3 and 4N1K peptides. Our pilot study results indicate both peptides affected the migratory ability of the SASP collected from MCF7 cells and LS174t cells but did not have any significant effect on emergence from CIS model of these cells. Speculating that this could be related to peptide stability, 4N1Ks peptide was proposed as a more stable alternative by exchanging the lysin amino acids on the N- and C- terminals to the D-form, which was proved later as 4N1Ks peptide was able to significantly prevent senescence escape in CIS model of MCF7 and LS174T, Figure 3-A.

It has been reported before that TSP1 inhibits cell cycle progression and induces senescence in endothelial cells [14]. However, in our case 4N1Ks did not induce senescence, as we found later that p53 and p21 (which are highly induced in senescent cells) were not expressed in cells treated with the peptides Figure 4-B&C. Moreover, we found that 4N1Ks peptide did not affect the cell cycle of both cell lines, Figure 5-C. Therefore, further experiments are essential to explain those results.

Results from cell cytotoxicity studies of MTT assay and colony forming assay showed that 4N1Ks has antiproliferative effect on MCF7 and LS174T cancer cell lines, which agrees with previous studies that showed 4N1K peptide and its analogue PKHB1 induce cell death in several types of cancer cells [19,20,37]. However, the effective concentration used in those studies (ranged between 100 to 300 µM) were much higher than the one we used. It is known

that MTT is used to indicate the metabolic activity in the cells. Therefore, it was interesting to investigate if 4N1Ks might affect the metabolic activity of the MCF7 senescent cells which might explain also the CIS escape results. Similar results were gained with MCF7 senescent cells, which proves that 4N1Ks influence the metabolic activity of those cells.

Low total protein content in cells treated with 4N1Ks peptide, Figure 6-A, pointed the possibility of autophagy or ER/UPR induction in the treated cells. Western blot results on cancer cells and senescent cells treated with 4N1Ks showed that 4N1Ks effects are mainly related to induction of autophagy. Moreover, the lower protein content plus the increased granularity of the cells treated with 4N1Ks is an additional proof of autophagy induction in those cells. It has been reported before that 4N1K peptide induced autophagy in cancer cells through immunodetection of LC3 in treated cells [21]. Anyhow, we have extra proof of autophagy induction through the downregulation of mTOR pathway and p62. In addition, induction of β-galactosidase activity could also be explained by autophagy program activation [38]. Moreover, MTT results on MCF7 cancer and senescent cells can also be explained by autophagy induction since it is highly correlated with cell metabolism activity [39].

In order to confirm or cut out the possibility of ER/UPR induction in cells treated with 4N1Ks, several experiments were proceeded. Although 4N1Ks increased the expression of IRE1-α, PERK, and the Bip proteins, it was not enough to prove UPR activation as 4N1Ks did not affect the mRNA expression of several UPR genes in treated cells. Moreover, our lab stated before the important role of mTOR and UPR stress in CIS escape and how mTOR inhibition block CIS escape. In that study it was also concluded that inhibition of mTOR resulted in reduction of several tRNA expression [35]. Based on that we checked the expression of several tRNA in MCF7 cancer and senescent cells treated with 4N1Ks. To our surprise, 4N1Ks treatment for 48h reduced the expression of each of the following: tRNA iMet, tRNA His, tRNA Cys, and CARS, but it was not the case in cells treated after 2 days of emergence as 4N1Ks did not alter the expression of any of the tRNA mentioned. Therefore, extra experiments are needed to confirm the relationship between 4N1Ks and UPR, unfortunately due to Covid-19 those experiments were cut and were not possible to pursue it later.

Higher autophagy with lower cellular protein content might also explain 4N1Ks effects on SASP migratory ability and its production as shown by Boyden chamber assay results. On the contrary, according to RT-qPCR results 4N1Ks peptide did not affect mRNA levels of several

SASP components. The Boyden chamber assay results in Figure 3 could be explained by the antiproliferative effect of 4N1Ks on both cancer cell lines, however when we tested the migratory ability of SASP produced by senescent cells treated with 4N1Ks peptide compared to normal SASP, this could indicate that 4N1Ks affect the production of SASP factors. These results oppose the fact that TSP1 promotes invasion and migration of endothelial cells osteosarcoma cells [40]. Anyhow, TSP1 effects are mediated by several receptors and since 4N1Ks is derived from the C-terminal domain it does not possess all TSP1 effectivity.

Lastly, CIS escape experiments on MCF7 and LS174t expressing an shRNA directed against CD47 were to prove any link of the above results with 4N1Ks interaction with CD47 receptor. Unfortunately, there was no difference in 4N1Ks effect on CIS escape between cells expression sh CD47 compared to control. Moreover, several recent studies have indicated that 4N1K peptide and 7N3 effects are not related to their interaction with CD47 [37,41]. Again, further experiments were not possible due to Covid-19 situation.

It is important to note that all the studies on 4N1K and its analogue PKHB1 effects were in cancer cells and there are no reports on their effect on senescent cells.

Taking all the results we had with 4N1Ks we speculated that its effect is more at protein level rather than transcriptional one.

5. Conclusions.

4N1Ks with its relatively small size of 10 amino acids and its significant ability to prevent senescence escape, reducing the migratory ability of SASP, and the metabolic activity of senescent cells, makes 4N1Ks an attractive candidate for Senotherapy in order to enhance the health-span and lifespan of cancer patients who have received chemotherapies.

6. References:

1. Borodkina, A. V; Deryabin, P.I.; Giukova, A.A.; Nikolsky, N.N. “Social Life” of Senescent Cells: What Is SASP and Why Study It? **2018**, *10*, 4–14.

2. Storer, M.; Mas, A.; Robert-Moreno, A.; Pecoraro, M.; Ortells, M.C.; Di Giacomo, V.; Yosef, R.; Pilpel, N.; Krizhanovsky, V.; Sharpe, J.; et al. Senescence is a developmental mechanism that contributes to embryonic growth and patterning. *Cell* **2013**, *155*, 1119, doi:10.1016/j.cell.2013.10.041.

3. Pignolo, R.J.; Passos, J.F.; Khosla, S.; Tchkonia, T.; Kirkland, J.L. Reducing Senescent Cell Burden in Aging and Disease. *Trends Mol. Med.* **2020**, *26*, 630–638, doi:10.1016/j.molmed.2020.03.005.

4. Milanovic, M.; Fan, D.N.Y.; Belenki, D.; Däbritz, J.H.M.; Zhao, Z.; Yu, Y.; Dörr, J.R.; Dimitrova, L.; Lenze, D.; Monteiro Barbosa, I.A.; et al. Senescence-associated reprogramming promotes cancer stemness. *Nature* **2018**, *553*, 96–100, doi:10.1038/nature25167.

5. Carné Trécesson, S. De; Guillemin, Y.; Bélanger, A.; Bernard, A.C.; Preisser, L.; Ravon, E.; Gamelin, E.; Juin, P.; Barré, B.; Coqueret, O. Escape from p21-mediated oncogene-induced senescence leads to cell dedifferentiation and

dependence on anti-apoptotic Bcl-xL and MCL1 proteins. *J. Biol. Chem.* **2011**, *286*, 12825–12838, doi:10.1074/jbc.M110.186437.

6. Vigneron, A.; Roninson, I.B.; Gamelin, E.; Coqueret, O. Src inhibits adriamycin-induced senescence and G2 checkpoint arrest by blocking the induction of p21waf1. *Cancer Res.* **2005**, *65*, 8927–8935, doi:10.1158/0008-5472.CAN-05-0461.

7. Vétillard, A.; Jonchère, B.; Moreau, M.; Toutain, B.; Henry, C.; Fontanel, S.; Bernard, A.C.; Campone, M.; Guette, C.; Coqueret, O. Akt inhibition improves irinotecan treatment and prevents cell emergence by switching the senescence response to apoptosis. *Oncotarget* **2015**, *6*, 43342–43362, doi:10.18632/oncotarget.6126.

8. Jonchère, B.; Vétillard, A.; Toutain, B.; Lam, D.; Bernard, A.C.; Henry, C.; Carné Trécesson, S. De; Gamelin, E.; Juin, P.; Guette, C.; et al. Irinotecan treatment and senescence failure promote the emergence of more transformed and invasive cells that depend on anti-apoptotic Mcl-1. *Oncotarget* **2015**, *6*, 409–426, doi:10.18632/oncotarget.2774.

9. Ansieau, S.; Collin, G. Senescence versus apoptosis in chemotherapy. *Oncotarget* 2015, *6*, 4551–4552.

10. Le Duff, M.; Gouju, J.; Jonchère, B.; Guillon, J.; Toutain, B.; Boissard, A.; Henry, C.; Guette, C.; Lelièvre, E.; Coqueret, O. Regulation of senescence escape by the cdk4-EZH2-AP2M1 pathway in response to chemotherapy. *Cell Death Dis.* **2018**, *9*, doi:10.1038/s41419-017-0209-y.

11. Saleh, T.; Tyutyunyk-Massey, L.; Murray, G.F.; Alotaibi, M.R.; Kawale, A.S.; Elsayed, Z.; Henderson, S.C.; Yakovlev, V.; Elmore, L.W.; Toor, A.; et al. Tumor cell escape from therapy-induced senescence. *Biochem. Pharmacol.* **2019**, *162*, 202–212, doi:10.1016/j.bcp.2018.12.013.

12. Roberson, R.S.; Kussick, S.J.; Vallieres, E.; Chen, S.Y.J.; Wu, D.Y. Escape from therapy-induced accelerated cellular senescence in p53-null lung cancer cells and in human lung cancers. *Cancer Res.* **2005**, *65*, 2795–2803, doi:10.1158/0008-5472.CAN-04-1270.

13. Guillon, J.; Petit, C.; Moreau, M.; Toutain, B.; Henry, C.; Roché, H.; Bonichon-Lamichhane, N.; Salmon, J.P.; Lemonnier, J.; Campone, M.; et al. Regulation of senescence escape by TSP1 and CD47 following chemotherapy treatment. *Cell Death Dis.* **2019**, *10*, doi:10.1038/s41419-019-1406-7.

14. Gao, Q.; Chen, K.; Gao, L.; Zheng, Y.; Yang, Y.G. Thrombospondin-1 signaling through CD47 inhibits cell cycle progression and induces senescence in endothelial cells. *Cell Death Dis.* **2016**, *7*, e2368-7, doi:10.1038/cddis.2016.155.

15. Kaur, S.; Martin-Manso, G.; Pendrak, M.L.; Garfield, S.H.; Isenberg, J.S.; Roberts, D.D. Thrombospondin-1 inhibits VEGF receptor-2 signaling by disrupting its association with CD47. *J. Biol. Chem.* **2010**, *285*, 38923–38932, doi:10.1074/jbc.M110.172304.

16. Sick, E.; Jeanne, A.; Schneider, C.; Dedieu, S.; Takeda, K.; Martiny, L. CD47 update: a multifaceted actor in the tumour microenvironment of potential therapeutic interest. *Br. J. Pharmacol.* **2012**, *167*, 1415–1430, doi:10.1111/j.1476-5381.2012.02099.x.

17. Huang, T.; Sun, L.; Yuan, X.; Qiu, H. Thrombospondin-1 is a multifaceted player in tumor progression. *Oncotarget* **2017**, *8*, 84546–84558, doi:10.18632/oncotarget.19165.

18. Resovi, A.; Pinessi, D.; Chiorino, G.; Taraboletti, G. Current understanding of the thrombospondin-1 interactome. *Matrix Biol.* **2014**, *37*, 83–91, doi:https://doi.org/10.1016/j.matbio.2014.01.012.

19. Ana-Carolina Martinez-Torres, Claire Quiney, Tarik Attout, H.B.; Linda Herbi, Laura Vela, Sandrine Barbier, D.C.; Elise Chapiro, Florence Nguyen-Khac, Frédéric Davi, M.L.G.-; Tavernier, Roba Moumné, Marika Sarfati11, Philippe Karoyan, H.M.-; Béral, P.L.S.A.S. CD47 Agonist Peptides Induce Programmed Cell Death in Refractory Chronic Lymphocytic Leukemia B Cells via PLC γ 1 Activation : Evidence from Mice and Humans. **2015**, *12*, 1–38, doi:10.1371/journal.pmed.1001796.

20. Denèfle, T.; Boullet, H.; Herbi, L.; Newton, C.; Martinez-Torres, A.C.; Guez, A.; Pramil, E.; Quiney, C.; Pourcelot, M.; Levasseur, M.D.; et al. Thrombospondin-1 Mimetic Agonist Peptides Induce Selective Death in Tumor Cells: Design, Synthesis, and Structure-Activity Relationship Studies. *J. Med. Chem.* **2016**, *59*, 8412–8421, doi:10.1021/acs.jmedchem.6b00781.

21. Kalas, W.; Swiderek, E.; Świtalska, M.; Wietrzyk, J.; Rak, J.; Strządała, L. Thrombospondin-1 receptor mediates autophagy of RAS-expressing cancer cells and triggers tumour growth inhibition. *Anticancer Res.* **2013**, *33*, 1429–1438.

22. McDonald, J.F.; Dimitry, J.M.; Frazier, W.A. An amyloid-like C-terminal domain of thrombospondin-1 displays CD47 agonist activity requiring both VVM motifs. *Biochemistry* **2003**, *42*, 10001–10011, doi:10.1021/bi0341408.

23. Campone, M.; Valo, I.; Jézéquel, P.; Moreau, M.; Boissard, A.; Campion, L.; Loussouarn, D.; Verriele, V.; Coqueret, O.; Guette, C. Prediction of recurrence and survival for triple-negative breast cancer (TNBC) by a protein

signature in tissue samples. *Mol. Cell. Proteomics* **2015**, *14*, 2936–2946, doi:10.1074/mcp.M115.048967.

24. Tugyi, R.; Uray, K.; Ra Ivá, D.; Perkins, A.; Hudecz, F. *Partial D-amino acid substitution: Improved enzymatic stability and preserved Ab recognition of a MUC2 epitope peptide*; 2005; Vol. 102;.

25. D'Adda Di Fagagna, F. Living on a break: Cellular senescence as a DNA-damage response. *Nat. Rev. Cancer* **2008**, *8*, 512–522, doi:10.1038/nrc2440.

26. Georgakilas, A.G.; Martin, O.A.; Bonner, W.M. p21: A Two-Faced Genome Guardian. *Trends Mol. Med.* **2017**, *23*, 310–319, doi:10.1016/j.molmed.2017.02.001.

27. Beauséjour, C.M.; Krtolica, A.; Galimi, F.; Narita, M.; Lowe, S.W.; Yaswen, P.; Campisi, J. Reversal of human cellular senescence: Roles of the p53 and p16 pathways. *EMBO J.* **2003**, *22*, 4212–4222, doi:10.1093/emboj/cdg417.

28. Noren Hooten, N.; Evans, M.K. Techniques to induce and quantify cellular senescence. *J. Vis. Exp.* **2017**, *2017*, 1–14, doi:10.3791/55533.

29. Meijles, D.N.; Sahoo, S.; Al Ghouleh, I.; Amaral, J.H.; Bienes-Martinez, R.; Knupp, H.E.; Attaran, S.; Sembrat, J.C.; Nouraie, S.M.; Rojas, M.M.; et al. The matricellular protein TSP1 promotes human and mouse endothelial cell senescence through CD47 and Nox1. *Sci. Signal.* **2017**, *10*, doi:10.1126/scisignal.aaj1784.

30. Valenzuela, C.A.; Quintanilla, R.; Olate-Briones, A.; Venturini, W.; Mancilla, D.; Cayo, A.; Moore-Carrasco, R.; Brown, N.E. SASP-dependent interactions between senescent cells and platelets modulate migration and invasion of cancer cells. *Int. J. Mol. Sci.* **2019**, *20*, doi:10.3390/ijms20215292.

31. Velarde, M.C.; Demaria, M.; Campisi, J. Senescent cells and their secretory phenotype as targets for cancer therapy. *Interdiscip. Top. Gerontol.* **2013**, *38*, 17–27, doi:10.1159/000343572.

32. Lecot, P.; Alimirah, F.; Desprez, P.Y.; Campisi, J.; Wiley, C. Context-dependent effects of cellular senescence in cancer development. *Br. J. Cancer* **2016**, *114*, 1180–1184, doi:10.1038/bjc.2016.115.

33. Gosselin, K.; Deruy, E.; Martien, S.; Vercamer, C.; Bouali, F.; Dujardin, T.; Slomianny, C.; Houel-Renault, L.; Chelli, F.; De Launoit, Y.; et al. Senescent keratinocytes die by autophagic programmed cell death. *Am. J. Pathol.* **2009**, *174*, 423–435, doi:10.2353/ajpath.2009.080332.

34. Pluquet, O.; Pourtier, A.; Abbadie, C. The unfolded protein response and cellular senescence. A Review in the Theme: Cellular Mechanisms of Endoplasmic Reticulum Stress Signaling in Health and Disease. *Am. J. Physiol. - Cell Physiol.* **2015**, *308*, C415–C425, doi:10.1152/ajpcell.00334.2014.

35. Guillon, J.; Toutain, B.; Boissard, A.; Guette, C.; Coqueret, O. tRNA biogenesis and specific Aminoacyl-tRNA Synthetases regulate senescence stability under the control of mTOR. *bioRxiv* **2020**, doi:10.1101/2020.04.30.068114.

36. Guha, P.; Kaptan, E.; Gade, P.; Kalvakolanu, D. V; Ahmed, H. Tunicamycin induced endoplasmic reticulum stress promotes apoptosis of prostate cancer cells by activating mTORC1. *Oncotarget* **2017**, *8*, 68191–68207, doi:10.18632/oncotarget.19277.

37. Leclair, P.; Kim, M.J.; Lim, C.J. Peptide analogues PKHB1 and 4N1K induce cell death through CD47-independent mechanisms. *Cancer Sci.* **2020**, *111*, 1028–1030, doi:10.1111/cas.14310.

38. Gerland, L.-M.; Peyrol, S.; Lallemand, C.; Branche, R.; Magaud, J.-P.; Ffrench, M. Association of increased autophagic inclusions labeled for beta-galactosidase with fibroblastic aging. *Exp. Gerontol.* **2003**, *38*, 887–895, doi:10.1016/s0531-5565(03)00132-3.

39. Capasso, S.; Alessio, N.; Squillaro, T.; Di Bernardo, G.; Melone, M.A.; Cipollaro, M.; Peluso, G.; Galderisi, U. Changes in autophagy, proteasome activity and metabolism to determine a specific signature for acute and chronic senescent mesenchymal stromal cells. *Oncotarget* **2015**, *6*, 39457–39468, doi:10.18632/oncotarget.6277.

40. Hu, C.; Wen, J.; Gong, L.; Chen, X.; Wang, J.; Hu, F.; Zhou, Q.; Liang, J.; Wei, L.; Shen, Y.; et al. Thrombospondin-1 promotes cell migration, invasion and lung metastasis of osteosarcoma through FAK dependent pathway. *Oncotarget* **2017**, *8*, 75881–75892, doi:10.18632/oncotarget.17427.

41. Leclair, P.; Lim, C.J. CD47-independent effects mediated by the TSP-derived 4N1K peptide. *PLoS One* **2014**, *9*, doi:10.1371/journal.pone.0098358.

Chapter 2:

Senolytic and Senostatic Sphingomyelin based Nanosystems.

Abstract:

Chemotherapeutic and anti-cancer agents have the ability to induce cellular senescence in proliferative and cancer cells. Cancer cells turning to senescent have cells have the capacity to escape senescence state and emerge as a more aggressive form of cancer leading to cancer relapse. Moreover, this therapy-induced senescence also plays an important role in several age-related diseases, linking chemotherapies to accelerated ageing. Therefore, developing senotherapeutics has become of interest to improve the health span and life span. Taking advantage of sphingomyelin-based nanosystems' (SNs) biocompatibility, biodegradability, and versatility to associate or encapsulate different therapeutic molecules, as previously shown [1–6] . We developed three distinctive SNs with 3 different therapeutic molecules that target senescent cells in a different way.

First therapeutic molecule is a lipid derivative of the 4N1Ks peptide (studied in the previous chapter), which was conveniently associated to the surface of SNs and exposed at the surface for an effective targeting of senescent cells. The second therapeutic candidate was ABT-737, which was encapsulated in the oily core of SNs. The last therapeutic component was oleuropein, similarly encapsulated into the oily core. All SNs nanosystems were extensively characterized regarding size, stability overtime, stability in different biological media, association/encapsulation efficiency, cytotoxicity, hemocompatibility, and most importantly, by their effect on senescence escape in chemotherapy-induced senescence model of breast cancer cells.

1. Materials and Methods:

1.1. Materials

Vitamin E (VitE, DL-α-Tocopherol) was purchased from Calbiochem (Merck-Millipore, Darmstadt, Germany). Sphingomyelin (SM, Lipoid E SM) was kindly provided by Lipoid GmbH (Ludwigshafen, Germany). C18-PEG-4N1Ks was synthesised by Covalab (Bron, France). ABT-737 were purchased from Abcam (Abcam, UK). Oleuropein was purchased from CAYMAN Chemical (Madrid, Spain). HPLC grade Acetonitrile (ACN) and Ethanol (EtOH), Dimethyl sulfoxide (DMSO) were purchased from Acros Organics (country). Methanol (MetOH) was purchased from Merck (Darmstadt, Germany). Alamar blue reagent was purchased from Fisher Chemicals (Thermo Fisher Scientific, USA). Trifluoroacetic acid (TFA) and MTT (3-(4,5-Dimethyl-2-thiazolyl)-2,5-diphenyl-2H-tetrazolium Bromide) were provided by Sigma-Aldrich (Madrid, Spain). RPMI cell culture medium, Fetal bovine serum (FBS) and

Doxorubicin hydrochloride (≥98%) were purchased from CAYMAN Chemical (Michigan, USA). All other chemicals used were HPLC or UPLC purity grade.

1.2. Methods:

1.2.1. Preparation of SNs

1.2.1.1. Preparation of SNs and association of 4N1Ks

SNs were prepared by the straightforward and very simple ethanol injection method, as previously reported by our research group [5–7]. In short, VitE and SM were dissolved in ethanol at a concentration of 200 mg/mL and 40 mg/mL, respectively. Next, VitE and SM solutions were subsequently mixed to obtain a mass ratio of 1:0.1 (V:SM), corresponding to 5 mg of vitamin E. The resulting volume was completed up to 100 µL with ethanol and then injected into 1 mL of ultrapure water under continuous magnetic stirring (<10% of ethanol in the final formulation).

SNs associating 4N1Ks on the surface were prepared as follows. Initially, 4N1Ks was first modified by covalently linking it with a PEGylated-lipid containing a carboxyl group (C18-PEG6-COOH) resulting in the amphiphilic molecule C18-PEG6-4N1Ks (C18-PEG-Ks), which was performed under request by Covalab (Bron, France). C18-PEG-Ks was dissolved at a concentration of 20 mg/mL in a mixture of ethanol and water (EtOH 70%). Similar as for blank SNs preparation, VitE (200 mg/mL) and SM (40 mg/mL) and C18-PEG-Ks were mixed to obtain different mass ratios of the peptide (VitE:SM:C18-PEG-Ks 1:0.1:0.025 to 1:0.1:0.2, corresponding to a peptide concentration of 0.125 to 1 mg/mL) and ethanol was added to complete 100 µL. This organic phase was then injected into 1 mL of ultrapure water under continuous magnetic stirring for a couple of minutes. The formulations containing all the components were named SNs-Ks. A control formulation with only the VitE and the peptide was named V-Ks.

The association efficiency (AE%) of C18-PEG-Ks into the nanosystems was determined by direct quantification of the peptide using gradient HPLC analysis method. The isolation of nanosystems from free molecules was performed as follows: 1.5 mL of nanosystems (SNs-Ks, V-Ks) were injected into a dialysis cassette (Slide-A-Lyzer™ G2 Dialysis Cassette, Thermo Fisher Scientific, US) with a membrane molecular-weight cut-off (MWCO) of 20 KDa. Then the cassette was immersed in 800 mL of ultra-pure water with gentle stirring at room temperature (RT). The dialysis procedure was done for 2 h first then change water; another 2 h

of dialysis and change water; then left for dialysis overnight. The new volume of nanosystems were measured after dialysis. Before injecting the nanosystems in HPLC column, they were dissolved in MetOH at a volume ratio of 1:20 (SNs:MetOH).

HPLC analysis was performed using a HPLC system 1260 Infinity II Agilent (Agilent Technologies, US) equipped with a pump G7111A, an autosampler G7129A, and an UV-Vis detector G7114A set at 220 nm wavelength. An Infinity Lab Poroshell 120 EC-C18 (100 mm x 4.6 mm, 4 µm pore size) Agilent column was used and operated at RT. The mobile phases used were (A) ultrapure water with 0.1 % (v/v) TFA, and (B) ACN with 0.1 % (v/v) TFA The following gradient conditions were used; 0 min B=20 %; 1 min, B=20 %; 8 min B=80 %; 10 min B=80 %, 12 min B=20 %, maintaining a flow rate of 0.5 mL/min. Standard calibration curves were linear in the range of 7.8 to 250 ppm (R2 = 0.9999).

The association efficiency of C18-PEG-Ks into the nanosystems was calculated using the following equation:

Equation 1: Direct measurement of the encapsulated fraction.

$$\boldsymbol{AE}\% = \left(\frac{\boldsymbol{Associated}\mu\boldsymbol{g}}{\boldsymbol{total}\mu\boldsymbol{g}}\right) \times 100$$

1.2.1.2. Preparation of SNs loaded with ABT-737

ABT-737 was dissolved in DMSO at a concentration of a 20 mg/mL. Similar as for blank SNs preparation, VitE (200 mg/mL) and SM (40 mg/mL) and ABT-737 were mixed to obtain different mass ratios of the peptide (VitE:SM:ABT-737 1:0.1:0.005 to 1:0.1:0.02, corresponding to ABT-737 concentration of 0.025 to 0.1 mg/mL) and ethanol was added to complete 100 µL. This organic phase was then injected into 1 mL of ultrapure water under continuous magnetic stirring for a couple of minutes. Those formulations were named SNs-ABT.

Encapsulation efficiency (EE%) of ABT-737 into the nanosystems was determined by direct quantification of ABT using gradient HPLC analysis method. The isolation of nanosystems from free molecules was performed as the dialysis procedure was done for 2 h first then change water and another 2 h of dialysis. The new volume of nanosystems were measured after dialysis. Before injecting the nanosystems in HPLC column, they were dissolved in MetOH at a volume ratio of 1:20 (SNs:MetOH).

HPLC analysis was performed using an HPLC system 1260 Infinity II Agilent (Agilent Technologies, US) equipped with a pump G7111A, an autosampler G7129A, and an UV-Vis detector G7114A set at 251 nm wavelength. An InfinityLab Poroshell 120 EC-C18 (100 mm x 4.6 mm, 4 µm pore size) Agilent column was used and operated at RT. The mobile phases used were (A) ultrapure water with 0.1 % (v/v) TFA, and (B) ACN with 0.1 % (v/v) TFA The following gradient conditions were used; 0 min B=20 %; 1 min, B=20 %; 8 min B=80 %; 10 min B=80 %, 12 min B=20 %, maintaining a flow rate of 1 mL/min. Standard calibration curves were linear in the range of 0.5 to 80 ppm (R2 = 0.9999).

The encapsulation efficiency of ABT-737 into the nanosystems was calculated using the following equation:

Equation 1: Direct measurement of the encapsulated fraction.

$$\boldsymbol{EE}\% = \frac{(\boldsymbol{Encapsulate}\mu\boldsymbol{g})}{(\boldsymbol{total}\mu\boldsymbol{g})} \times 100$$

1.2.1.3. Preparation of SNs loaded with Oleuropein.

Oleuropein was dissolved in ethanol at a concentration of a 20 mg/mL. Similar as for blank SNs preparation, VitE (200 mg/mL) and SM (40 mg/mL) and ABT-737 were mixed to obtain different mass ratios of the peptide (VitE:SM:Ole 1:0.1:0.01 to 1:0.1:0.05, corresponding to Oleuropein concentration of 0.05to 0.25 mg/mL) and ethanol was added to complete 100 µL. This organic phase was then injected into 1 mL of ultrapure water under continuous magnetic stirring for a couple of minutes. Those formulations were named SNs-Ole.

1.2.2. Physicochemical characterisation of the nanosystems

Particle size and polydispersity index (PdI) of the nanoemulsions were determined by dynamic light scattering (DLS) after a dilution 1:20 (v/v) in water. The surface charge (Z-potential, ZP) values were obtained by Laser Doppler Anemometry (LDA) (Zetasizer NanoZS®, Malvern Instruments, Worcestershire, United Kingdom). Additionally, extended nanoemulsion characterisation was performed by Nanoparticle Tracking Analysis (NTA) and Multiple-Angle Dynamic Light Scattering (MA-DLS). For NTA, the nanosystems were diluted at 1:1000 (v/v) in ultrapure water (NanoSight LM20, Amesbury, United Kingdom). Data collection was settled with 3 repeats/60s capture time, with both shutter and gain manually determined for each sample. NTA 2.0 Build 127 software was used for measurement and subsequent data analysis.

MA-DLS analyses were performed using an ALV SP−86 goniometer with an ALV 5000 Multi-tau correlator and a Coherent Sapphire optically pumped semiconductor laser operating at λ = 488 nm and 200 mW power. Un-dialyzed samples were diluted 10 times with ultrapure water, while dialyzed samples were diluted 100 times. Measurements were performed at 25 °C and scattering angles between θ = 30° and 150° with increments of 10° and measuring times of 300s. Results were analysed using the ALV Correlator Software (ALV-5000/E version 3.0) based on the CONTIN algorithm adapted to the specific correlator noise. The logarithmically sampled relaxation time spectra (amplitude vs. log(τ)) were obtained from the CONTIN inversion of the normalised correlation functions. Assuming homodyne light beating, the distribution of diffusivities were obtained applying the relation $D = 1 / (q^2\tau)$, and transformed using the Stokes-Einstein relation, the solvent viscosity (η_0) and refractive index (n) at the actual temperature (T) in order to yield the hydrodynamic radius $R_H = kTq^2\tau / 6\pi\eta_0$ where k is the Boltzmann constant, $q = (4\pi n/\lambda) \sin(\theta/2)$ is the scattering vector as a function of wavelength in vacuum (λ), and scattering angle (θ).

The topography of the nanoemulsion systems was studied with Non-Contact Atomic Force Microscopy (NC-AFM) under ambient conditions. For this, AFM analysis samples were diluted with ultrapure water 100 times and 10 µL were deposited onto a mica substrate (SPI Supplies, Grade V−1 Muscovite), allowed to dry and then viewed using a XE−100 instrument (Park Systems, Korea) with a non-contact silicon cantilever probe with high resonant frequency (325 kHz) and backside aluminum reflex coating (ACTA, supplied by Park Systems).

1.2.3. Colloidal stability

The colloidal stability of the nanoemulsions was determined upon incubation with different medium as PBS 5 mM (1:2 v/v), cell culture medium RPMI (1:6 v/v) supplemented or not with 1% (v/v) FBS, and human serum previously filtered and diluted 10x in water (1:10, v/v) up to 24 h at 37 ºC and horizontal agitation. The colloidal stability of the nanosystems stored at 4 ºC was also determined. Prior to DLS analysis, using Zetasizer NanoZS® (Malvern Instruments, Worcestershire, United Kingdom), all the samples were further diluted in ultrapure water at 1:10 (v/v)

1.2.4. *In vitro* toxicity.

1.2.4.1. Metabolic activity assay.

MCF7 breast cancer cells (ATCC, HTB-22) were seeded at a density of 1500 cells/well in 96-well plates and cultured in RPMI supplemented with 3% (v/v) FBS, at 37 ºC in 5% CO_2

atmosphere. The next day, the cell culture medium was replaced by increasing concentrations of C18-PEG-Ks (0.25 µM to 1 µM) or ABT-737 (1 µM to 15 µM) diluted in supplemented RPMI to a final volume of 150 µL per well. After 72 h of incubation with C18-PEG-Ks/ ABT-737, the medium was aspirated and cells were washed with PBS 2x, and then 100 µL of MTT solution (5 mg/mL in PBS) were added to each well and incubated for 4 h. Afterwards, the formazan crystals were solubilised with 100µl of DMSO and the absorbance was measured at 540 nm using a microplate reader (Multiskan EX, Thermo Labsystems). Cell viability (%) was calculated in percentage related to untreated (control) cells.

1.2.4.2. Colony forming assay (CFA).

MCF7 breast cancer cells were seeded in a 12-well plate at a density of 500 cells/well and cultured in RPMI supplemented with 10 % (v/v) FBS, at 37 ºC in 5 % CO_2 atmosphere. After 24 h, cells were treated with increasing concentration of SNs-Ks and V-Ks (0.25 µM to 1µM). SNs-blank and C18-PEG-Ks were used as positive controls. The cells remained in contact with treatment the whole period of the experiment, 10 days, which is the time needed for visible colonies to be formed. After this period, cells were incubated with MTT solution (5 mg/mL in PBS) for 4 h and subsequently dried and scanned. The obtained images were analysed using ImageJ software [8].

1.2.4.3. Blood compatibility

Haemolysis assay was performed as follows, 100 µL of a 3% (w/v) suspension of heparin-stabilised erythrocytes were plated in a rounded bottom 96 well plate and incubated with the nanosystems for 4 h, SNs-blank and SNs-Ks at concentrations from 0.25 to 1µM, SNs-ABT from 0.25 to 1µM, and SNs-Ole at concentrations from 0.5 to 5µM (added in a 50 µL total volume). Positive and negative controls were 50 µL /well of 1% Triton X-100 and PBS respectively. After incubation time, the plate was centrifuged at 1000 RPM for 10 min at 4 ºC. Subsequently, 80 µL of the supernatant were transferred to another 96 well plate and read at 570 nm (absorption maxima of deoxyhaemoglobin and oxyhaemoglobin). Haemolysis percentage was calculated following the next equation.

Equation 2: Formula for calculation of the haemolysis percentage.

$$\boldsymbol{Haemolysis}\% = \frac{\boldsymbol{Sample - PBScontrol}}{\boldsymbol{TritonX}100 - \boldsymbol{PBScontrol}}$$

1.2.5. Cell uptake

The internalisation of SNs, SNs-Ks was evaluated in MCF7 breast cancer cells by confocal laser scan microscopy (Leica microscope TCS SP8, Germany). Fluorescent SNs-blank and SNs-Ks were first prepared by supplementing a percentage of SM with the modified lipid TopFluor®-SM (5.6 µg/mL to achieve 25 ng/well of fluorescent matter). Cells were seeded in 8-well chamber slides 24 h before the experiment at a density of 50000 cells/well and cultured in RPMI supplemented with 10 % (v/v) FBS. The next day, cells were treated with fluorescently labelled nanosystems at a concentration of 0.5 µM (peptide) for 10 min, 30 min, 1 h, 2 h and 4 h. After the desired incubation time, cells were washed twice with PBS and fixed with paraformaldehyde (PFA) 4 % (w/v) for 15 min at RT. Later, cellular nuclei were stained with Hoescht for 5 min and washed three times with PBS. Finally, the coverslips were mounted over the microscopy slides using Mowiol™ mounting medium (Calbiochem, UK), left to dry in darkness overnight and stored at -20 °C until visualisation.

Furthermore, the internalisation of SNs and SNs-Ks was also determined in MCF 7 cells by flow cytometry. In brief, cells were seeded in 6 well-plates at a density of 300000 cells/well in RPMI supplemented with 10% (v/v) FBS. After 24 h, cells were treated with the fluorescently labelled nanosystems at a concentration of 0.5 µM (peptide) for 10 min, 30 min, 1 h, 2 h, and 4 h. Following these incubation times, cells were washed twice with PBS, and after trypsinization they were collected, resuspended and finally fixed in 500 µL of PFA 4% (w/v) for 15 min at RT. Samples were kept at 4 °C, protected from light, until flow cytometry analysis.

1.2.6. *In vitro* evaluation of SNs-Ks

1.2.6.1. Senescence escape assay

In order to determine the efficiency of SNs-Ks/ SNs-ABT in preventing senescence escape and study their possible senolytic effects in chemotherapy-induced senescence model, a senescence escape assay was performed using MCF7 breast cancer cells. Cells were seeded in 6 well-plates at a density of 50000 cells/well and cultured in RPMI supplemented with 3% (v/v) FBS, at 37 ºC in 5 % CO_2 atmosphere. After 24 h, cells were treated with doxorubicin at a concentration of 25 ng/mL for 96 h to generate MCF7 senescent cells [9]. After that, cell culture medium was aspirated, cells were washed with PBS and treated with the nanosystems for 24 h. Afterwards, the cells were washed with PBS and restimulated with fresh RPMI (10% v/v FBS) for 14 days. Emerged colonies were incubated with MTT solution (5 mg/mL in PBS) for 4 h and subsequently dried and scanned. Obtained images were analysed using ImageJ software.

In order to make sure that after chemotherapy treatment (doxorubicin 25 ng/mL for 96 h) MCF7 cancer cell became senescent, the expression of cellular senescence markers such as β-galactosidase and p53/p21 were determined.

For β-galactosidase analysis, after doxorubicin treatment, the cells were fixed for 15 min at RT in 1% formaldehyde, then washed with PBS and incubated at 37 °C (in the absence of CO_2) with fresh staining solution (0.3 mg/mL of 5-bromo4-chloro-3 indolyl β-D-galactoside (X-Gal, Fermentas), 40 mM citric acid, 40 mM sodium phosphate at pH 6, 5 mM potassium ferrocyanide, 5 mM potassium ferricyanide, 150 mM NaCl, 150 mM $MgCl_2$ (all reagents were acquired from Sigma-Aldrich (Madrid, Spain)). SA-β-GAL-positive cells were quantified after 20 h.

The expression of p53 and p21 was assessed after 24 h of doxorubicin treatment, as p53 expression starts to decrease after this period. The expression of p21 and p53 was determined by western blot after protein extraction from the treated cells. The following antibodies were used: anti-p21Waf1 (Cell Signaling, 2947S), anti p-p53ser15 (Cell Signaling, 9284). Visualization was performed by chemiluminescence with a Bio-Rad Chemi Doc XRS imaging device (Bio-Rad) and Fusion Solo (Vilber).

1.2.7. Statistical analysis

All values were expressed as mean +/− standard deviation (SD). Differences were analysed using non- parametric tests (t test, Mann–Whitney, Kolmogorov–Smirnov, and one-way ANOVA). Statistical analysis was performed using GraphPad Prism (Version 6.0 software) (GraphPad Software, San Diego, CA, USA). A p value < 0.05 was considered to be significant.

This chapter is divided into 3 parts, each one represents one of the SNs prepared to specifically associate the described therapeutic molecules.

Part 1:

Sphingomyelin nanosystems decorated with TSP-1 derived peptide targeting senescent cells

1. Abstract

Senescent cells accumulation can contribute to the development of several age-related diseases, including cancer. Targeting and eliminating senescence cells, would allow the development of new therapeutic approaches for the treatment of different diseases. The 4N1Ks peptide; a 10 amino acid peptide derived from TSP1 protein, combines both features by targeting the CD47 receptor present in the surface of senescent cells and demonstrating senolytic activity, thereby representing a new strategy to take into account. Nonetheless, peptide drugs are known for their biopharmaceutical issues, such as low short half-life and tendency to aggregate, which reduces their bioavailability and limits their therapeutic potential. In order to overcome this problem, herein we propose the use of biodegradable and biocompatible sphingomyelin nanosystems (SNs), decorated with this peptide for the targeting of senescent cells. In order to efficiently associate the 4N1Ks peptide to the nanosystems while exposing it on their surface for an effective targeting of senescent cells, the 4N1Ks peptide was chemically conjugated to a PEGylated hydrophobic chain. The resulting 4N1Ks-loaded SNs (SNs-Ks), were extensively characterized for their physicochemical properties, by dynamic light scattering, multiple-angle dynamic light scattering, nanoparticle tracking analysis and atomic force microscopy. The SNs-Ks demonstrated suitable features in terms of size (~ 100 nm), association efficiency (87.2 ± 6.9%) and stability in different biorelevant media. Cell toxicity experiments in MCF7 cancer cells indicated an improved cytotoxic effect of SNs-Ks, decreasing cancer cells capacity to form colonies, with respect to free peptide, and an improved hemocompatibility. Lastly, senescence escape preliminary experiments demonstrated the improvement of SNs-Ks senolytic activity of in chemotherapy-induced senescence model of breast cancer cells. Therefore, these results demonstrate for the first time the potential of the combination of SNs with 4N1Ks peptide for the development of innovative senolytic therapies to battle cancer.

Keywords: Cellular senescence, TSP-1, sphingomyelin nanoemulsions

2.Introduction

Peptides' potency and high value to medicine has pushed them to come a long way. Currently, there are 86 peptide drugs on the market for the management of several human diseases [10]. Among small-drugs and biologicals, in 2019 peptide drugs accounted for 5% of the pharmaceutical market, with sales above $50 billion [11]. By 2025 it is expected that the protein market will reach $155.06 billion [12]. However, peptide delivery presents several limitations such as short half-life and low bioavailability due to enzymatic degradation, instability and fast renal clearance; as well as immunogenicity, which limits their full exploitation [13,14]. Nanomedicine, among other strategies, can overcome peptides' stability issues, improve their half-life and bioavailability, and consequently their therapeutic effect [10,14]. Among the different types of nanocarriers, liposomes, polymeric nanoparticles and solid lipid nanoparticles have been widely used for peptide delivery [15]. Depending on the intended application, peptides can be either encapsulated in the nanoparticles core or associated on their surface [16,17]. In this work, we aim at decorating the surface of nanocarriers with 4N1Ks peptide for the targeting of CD47 receptor, expressed on the surface of the targeted senescent cells.

Milanovic *et al.* has recently contradicted the concept of irreversible cell cycle arrest as the main feature of cellular senescence, by demonstrating that chemotherapy-induced senescent cells can escape this stage turning into a more aggressive form of cancer cells (cancer stem cells) with enhanced growth potential [18]. The accumulation of these cells due to the immune surveillance system failure, provides a proinflammatory niche that results in several age-related diseases, including cancer. In addition, it was demonstrated that tumour sites rich in senescent cells are directly linked to cancer relapse [18,19]. In this sense, the elimination of senescent cells using senolytic drugs has been the centre of attention of several researchers to improve cancer and age-related diseases outcome [20–22]. Nowadays there are several drugs described in literature for their senolytic activity for cancer and other age-related diseases. Dasatinib, quercetin and rapamycin are some examples of senolytic drugs currently under clinical evaluation [23]. In addition, considering that cellular senescence is a highly dynamic biological phenomenon, great efforts are being made to find senescence specific markers which will allow the development of senotherapies specifically targeted to these cells. In this regard, we have recently shown that homotrimer glycoprotein TSP-1/CD47 receptor is able to avoid senescence escape in chemotherapy-induced colon and breast cancer cells by inhibiting self-renewal and cell proliferation [9]. In addition, our group has recently shown that 4N1Ks, a 10 amino acid peptide derived from the C-terminal domain of TSP-1, has also the ability to prevent senescent

cells escape by promoting autophagy in senescent and cancer cells [24]. Maintaining the senolytic activity while decreasing the molecular weight (MW) of the therapeutic molecule is a great advantage since peptides are cheaper to synthesize, present lower immunogenicity and enhanced tissue penetration in comparison to high MW proteins.

To the best of our knowledge, among the different senescence therapeutic drugs described in the literature, up to date, there are only a few publications referring to the use of nanomedicine for targeting cellular senescence [25–33]. Most of these consist of inorganic (silica, calcium carbonate, iron oxide, molybdenum) drug delivery systems that exploit the characteristic β-galactosidase activity of the senescent cells to achieve a controlled intracellular delivery of the senolytic drugs as navitoclax [26]. Quercetin and CD9 monoclonal antibody functionalized inorganic nanoparticles are other strategies exploited for senescent cells targeting [27,28].

In this study we propose the association of 4N1Ks peptide to nanoemulsions composed of sphingomyelin, which is present in cell membranes, and vitamin E, which has been extensively used in several formulations intended for clinical and characterized for a good biodegradability and versatility for association and encapsulation of a variety of therapeutic molecules [1,3–7]. In addition, our previous works have shown that the sphingomyelin nanosystems (SNs) prepared by the simple and straightforward injection method present a great colloidal stability, low toxicity and high cell internalization [1,3–7]. In order to incorporate 4N1Ks peptide into our nanosystem structure but still presenting it on their surface, our strategy was to chemically conjugate the peptide to a lipid (C18)-PEG (polyethylene glycol) derivative. We have previously observed that by using this strategy with another peptide we could improve the targeting of metastatic colorectal cancer cells [7].

While the stearic acid chain would allow the anchorage of the peptide to the SNs structure, the PEG moiety could reduce possible interactions with blood components like proteins (opsonisation), providing ‘stealth’ properties to nanosystems [34]. An extensive physicochemical characterization of the peptide nanocarriers was performed through different methods. Their effect on cancer cells viability and colony forming capacity was studied *in vitro* breast cancer cells and a chemotherapy-induced senescence model was used in a preliminary study to determine the capacity of the peptide-functionalized SNs to eliminate senescence cells.

3.Results and discussion

Due to their specificity and potency, peptide drugs have accomplished a milestone with more than 80 products available on the market for different human conditions (cancer, diabetes,

among others) and a serious investment ongoing. However, they still present limitations as short half-life and low bioavailability which limits their translation from the bench to the market [19,20]. Such issues can be improved by combining peptides with nanotechnology. Lipidic and polymeric nanocarriers have been described in the literature for protein and peptide delivery [19–21]. In the case of lipidic carriers, the peptide can be chemically conjugated to a hydrophobic chain thereby improving its encapsulation. In the case of the work herein described, this would not only enable the incorporation of the peptide into the nanosystems structure, but also to present the 4N1Ks peptide on the surface of the nanosystems to be available to interact with the respective receptor (CD47) expressed on the surface of the targeted senescent cells. The development of new strategies targeting senescent cells is of great relevance due to their role in age related diseases and cancer recurrence, thereby different pre-clinical and clinical studies are being conducted to address this avenue to further understand and fight such diseases.

3.1. Development and characterisation of SNs-Ks

In order to incorporate 4N1Ks peptide into SNs structure and potentiate its presentation on their surface, our strategy was to chemically conjugate the peptide to a PEGylated stearic acid carbon chain (C18). PEGylated lipids have been used as a base to conjugate biomolecules like peptides and antibodies to the surface of nano-formulations [7]. In addition, PEG has been extensively used in drug delivery formulation as it prolongs blood circulation time and reduces possible interactions with blood components like proteins (opsonisation), providing ‘stealth’ properties to nanosystems [34].

In this work, the nanosystems were prepared by the single-step ethanol injection method, where the modified peptide was mixed with the other organic phase components and injected in ultra-pure water and these were named SNs-Ks. We hypothesised, that through the formulation process the modified peptide would rearrange itself so the hydrophobic part (stearic acid chain) would be incorporated in the oil core while the PEG-Ks part would be exposed on the surface of the nanosystems, as illustrated in Figure 1. In this way the PEG moiety could also improve the nanosystems colloidal stability. In fact, due to the new structure, the modified peptide might work as a surfactant and promote the disposition of the peptide on the surface of the nanosystems. In order to address this hypothesis, we decided to formulate simply with VitE and C18-PEG-Ks (V-Ks). In this way we could determine if in the absence of sphingomyelin, the modified peptide in combination with VitE would be able to form nanostructures as SM is able to. Thereby, in this work V-Ks nanosystems were simply used as controls in order to provide

evidence regarding the capacity of the modified peptide to emulsify and its arrangement on the nanosystems structure.

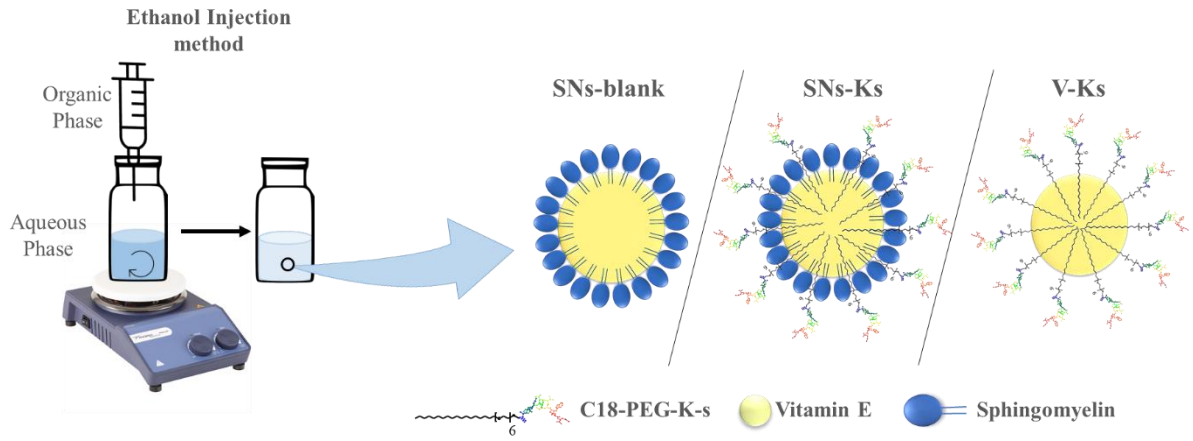

Figure 1: Schematic illustration of the nanosystems (SNs-blank, SNs-Ks and V-Ks) preparation by ethanol injection method.

Based on a previous study from our group, showing the great colloidal stability under accelerated storage conditions of the VitE:SM at 1:0.1 ratio, with around 100 nm of size and slightly negative zeta potential, this ratio was selected for the present work [1]. As shown in Figure 2 (upper panel), the incorporation of the peptide at the weight ratios 0.025, 0.05 and 0.1 (respective to VitE) did not significantly alter the hydrodynamic diameter of the nanosystems, however doubling the ratio of the peptide to 0.2 led to an increase of the size from 106 to 167 nm. Regarding the control V-Ks, C18-PEG-Ks ratios ranging from 0.025 to 0.1 resulted in the formation of nanostructures with a hydrodynamic diameter below 120 nm (Figure 2), similar to SNs-blank (1:0.1:0) and SNs-Ks (1:0.1:0.025 to 1:0.1:0.1). As observed for SNs-Ks, increasing the ratio of the modified peptide to 0.2 resulted in a bigger size of 220 nm but also to less homogeneous population as indicated by the bigger PdI (0.38). This can be explained due to the surfactant-like characteristics of the peptide conjugated to a PEGylated hydrophobic chain that, as reported in several studies, increasing amounts of surfactants lead to a smaller size of the oil droplets, however when exceeding a specific concentration lead to an increase in the particle size and can also result in unstable nanosystems [35–37]. In addition, unlike SNs-blank (without peptide) both SNs-Ks and V-Ks presented a positive zeta potential which was expected due to the 4N1Ks peptide's positively charged amino acids (lysin and arginine). Both the capacity of C18-PEG-Ks to form nanostructures with VitE and the positive surface charge of SNs-Ks and V-Ks provide evidence regarding the peptide surfactant properties and its availability on the nanosystems surface.

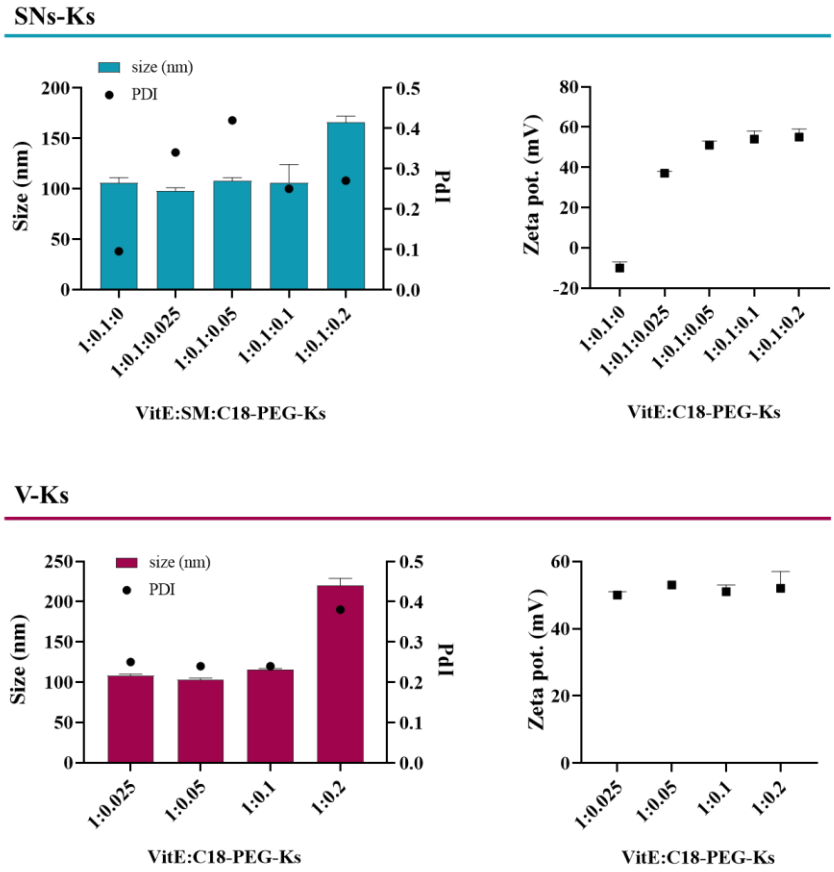

Figure 2: Effect of increasing weight ratios of C18-PEG-Ks (from 0.0025 to 0.2, respective to VitE) on SNs-Ks' (composed of VitE, SM and C18-PEG-Ks) and V-Ks' (composed of VitE and) size, polydispersity index (PdI) and zeta potential, determined by DLS.

In order to further characterize the physicochemical properties of SNs-Ks at 1:0.1:0.1 (VitE:SM:C18-PEG-Ks, w/w), other methods namely NTA, MA-DLS and AFM were used. SNS-blank (1:0.1, VitE:SM) and V-Ks (1:0.1, VitE:C18-PEG-Ks) were used as controls. The nanosystems loading C18-PEG-Ks at the ratio 0.1 were selected for further characterization considering their size (about 100 nm) as well as population homogeneity (PdI<0.3) and 4N1Ks peptide senolytic effective dose (50 µM).

As shown in Figure 3 these nanosystems were dialysed and characterized once again by DLS (before and after dialysis) in order to understand if this mild process could impair SNs-Ks physicochemical properties. This method was selected to isolate the nanosystems from the free C18-PEG-Ks molecules, as well as to determine the association efficiency of the peptide. DLS analysis showed that neither particle size or PdI (Figure 3) nor surface charge (data not shown) were affected during the dialysis process. In addition, two weeks after dialysis, DLS analysis was repeated without showing significant changes in size, PdI nor zeta potential (data not shown). The nanosystems were also characterized by NTA and MA-DLS before and after

dialysis, as complementary methods of DLS. NTA combines laser light scattering microscopy with a charge-coupled device camera and therefore grants identifying and tracking individual nanoparticles moving under Brownian motion, determining particle size and calculating particle concentration [38]. NTA data (Table 1) shows that dialysed nanosystems presented a slightly smaller mean particle size as well as span value, which indicates a smaller size distribution and a more homogenous sample. The dialysed nanosystems homogeneity is also observed in Figure 3 (lower panel). This probably indicates that the SM and modified peptide free molecules were exchanged through dialysis. D-values D10, D50, and D90, are representative of the particle diameter at 10, 50 and 90% cumulative distribution (Table 1). In general, these results are compatible with the DLS data.

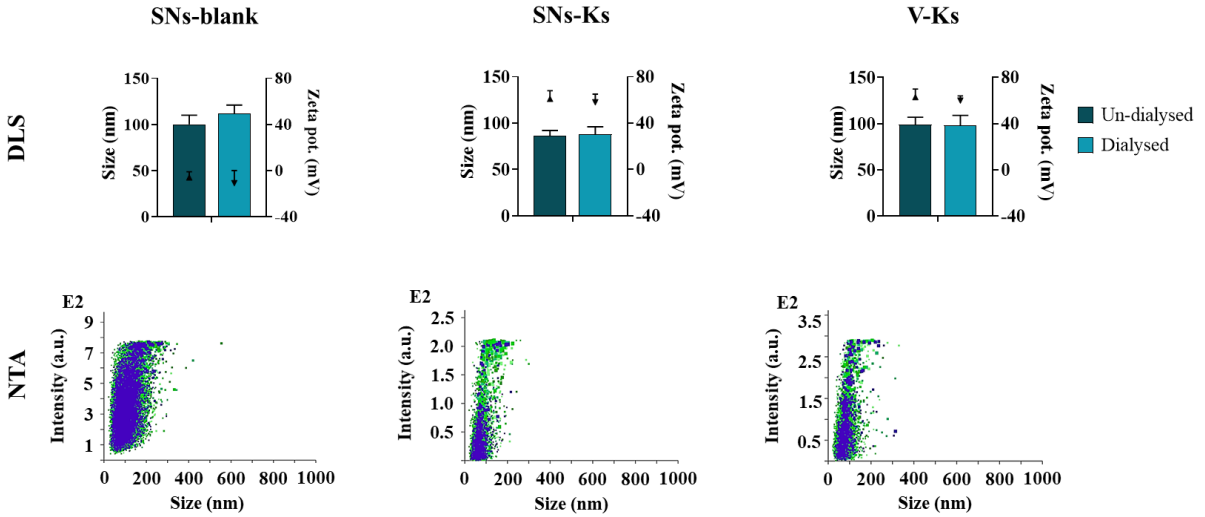

Figure 3: Physiochemical characterisation of dialysed vs un-dialysed SNs-blank (left), SNs-Ks (middle), and V-Ks (right) nanosystems by Dynamic light scattering (DLS) and dialysed nanosystems by Nanoparticle tracking analysis (NTA) (n≥3).

Table 1: Physicochemical properties of SNs-blank (1:0.1), SNs-Ks (1:0.1:0.1) and V-Ks (1:0.1) before and after dialysis, determined by NTA. Mean particle size (diameter), D-values (D10, D50, D90), calculated SPAN value and sample concentration in particles per millilitre (particle/mL) (mean ± SD, n= 3).

Nanosystems	Mean size (nm)	D10	D50	D90	Span	Concentration (particles/mL)
SNs-blank	122 ± 1	93± 1	113 ± 1	166 ± 3	0.64	1.8×10^{12}
SNs-blank dialysed	123 ± 1	96± 1	116 ± 1	155 ± 3	0.50	5.1×10^{11}
SNs-Ks	108 ± 27	76 ± 18	96 ± 26	159± 34	0.87	3.7×10^{11}
SNs-Ks dialysed	74 ± 19	58.8 ± 1	69 ± 1	98 ± 6	0.57	2.8×10^{11}
V-Ks	111 ± 32	81 ± 15	101 ± 30	152 ± 52	0.67	4.3×10^{11}
V-Ks dialysed	90 ± 3	69 ± 2	84 ± 1	121 ± 13	0.54	6.5×10^{11}

The second complementary method selected for the characterisation of the nanosystems' physicochemical properties was MA-DLS. The results show that only a single relaxation mode is observed. This mode is angular-dependent, as expected for translational Brownian diffusion of the nanosystems. Linearly-fitting the angular dependence of the inverse relaxation times for these diffusion modes (τ^{-1} vs. q^2), we can obtain an average diffusion coefficient for the nanoemulsions. The analysis revealed the existence of a single and clear relaxation mode for blank SNs, SNs-Ks and V-Ks in the whole scattering range (Figure 4). For the SNs-blank sample, the diffusion coefficient is D = 4.454 ± 0.006 $\mu m^2/s$, which corresponds to an average hydrodynamic radius of $R_H \approx 55.04 \pm 0.08$ nm. For the SNs-Ks sample, the diffusion coefficient is D = 5.476 ± 0.017 $\mu m^2/s$, which corresponds to an average hydrodynamic radius of $R_H \approx$ 44.76 ± 0.14 nm. And finally, for the V-Ks sample, the diffusion coefficient is D = 5.564 ± 0.007 $\mu m^2/s$, which corresponds to an average hydrodynamic radius of $R_H \approx$ 44.06 ± 0.06 nm. The results summarized in Table 2 show that, in general, are very consistent with the ones observed by both DLS (Figure 3) and NTA (Figure 3 and Table 1) analysis.

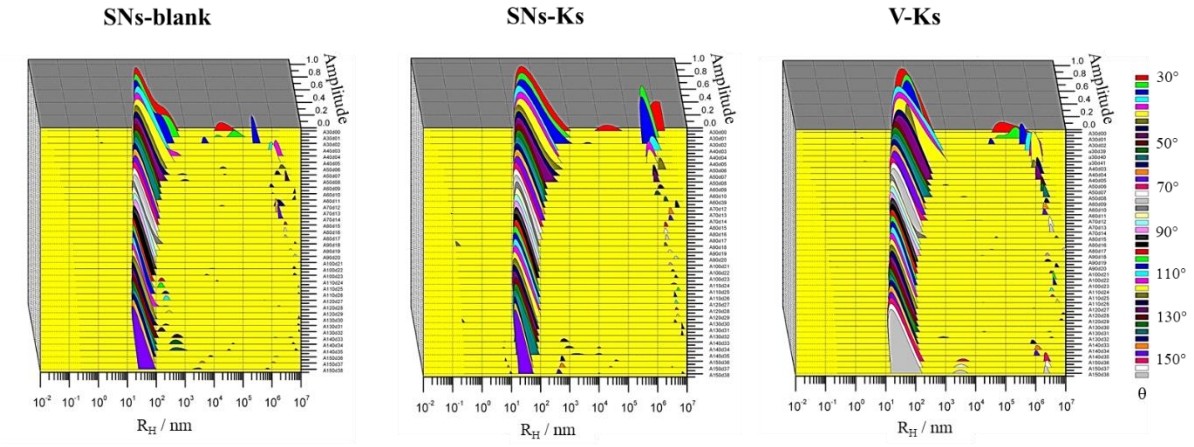

Figure 4: Physicochemical characterisation of dialysed nanosystems by Multi angle dynamic light scattering (MA-DLS) (n=3). The 3D plots show CONTIN-derived hydrodynamic radii distributions for different scattering angles (θ = 30 to 150º)

Table 2: Physicochemical characterization of nanosystems (before and after dialysis) by MA-DLS and AFM.

Nanosystems	Average Diffusion Coefficient, D (μm²/s)	Average Hydrodynamic Radius, R_H (nm)	Average Peak-to-Valley distance, R_{pv} (nm)
SNs-Blank	4.454 ± 0.006	55.04 ± 0.08	-
SNs-Blank dialysed	5.108 ± 0.018	47.99 ± 0.17	51.2 ± 29.6
SNs-Ks	5.476 ± 0.017	44.76 ± 0.14	-
SNs-Ks dialysed	6.598 ± 0.004	37.17 ± 0.02	22.0 ± 11.2
V-Ks	5.564 ± 0.007	44.06 ± 0.06	-
V-Ks dialysed	5.569 ± 0.007	44.02 ± 0.06	88.1 ± 29.7

Atomic force microscopy was also explored in order to check the heterogeneity of the particle population. Regarding this technique, only the dialyzed samples were analysed because the un-dialysed ones showed a bed of material deposited on the mica surface caused by the different components of the nanosystems that probably were solubilized outside the nanoemulsion. The AFM images were acquired immediately after deposition of the samples on the mica surface, showing clearly the characteristic spherical shape of the SNs (Figure 5), previously observed in other works through TEM analysis [1]. This spherical shape did not seem to be affected by the incorporation of the modified peptide. As shown in Table 2, in most of the depositions, the average peak-to-valley distance (R_{pv}), obtained for the nanoemulsions are below the expected sizes observed in solution. This was an expected result because the nanoemulsion droplets are spread on the mica surface after deposition and drying. The AFM heights observed for the nanoemulsion droplets of SNs, and SNs-Ks did not show a clear decrease in height with time (at least during several hours), pointing out the good stability of these nanosystems. Regarding V-Ks a phase segregation of some components was observed with time, finally resulting in the coalescence of several nanoemulsion droplets (Figure 5, bottom right). This evolution over time was also observed by B. Ruozi et al. [39]. This control formulation also led us to understand that despite the capacity of the modified peptide to behave as a surfactant due to its amphiphilic structure, it requires the presence of another component as sphingomyelin to form stable nanosystems, as it is the case of SNs-Ks.

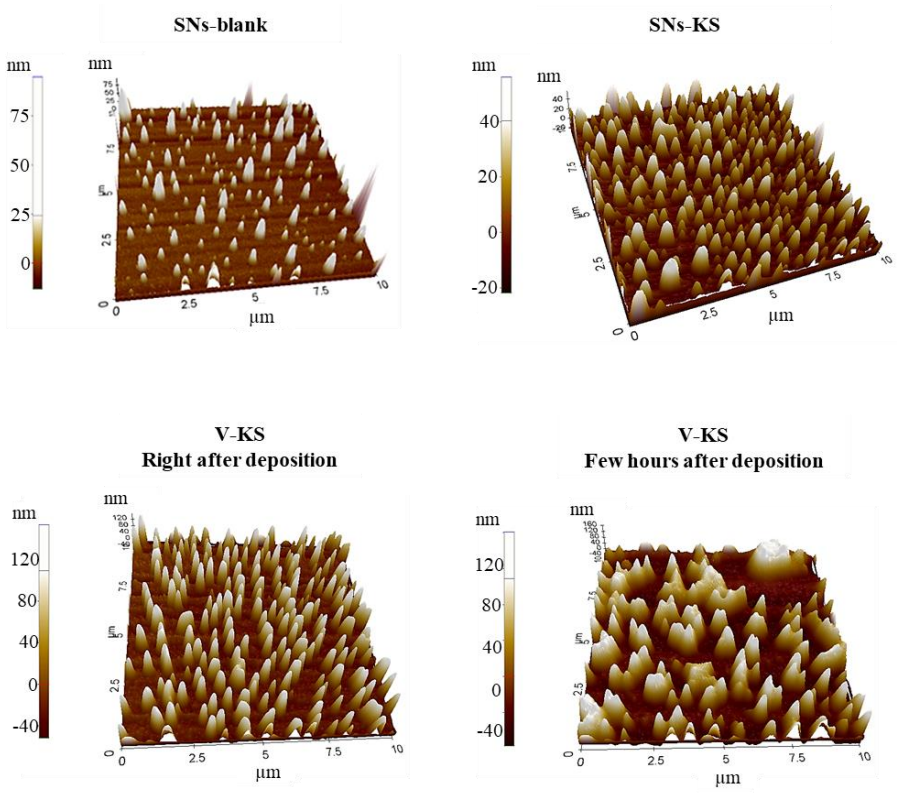

Figure 5: Physicochemical characterisation of dialysed nanosystems by Atomic force microscopy (AFM) (n=3).

Regarding the AE of the modified peptide to SNs-Ks (1:0.1:0.1), determined by HPLC after dialysis, the results showed a high AE of 87.2 ± 6.9 %, which correlates with a loading capacity (LC%) of 7.3% for SNs-Ks (1:0.1:0.1). The control formulation V-Ks (1:0.1) also presented a similar AE (90.3 ± 10.6 %), which once again indicates that C18-PEG-Ks is acting as a surfactant being able to emulsify with VitE (and SM) and form nanostructures. Note that in order to ensure that none of the nanosystems components affected the HPLC signal of the peptide, mixtures of Vit E/C18-PEG-Ks and SM/C18-PEG-Ks were also analysed.

As verified by DLS, NTA, MALS, AFM and HPLC quantification, the modified peptide was efficiently incorporated in SNs structure. C18-PEG-Ks did not lead to significant changes in SNs mean particle size, nonetheless, an excess of the peptide (namely at the ratio 1:0.1:0.2, VitE:SM:C18-PEG-Ks) led to an increase of about 60 nm was observed. As expected, the incorporation of the modified peptide to SNs and its exposure on SNs surface was clearly indicated by the increase of the surface charge from about -10 mV to about +50 mV, when compared to the control SNs-blank. The same trend was observed in the control V-Ks, which further demonstrated the surfactant-like profile of the modified peptide that was able to emulsify with VitE and form nanostructures with a mean particle size similar to SNs-blank and SNs-Ks. Therefore, as initially hypothesized, the chemical conjugation of the 4N1Ks peptide to

PEGylated carbon chain (stearic acid, C18) provided an amphiphilic character to the peptide, and therefore surfactant-like properties. Nonetheless, AFM data showed that despite being able to form nanostructures with VitE, these are not stable and require the presence of another surfactant, in this case sphingomyelin. In addition, this extensive characterization before and after dialysis is of extreme importance in order to guarantee that the formulations maintain their features and can be used either in an *in vitro* or *in vivo* scenario.

3.2. SNs-Ks stability over time and in biorelevant media

Evaluating the stability of prepared nanosystems overtime and in different biological media is essential to predict the fate of nanosystems especially after administration [40]. Storage stability at 4 °C was studied and the analysis by DLS showed that SNs-Ks (103± 17 nm, PdI 0.16, +51 ± 9 mV) and V-Ks (112 ± 14, PdI 0.16, +51 ± 3 mV) were stable at least for 6 months. In addition, the stability of SNs (with and without the modified peptide) was determined in different biological media, PBS 5 mM, RPMI (supplemented or not with 1 % FBS) and human plasma. According to DLS measurements and optical visualisation of the samples after incubation with the different media, it was possible to observe that SNs-Ks (1:0.1:0.1) was stable in cell culture medium containing proteins (FBS). This could be related to the adsorption of serum proteins to the surface of the strongly positively charged SNs-Ks nanosystems, through electrostatic interactions which can also explain the increase in size to 272 ± 10 nm and surface charge decrease to -11 ± 1 mV, after 24 h of incubation in RPMI supplemented with 1 % FBS. Based on the possibility that a lower content of modified peptide could result in better colloidal stability due to a lower positive surface charge of the nanosystems, the colloidal stability of SNs-Ks prepared at 1:0.1:0.025 ratio was also assessed in supplemented RMPI. However, this nanosystem was only stable in RPMI supplemented with 1% FBS showing a final hydrodynamic size of 206 ± 7 nm (after 24 h incubation), which was a smaller increment in comparison to 1:0.1:0.1 SNs-Ks. Such behaviour is reported for other positively charged nanosystems [41]. On the other hand, the colloidal stability in plasma gives an indication of the nanosystems' fate after intravenous (IV) administration. The plasma was diluted 10 times in ultra-pure water before mixing it with the prepared nanosystems, so that the plasma contents did not interfere with the DLS. As it is clear from Figure 6, SNs-blank and SNs-Ks nanosystems were both stable in plasma for 24 h presenting a mean particle size of 101 ± 11 nm and 149 ± 3 nm for SNs-Ks and SNs-blank, respectively, at the end of the experiment.

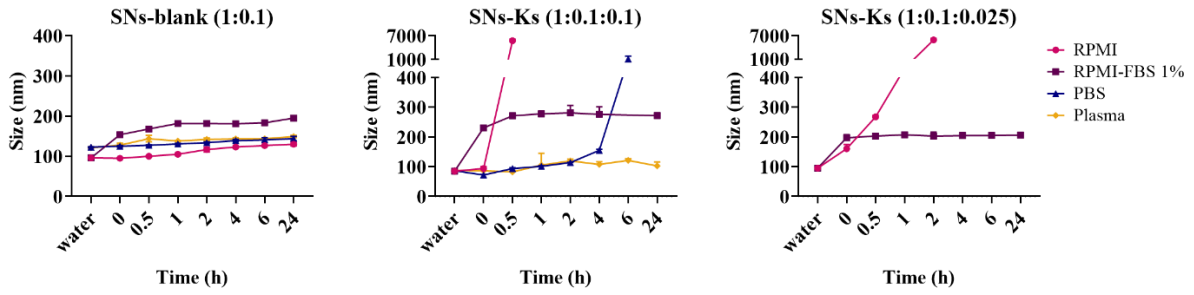

Figure 6: Stability of SNs-blank (1:0.1) and SNs-Ks (1:0.1:0.1 and 1:0.1:0.025) upon incubation in different relevant media (PBS 5 mM, non-supplemented RPMI, RPMI supplemented with 1% FBS and plasma) up to 24 h. PBS: Phosphate Buffer Saline; FBS: Fetal Bovine Serum.

3.3. *In vitro* evaluation of the nanosystems

3.3.1. SNs-Ks effects on MCF7 and red blood cells

Assessing the cytotoxic profile of the nanosystems is an important requirement for newly formulated therapeutic nanosystems [42] since it provides an estimation of possible undesired side effects. The toxicity profile of the nanosystems containing the peptide (SNs-Ks and V-Ks) in comparison with SNs-blank was assessed through proliferation studies namely cells' colony forming and metabolic activity, as well as haemolytic assay.

Essentially, colony forming assay is the method of choice to determine cell reproductive death after treatment (ionising radiation, genetic manipulation, etc.) as well as the effectiveness of cytotoxic drugs [43]. It determines the ability of a single cell in the population, undergoing treatment, to grow into a colony of at least 50 cells by clonal expansion. To make sure that the chemical modification did not alter its efficacy C18-PEG-Ks cytotoxicity as well as capacity to impair the formation of tumoral cells colonies were assessed by MTT and colony forming assays MCF7 cells were treated with a range of C18-PEG-Ks concentrations (1 to 50 µM). Regarding cell viability assays, cells were treated for 72 h, while in the case of CFA, cells were treated for 24 h and left in culture in cell culture medium for another 10 days (period required to observe the formation of colonies). Figure 5A shows that C18-PEG-Ks maintained its dose-dependent cytotoxic profile which at 50 µM led to about 90 % mortality of MCF7 cells. On the other hand, its antiproliferative capacity and thereby impairment of colonies formation was also not affected since the wells treated with 15 to 50 µM were totally clear, while at 5 µM MCF7 cells capacity to form colonies was only decreased by 50% (Figure 7 B and C). The C18-PEG-Ks cytotoxic profile is similar to 4N1Ks peptide, as previously observed [24], indicating that C18-PEG modification did not alter 4N1Ks efficacy.

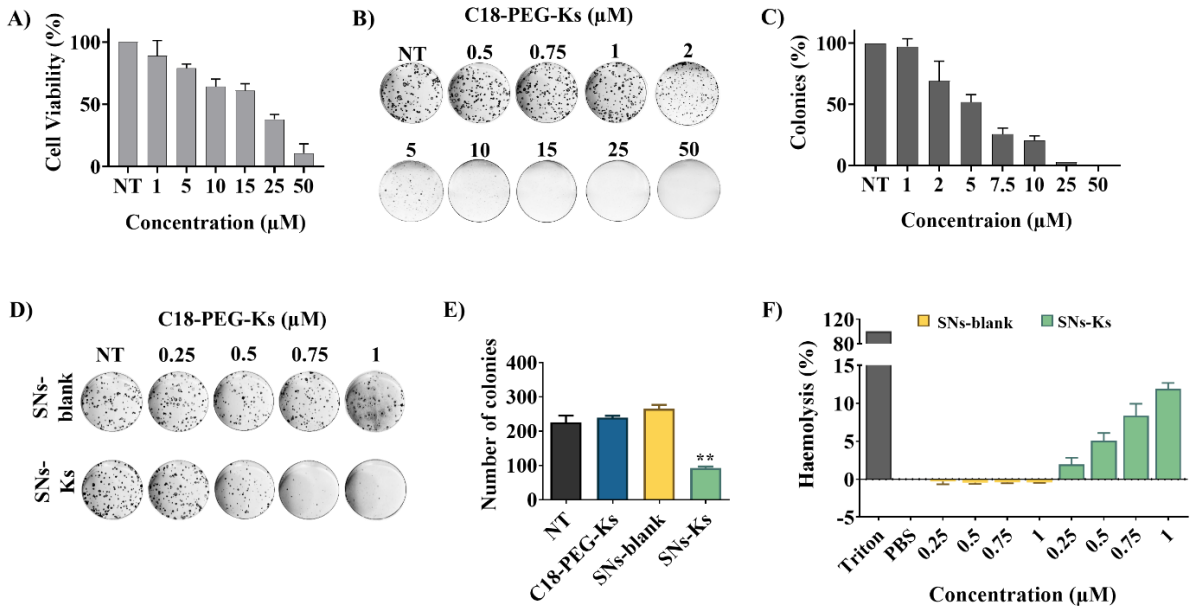

Figure 7: Effect of C18-PEG-Ks and SNs-Ks on MCF7 breast cancer cells and red blood cells. A) MCF7 cells viability determined by MTT assay after treatment with the modified peptide (1 to 50 µM) for 72 h. B) Macroscopic photos of MCF7 colonies formed after C18-PEG-Ks treatment. C) Evaluation of cell proliferation activity by colony forming assay of MCF7 treated with C18-PEG-Ks (1 to 50 µM) for 10 days. D) Representative macroscopic images of MCF7 colonies. MCF7 cells after treatment for 9 days with C18-PEG-Ks, SNs-blank and SNs-Ks (peptide concentration 0.25 to 1 µM). E) Graphical representation of MCF7 colony forming capacity upon treatment with cell culture medium (NT, non-treated), C18-PEG-Ks, SNs-blank and SNs-Ks at 0.5 µM (peptide concentration). Data are presented as mean ± SD (n=6). ** $p < 0.01$. F) Human red blood cells were haemolysis (%) upon exposure to SNs-blank and SNs-Ks nanosystems up to 1 µM (peptide). Triton X-100 and PBS were used as positive and negative controls representing 100% and 0% of haemolysis, respectively (n=3). Data are presented as mean ± SD.

Considering that we expected an improved efficacy by formulating the modified peptide into a nanosystem, we decided to continue the study using C18-PEG-Ks concentrations below 5 µM. In addition, before studying the cytotoxicity of the nanosystems containing the peptide, it was important to determine if the SNs-blank did not cause any toxic effects at the concentrations of interest. According to the results presented in Figure 7D, the SNs-blank were toxic at 1 µM while no apparent toxicity was observed at 0.5 µM compared to not-treated wells. Therefore, the effect of SNs-Ks was assessed from 0.25 up to 1 µM. Interestingly, at 0.5 µM SNs-Ks were able to significantly decrease (p<0.01) the proliferative capacity of MCF7 cells by almost 50% in comparison to non-treated cells (Figure 7E). Decreasing the effective concentration 10 times (from 5 to 0.5 µM) is quite remarkable and could be attributed to the association of 4N1Ks peptide to the nanosystems and its exposure on their surface. Such results demonstrate the capacity of the nanoformulated systems to improve drug's effectiveness, thereby requiring lower doses.

The nanosystems' surface charge, concentration, shape and size can also be responsible for toxic effects on red blood cells once administered IV [44]. Thereby, hemocompatibility is a crucial

requirement for any newly formulated therapeutic nanosystem intended to be delivered intravenously. For that, we assessed the blood compatibility of SNs-Ks (1:0.1:0.1) in comparison with SNs-blank nanosystems. The results presented in Figure 7F, indicate that while triton caused RBCs' haemolysis, SNs-blank did not affect RBCs integrity (as previously reported by our group [28]) and as expected SNs-Ks haemolytic activity was very low with 12% ± 1 haemolysis at the highest concentration tested (1 µM). These results indicate that SNs-Ks nanosystems are suitable for IV administration.

3.3.2. Internalization by MCF7 cells.

In order to elucidate the effect of 4N1Ks peptide association to the surface of SNs nanosystems on cellular uptake, SNs-Ks with fluorescently labelled sphingomyelin were prepared and internalisation studies in MCF7 cells was assessed by confocal microscopy and flow cytometry. Confocal microscopy images illustrated in Figure 8, show an early detection of SNs-Ks (1:0.1:0.1) in and around MCF7 cells after 30 minutes of treatment and the highest fluorescent signal was detected 2 h after treatment. On the other hand, the highest fluorescent signal for SNs-blank was only detected 4 h after treatment. Similarly, and more interesting observations were found by flow cytometry analysis, which indicated that about 83% of MCF7 cells were fluorescent after only 10 minutes of treatment with SNs-Ks nanosystems reaching 96% after 1 h of treatment. In the case of SNs-blank, a similar percentage of fluorescent MCF7 cells was only achieved 2 h after treatment. These results can be explained by i) the positive surface charge of SNs-Ks can play a role in the enhanced cellular uptake through electrostatic interactions with the negatively charged cells' membrane [45]; ii) several papers point out that the presence of conjugated ligands on nanoparticles improve cellular uptake [46,47]; iii) most importantly, 4N1Ks peptide target is CD47 receptor which is expressed on the surface of MCF7 breast cancer cells as well as of senescent cells which can improve cell uptake of SNs-Ks nanosystems.

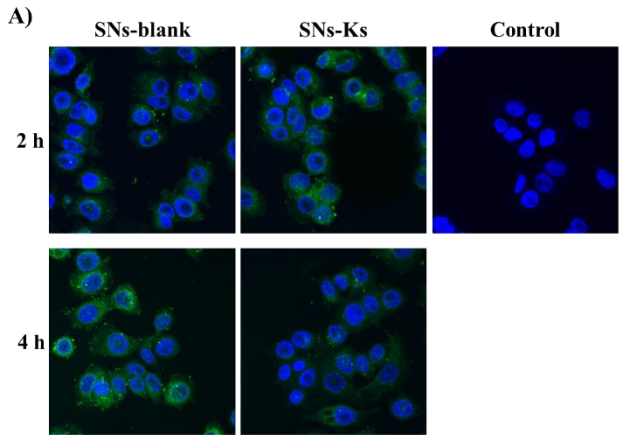

	TopFluor-Positive cells (%)				
	10 min	30 min	1 h	2 h	4 h
SNs-blank	22	50	81	93	99
SNs-Ks	83	92	96	97	99

Figure 8: Cell internalization studies of SNs-Ks and SNs-blank over time. (A) Confocal microscopy images showing the internalization of SNs-Ks and SNs-blank, labelled with TopFluor®-SM,in MCF7 cells after 30 min, 1 h and 2 h of treatment. Green channel: TopFluor®-SM labelled SNs. Blue channel: nuclei staining with DAPI. (B) Flow cytometry analysis and respective percentage of MCF7 cells internalizing TopFluor-SM SNs over time (10 min to 4 h).

3.4. Senescence escape.

After assessing the capacity of SNs-Ks to i) efficiently associate the modified peptide, ii) improve SNs internalization in cells, iii) potentiate 4N1Ks peptide effect on decreasing MCF7 colony forming capacity while iv) showing a reduced haemolytic effect on RBCs, the last and most important study in this work was to determine if SNs-Ks nanosystems improved the senolytic effect of 4N1Ks peptide.

Senescent cells were initially considered to be involved in tumour suppressor mechanisms for being in cell cycle arrest, as well as for the senescence-associated secretory phenotype (SASP) which secretes cytokines, chemokines, among other molecules, that attract different immune cells responsible for the elimination of anomalous cells (cancerous, senescent...). Nonetheless, cellular senescence is a highly dynamic and heterogeneous state and thereby the accumulation of these cells and due to SASP activity they can also be harmful behaving as pro-tumorigenic through different mechanisms. Several anticancer therapeutics (chemotherapy, radiotherapy, among others) have been recognized to induce cellular senescence either in tumoral and healthy cells. However, the tumoral cells that can escape senescence state end up being more aggressive with higher proliferation rates [18,48,49].

SNs-Ks senolytic activity was assessed using a chemotherapy-induced model of MCF7 cells. For that, first senescent MCF7 cells were generated upon the treatment with doxorubicin (25 ng/mL for 4 days). The senescence-like phenotype of MCF7 cells was displayed by their changed morphology (larger size, flattened shape, cytoplasmic granularity), increased β-galactosidase activity as well as increased expression of senescence markers p53 and p21

(Figure 9A). The senescent cells were treated with SNs-Ks and SNs-blank (as control) for 24 h. The treated cells were left for 14 more days in cell culture medium, in order to observe the establishment of macroscopic colonies. In this way we could determine if SNs-Ks were able to deplete the senescent cells and therefore avoid or decrease their capacity to escape senescent state. If the cells can recover their proliferative state after being senescent, they would not only be able to form colonies, as we assessed in this study, but also to become more aggressive, as shown in other studies [18,49].

Despite the extensive research on cellular senescence, therapeutic drugs aiming to impair their pro-tumorigenic effects and the several benefits of nanotechnology, only a few studies have combined these drugs with a nanocarrier. In addition, such studies have been mainly focused on the use of inorganic nanoparticles (mesoporous, metallic, calcium carbonate NPs) mainly targeting senescent cells based on their high β-galactosidase activity [25,26] but also making use of quercetin [27] and CD9 monoclonal antibody [29]. More recently, Belcastro et al developed maleimide-decorated Labrafac nanoemulsions for the grafting of anti-VCAM-1 antibody, aiming at the targeting of endothelial senescent cells [31]. Aside from being developed as a therapeutic approach, when loading lipophilic fluorescent dyes, these nanosystems can also be considered for diagnosis.

Unlike these nanosystems, in the present work we used natural components as Vitamin E and sphingomyelin for the main composition, formulated using the single-step ethanol injection method, which is highly reproducible, simple and straightforward. For senescent cells targeting, we selected peptide 4N1Ks which is derived from the C-terminal domain of TSP-1 (that targets CD47 receptor) and has the ability to prevent senescent cells escape by promoting autophagy in senescent and cancer cells [24]. The results presented in Figures 9B-C show that SNs-Ks significantly reduced the number of emergent colonies in comparison to non-treated as well as SNs-blank treated cells, specially at 0.5 µM (peptide). A similar effect on colony forming capacity was also observed on cancer MCF7 cells' CFA. Considering the results, these nanosystems might present a viable approach for reducing the burden of accumulated senescent cells caused due to anticancer treatments as chemotherapeutics, and therefore make a step forward in the management of this disease. Still, further in vivo studies will be needed to confirm the therapeutic potential.

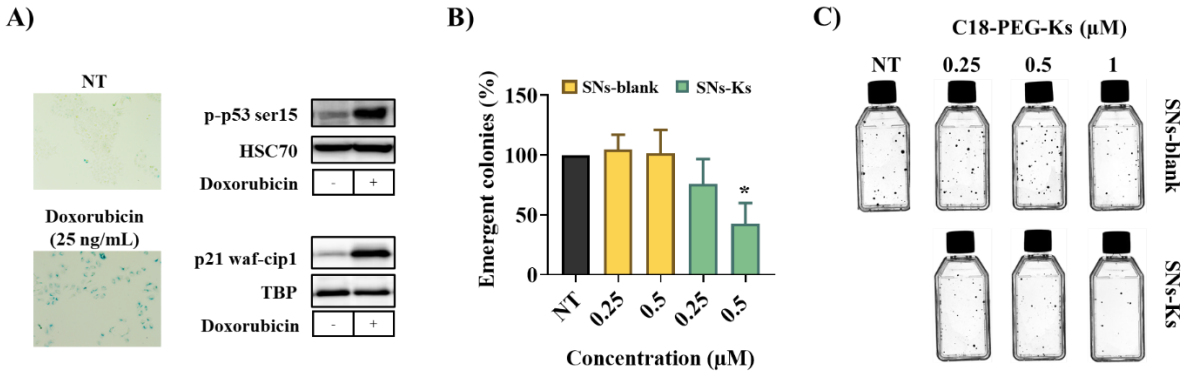

Figure 9: SNs-Ks effect on senescence escape. A) Ninety-six h treatment of doxorubicin (25 ng/mL) induces senescence in MCF7 breast cancer cells. Microscopic photos of the increased β-galactosidase activity (blue signal) in comparison to non-treated (NT) cells. Increased expression of senescence markers p-p53 ser15 and p21 waf-cip1, determined by western blot. B) Chemotherapy-induced senescent MCF7 cells were treated with SNs-Ks at 0.25 to 1 µM (peptide dose) and SNs-blank as negative control for 24 h and left for 14 days in culture. Non-treated (NT) cells were used as positive control. (n=1). * $p < 0.05$. C) Macroscopic images of chemotherapy-induced senescent MCF7 cells 14 days post-treatment with SNs and SNs-Ks.

4. Conclusions

In this study we successfully prepared promising Vitamin E-sphingomyelin nanosystems, through a the very simple and efficient method of ethanol injection, able to incorporate with high a high efficiency the 4N1Ks peptide (chemically conjugated to a C18-PEG). In this way, the peptide's C18 chain was incorporated in the lipidic carrier structure, while the peptide was exposed on its surface being available for senescent cells targeting. Extensive physicochemical characterisation shows that the dialysis purification method did not impair the nanosystems features and that these present a small particle size and are stable in different biological media. SNs-Ks demonstrated a higher internalization by cancer cells in comparison to the blank nanosystems. In addition, SNs improved 4N1Ks senolytic activity lowering its effective dose to impair cancer and senescent cancer cells' capacity to proliferate and form colonies. Considering the results presented in this work, next steps will involve further investigation of the therapeutic effect of SNs-Ks *in vivo*.

Part 2: Sphingomyelin based nanosystems loaded with the senolytic drug ABT-737.

1. Introduction:

One of the characteristic features of cellular senescence is its resistance to apoptosis by the upregulation of several survival pathways. This also contributes in the accumulation of senescent cells, which promote cancer and several age-related diseases [50]. BCL-2 protein family consist of pro-apoptotic proteins and anti-apoptotic proteins that orchestrate the mitochondria-mediated intrinsic pathway of apoptosis [51]. Several studies featured the upregulation of anti-apoptotic proteins in senescent cells [22,52]. Disrupting the balance of the BCL-2 protein family towards apoptosis represent an attractive strategy to eliminate senescent cells, which is the exact mechanism of the senolytic drug ABT-737.

ABT-737 is a BH3 mimetic small-molecule inhibitor that binds with high affinity to Bcl-xL, Bcl-2 and Bcl-w, triggering apoptosis by disrupting the balance between pro- and anti-apoptotic proteins. An interesting study by Yosef and his colleagues stated that ABT-737 efficiently eliminates two types of senescent cells in their mice models, and improved hair-follicle stem cell proliferation resulting in regrowth of hair [52]. Despite of the potential of this drug, preclinical studies faced two problems: i) low solubility and poor bioavailability, and ii) toxicity effects due to a decrease of the platelet half-life (t1/2), which result in acute thrombocytopenia in a dose-dependent manner [53–55]. To overcome these constraints, the aim was to encapsulate the ABT-737 in SNs.

There are already several studies that have developed ABT-737 encapsulated nanosystems targeting different types of cancer [56–59], mostly referring to polymeric based nanoparticles, namely pegylated PLGA NPs [57-59], which improved ABT-737 cytotoxic effects through the incorporation of other anti-cancer drugs; such as y IRAK1/4 inhibitor [57], Notch-1 Antibodies [58], camptothecin [59] and the diacid metabolite of norcantharidin [56]. These Combinatory therapies reduced the ABT-737 systemic toxicity related to thrombocytopenia. To the best of our knowledge, there are no works referring to the use of ABT-737-loaded nanosystems targeting senescent cells. However, there is an interesting publication based on the galacto-oligosaccharides nanoparticles, already mentioned in the thesis introduction, where the higher β-galactosidase activity in senescent cells were exploited for specific release of the cargo in

senescent cells. In this study they prepared a prodrug of navitoclax (by galacto-conjugation), an analogue of ABT-737. Navitoclax will only be released in senescent cells due to their high β-galactosidase activity which improved the senolytic activity of the navitoclax and reduced platelet apoptosis in human blood samples [60].

2. Results and discussion:

2.1.Development and characterisation of ABT-737 loaded SNs (SNs-ABT)

As we mentioned earlier, ABT-737 has a poor solubility profile. In order to encapsulate the drug in SNs, ABT-737 had to be dissolved in chloroform and was mixed in different weight ratios (0.008 - 0.012 in respect to the VitE amount in SNs) in the ethanol phase (together with Vit E and SM). ABT-737-loadedd SNs (SNs-ABT) were, then prepared by injecting the previous ethanol mixture into ultra-pure water (Figure 1). Unfortunately, the resulting nanosystems were unstable and separated after a while, most probably due to evaporation of chloroform. DMSO was selected as an alternative solvent. A 20mg/ml stock solution was prepared to prepare SNs-ABT with different weight ratios (0.005, 0.01, 0.02) with respect to the content of VitE in the SNs (5mg of VitE in 1mL of formulation). Importantly, these SNs-ABT were more stable with respect to the previous formulations prepared in the presence of chloroform. Additionally, they remained stable after centrifugation at 7000 rpm for 1h. Besides, the absence of ABT-737 sedimentation proves the solubility of this drug in those nanosystems [61].

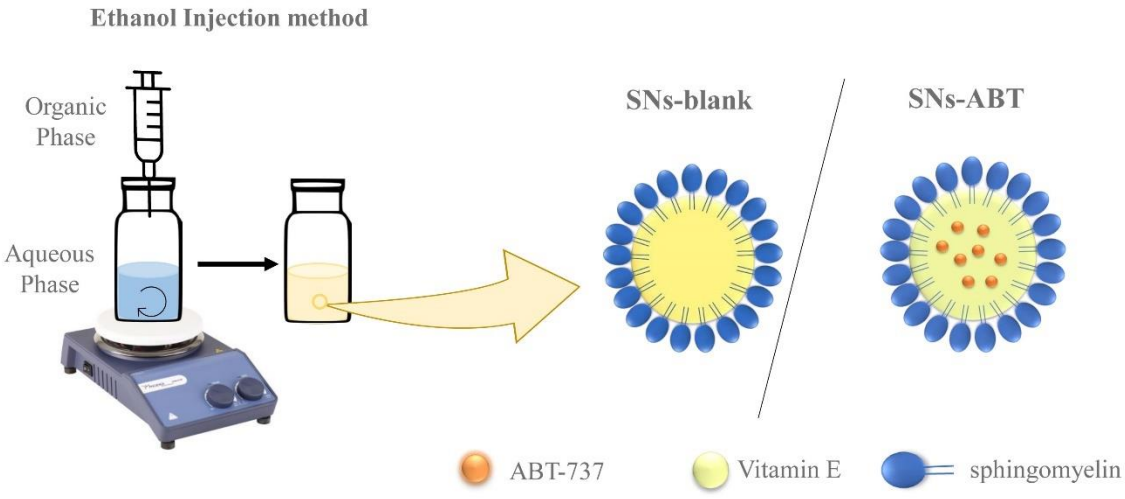

Figure 1: Schematic illustration of the nanosystems (SNs-blank, SNs-ABT) preparation by ethanol injection method.

SNs-ABT were characterized by DLS. As it can be observed from table 1, incorporation of ABT-737 increased the size of the nanoemulsion to 139.5 nm ±19 nm at ratio of 0.02 and resulted in gradient zeta potential ranging from -0.96mV to +9.2 mV. The increase of surface positive charge compared to SNs-blank could be related to DMSO or ABT-737 incorporation. DMSO has a positive charge related to the presence of a sulphur atom [62]. It is important mentioning that the total amount of DMSO did not exceed 0.5%, which is the highest acceptable for IV formulations [63].

Table 1: SNs-blank[1] (1:0.1) [1] and SNs-ABT nanosystems physicochemical characterisation by DLS and LDA (mean ± SD, n=12).

	VitE: SM : ABT	DMSO%	Size (nm)	PDI	ZP (mV)
SNs-blank	1:0.1:0	0	98.2 ± 1.4	0.09 ± 0.02	-10.2 ± 0.8
SNs-ABT	1:0.1:0.005	0.125	130.7 ± 5.5	0.09 ± 0.04	-0.96 ± 1.7
	1:0.1:0.01	0.25	119.5 ± 8	0.08 ± 0.03	+8.9 ± 2.8
	1:0.1:0.02	0.5	139.5 ± 19	0.08 ± 0.04	+9.2 ± 3.9

Vit E, Vitamin E; nm, nanometre; PdI, Polydispersity index; ZP, zeta potential; mV, millivolts; ABT, ABT-737.
Total volume of the nanoparticle suspension: 1 mL. Size refers to diameter.

SNs-ABT nanosystems were dialyzed in order to separate the nanosystems from the free drug and other molecules. Unfortunately, the dialysis process affected the stability of SNs-ABT nanosystems (1:0.1:0.02 and 1:0.1:0.01) as they disintegrate at the end of the process. This might be related to the poor solubility of the ABT-737. As we concluded from the formulations prepared with chloroform that ABT-737 is not soluble in our SNs nanosystems, and with the dialysis process, we might be losing part of the DMSO that stabilises those nanosystems. Therefore, we repeated the formulation process with 10mg/mL ABT-737 in DMSO stock solution. However, in this case, the highest acceptable loading ratio of ABT-737 is 0.01 in order not to exceed the 0.5% of DMSO in our formulations.

SNs-ABT (1:0.1:0.01) prepared from the new stock solution were 126.9 ± 9.8 nm in size, had PDI of 0.1 ± 0.02 and ZP of +5.55 ± 1.06. Those nanosystems properties were not affected by the dialysis process. According to the characterization results, the dialysis process increased SNs-ABT (1:0.1:0.01) size slightly (135.8 ± 1.9 nm), and also had increased the zeta potential (+10.4 ± 1.5). Additional characterization was performed by NTA, MADLS and AFM. Results

[1] SNs-blank refers to SNs nanosystems prepared with Vit E and SM only. They are used here as a control.

also proved that the dialysis process did not compromise the integrity of the nanosystems, in agreement with previous characterization results (Figure 2 & table 2). Interestingly, we found an increase in the average size in SNs-ABT samples after 13h and 37h of deposition. We speculated that such increase in size could be related to coalescence between some nanosystems droplets overtime. However, we also observed that the majority of the small droplets maintained their size over the whole course of the experiment. It is important to note that this polydispersity was not noticed with DLS, NTA nor MADLS.

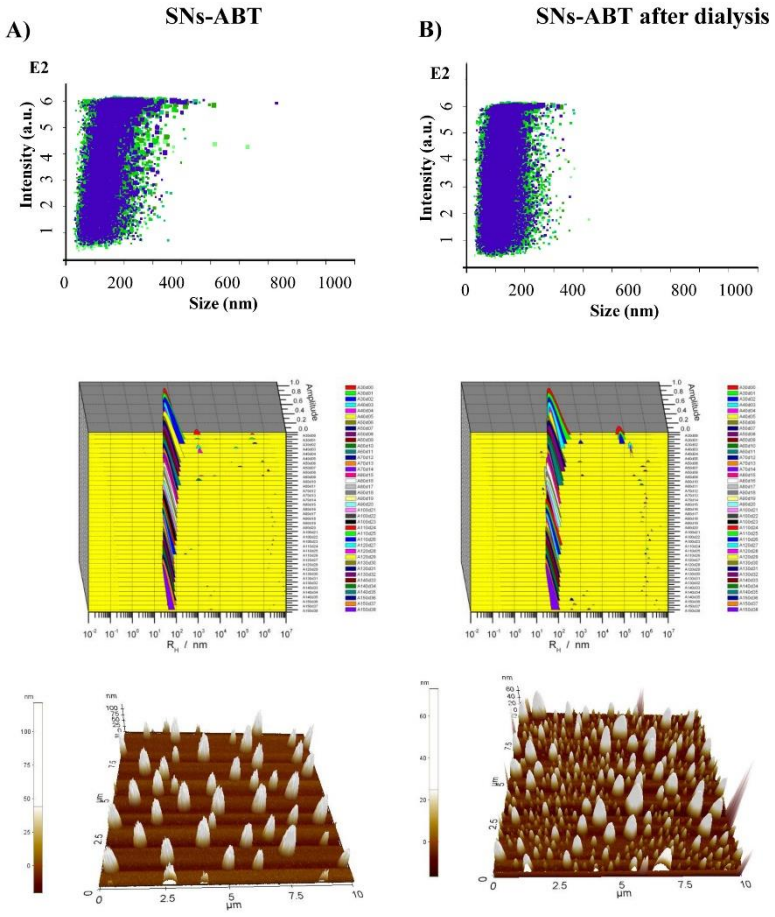

Figure 2: Physicochemical characterization of SNs-ABT (1:0.1:0.01) with NTA, MADLS and AFM A) before dialysis & B) after dialysis (n=3).

Table 2: Physicochemical characterization of nanosystems (before and after dialysis) by NTA and MA-DLS.

Nanosystems	NTA size measurement	Average Diffusion Coefficient, D (µm²/s)	Average Hydrodynamic Radius, R_H (nm)
SNs-ABT	143.5 ± 1.7	3.6 ± 0.004	68.28 ± 0.08
SNs-ABT dialyzed	119.1 ± 0.4	3.2 ± 0.005	76.39 ±0.01

The encapsulation efficiency (EE%) of ABT-737 (1:0.1:0.01), was determined by HPLC after dialysis, being 87.86 ± 4.24 %, in line with other studies (71.4% and 95% for folate-modified lipid bilayer-coated mesoporous silica and N1-ABT-NPs (PLGA NPs) nanocarriers [56,57,58]) which in our case correlates with a loading capacity (LC%) of 0.007%. However, the first nanosystem were based on mesoporous nanoparticles [56] which is known to have biocompatibility issues [64]. Also, the other nanosystems were polymeric nanoparticles [57,58]. Therefore, our SNs nanosystems are more appealing due to their biodegradability and biocompatibility. Besides the preparation of these nanosystems were much complicated compared to the ethanol injection method.

2.2. SNs-ABT stability studies.

Colloidal short-term stability of SNs-ABT was assessed in different biological media after 24h of incubation to estimate their fate after administration both *in vitro* an *in vivo* [40]. SNs-ABT showed good colloidal stability profile in both PBS and plasma, Figure 3-A. Regarding stability in plasma, SNs-ABT slightly increased in size at the very end of the experiment (after 24 h of incubation) with a final hydrodynamic size of 175.4 ±6.6 nm and ZP of -19.6 ±1.3 mV. The slight increase in size and the final strong negative surface charge can be explained by plasma proteins adsorption and formation of a protein corona [65,66]. In case of stability in PBS, SNs-ABT maintained their size throughout the entire study. However, in RPMI, SNs-ABT gradually increased in size reaching 418 ±52 nm and ZP of –37.6 ±1 mV after 24h of incubation, while the PDI remained less than 0.3. This could be related to the higher content of salts in RPMI compared to PBS. It is important to note, dialyzed SNs-ABT showed improved stability compared to undialyzed nanosystems.

2.3. *In vitro* cytotoxicity evaluation of SNs-ABT

2.3.1. Haemolysis assay.

SNs-ABT showed good hemocompatibility profile with no haemolytic activity in all concentration tested, Figure 3-B. This provides a great advantage for IV administration, as ABT-737 encapsulation in SNs nanosystems prevents its interaction with blood contents and reduces its toxicity, which was one of the reasons why clinical studies of ABT-737 did not move forward.

2.3.2. *In vitro* evaluation of prepared nanosystems. (Senescence escape assay)

SNs-ABT senolytic activity were evaluated in chemotherapy-induced model of MCF7 cells. For that, first senescent MCF7 cells were generated upon the treatment with doxorubicin (25 ng/mL for 4 days). The senescent cells were treated with SNs-ABT and SNs-blank (as control) for 24 h. The treated cells were left for 2 weeks in cell culture medium, which is the time needed for visible emergent colonies to form.

Results presented in Figure 3-D&E manifest that SNs-ABT at 0.5 µM reduced emergent clones by 72% compared to not treated (NT) plates.

Compared to the other nanosystems encapsulating ABT-737 [56–58,58,59], although they are targeting cancer cells and not senescent cells, those nanosystems achieved their therapeutic target by co-encapsulation of other cytotoxic drugs [56,57,59] or ligands [58]. However, our SNs-ABT nanosystems were able to reduce the number of emergent clones by encapsulating ABT-737 alone and with LC% much lower compared to the other nanosystems.

SNs-ABT nanosystems effect on senescence escape were more potent in comparison to SNs-Ks nanosystems. ABT-737 promote apoptosis in senescent cells while 4N1Ks peptide induce autophagy. Therefore, it would be interesting to combine the two therapies together, especially as ABT-737 will be encapsulated in the oil phase while 4N1Ks will be associated on the surface. Such combinatory therapy might have higher impact on senescent cells, which has already been established in our lab with a similar study by associating uroguanylin on the surface of SNs while encapsulating etoposide in the oil phase [7]. This combinatory therapy had higher cytotoxic effect on colorectal cancer cells in comparison to SNs with etoposide alone [7].

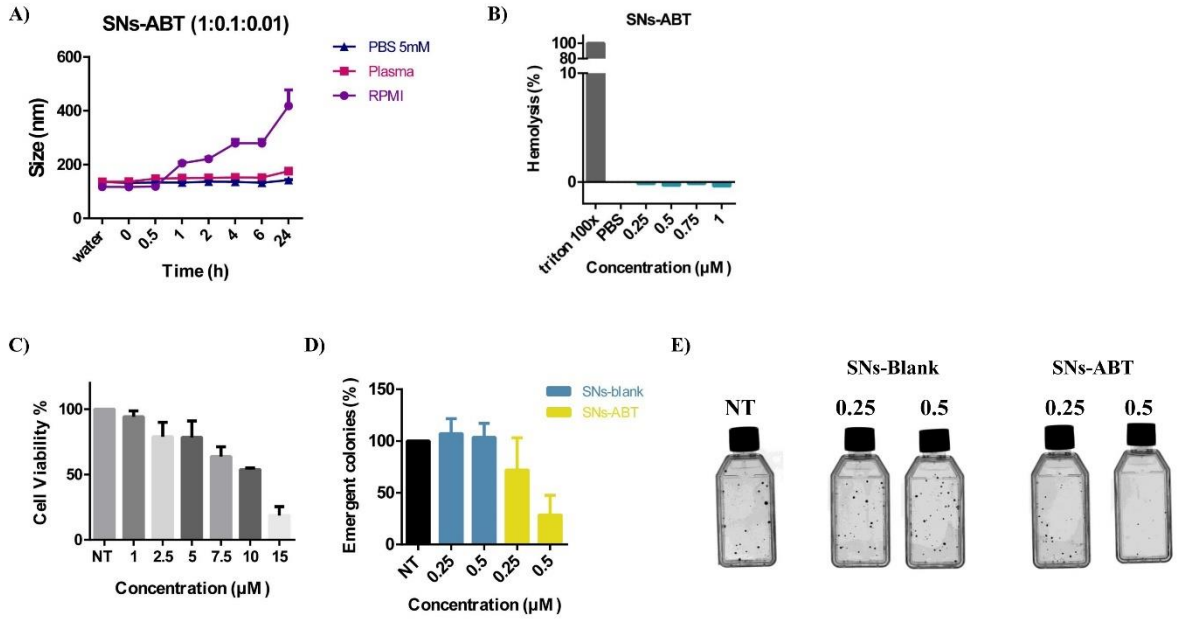

Figure 3: A) Stability of SNs-ABT (1:0.1:0.01) upon incubation in different relevant media (PBS 5 mM, non-supplemented RPMI, and plasma) up to 24 h. PBS: Phosphate Buffer Saline. B) Human red blood cells were haemolysis (%) upon exposure to SNs-ABT nanosystems up to 1 µM (ABT-737). Triton X-100 and PBS were used as positive and negative controls representing 100% and 0% of haemolysis, respectively (n=3). Data are presented as mean ± SD. C) MCF7 cells viability determined by MTT assay after treatment with ABT-737 (1 to 15 µM) for 72 h. D) Chemotherapy-induced senescent MCF7 cells were treated with SNs-ABT at 0.25 and 0.5 µM (ABT-737) and SNs-blank as negative control for 24 h and left for 14 days in culture. Non-treated (NT) cells were used as positive control. (n=3). * $p < 0.05$. E) Macroscopic images of chemotherapy-induced senescent MCF7 cells 14 days post-treatment with SNs and SNs-ABT.

3. Conclusions.

Through the straightforward method of ethanol injection, we successfully encapsulated ABT-737 in SNs nanosystems with high EE%. NTA, MADLS and AFM results proved that we obtained small homogenous nanosystems with around 140 nm in size and slightly positive zeta potential. SNs-ABT were stable in different biological media and did not induce any haemolytic activity upon incubation with human blood. SNs-ABT had senolytic properties proved by reducing the emergent clones from a chemotherapy- induced senescence. Encapsulating ABT improved its hemocompatibility. Further experiments are essential to evaluate the therapeutic potential of SNs-ABT such as *in vivo* studies. Combinatory therapies with the peptide could also be envisioned especially as ABT-737 and 4N1Ks acts on different molecular pathways in senescent cells. Moreover, 4N1Ks will be attached to the surface while ABT-737 can be encapsulated in the oil phase of SNs. Such combination might improve the senolytic capacity and reduce dose-dependent toxicities.

Part 3: Sphingomyelin based nanosystems encapsulated with Oleuropein.

1. Introduction.

Oleuropein is a polyphenol that possess antioxidant, anti-inflammatory, and senolytic properties [67–69]. These properties are related to oleuropein downregulation of IL-1ß, IL-6 and COX-2 gene expression and NF-kB activation [68,69]. A recent study on osteoarthritic chondrocytes (OACs) treatment with oleuropein, showed that oleuropein reduced inflammatory factors, promoted cartilage tissue redifferentiation, in addition it reduced cellular senescence in osteoarthritic chondrocytes, synovial and bone cells [69]. Therefore, it would be interesting to prepare SNs with oleuropein and investigate their senolytic potential on chemotherapy induced model of MCF7 cancer cells.

2. Results and Discussion:

It is important to note that several experiments were hindered from moving forward due to Covid-19 pandemic. Therefore, results obtained with SNs-Ole represent preliminary study.

2.1. Development and characterization of SNs-Ole nanosystems.

Oleuropein was dissolved in ethanol and mixed with VitE and sphingomyelin, following the same procedure as for ABT-737, in weight ratios of (0.01 - 0.05) in respect to Vit E amount in SNs. SNs-Ole nanosystems were prepared as previously described, by following the ethanol injection method, as represented in Figure 4.

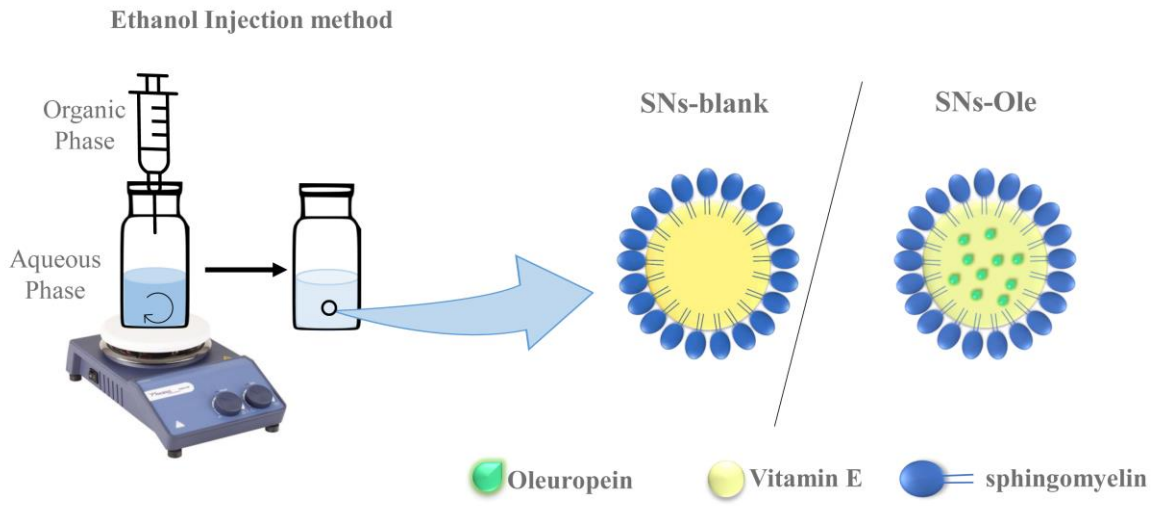

Figure 4: Schematic illustration of the nanosystems (SNs-blank, SNs-ABT) preparation by ethanol injection method.

All prepared SNs-Ole nanosystems, with different ratios of loaded oleuropein (0.01, 0.02, 0.05) were around 100 nm in size and possessed negative surface charge, Figure 5-A. Similar to SNs-Ks and SNs-ABT, those nanosystems were extensively characterized by NTA (Figure 5-B), MADLS (Figure 5-C) and AFM (Figure 5-D), proving that small (< 100 nm), and homogeneous nanosystems were formed. A previous study indicated the presence of Ole on the bilayer membrane and core of liposomes due to its amphiphilic nature [70]. Therefore, the increase of negative surface charge can be explained by the presence of part of Ole on the surface of the SNs due to its amphiphilic nature [70,71]. Moreover, this amphiphilic nature of Ole facilitate the formation of small vesicles which has been reported before [71]. SNs-Ole with a composition (1:0.1:0.05), which are the ones with the highest content in Oleuropein, were selected for the next experiments.

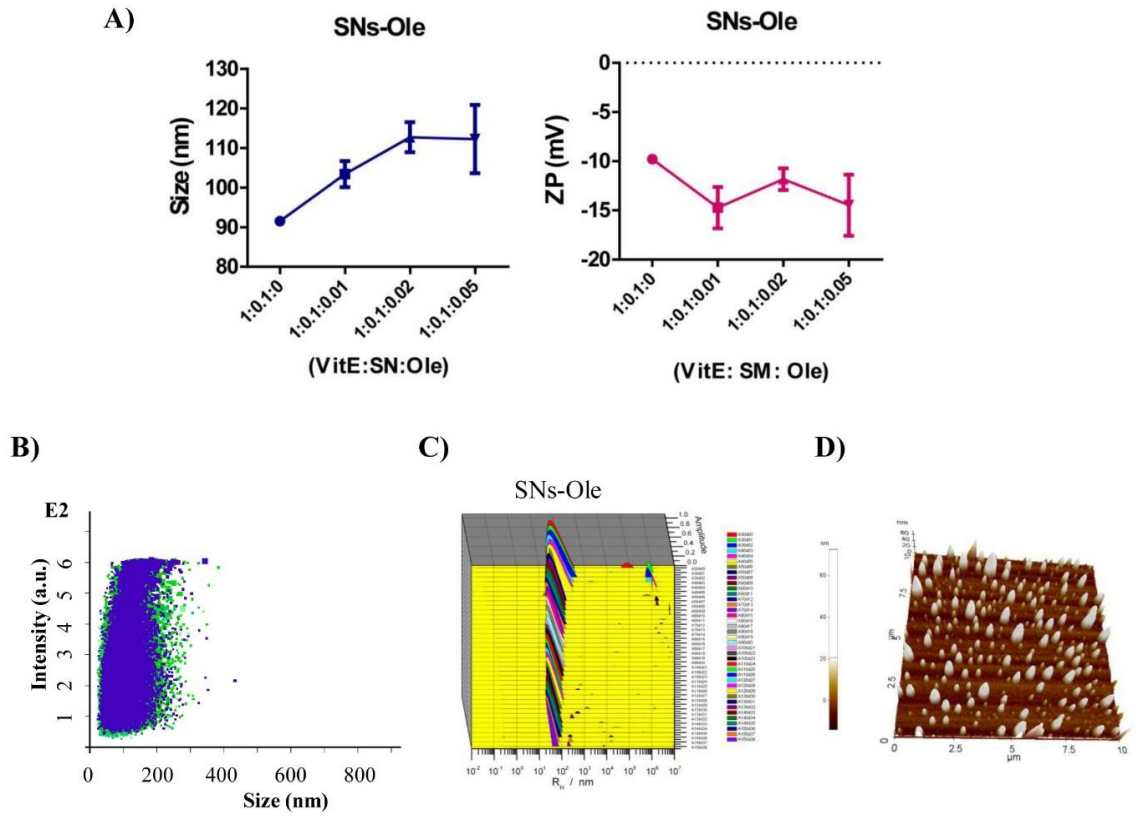

Figure 5: A) Effect of increasing weight ratios of Oleuropein (from 0.01 to 0.5, respective to VitE) on SNs-Ole' (composed of VitE, SM and Oleuropein) size, polydispersity and zeta potential, determined by DLS. Physiochemical characterisation of SNs-Ole (1:0.1:0.05) by **B)** NTA**, C)** MADLS and **D)** AFM. (n=3).

2.2. SNs-Ole stability studies.

Storage stability at 4 °C was studied and the analysis by DLS showed that SNs-Ole (1:0.1:0.05) (121.9± 4.7 nm, PdI 0.07, -16.5 ± 2 mV) were stable at least for 4 months, Figure 6-A. Moreover, colloidal short-term stability of SNs-Ole were assessed in different biological media, Figure 6-B. The results indicated that SNs-Ole nanosystems were stable in RPMI supplemented with1%FBS and in PBS 5mM as the nanosystems maintained their particle size throughout the entire study. However, in plasma, SNs-Ole maintained their particle size for 6 h only as a spike increase in their mean hydrodynamic size appeared at 24h of incubation reaching 418 ± 60 nm and ZP of -16 ± 1 mV. The high colloidal stability of SNs-Ole was not a surprise as oleuropein is used as a stabilising agent for many metallic nanoparticles such as gold and silver nanoparticles [71–73].

2.3. *In vitro* cytotoxicity evaluation of SNs-Ole

2.3.1. Haemolysis assay

We checked the hemocompatibility of SNs-Ole (1:0.1:0.05) nanosystems as it is an essential requirement for IV administration. As it is clear in Figure 6-C, SNs-Ole did not lead to any haemolytic activity in all concentrations tested.

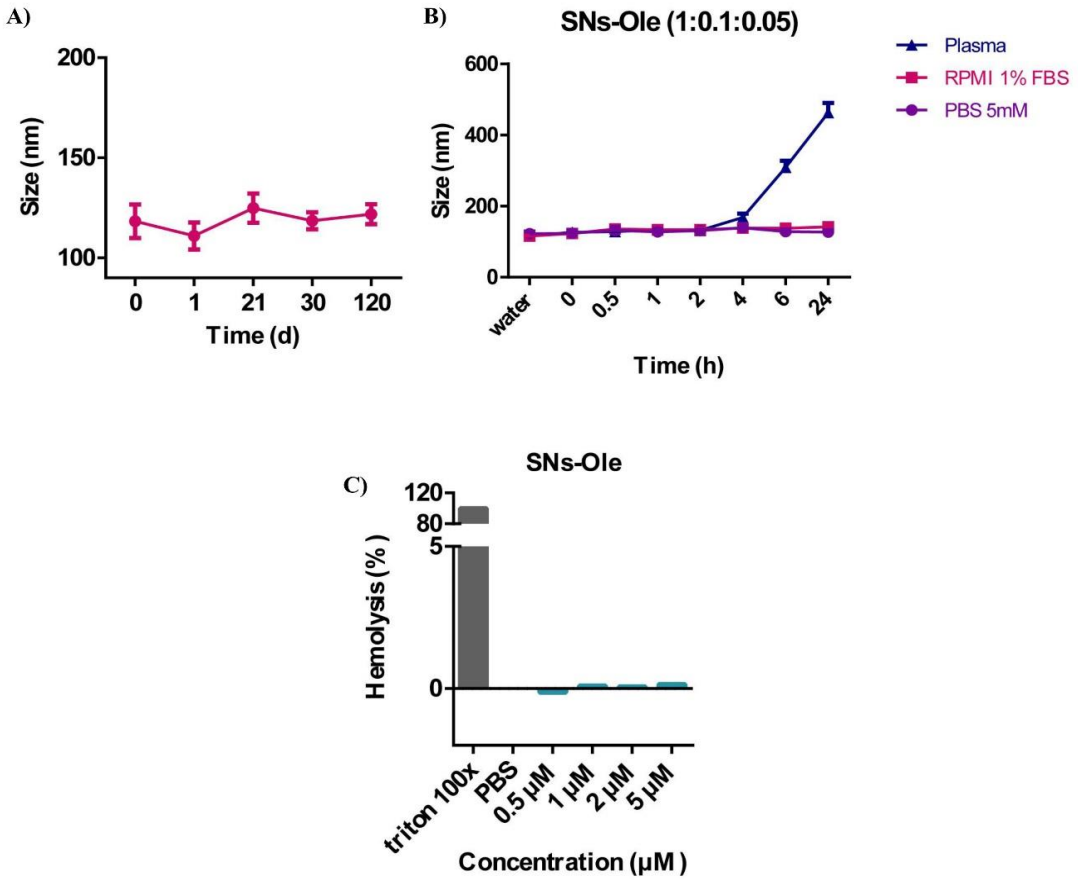

Figure 6: A) storage stability of SN-Ole (1:0.1:0.05) at 4 ºC over 4 months, size measurements were determined by DLS. **B)** Stability of SNs-Ole (1:0.1:0.05) upon incubation in different relevant media (PBS 5 mM, RPMI supplemented with 1% FBS, and plasma) up to 24 h. PBS: Phosphate Buffer Saline, FBS: Fetal Bovine Serum. **C)** Human red blood cells were haemolysis (%) upon exposure to SNs-Ole nanosystems up to 5 µM (Oleuropein). Triton X-100 and PBS were used as positive and negative controls representing 100% and 0% of haemolysis, respectively (n=3). Data are presented as mean ± SD.

3. Conclusions:

SNs prepared with Oleuropein possessed small hydrodynamic size of around 100 nm, were stable in different biological media and did not lead to any haemolytic activity. Therefore, these data are promising and will justify additional future studies to evaluate their possible senotherapeutic potential.

References:

1. Bouzo, B.L.; Calvelo, M.; Martín-Pastor, M.; García-Fandiño, R.; de la Fuente, M. In Vitro–In Silico Modeling Approach to Rationally Designed Simple and Versatile Drug Delivery Systems. J. Phys. Chem. B 2020, 124, 5788–5800, doi:10.1021/acs.jpcb.0c02731.

2. Bouzo, B.; Lores, S.; Jatal, R.; Alijas, S.; Alonso, M.J.; Conejos-Sánchez, I.; Fuente, M. de la Uroguanylin-decorated Nanosystems

Containing Etoposide, a Potential Targeted Combination Therapy for Colorectal Cancer 2020.

3. Díez-Villares, S.; Ramos-Docampo, M.A.; Silva-Candal, A. da; Hervella, P.; Vázquez-Ríos, A.J.; Dávila-Ibáñez, A.B.; López-López, R.; Iglesias-Rey, R.; Salgueiriño, V.; de la Fuente, M. Manganese Ferrite Nanoparticles Encapsulated into Vitamin E/Sphingomyelin Nanoemulsions as Contrast Agents for High-Sensitive Magnetic Resonance Imaging. Adv. Healthc. Mater. 2021, 2101019, doi:10.1002/ADHM.202101019.

4. Díez-Villares, S.; Pellico, J.; Gómez-Lado, N.; Grijalvo, S.; Alijas, S.; Eritja, R.; Herranz, F.; Aguiar, P.; de la Fuente, M. Biodistribution of 68/67Ga-Radiolabeled Sphingolipid Nanoemulsions by PET and SPECT Imaging. Int. J. Nanomedicine 2021, 16, 5923–5935, doi:10.2147/IJN.S316767.

5. Nagachinta, S.; Bouzo, B.L.; Vazquez-Rios, A.J.; Lopez, R.; de la Fuente, M. Sphingomyelin-based nanosystems (SNs) for the development of anticancer miRNA therapeutics. Pharmaceutics 2020, 12, 1–16, doi:10.3390/pharmaceutics12020189.

6. Nagachinta, S.; Becker, G.; Dammicco, S.; Serrano, M.E.; Leroi, N.; Bahri, M.A.; Plenevaux, A.; Lemaire, C.; Lopez, R.; Luxen, A.; et al. Radiolabelling of lipid-based nanocarriers with fluorine-18 for in vivo tracking by PET. Colloids Surfaces B Biointerfaces 2020, 188, 110793, doi:10.1016/j.colsurfb.2020.110793.

7. Bouzo, B.L.; Lores, S.; Jatal, R.; Alijas, S.; Alonso, M.J.; Conejos-Sánchez, I.; Fuente, M. de la Sphingomyelin nanosystems loaded with uroguanylin and etoposide for treating metastatic colorectal cancer. Sci. Rep. 2021.

8. Schneider, C.A.; Rasband, W.S.; Eliceiri, K.W. NIH Image to ImageJ: 25 years of image analysis. Nat. Methods 2012, 9, 671–675, doi:10.1038/nmeth.2089.

9. Guillon, J.; Petit, C.; Moreau, M.; Toutain, B.; Henry, C.; Roché, H.; Bonichon-Lamichhane, N.; Salmon, J.P.; Lemonnier, J.; Campone, M.; et al. Regulation of senescence escape by TSP1 and CD47 following chemotherapy treatment. Cell Death Dis. 2019, 10, doi:10.1038/s41419-019-1406-7.

10. Durán-Lobato, M.; López-Estévez, A.M.; Cordeiro, A.S.; Dacoba, T.G.; Crecente-Campo, J.; Torres, D.; Alonso, M.J. Nanotechnologies for the delivery of biologicals: Historical perspective and current landscape. Adv. Drug Deliv. Rev. 2021, 176, 113899.

11. Muttenthaler, M.; King, G.F.; Adams, D.J.; Alewood, P.F. Trends in peptide drug discovery. Nat. Rev. Drug Discov. 2021, 20, 309–325.

12. Therapeutic Proteins Global Market Report 2021: COVID-19 Impact and Recovery to 2030 - ResearchAndMarkets.com | Business Wire.

13. Bruno, B.J.; Miller, G.D.; Lim, C.S. Basics and recent advances in peptide and protein drug delivery. Ther Deliv 2013, 4, 1443–1467, doi:10.4155/tde.13.104.

14. Fosgerau, K.; Hoffmann, T. Peptide therapeutics: Current status and future directions. Drug Discov. Today 2015, 20, 122–128, doi:10.1016/j.drudis.2014.10.003.

15. Solaro, R.; Chiellini, F.; Battisti, A. Targeted delivery of protein drugs by nanocarriers. Materials (Basel). 2010, 3, 1928–1980.

16. Pudlarz, A.; Szemraj, J. Nanoparticles as carriers of proteins, peptides and other therapeutic molecules. Open Life Sci. 2018, 13, 285–298.

17. Jeong, W. jin; Bu, J.; Kubiatowicz, L.J.; Chen, S.S.; Kim, Y.S.; Hong, S. Peptide–nanoparticle conjugates: a next generation of diagnostic and therapeutic platforms? Nano Converg. 2018, 5, 1–18, doi:10.1186/s40580-018-0170-1.

18. Milanovic, M.; Fan, D.N.Y.; Belenki, D.; Däbritz, J.H.M.; Zhao, Z.; Yu, Y.; Dörr, J.R.; Dimitrova, L.; Lenze, D.; Monteiro Barbosa, I.A.; et al. Senescence-associated reprogramming promotes cancer stemness. Nature 2017, 553, 96.

19. Saleh, T.; Tyutyunyk-Massey, L.; Gewirtz, D.A. Tumor cell escape from therapy-induced senescence as a model of disease recurrence after dormancy. Cancer Res. 2019, 79, 1044–1046, doi:10.1158/0008-5472.CAN-18-3437.

20. Paez-Ribes, M.; González-Gualda, E.; Doherty, G.J.; Muñoz-Espín, D. Targeting senescent cells in translational medicine. EMBO Mol. Med. 2019, e10234, doi:10.15252/emmm.201810234.

21. Wissler Gerdes, E.O.; Zhu, Y.; Tchkonia, T.; Kirkland, J.L. Discovery, development, and future application of senolytics: theories and predictions. FEBS J. 2020, 287, 2418–2427, doi:10.1111/febs.15264.

22. Zhu, Y.; Tchkonia, T.; Pirtskhalava, T.; Gower, A.C.; Ding, H.; Giorgadze, N.; Palmer, A.K.; Ikeno, Y.; Hubbard, G.B.; Lenburg, M.; et al. The Achilles' heel of senescent cells: from transcriptome to senolytic drugs. Aging Cell 2015, 14, 644–658, doi:10.1111/acel.12344.

23. Borghesan, M.; Hoogaars, W.M.H.; Varela-Eirin, M.; Talma, N.; Demaria, M. A Senescence-Centric View of Aging: Implications for Longevity and Disease. Trends Cell Biol. 2020, 30, 777–791.

24. Jatal, R.; Lelievre, E.; Coqueret, O. TSP-1 C-terminal derived peptide and its effect on chemotherapy-induced senescence. submitted 2021.

25. Agostini, A.; Mondragõn, L.; Bernardos, A.; Martínez-Máñez, R.; Dolores Marcos, M.; Sancenõn, F.; Soto, J.; Costero, A.; Manguan-García, C.; Perona, R.; et al. Targeted cargo delivery in senescent cells using capped mesoporous silica nanoparticles. Angew. Chemie - Int. Ed. 2012, 51, 10556–10560, doi:10.1002/anie.201204663.

26. Muñoz-Espín, D.; Rovira, M.; Galiana, I.; Giménez, C.; Lozano-Torres, B.; Paez-Ribes, M.; Llanos, S.; Chaib, S.; Muñoz-Martín, M.; Ucero, A.C.; et al. A versatile drug delivery system targeting senescent cells. EMBO Mol. Med. 2018, 10, 1–18, doi:10.15252/emmm.201809355.

27. Lewinska, A.; Adamczyk-Grochala, J.; Bloniarz, D.; Olszowka, J.; Kulpa-Greszta, M.; Litwinienko, G.; Tomaszewska, A.; Wnuk, M.; Pazik, R. AMPK-mediated senolytic and senostatic activity of quercetin surface functionalized Fe3O4 nanoparticles during oxidant-induced senescence in human fibroblasts. Redox Biol. 2020, 28, 101337, doi:10.1016/j.redox.2019.101337.

28. Ke, S.; Lai, Y.; Zhou, T.; Li, L.; Wang, Y.; Ren, L.; Ye, S. Molybdenum Disulfide Nanoparticles Resist Oxidative Stress-Mediated Impairment of Autophagic Flux and Mitigate Endothelial Cell Senescence and Angiogenic Dysfunctions. ACS Biomater. Sci. Eng. 2018, 4, 663–674, doi:10.1021/acsbiomaterials.7b00714.

29. Thapa, R.K.; Nguyen, H.T.; Jeong, J.H.; Kim, J.R.; Choi, H.G.; Yong, C.S.; Kim, J.O. Progressive slowdown/prevention of cellular senescence by CD9-targeted delivery of rapamycin using lactose-wrapped calcium carbonate nanoparticles. Sci. Rep. 2017, 7, 1–11, doi:10.1038/srep43299.

30. Ekpenyong-Akiba, A.E.; Canfarotta, F.; Abd, B.; Poblocka, M.; Casulleras, M.; Castilla-Vallmanya, L.; Kocsis-Fodor, G.; Kelly, M.E.; Janus, J.; Althubiti, M.; et al. Detecting and targeting senescent cells using molecularly imprinted nanoparticles. Nanoscale Horizons 2019, 4, 757–768, doi:10.1039/c8nh00473k.

31. Belcastro, E.; Rehman, A.U.; Remila, L.; Park, S.H.; Gong, D.S.; Anton, N.; Auger, C.; Lefebvre, O.; Goetz, J.G.; Collot, M.; et al. Fluorescent nanocarriers targeting VCAM-1 for early detection of senescent endothelial cells. Nanomedicine Nanotechnology, Biol. Med. 2021, 34, 102379, doi:10.1016/j.nano.2021.102379.

32. Wang, H.H.; Lin, C.A.J.; Tseng, Y.M.; Lee, H.I.; Lee, Y.N.; Yeh, H.I.; Yang, P.S.; Peng, H.Y.; Wu, Y.J. Dihydrolipoic acid-coated gold nanocluster bioactivity against senescence and inflammation through the mitochondria-mediated JNK/AP-1 pathway. Nanomedicine Nanotechnology, Biol. Med. 2021, 36, 102427, doi:10.1016/j.nano.2021.102427.

33. Pham, L.M.; Kim, E.C.; Ou, W.; Phung, C.D.; Nguyen, T.T.; Pham, T.T.; Poudel, K.; Gautam, M.; Nguyen, H.T.; Jeong, J.H.; et al. Targeting and clearance of senescent foamy macrophages and senescent endothelial cells by antibody-functionalized mesoporous silica nanoparticles for alleviating aorta atherosclerosis. Biomaterials 2021, 269, 120677, doi:10.1016/j.biomaterials.2021.120677.

34. Berrecoso, G.; Crecente-Campo, J.; Alonso, M.J. Unveiling the pitfalls of the protein corona of polymeric drug nanocarriers. Drug Deliv. Transl. Res. 2020 103 2020, 10, 730–750, doi:10.1007/S13346-020-00745-0.

35. Kommuru, T.R.; Gurley, B.; Khan, M.A.; Reddy, I.K. Self-emulsifying drug delivery systems (SEDDS) of coenzyme Q10: Formulation development and bioavailability assessment. Int. J. Pharm. 2001, 212, 233–246, doi:10.1016/S0378-5173(00)00614-1.

36. Saberi, A.H.; Fang, Y.; McClements, D.J. Fabrication of vitamin E-enriched nanoemulsions: Factors affecting particle size using spontaneous emulsification. J. Colloid Interface Sci. 2013, 391, 95–102, doi:10.1016/j.jcis.2012.08.069.

37. L, W.; J, D.; J, C.; J, E.; X, L. Design and optimization of a new self-nanoemulsifying drug delivery system. J. Colloid Interface Sci. 2009, 330, 443–448, doi:10.1016/J.JCIS.2008.10.077.

38. Filipe, V.; Hawe, A.; Jiskoot, W. Critical evaluation of nanoparticle tracking analysis (NTA) by NanoSight for the measurement of nanoparticles and protein aggregates. Pharm. Res. 2010, 27, 796–810, doi:10.1007/s11095-010-0073-2.

39. Ruozi, B.; Tosi, G.; Forni, F.; Fresta, M.; Vandelli, M.A. Atomic force microscopy and photon correlation spectroscopy: Two techniques for rapid characterization of liposomes. Eur. J. Pharm. Sci. 2005, 25, 81–89, doi:10.1016/j.ejps.2005.01.020.

40. Wu, L.; Zhang, J.; Watanabe, W. Physical and chemical stability of drug nanoparticles. Adv. Drug Deliv. Rev. 2011, 63, 456–469, doi:10.1016/j.addr.2011.02.001.

41. Aramesh, M.; Shimoni, O.; Ostrikov, K.; Prawer, S.; Cervenka, J. Surface charge effects in protein adsorption on nanodiamonds. Nanoscale 2015, 7, 5726–5736, doi:10.1039/c5nr00250h.

42. Fornaguera, C.; Solans, C. Methods for the in vitro characterization of nanomedicines—biological component interaction. J. Pers. Med. 2017, 7, doi:10.3390/jpm7010002.

43. Franken, N.A.P.; Rodermond, H.M.; Stap, J.; Haveman, J.; van Bree, C. Clonogenic assay of cells in vitro. Nat. Protoc. 2006, 1, 2315–2319, doi:10.1038/nprot.2006.339.

44. Harpe, K.M. de la; Kondiah, P.P.D.; Choonara, Y.E.; Marimuthu, T.; Toit, L.C. du; Pillay, V. The Hemocompatibility of Nanoparticles: A Review of Cell–Nanoparticle Interactions and Hemostasis. Cells 2019, 8, doi:10.3390/CELLS8101209.

45. Forest, V.; Cottier, M.; Pourchez, J. Electrostatic interactions favor the binding of positive nanoparticles on cells: A reductive theory. Nano Today 2015, 10, 677–680, doi:https://doi.org/10.1016/j.nantod.2015.07.002.

46. Fakhari, A.; Baoum, A.; Siahaan, T.J.; Le, K.B.; Berkland, C. Controlling ligand surface density optimizes nanoparticle binding to ICAM-1. J. Pharm. Sci. 2011, 100, 1045–1056, doi:10.1002/jps.22342.

47. Gao, H.; Yang, Z.; Zhang, S.; Cao, S.; Shen, S.; Pang, Z.; Jiang, X. Ligand modified nanoparticles increases cell uptake, alters endocytosis and elevates glioma distribution and internalization. Sci. Rep. 2013, 3, 1–8, doi:10.1038/srep02534.

48. Acosta, J.C.; Gil, J. Senescence: A new weapon for cancer therapy. Trends Cell Biol. 2012, 22, 211–219.

49. Yang, L.; Fang, J.; Chen, J. Tumor cell senescence response produces aggressive variants. Cell Death Discov. 2017, 3, 1–11, doi:10.1038/cddiscovery.2017.49.

50. Soto-Gamez, A.; Quax, W.J.; Demaria, M. Regulation of Survival Networks in Senescent Cells: From Mechanisms to Interventions. J. Mol. Biol. 2019, 431, 2629–2643, doi:10.1016/j.jmb.2019.05.036.

51. Akl, H.; Vervloessem, T.; Kiviluoto, S.; Bittremieux, M.; Parys, J.B.; De Smedt, H.; Bultynck, G. A dual role for the anti-apoptotic Bcl-2 protein in cancer: Mitochondria versus endoplasmic reticulum. Biochim. Biophys. Acta - Mol. Cell Res. 2014, 1843, 2240–2252, doi:10.1016/j.bbamcr.2014.04.017.

52. Yosef, R.; Pilpel, N.; Tokarsky-Amiel, R.; Biran, A.; Ovadya, Y.; Cohen, S.; Vadai, E.; Dassa, L.; Shahar, E.; Condiotti, R.; et al. Directed elimination of senescent cells by inhibition of BCL-W and BCL-XL. Nat. Commun. 2016, 7, doi:10.1038/ncomms11190.

53. Zhang, X.; Liu, X.; Zhou, D.; Zheng, G. Targeting anti-apoptotic BCL-2 family proteins for cancer treatment. Future Med. Chem. 2020, 12, 563–565, doi:10.4155/fmc-2020-0004.

54. Zhang, H.; Nimmer, P.M.; Tahir, S.K.; Chen, J.; Fryer, R.M.; Hahn, K.R.; Iciek, L.A.; Morgan, S.J.; Nasarre, M.C.; Nelson, R.; et al. Bcl-2 family proteins are essential for platelet survival. Cell Death Differ. 2007, 14, 943–951, doi:10.1038/sj.cdd.4402081.

55. Wilson, W.H.; O'Connor, O.A.; Czuczman, M.S.; LaCasce, A.S.; Gerecitano, J.F.; Leonard, J.P.; Tulpule, A.; Dunleavy, K.; Xiong, H.; Chiu, Y.L.; et al. Navitoclax, a targeted high-affinity inhibitor of BCL-2, in lymphoid malignancies: A phase 1 dose-escalation study of safety, pharmacokinetics, pharmacodynamics, and antitumour activity. Lancet Oncol. 2010, 11, 1149–1159, doi:10.1016/S1470-2045(10)70261-8.

56. Liu, M.; Tu, J.; Feng, Y.; Zhang, J.; Wu, J. Synergistic co-delivery of diacid metabolite of norcantharidin and ABT-737 based on folate-modified lipid bilayer-coated mesoporous silica nanoparticle against hepatic carcinoma. J. Nanobiotechnology 2020, 18, 1–8, doi:10.1186/s12951-020-00677-4.

57. Wu, X.; Wang, L.; Qiu, Y.; Zhang, B.; Hu, Z.; Jin, R. Cooperation of IRAK1/4 inhibitor and ABT-737 in nanoparticles for synergistic therapy of T cell acute lymphoblastic leukemia. Int. J. Nanomedicine 2017, 12, 8025–8034, doi:10.2147/IJN.S146875.

58. Valcourt, D.M.; Dang, M.N.; Scully, M.A.; Day, E.S. Nanoparticle-Mediated Co-Delivery of Notch-1 Antibodies and ABT-737 as a Potent Treatment Strategy for Triple-Negative Breast Cancer. ACS Nano 2020, 14, 3378–3388, doi:10.1021/acsnano.9b09263.

59. Schmid, D.; Jarvis, G.E.; Fay, F.; Small, D.M.; Greene, M.K.; Majkut, J.; Spence, S.; McLaughlin, K.M.; McCloskey, K.D.; Johnston, P.G.; et al. Nanoencapsulation of ABT-737 and camptothecin enhances their clinical potential through synergistic antitumor effects and reduction of systemic toxicity. Cell Death Dis. 2014, 5, e1454-11, doi:10.1038/cddis.2014.413.

60. González-Gualda, E.; Pàez-Ribes, M.; Lozano-Torres, B.; Macias, D.; Wilson, J.R.; González-López, C.; Ou, H.L.; Mirón-Barroso, S.; Zhang, Z.; Lérida-Viso, A.; et al. Galacto-conjugation of Navitoclax as an efficient strategy to increase senolytic specificity and reduce platelet toxicity. Aging Cell 2020, 19, doi:10.1111/acel.13142.

61. Minelli, C.; Sikora, A.; Garcia-Diez, R.; Sparnacci, K.; Gollwitzer, C.; Krumrey, M.; Shard, A.G. Measuring the size and density of nanoparticles by centrifugal sedimentation and flotation. Anal. Methods 2018, 10, 1725–1732, doi:10.1039/c8ay00237a.

62. Zierkiewicz, W.; Privalov, T. A theoretical study of the essential role of DMSO as a solvent/ligand in the Pd(OAc)2/DMSO catalyst system for aerobic oxidation. Organometallics 2005, 24, 6019–6028, doi:10.1021/om0506217.

63. Weaver Jr, C.E.; Marek, P.; Park-Chung, M.; Tam, S.W.; Farb, D.H. Neuroprotective activity of a new class of steroidal inhibitors of the N-methyl-D-aspartate receptor. Proc. Natl. Acad. Sci. U. S. A. 1997, 94, 10450–10454, doi:10.1073/pnas.94.19.10450.

64. Asefa, T.; Tao, Z. Biocompatibility of Mesoporous Silica Nanoparticles. Chem. Res. Toxicol. 2012, 25, 2265–2284, doi:10.1021/tx300166u.

65. Wang, H.-X.; Zuo, Z.-Q.; Du, J.-Z.; Wang, Y.-C.; Sun, R.; Cao, Z.-T.; Ye, X.-D.; Wang, J.-L.; Leong, K.W.; Wang, J. Surface charge critically affects tumor penetration and therapeutic efficacy of cancer nanomedicines. Nano Today 2016, 11, 133–144, doi:https://doi.org/10.1016/j.nantod.2016.04.008.

66. Cagliani, R.; Gatto, F.; Bardi, G. Protein adsorption: A feasible method for nanoparticle functionalization? Materials (Basel). 2019, 12.

67. Le Tutour, B.; Guedon, D. Antioxidative activities of Olea europaea leaves and related phenolic compounds. Phytochemistry 1992, 31, 1173–1178, doi:10.1016/0031-9422(92)80255-D.

68. Castejón, M.L.; Rosillo, M.Á.; Montoya, T.; González-Benjumea, A.; Fernández-Bolaños, J.M.; Alarcón-De-La-Lastra, C. Oleuropein down-regulated IL-1β-induced inflammation and oxidative stress in human synovial fibroblast cell line SW982. Food Funct. 2017, 8, 1890–1898, doi:10.1039/c7fo00210f.

69. Varela-Eirín, M.; Carpintero-Fernández, P.; Sánchez-Temprano, A.; VarelaVázquez, A.; Paíno, C.L.; Casado-Díaz, A.; Continente, A.C.; Mato, V.; Fonseca, E.; Kandouz, M.; et al. Senolytic activity of small molecular polyphenols from olive restores chondrocyte redifferentiation and promotes a pro-regenerative environment in osteoarthritis. Aging (Albany. NY). 2020, 12, 15882–15905, doi:10.18632/aging.103801.

70. González-Ortega, R.; Šturm, L.; Skrt, M.; Di Mattia, C.D.; Pittia, P.; Poklar Ulrih, N. Liposomal Encapsulation of Oleuropein and an Olive Leaf Extract: Molecular Interactions, Antioxidant Effects and Applications in Model Food Systems. Food Biophys. 2021, 16, 84–97.

71. Jimenez-Ruiz, A.; Prado-Gotor, R.; Fernández-Bolaños, J.G.; González-Benjumea, A.; Carnerero, J.M. Encased gold nanoparticle synthesis as a probe for oleuropein self-assembled structure formation. Materials (Basel). 2021, 14, 1–16, doi:10.3390/ma14010050.

72. Khalil, M.M.H.; Ismail, E.H.; El-Magdoub, F. Biosynthesis of Au nanoparticles using olive leaf extract: 1st Nano Updates. Arab. J. Chem. 2012, 5, 431–437, doi:https://doi.org/10.1016/j.arabjc.2010.11.011.

73. Khalil, M.M.H.; Ismail, E.H.; El-Baghdady, K.Z.; Mohamed, D. Green synthesis of silver nanoparticles using olive leaf extract and its antibacterial activity. Arab. J. Chem. 2014, 7, 1131–1139, doi:https://doi.org/10.1016/j.arabjc.2013.04.007.

Overall Discussion

Cellular Senescence is initially a tumour suppressive mechanism that is characterised by cell cycle arrest, distinct secretory phenotype (SASP), and resistance to apoptosis [1]. Senescent cells also play an important role in wound healing and tissue regeneration [2,3]. All these beneficial effects are linked to their temporary presence as senescent cells should be eliminated by the immune system. However, these cells tent to accumulate chronically over age or due to some therapies such as genotoxic chemotherapy, and with their proinflammatory secretome they promote several age-related diseases including cancer. In addition, recent studies pointed out that cancer cells turning to senescent state due to chemotherapy treatment have the capacity to regain full proliferative potential which leads them to escape this state and emerge in a more aggressive form of cancer, leading to cancer relapse [4–12]. Interestingly it was found out that cancer cells turning to senescent have characteristics similar to tumour dormancy [4,5,13]. Consequently, numerous studies are investigating possible therapeutic strategies targeting senescent cells or their secretory phenotype SASP. Molecular pathways governing senescent cells are the main source for developing such senotherapies. Besides, very recent studies are exploiting nanomedicine advantages for delivering senolytics and senostatic agents.

Within this frame, the main target of this PhD thesis has been to explore and investigate therapeutic agents that can hinder the emergence from chemotherapy induced senescence (CIS) for the long-term goal of improving the health span and life span of cancer patients received senescence-inducing therapies. Our therapeutic candidate was a 10 amino acids peptide (4N1Ks) derived from the C-terminal domain of TSP-1 and was chosen based on a previous study proving that TSP-1 prevents emergence from CIS model of colorectal and breast cancer. Therefore, we explored the effect of this peptide on both MCF7 and LS174t cancer and senescent cells as well as its effect on senescence escape from CIS (chapter1). Additionally, several western blot experiments for different cellular proteins expression were carried out as well as flow cytometry, RT-qPCR, MTT, Colony forming assay, and Boyden chamber assay, in order to understand the exact molecular mechanism of 4N1Ks peptide.

The second part of this thesis was to incorporate 4N1Ks peptide on the surface of nanosystems to improve its efficacy (chapter 2, part1). Sphingomyelin based nanosystems SNs were chosen for this purpose due to their bioavailability, biocompatibility, and versatility for association and encapsulation of a variety of therapeutic molecules [14–19]. To facilitate 4N1Ks assembling to the surface of SNs, it was chemically conjugated to PEGylated hydrophobic chain. The prepared nanosystems were heavily characterised by DLS, NTA, MADLS, and AFM. Additionally, the

therapeutic efficacy of those nanosystems were evaluated by several *in vitro* studies including emergence assay on CIS model of MCF7 breast cancer cells.

Due to SNs versatility for associating and encapsulating several therapeutic molecules in addition to the simple and straightforward preparation method, we were eager to formulate SNs with other senotherapies targeting senescent cells. For that we chose two different senotherapeutic agents: i) ABT-737 a senolytic drug that induces apoptosis in senescent cells by inhibiting anti-apoptotic proteins (BCL-2, BCL-XL and BCL-W) [20,21] (chapter2, part 2). ii) Oleuropein, an antioxidant that possess senolytic and anti-inflammatory effects by downregulating IL-1ß, IL-6 and COX-2 gene expression and NF-kB activation [22,23] (chapter2, part 3). Each of these senolytic drug were encapsulated in the oil phase of the SNs. Both SNs prepared were heavily characterised by DLS, NTA, MADLS, and AFM. Also, several *in vitro* studies were followed to demonstrate their safety and therapeutic potential.

It is important to indicate that an absolute elimination of all senescent cells is not necessary. As a decrease in 30% of senescent cells in the body were able to alleviate age-related pathologies and extended health-span in progeroid and normal chronologically aged mice [1].

1. 4N1Ks, a TSP-1 C-terminal derived peptide and its effect on Chemotherapy-Induced Senescence.

Senescence escape and Boyden chamber assay were the first two experiments to evaluate 4N1Ks therapeutic potential and compare it with TSP-1 results gained in a previous study. The senescence escape essay would give an indication of 4N1Ks effects on senescent cells, while the Boyden chamber assay would specify 4N1Ks effect on senescent cells secretome (SASP). 4N1Ks peptide was able to significantly prevent senescence escape in the CIS model of MCF7 and LS174T and greatly affect the migratory ability of the SASP in both cell lines.

From this point, several experiments were followed to understand the exact molecular mechanism the peptide work by. Obviously, we had to check p53, p21, expression as they are essential for establishing and maintaining the cellular senescence program [24,25]. 4N1Ks peptide did not have any effect on p53 and p21 expression in both cell lines. In addition, β-galactosidase activity was increased by in (33%) MCF7 and by (22%) in LS174T cells upon treatment with 4N1Ks. Those results were quite confusing, and further experiments were essential to explain those results.

Cell cytotoxicity studies of MTT assay and colony forming assay showed that 4N1Ks has an antiproliferative effect on MCF7 and LS174T cancer cell lines, which agrees with previous studies that showed 4N1K peptide and its analogue PKHB1 induce cell death in several types of cancer cells [26–28]. However, the effective concentration used in those studies (ranged between 100 to 300 µM) were much higher than the one we used (50µM). Based on these results and 4N1Ks effect on senescence escape, it was interesting to detect the cell cycle of treated cells by flow cytometry, where we found that there was a slight insignificant increase in the number of cells in G2M phase after 4N1Ks treatment. This proves that 4N1Ks did not have any effect on the cell cycle of treated cells.

The rest of the experiments were conducted on MCF7 only as it was more responsive than LS174T. We noticed a low protein content in cancer and emergent cells treated with 4N1Ks, raising the hypothesis of ER stress [29], UPR [30], and autophagy induction [31]. Western blot studies on cancer cells and senescent cells treated with 4N1Ks showed that 4N1Ks effects are mainly related to induction of autophagy. Moreover, the increased granularity of the cells treated with 4N1Ks is additional proof of autophagy induction in those cells [32]. It has been reported before that 4N1K peptide-induced autophagy in cancer cells through immunodetection of LC3 in treated cells [33]. Anyhow, we have extra proof of autophagy induction through the downregulation of the mTOR pathway [34] and p62 [31]. In addition, slight increase of β-galactosidase activity could also be explained by autophagy program activation.

Regarding the UPR induction hypothesis, 4N1Ks treatment increase the expression of Bip, which is an ER chaperon protein [35] and considered as a master regulator of the unfolded protein response UPR [36]. In addition, treated cells showed higher cellular granularity which is usually observed in physiological processes like autophagy [32] and UPR [37]. Unfortunately, these results were not backed up by the results obtained from RT-qPCR of several UPR markers, as it indicates that treatment with 4N1Ks did not alter the expression of any of the UPR genes. It is important to note that although 4N1Ks treatment increased the expression of IRE1α and PERK, which are ER stress sensors [38], this represents the whole protein and not the active phosphorylated form. Therefore, further experiments are needed to strength this hypothesis.

Already mentioned in the general introduction the essential roles of UPR and autophagy in senescent cells survival. As senescent cells tend to accumulate oxidised lipids, proteins, and nucleic acids due increased levels of ROS [39]. Consequently, UPR and autophagy are activated

to regain the intracellular balance [40]. However, the relationship between senescence and those mechanisms are quite complicated specially for autophagy. As high levels of autophagy can result in cellular organelle destruction leading to cell death [41].

Regarding the 4N1Ks effect on the SASP, we already indicated that 4N1Ks affect the migratory ability of the SASP by Boyden chamber assay. These could be more related to the antiproliferative effect of the peptide we found with clonogenic assay and MTT.

Autophagy [42,43] and mTOR [44,45] play and essential role in the production of several SASP components and since 4N1Ks induce autophagy and downregulate mTOR, in addition to low cellular protein content, we speculated that 4N1Ks might also affect the production of SASP factors. Unfortunately, we could not prove if 4N1Ks affect mRNA levels of several SASP components. We also repeated the Boyden chamber assay, but instead of mixing the peptide with the SASP, we tested the migratory ability of SASP produced by senescent cells treated with 4N1Ks peptide compared to normal SASP. This could indicate that 4N1Ks affect the production of SASP factors. These results oppose the fact that TSP1 promotes invasion and migration of endothelial cells osteosarcoma cells [46]. Anyhow, TSP1 effects are mediated by several receptors, and since 4N1Ks is derived from the C-terminal domain, it does not possess all TSP1 effectivity.

Additionally, we checked the metabolic activity of MCF7 senescent cells treated with 4N1Ks peptide through an MTT assay. 4N1Ks was able to reduce the metabolic activity of MCF7 senescent cells significantly.

Considering all these results, we speculate that 4N1Ks mediates its effects at a post-transcriptional level.

In the end, 4N1Ks with its relatively small size of 10 amino acids and its significant ability to prevent senescence escape, reducing the migratory capacity of SASP, and the metabolic activity of senescent cells, makes 4N1Ks an attractive candidate for Senotherapy.

2. Senolytic and Senostatic Sphingomyelin based Nanosystems.

Based on the molecular pathways that govern senescent cells, there are several mechanisms to target senescent cells. For example, activating apoptotic pathways in senescent cells, targeting SASP components or improving the immune system capacity in eliminating senescent cells. All this has been discussed extensively in the thesis introduction. Many of those senotherapies have

reached clinical studies, but the high toxicity profile of some of them is hindering them from moving forward. Nanomedicine can be the solution for such problems by maximising efficacy while minimising side effects by specific targeting and reducing the loaded dose.

In this chapter we took advantage of sphingomyelin based nanosystems versatility to associate and encapsulate different therapeutic agents targeting senescent cells.

Part 1: SNs-Ks.

4N1Ks peptide were first chemically modified with a PEGylated hydrophobic chain (PEG-C18), resulting in C18-PEG-Ks. Such modification was essential to facilitate the association of the peptide to the surface of SNs. Moreover, the modified peptide resembled surfactant-like properties, which was proved by successfully formulation nanosystems based on VitE and the C18-PEG-Ks (V-Ks). V-Ks nanosystems serve another poof of the rearrangement of the modified peptide.

DLS measurements of SNs-blank nanosystems of VitE:SM 1:0.1 ratio indicate a 100 nm in size and a slightly negative zeta potential. Incorporating the modified peptide at the weight ratios 0.025, 0.05 and 0.1 (respective to VitE) did not significantly alter the hydrodynamic diameter of the nanosystems; however, doubling the ratio of the peptide to 0.2 led to an increase of the size from 106 to 167 nm. Similar results were also gained with V-Ks nanosystems, table 1. Increasing the ratio of the modified peptide to 0.2 did not only result in a bigger size but also led to a less homogeneous population, as indicated by the bigger PdI. explained due to the surfactant-like characteristics of the peptide conjugated to a PEGylated hydrophobic chain that, as reported in several studies, increasing amounts of surfactants lead to a smaller size of the oil droplets, however when exceeding a specific concentration lead to an increase in the particle size and can also result in unstable nanosystems [47–49]. SNs-Ks and V-Ks presented a positive zeta potential due to the 4N1Ks peptide's positively charged amino acids (lysine and arginine). This provides another evidence of PEG-Ks part presence on the surface of the nanosystems.

Table 1: SNs-blank (1:0.1) and SNs-Ks nanosystems physicochemical characterisation by DLS and LDA (mean ±SD, n=3).

VitE:SM:C18-PEG-Ks	Size (nm)	PdI	ZP (mV)
1:0.1:0	106 ± 5	0.095 ± 0.02	-10 ± 3
1:0.1:0.025	98± 3	0.34 ± 0.03	+37 ± 1
1:0.1:0.05	108 ± 3	0.42 ± 0.01	+51 ± 2
1:0.1:0.1	106 ± 18	0.25 ± 0.1	+54 ± 4
1:0.1:0.2	166 ± 6	0.27 ± 0.07	+55 ± 4

Vit E, Vitamin E; SM, Sphingomyelin; nm, nanometre; PdI, Polydispersity index; ZP, zeta potential; mV: millivolts.
Total volume of the nanoparticle suspension: 1 mL. Size refers to diameter.

Table 2: V-Ks nanosystems physicochemical characterisation by DLS and LDA (mean ± SD, n=3).

VitE:C18-PEG-Ks	Size (nm)	PdI	ZP (mV)
1:0.025	108 ± 2	0.25 ± 0.01	+50± 1
1:0.05	103 ± 2	0.24 ± 0.01	+53 ± 0
1:0.1	116 ± 1	0.24 ± 0.007	+51 ± 2
1:0.2	220 ± 9	0.38 ±0.01	+52 ± 5

Vit E, Vitamin E; nm, nanometre; PdI, Polydispersity index; ZP, zeta potential; mV, millivolts.
Total volume of the nanoparticle suspension: 1 mL. Size refers to diameter.

The nanosystems loading C18-PEG-Ks at the ratio 0.1 were selected for further characterisation considering their size (about 100 nm) as well as population homogeneity (PdI<0.3) and 4N1Ks peptide senolytic effective dose (50 µM). V-Ks and SNs-blank nanosystems were used as controls.

A dialysed method was chosen to separate nanosystems from free molecules to determine the association efficiency of the peptide. Dialyzed nanosystems were heavily characterised by DLS, NTA, MADLS and AFM. DLS measurements showed that the dialysis process did not affect the integrity of those nanosystems. Moreover, NTA, MADLS and AFM results were compatible with the measurements gained with DLS. During the AFM measurement process, we noticed the V-Ks sample show a phase segregation of some components over time, finally resulting in the coalescence of several nanoemulsion droplets, Figure 6-D. Such behaviour was not noticed with SNs and SNs-Ks nanosystems, proofing the necessity of sphingomyelin for the stability of those nanosystems.

Both SNs-Ks (1:0.1:0.1), and V-Ks (1:0.1) showed high association efficiency AE of 87.2 ± 6.9 % and 90.3 ±10.6 %, which once again indicates that C18-PEG-Ks is acting as a surfactant being able to emulsify with VitE (and SM) and form nanostructures.

The stability of prepared nanosystems was evaluated over time and in different biological media, and it is essential to predict the fate of nanosystems, especially after administration [50]. All nanosystems prepared were relatively stable for at least 6 months of storage at 4 °C. SNs-Ks was stable in RPMI supplemented with 1%FBS for 24h with a final hydrodynamic size of 272 ±10 nm and surface charge decrease to -11 ±1 mV. Such an increase in size can be explained by the adsorption of serum proteins to the surface of the strongly positively charged SNs-Ks nanosystems through electrostatic interactions. Regarding stability in plasma, SNs-Ks showed improved stability compared to SNs-blank nanosystems as SNs-Ks maintained their size the whole experiment presenting a final mean particle size of 101 ±11 nm. This could be related to the PEG-C18 part, as several studies have indicated the role of PEG chains in stabilising the particles in a cellular medium by steric hydration repulsions and preventing or reducing protein adsorption [51].

MTT and CFA experiments conducted on MCF7 cells treated with different concentrations of C18-PEG-Ks, indicate that the chemical modification on 4N1Ks peptide did not alter its therapeutic capacity. According to CFA results, C18-PEG-Ks reduced the number of growing colonies by 50% at a concentration of 5 µM compared to nontreated cells. Interestingly, SNs-Ks achieved similar results at 0.5 µM. Decreasing the effective concentration 10 times (from 5 to 0.5 µM) is quite remarkable and could be attributed to the association of 4N1Ks peptide to the nanosystems and its exposure on their surface. Such results demonstrate the capacity of nanoformulated systems as to improve drug's effectiveness requiring lower doses.

The hemocompatibility of SNs-Ks nanosystems were evaluated in vitro compared to SNs-blank. Haemolysis assay is an essential requirement for newly formulated therapeutic nanosystem intended to be delivered intravenously, especially if those nanosystems were positively charged as they tend to be more toxic. SNs-Ks haemolytic activity was very low with 12% ±1 haemolysis at the highest concentration tested (1 µM).

SNs-Ks with fluorescently labelled sphingomyelin were prepared for internalisation studies on MCF7 cells which were assessed by confocal microscope and flow cytometry. This will give an insight of 4N1Ks effect on SNs cell uptake. Confocal microscope images and Flow

cytometry results showed high cellular uptake of SNs-Ks compared to SNs-blank. Flowcytometry results indicate that 83% of the cells were fluorescent after 10 min of treatment with SNs-Ks and reaches 96% after 1 h, while such percent where achieved after 4h in case of cells treated with SNs-blank.

Lastly, the most crucial experiment of this part was assessing the SNs-Ks senolytic capacity on the CIS model of MCF cells by senescence escape experiment. As it is clear from Figure 9, SNs-Ks significantly decreases the number of emergent clones at 0.5 µM compared to nontreated cells and cells treated with SNs-blank, which is similar to what we observed in CFA. Considering all results, SNs-Ks nanosystems represent an interesting approach to ease the burden of accumulated senescent cells due to chemotherapy treatment and, therefore, make a step forward in the management of this disease. Of course, further studies, especially *in vivo*, are needed to further strengthen our findings.

Part 2: SNs-ABT:

ABT-737 is a small molecule that binds with high affinity to the anti-apoptotic proteins (BCL-2 family), shifting the survival/ apoptosis balance towards apoptosis [21]. ABT-737 is a potent anti-cancer and senolytic drug; however, its low solubility and bioavailability, plus its high toxicity, hindered several clinical studies from moving forward [52]. Several studies exploited nanotechnology advances in improving ABT-737 bioavailability and reducing its toxicity against platelets. However, these nanoparticles were intended to treat cancer. Up until now, there has been no study indicating senolytic ABT-737 loaded nanoparticles.

SNs-ABT nanosystems prepared from ABT-737 dissolved in chloroform were not stable and disintegrated after a while, most probably due to evaporation of chloroform. DMSO was selected as an alternative solvent. A 20mg/ml stock solution was prepared to prepare SNs-ABT with different weight ratios (0.005, 0.01, 0.02) with respect to the content of VitE in the SNs (5mg of VitE in 1mL of formulation). Importantly, these SNs-ABT were more stable with respect to the previous formulations prepared in the presence of chloroform. Additionally, they remained stable after centrifugation at 7000 rpm for 1h. Besides, the absence of ABT-737 sedimentation proves the solubility of this drug in those nanosystems [61].

SNs-ABT were characterized by DLS. As it is clear from table 3, incorporation of ABT-737 increased the size of the nanoemulsion to 139.5 nm ±19 nm at a ratio of 0.02 and resulted in gradient zeta potential ranging from -0.96mV to +9.2 mV. The increase of surface positive

charge compared to SNs-blank ZP could be related to DMSO or ABT-737 incorporation as DMSO contain positively charged sulphur. Moreover, The PdI of all nanosystems prepared were below 0.1, referring to their homogeneity. It is important that we did not exceed 0.5% of DMSO in our formulation, which is the highest acceptable for IV formulations [53].

Table 3: SNs-blank (1:0.1) and SNs-ABT nanosystems physicochemical characterisation by DLS and LDA (mean ±SD, n=12).

VitE: SM : ABT	DMSO%	Size nm	PDI	ZP mV
1:0.1:0	0	98.2 ± 1.4	0.09 ± 0.02	-10.2 ± 0.8
1:0.1:0.005	0.125	130.7 ± 5.5	0.09 ± 0.04	-0.96 ± 1.7
1:0.1:0.01	0.25	119.5 ± 8	0.08 ± 0.03	+8.9 ± 2.8
1:0.1:0.02	0.5	139.5 ± 19	0.08 ± 0.04	+9.2 ± 3.9

Vit E, Vitamin E; nm, nanometre; PdI, Polydispersity index; ZP, zeta potential; mV, millivolts; ABT, ABT-737. The total volume of the nanoparticle suspension: 1 mL. Size refers to diameter.

SNs-ABT nanosystems were dialyzed in order to separate the nanosystems from the free drug and other molecules. Unfortunately, the dialysis process affected the stability of SNs-ABT nanosystems (1:0.1:0.02 and 1:0.1:0.01) as they disintegrate at the end of the process. This might be related to the poor solubility of the ABT-737. and with the dialysis process, we might be losing part of the DMSO that stabilises those nanosystems. As we concluded from the formulations prepared with chloroform that ABT-737 is not soluble in our SNs nanosystems. Therefore, we repeated the formulation process with 10mg/mL ABT-737 in DMSO stock solution. However, in this case, the highest acceptable loading ratio of ABT-737 is 0.01 in order not to exceed the 0.5% of DMSO in our formulations.

SNs-ABT (1:0.1:0.01) prepared from the new stock solution were 126.9 ± 9.8 nm in size, had PDI of 0.1 ± 0.02 and ZP of +5.55 ± 1.06. Those nanosystems properties were not affected by the dialysis process. According to the characterization results, the dialysis process increased SNs-ABT (1:0.1:0.01) size slightly (135.8 ± 1.9 nm), and also had increased the zeta potential (+10.4 ± 1.5). Additional characterization was performed by NTA, MADLS and AFM. Results also proved that the dialysis process did not compromise the integrity of the nanosystems, in agreement with previous characterization results. However, we found an increase in the average size in SNs-ABT samples after 13h and 37h of deposition. We speculated that such increase in size could be related to coalescence between some nanosystems droplets overtime. However, we also observed that the majority of the small droplets maintained their size over the whole

course of the experiment. It is important to note that this polydispersity was not noticed with DLS, NTA nor MADLS.

The encapsulation efficiency (EE%) of ABT-737 in SNs-ABT (1:0.1:0.01), was determined by HPLC after dialysis, being 87.86 ± 4.24 %, which correlates with a loading capacity (LC%) of 0.007%. Other studies reported similar high EE% of 71.4% and 95% for folate-modified lipid bilayer-coated mesoporous silica and N1-ABT-NPs (PLGA NPs) nanocarriers [56,57,58]. However, the first nanosystem were based on mesoporous nanoparticles [56] which is known to have biocompatibility issues [64]. Also, the other nanosystems were polymeric nanoparticles (PLGA NPs) [57,58]. Therefore, our SNs nanosystems are more appealing due to their biodegradability and biocompatibility. Besides the preparation of these nanosystems were much complicated compared to the ethanol injection method.

Colloidal short-term stability of SNs-ABT was assessed in different biological media after 24h of incubation to estimate their fate after administration both *in vitro* and *in vivo* [37]. SNs-ABT showed a good colloidal stability profile in both PBS and plasma. Regarding stability in plasma, SNs-ABT slightly increased in size at the very end of the experiment (after 24 h of incubation) with a final hydrodynamic size of 175.4 ±6.6 nm and ZP of -19.6 ±1.3 mV. The slight increase in size and the final strong negative surface charge can be explained by plasma proteins adsorption and formation of a protein corona [54,55]. In the case of stability in PBS, SNs-ABT maintained their size throughout the entire study. However, in RPMI, SNs-ABT gradually increased in size, reaching 418 ±52 nm and ZP of –37.6 ±1 mV after 24h of incubation, while the PDI remained less than 0.3. This could be related to the higher content of salts in RPMI compared to PBS.

Encapsulating ABT-737 in SNs nanosystems improved its hemocompatibility profile as no haemolytic activity were detected with SNs-ABT (1:0.1:0.01) in all concentrations tested. This provides a great advantage for IV administration, as ABT-737 encapsulation in SNs nanosystems prevents its interaction with blood contents and reduces its toxicity which was one of the reasons why clinical studies of ABT-737 did not move forward.

Lastly, we tested the senolytic capacity of SNs-ABT on the CIS of MCF7 cells. Results presented in chapter 2 (Part 2, Figure 3, page 135) manifest that SNs-ABT at 0.5 µM reduced emergent clones by 72% compared to NT plates.

SNs-ABT nanosystems effect on senescence escape were more potent in comparison to SNs-Ks nanosystems. ABT-737 promote apoptosis in senescent cells while 4N1Ks peptide induce autophagy. Therefore, it would be interesting to combine the two therapies together, especially as ABT-737 will be encapsulated in the oil phase while 4N1Ks will be associated on the surface. Such combinatory therapy might have higher impact on senescent cells, which has already been established in our lab with a similar study by associating uroguanylin on the surface of SNs while encapsulating etoposide in the oil phase [7]. This combinatory therapy had higher cytotoxic effect on colorectal cancer cells in comparison to SNs with etoposide alone [7].

Encapsulating ABT-737 in SNs provides advantages compared to other nanosystems encapsulating ABT-737 [56-59]. Most of those nanosystems co-encapsulate other cytotoxic drugs and ligands to achieve the desirable therapeutic effect. Moreover, the biodegradability and biocompatibility of SNs nanosystems is an extra feature compared to the mesoporous [58] or polymeric nanoparticles [56].

Unfortunately, further cytotoxicity experiments and replicates were already in process, but due to the Covid-19 situation, we could not continue working on them.

Part3: SNs-Ole.

Since oleuropein senolytic properties [23] are based on molecular pathways different than ABT-737 and 4N1Ks, it was interesting to encapsulate it in SNs nanosystems and study its effect on the CIS model of MCF7 cells.

Luckily, oleuropein dissolves in ethanol; therefore, a stock solution of Ole in ethanol was prepared and mixed in different weight ratios (0.01- 0.05) with Vit E and sphingomyelin for the preparation of SNs-Ole by the ethanol-injection method. All prepared SNs-Ole nanosystems, with different ratios of loaded oleuropein (0.01, 0.02, 0.05) were around 100 nm in size and possessed negative surface charge. Results obtained from NTA and MADLS, proved that small (< 100 nm), and homogeneous nanosystems were formed. A previous study indicated the presence of Ole on the bilayer membrane and core of liposomes due to its amphiphilic nature [60]. Therefore, the increase of negative surface charge can be explained by the presence of part of Ole on the surface of the SNs due to its amphiphilic nature [60,61].

AFM measurements were smaller compared to others, and that can be explained by the spread of the nanosystems on the mica surface and the drying of the sample over time. In addition, we

noticed a smaller population with AFM, which could be related to the ability of Ole to form small vesicles due to its amphiphilic nature [60,61].

SNs-Ole with a composition (1:0.1:0.05), which are the ones with the highest content in Oleuropein, were selected for the next experiments.

Storage stability at 4 °C was studied, and the analysis by DLS showed that SNs-Ole (121.9 ± 4.7 nm, PdI 0.07, -16.5 ±2 mV) were stable at least for 4 months. Moreover, the short-term colloidal stability of SNs-Ole was assessed in different biological media. The results indicated that SNs-Ole nanosystems were stable in RPMI supplemented with 1%FBS and in PBS 5mM as the nanosystems maintained their particle size throughout the entire study. Again, the Ole amphiphilic nature might play a role in the high colloidal stability of those nanosystems [60,61]. As the presence of two types of surfactants can prevent aggregation and increase their colloidal stability [62].

We assessed the cytotoxicity profile of SNs-Ole on red blood cells by haemolysis assay. SNs-Ole nanosystems were hemocompatible as they did not lead to any haemolytic activity in all concentrations tested.

Unfortunately, due to the Covid-19 situation, we could not continue further experiments regarding cytotoxicity and senescence escape. However, we thought that the results obtained with these nanosystems were promising to be continued for future studies.

A comparison between SNs-Ks, SNs-ABT and SNs-Ole:

All prepared SNs nanosystems were around 100 nm in size. Extensive characterisation by DLS, MADLS, NTA and AFM proved the population homogeneity of those nanosystems. Moreover, all SNs nanosystems showed great colloidal stability profile over time and in different biological media including plasma. Regarding SNs-Ks and SNs-Ole, both C18-PEG-Ks and Ole molecules have amphiphilic nature, however in case of SNs-Ks the C18 part will be incorporated in the oil core while the PEG-Ks will be associated to the surface. In the case of Ole, it is speculated the presence of Ole on the surface of SNs-Ole and in the oil core, as it has been reported before with liposomes encapsulating Ole [61]. Alternatively, ABT-737 due to its hydrophobic nature it is most probably encapsulated in the oil core. This eventually had an impact on the surface charge of each nanosystems. SNs-Ks have strong positive ZP due to the 4N1Ks peptide's positively charged amino acids (lysine and arginine). SNs-ABT nanosystems

also possessed positive ZP; however, it is not as strong as SNs-Ks, and it is most probably related to DMSO positive charge based on the presence of a sulphur atom. On the other hand, SNs-Ole formulation had negative ZP due to the presence of part of Ole on the surface of those nanosystems.

Regarding loading capacity, SNs-Ks (1:0.1:0.1) nanosystems had a high loading capacity of 7.3%. This could be explained by the amphiphilic nature, and the emulsifying ability of C18-PEG-Ks, which V-Ks formulations have already proved. Contrarily, SNs-ABT (1:0.1:0.01) had low LC% of 0.007%, and it is related to the low solubility of ABT-737 in SNs nanosystems; however, the encapsulation efficiency of ABT was relatively high 87.86 ± 4.24 %.

Finally, each SNs prepared nanosystems deliver their senolytic effect by targeting a different molecular pathway in the senescent cells. SNs-Ks nanosystems with the 4N1Ks peptide associated to the surface target specific receptor on the surface of senescent cells and, as a result, induce autophagy in senescent cells. Alternatively, SNs-ABT nanosystems target is intracellular and achieve their senolytic effect by disrupting the balance between anti-apoptotic and pro-apoptotic proteins. In the case of SNs-Ole, although we have not tested its therapeutic potential on senescent cells, however, based on previous studies, we assume they might possess senolytic effect by the downregulation of IL-1ß, IL-6, COX-2 gene expression and supressing NF-kB activation [22,23].

In the end, we were able to prepare senolytic SNs nanosystems by encapsulating different senolytic drugs that target senescent cells based on different molecular pathways. Therefore, these nanosystems present an interesting approach for senolytic drug delivery intended to prevent cancer relapse or age-related diseases. Further *in-vivo* studies are necessary to evaluate their therapeutic potential. Also, it will be interesting to test those nanosystems on other cellular senescence model, like oncogene-induced senescence or replicative senescence.

References:

1. Pignolo, R.J.; Passos, J.F.; Khosla, S.; Tchkonia, T.; Kirkland, J.L. Reducing Senescent Cell Burden in Aging and Disease. *Trends Mol. Med.* **2020**, *26*, 630–638, doi:10.1016/j.molmed.2020.03.005.
2. Watanabe, S.; Kawamoto, S.; Ohtani, N.; Hara, E. Impact of senescence-associated secretory phenotype and its potential as a therapeutic target for senescence-associated diseases. *Cancer Sci.* **2017**, *108*, 563–569, doi:10.1111/cas.13184.
3. Demaria, M.; Ohtani, N.; Youssef, S.A.; Rodier, F.; Toussaint, W.; Mitchell, J.R.; Laberge, R.M.; Vijg, J.; VanSteeg, H.; Dollé, M.E.T.; et al. An essential role for senescent cells in optimal wound healing through secretion of PDGF-AA. *Dev. Cell* **2014**, *31*, 722–733, doi:10.1016/j.devcel.2014.11.012.
4. Pluquet, O.; Abbadie, C.; Coqueret, O. Connecting cancer relapse with senescence. *Cancer Lett.* **2019**, *463*, 50–58, doi:10.1016/j.canlet.2019.08.004.
5. Saleh, T.; Tyutyunyk-Massey, L.; Gewirtz, D.A. Tumor cell escape from therapy-induced senescence as a model of disease recurrence after dormancy. *Cancer Res.* **2019**, *79*, 1044–1046, doi:10.1158/0008-5472.CAN-18-3437.

6. Guillon, J.; Petit, C.; Moreau, M.; Toutain, B.; Henry, C.; Roché, H.; Bonichon-Lamichhane, N.; Salmon, J.P.; Lemonnier, J.; Campone, M.; et al. Regulation of senescence escape by TSP1 and CD47 following chemotherapy treatment. *Cell Death Dis.* **2019**, *10*, doi:10.1038/s41419-019-1406-7.

7. Milanovic, M.; Fan, D.N.Y.; Belenki, D.; Däbritz, J.H.M.; Zhao, Z.; Yu, Y.; Dörr, J.R.; Dimitrova, L.; Lenze, D.; Monteiro Barbosa, I.A.; et al. Senescence-associated reprogramming promotes cancer stemness. *Nature* **2018**, *553*, 96–100, doi:10.1038/nature25167.

8. Haugstetter, A.M.; Loddenkemper, C.; Lenze, D.; Gröne, J.; Standfu, C.; Petersen, I.; Dörken, B.; Schmitt, C.A. Cellular senescence predicts treatment outcome in metastasised colorectal cancer. *Br. J. Cancer* **2010**, *103*, 505–509, doi:10.1038/sj.bjc.6605784.

9. Roberson, R.S.; Kussick, S.J.; Vallieres, E.; Chen, S.Y.J.; Wu, D.Y. Escape from therapy-induced accelerated cellular senescence in p53-null lung cancer cells and in human lung cancers. *Cancer Res.* **2005**, *65*, 2795–2803, doi:10.1158/0008-5472.CAN-04-1270.

10. Elmore, L.W.; Di, X.; Dumur, C.; Holt, S.E.; Gewirtz, D.A. Evasion of a single-step, chemotherapy-induced senescence in breast cancer cells: Implications for treatment response. *Clin. Cancer Res.* **2005**, *11*, 2637–2643, doi:10.1158/1078-0432.CCR-04-1462.

11. Saleh, T.; Tyutyunyk-Massey, L.; Murray, G.F.; Alotaibi, M.R.; Kawale, A.S.; Elsayed, Z.; Henderson, S.C.; Yakovlev, V.; Elmore, L.W.; Toor, A.; et al. Tumor cell escape from therapy-induced senescence. *Biochem. Pharmacol.* **2019**, *162*, 202–212, doi:10.1016/j.bcp.2018.12.013.

12. Wang, Q.; Wu, P.C.; Roberson, R.S.; Luk, B. V.; Ivanova, I.; Chu, E.; Wu, D.Y. Survivin and escaping in therapy-induced cellular senescence. *Int. J. Cancer* **2011**, *128*, 1546–1558, doi:10.1002/ijc.25482.

13. Triana-Martínez, F.; Loza, M.I.; Domínguez, E. Beyond Tumor Suppression: Senescence in Cancer Stemness and Tumor Dormancy. *Cells* **2020**, *9*, doi:10.3390/cells9020346.

14. Bouzo, B.L.; Calvelo, M.; Martín-Pastor, M.; García-Fandiño, R.; de la Fuente, M. In Vitro–In Silico Modeling Approach to Rationally Designed Simple and Versatile Drug Delivery Systems. *J. Phys. Chem. B* **2020**, *124*, 5788–5800, doi:10.1021/acs.jpcb.0c02731.

15. Bouzo, B.; Lores, S.; Jatal, R.; Alijas, S.; Alonso, M.J.; Conejos-Sánchez, I.; Fuente, M. de la Uroguanylin-decorated Nanosystems Containing Etoposide, a Potential Targeted Combination Therapy for Colorectal Cancer 2020.

16. Díez-Villares, S.; Ramos-Docampo, M.A.; Silva-Candal, A. da; Hervella, P.; Vázquez-Ríos, A.J.; Dávila-Ibáñez, A.B.; López-López, R.; Iglesias-Rey, R.; Salgueiriño, V.; de la Fuente, M. Manganese Ferrite Nanoparticles Encapsulated into Vitamin E/Sphingomyelin Nanoemulsions as Contrast Agents for High-Sensitive Magnetic Resonance Imaging. *Adv. Healthc. Mater.* **2021**, 2101019, doi:10.1002/ADHM.202101019.

17. Díez-Villares, S.; Pellico, J.; Gómez-Lado, N.; Grijalvo, S.; Alijas, S.; Eritja, R.; Herranz, F.; Aguiar, P.; de la Fuente, M. Biodistribution of 68/67Ga-Radiolabeled Sphingolipid Nanoemulsions by PET and SPECT Imaging. *Int. J. Nanomedicine* **2021**, *16*, 5923–5935, doi:10.2147/IJN.S316767.

18. Nagachinta, S.; Bouzo, B.L.; Vazquez-Rios, A.J.; Lopez, R.; de la Fuente, M. Sphingomyelin-based nanosystems (SNs) for the development of anticancer miRNA therapeutics. *Pharmaceutics* **2020**, *12*, 1–16, doi:10.3390/pharmaceutics12020189.

19. Nagachinta, S.; Becker, G.; Dammicco, S.; Serrano, M.E.; Leroi, N.; Bahri, M.A.; Plenevaux, A.; Lemaire, C.; Lopez, R.; Luxen, A.; et al. Radiolabelling of lipid-based nanocarriers with fluorine-18 for in vivo tracking by PET. *Colloids Surfaces B Biointerfaces* **2020**, *188*, 110793, doi:10.1016/j.colsurfb.2020.110793.

20. Yosef, R.; Pilpel, N.; Tokarsky-Amiel, R.; Biran, A.; Ovadya, Y.; Cohen, S.; Vadai, E.; Dassa, L.; Shahar, E.; Condiotti, R.; et al. Directed elimination of senescent cells by inhibition of BCL-W and BCL-XL. *Nat. Commun.* **2016**, *7*, 1–11, doi:10.1038/ncomms11190.

21. Kline, M.P.; Rajkumar, S. V.; Timm, M.M.; Kimlinger, T.K.; Haug, J.L.; Lust, J.A.; Greipp, P.R.; Kumar, S. ABT-737, an inhibitor of Bcl-2 family proteins, is a potent inducer of apoptosis in multiple myeloma cells. *Leukemia* **2007**, *21*, 1549–1560, doi:10.1038/sj.leu.2404719.

22. Castejón, M.L.; Rosillo, M.Á.; Montoya, T.; González-Benjumea, A.; Fernández-Bolaños, J.M.; Alarcón-De-La-Lastra, C. Oleuropein down-regulated IL-1β-induced inflammation and oxidative stress in human synovial fibroblast cell line SW982. *Food Funct.* **2017**, *8*, 1890–1898, doi:10.1039/c7fo00210f.

23. Varela-Eirín, M.; Carpintero-Fernández, P.; Sánchez-Temprano, A.; VarelaVázquez, A.; Paíno, C.L.; Casado-Díaz, A.; Continente, A.C.; Mato, V.; Fonseca, E.; Kandouz, M.; et al. Senolytic activity of small molecular polyphenols from olive restores chondrocyte redifferentiation and promotes a pro-regenerative environment in osteoarthritis. *Aging (Albany. NY).* **2020**, *12*, 15882–15905, doi:10.18632/aging.103801.

24. Georgakilas, A.G.; Martin, O.A.; Bonner, W.M. p21: A Two-Faced Genome Guardian. *Trends Mol. Med.* **2017**, *23*, 310–319, doi:10.1016/j.molmed.2017.02.001.

25. Jackson, J.G.; Pant, V.; Li, Q.; Chang, L.L.; Quintás-Cardama, A.; Garza, D.; Tavana, O.; Yang, P.; Manshouri, T.; Li, Y.; et al. P53-Mediated Senescence Impairs the Apoptotic Response to Chemotherapy and Clinical Outcome in Breast Cancer. *Cancer Cell* **2012**, *21*, 793–806, doi:10.1016/j.ccr.2012.04.027.

26. Denèfle, T.; Boullet, H.; Herbi, L.; Newton, C.; Martinez-Torres, A.C.; Guez, A.; Pramil, E.; Quiney, C.; Pourcelot, M.; Levasseur, M.D.; et al. Thrombospondin-1 Mimetic Agonist Peptides Induce Selective Death in Tumor Cells: Design, Synthesis, and Structure-Activity Relationship Studies. *J. Med. Chem.* **2016**, *59*, 8412–8421, doi:10.1021/acs.jmedchem.6b00781.

27. Ana-Carolina Martinez-Torres, Claire Quiney, Tarik Attout, H.B.; Linda Herbi, Laura Vela, Sandrine Barbier, D.C.; Elise Chapiro, Florence Nguyen-Khac, Frédéric Davi, M.L.G.-; Tavernier, Roba Moumné, Marika Sarfati11, Philippe Karoyan, H.M.-; Béral, P.L.S.A.S. CD47 Agonist Peptides Induce Programmed Cell Death in Refractory Chronic Lymphocytic Leukemia B Cells via PLC γ 1 Activation : Evidence from Mice and Humans. **2015**, *12*, 1–38, doi:10.1371/journal.pmed.1001796.

28. Leclair, P.; Kim, M.J.; Lim, C.J. Peptide analogues PKHB1 and 4N1K induce cell death through CD47-independent mechanisms. *Cancer Sci.* **2020**, *111*, 1028–1030, doi:10.1111/cas.14310.

29. Cao, S.S.; Luo, K.L.; Shi, L. Endoplasmic Reticulum Stress Interacts With Inflammation in Human Diseases. *J Cell Physiol* **2016**, *231*, 288–294, doi:10.1002/jcp.25098.Endoplasmic.

30. Diehl, J.A.; Fuchs, S.Y.; Koumenis, C. The cell biology of the unfolded protein response. *Gastroenterology* **2011**, *141*, 38-41.e412, doi:10.1053/j.gastro.2011.05.018.

31. Guha, P.; Kaptan, E.; Gade, P.; Kalvakolanu, D. V; Ahmed, H. Tunicamycin induced endoplasmic reticulum stress promotes apoptosis of prostate cancer cells by activating mTORC1. *Oncotarget* **2017**, *8*, 68191–68207, doi:10.18632/oncotarget.19277.

32. Haynes, M.K.; Strouse, J.J.; Waller, A.; Leitao, A.; Curpan, R.F.; Bologa, C.; Oprea, T.I.; Prossnitz, E.R.; Edwards, B.S.; Sklar, L.A.; et al. Detection of intracellular granularity induction in prostate cancer cell lines by small molecules using the HyperCyt high-throughput flow cytometry system. *J. Biomol. Screen.* **2009**, *14*, 596–609, doi:10.1177/1087057109335671.

33. Kalas, W.; Swiderek, E.; Świtalska, M.; Wietrzyk, J.; Rak, J.; Strządała, L. Thrombospondin-1 receptor mediates autophagy of RAS-expressing cancer cells and triggers tumour growth inhibition. *Anticancer Res.* **2013**, *33*, 1429–1438.

34. Jung, C.H.; Ro, S.-H.; Cao, J.; Otto, N.M.; Kim, D.-H. mTOR and autophagy. *NIH Public Access* **2010**, *584*, 1287–1295, doi:10.1016/j.febslet.2010.01.017.mTOR.

35. Wang, M.; Wey, S.; Zhang, Y.; Ye, R.; Lee, A.S. Role of the Unfolded Protein Response Regulator GRP78/BiP in Development, Cancer, and Neurological Disorders. *Antioxid. Redox Signal.* **2009**, *11*, 2307–2316, doi:10.1089/ars.2009.2485.

36. Cerezo, M.; Rocchi, S. New anti-cancer molecules targeting HSPA5/BIP to induce endoplasmic reticulum stress, autophagy and apoptosis. *Autophagy* **2017**, *13*, 216–217, doi:10.1080/15548627.2016.1246107.

37. Raschmanová, H.; Zamora, I.; Borčinová, M.; Meier, P.; Weninger, A.; Mächler, D.; Glieder, A.; Melzoch, K.; Knejzlík, Z.; Kovar, K. Single-Cell Approach to Monitor the Unfolded Protein Response During Biotechnological Processes With Pichia pastoris . *Front. Microbiol.* 2019, *10*, 335.

38. Senft, D.; Ronai, Z.A. UPR, autophagy, and mitochondria crosstalk underlies the ER stress response. *Trends Biochem. Sci.* **2015**, *40*, 141–148, doi:10.1016/j.tibs.2015.01.002.

39. Pole, A.; Dimri, M.; P. Dimri, G. Oxidative stress, cellular senescence and ageing. *AIMS Mol. Sci.* **2016**, *3*, 300–324, doi:10.3934/molsci.2016.3.300.

40. Ogata, M.; Hino, S.; Saito, A.; Morikawa, K.; Kondo, S.; Kanemoto, S.; Murakami, T.; Taniguchi, M.; Tanii, I.; Yoshinaga, K.; et al. Autophagy Is Activated for Cell Survival after Endoplasmic ReticulumStress. *Mol. Cell. Biol.* **2006**, *26*, 9220–9231, doi:10.1128/mcb.01453-06.

41. Gosselin, K.; Deruy, E.; Martien, S.; Vercamer, C.; Bouali, F.; Dujardin, T.; Slomianny, C.; Houel-Renault, L.; Chelli, F.; De Launoit, Y.; et al. Senescent keratinocytes die by autophagic programmed cell death. *Am. J. Pathol.* **2009**, *174*, 423–435, doi:10.2353/ajpath.2009.080332.

42. Young, A.R.J.; Narita, M.; Ferreira, M.; Kirschner, K.; Sadaie, M.; Darot, J.F.J.; Tavaré, S.; Arakawa, S.; Shimizu, S.; Watt, F.M.; et al. Autophagy mediates the mitotic senescence transition. *Genes Dev.* **2009**, *23*, 798–803, doi:10.1101/gad.519709.

43. Kwon, Y.; Kim, J.W.; Jeoung, J.A.; Kim, M.-S.; Kang, C. Autophagy Is Pro-Senescence When Seen in Close-Up, but Anti-Senescence in Long-Shot. *Mol. Cells* **2017**, *40*, 607–612, doi:10.14348/molcells.2017.0151.

44. Laberge, R.M.; Sun, Y.; Orjalo, A. V; Patil, C.K.; Freund, A.; Zhou, L.; Curran, S.C.; Davalos, A.R.; Wilson-Edell, K.A.; Liu, S.; et al. MTOR regulates the pro-tumorigenic senescence-associated secretory phenotype by promoting IL1A translation. *Nat. Cell Biol.* **2015**, *17*, 1049–1061, doi:10.1038/ncb3195.

45. Dulic, V. Senescence Regulation by mTOR. In *Cell Senescence: Methods and Protocols*; Galluzzi, L., Vitale, I., Kepp, O., Kroemer, G., Eds.; Humana Press: Totowa, NJ, 2013; pp. 15–35 ISBN 978-1-62703-239-1.

46. Hu, C.; Wen, J.; Gong, L.; Chen, X.; Wang, J.; Hu, F.; Zhou, Q.; Liang, J.; Wei, L.; Shen, Y.; et al. Thrombospondin-1 promotes cell migration, invasion and lung metastasis of osteosarcoma through FAK dependent pathway. *Oncotarget* **2017**, *8*, 75881–75892, doi:10.18632/oncotarget.17427.

47. Kommuru, T.R.; Gurley, B.; Khan, M.A.; Reddy, I.K. Self-emulsifying drug delivery systems (SEDDS) of coenzyme Q10: Formulation development and bioavailability assessment. *Int. J. Pharm.* **2001**, *212*, 233–246, doi:10.1016/S0378-5173(00)00614-1.

48. Saberi, A.H.; Fang, Y.; McClements, D.J. Fabrication of vitamin E-enriched nanoemulsions: Factors affecting particle size using spontaneous emulsification. *J. Colloid Interface Sci.* **2013**, *391*, 95–102, doi:10.1016/j.jcis.2012.08.069.

49. Wang, L.; Dong, J.; Chen, J.; Eastoe, J.; Li, X. Design and optimization of a new self-nanoemulsifying drug delivery system. *J. Colloid Interface Sci.* **2009**, *330*, 443–448, doi:10.1016/j.jcis.2008.10.077.

50. Wu, L.; Zhang, J.; Watanabe, W. Physical and chemical stability of drug nanoparticles. *Adv. Drug Deliv. Rev.* **2011**, *63*, 456–469,

doi:10.1016/j.addr.2011.02.001.

51. Milton Harris, J.; Chess, R.B. Effect of pegylation on pharmaceuticals. *Nat. Rev. Drug Discov.* 2003, *2*, 214–221.

52. Zhang, X.; Liu, X.; Zhou, D.; Zheng, G. Targeting anti-apoptotic BCL-2 family proteins for cancer treatment. *Future Med. Chem.* **2020**, *12*, 563–565, doi:10.4155/fmc-2020-0004.

53. Weaver Jr, C.E.; Marek, P.; Park-Chung, M.; Tam, S.W.; Farb, D.H. Neuroprotective activity of a new class of steroidal inhibitors of the N-methyl-D-aspartate receptor. *Proc. Natl. Acad. Sci. U. S. A.* **1997**, *94*, 10450–10454, doi:10.1073/pnas.94.19.10450.

54. Wang, H.-X.; Zuo, Z.-Q.; Du, J.-Z.; Wang, Y.-C.; Sun, R.; Cao, Z.-T.; Ye, X.-D.; Wang, J.-L.; Leong, K.W.; Wang, J. Surface charge critically affects tumor penetration and therapeutic efficacy of cancer nanomedicines. *Nano Today* **2016**, *11*, 133–144, doi:https://doi.org/10.1016/j.nantod.2016.04.008.

55. Cagliani, R.; Gatto, F.; Bardi, G. Protein adsorption: A feasible method for nanoparticle functionalization? *Materials (Basel).* 2019, *12*.

56. Wu, X.; Wang, L.; Qiu, Y.; Zhang, B.; Hu, Z.; Jin, R. Cooperation of IRAK1/4 inhibitor and ABT-737 in nanoparticles for synergistic therapy of T cell acute lymphoblastic leukemia. *Int. J. Nanomedicine* **2017**, *12*, 8025–8034, doi:10.2147/IJN.S146875.

57. Valcourt, D.M.; Dang, M.N.; Scully, M.A.; Day, E.S. Nanoparticle-Mediated Co-Delivery of Notch-1 Antibodies and ABT-737 as a Potent Treatment Strategy for Triple-Negative Breast Cancer. *ACS Nano* **2020**, *14*, 3378–3388, doi:10.1021/acsnano.9b09263.

58. Liu, M.; Tu, J.; Feng, Y.; Zhang, J.; Wu, J. Synergistic co-delivery of diacid metabolite of norcantharidin and ABT-737 based on folate-modified lipid bilayer-coated mesoporous silica nanoparticle against hepatic carcinoma. *J. Nanobiotechnology* **2020**, *18*, 1–8, doi:10.1186/s12951-020-00677-4.

59. Schmid, D.; Jarvis, G.E.; Fay, F.; Small, D.M.; Greene, M.K.; Majkut, J.; Spence, S.; McLaughlin, K.M.; McCloskey, K.D.; Johnston, P.G.; et al. Nanoencapsulation of ABT-737 and camptothecin enhances their clinical potential through synergistic antitumor effects and reduction of systemic toxicity. *Cell Death Dis.* **2014**, *5*, e1454-11, doi:10.1038/cddis.2014.413.

60. Jimenez-Ruiz, A.; Prado-Gotor, R.; Fernández-Bolaños, J.G.; González-Benjumea, A.; Carnerero, J.M. Encased gold nanoparticle synthesis as a probe for oleuropein self-assembled structure formation. *Materials (Basel).* **2021**, *14*, 1–16, doi:10.3390/ma14010050.

61. González-Ortega, R.; Šturm, L.; Skrt, M.; Di Mattia, C.D.; Pittia, P.; Poklar Ulrih, N. Liposomal Encapsulation of Oleuropein and an Olive Leaf Extract: Molecular Interactions, Antioxidant Effects and Applications in Model Food Systems. *Food Biophys.* 2021, *16*, 84–97.

62. Pucek-kaczmarek, A. Nanoparticles by an Ultrasonic-Nanoemulsification Method. **2021**.

Conclusions & Future perspectives

Conclusions concluded from each chapter are listed here as points, in addition to future remarks.

Chapter 1: TSP1 C-terminal Derived Peptides and their Effect on Cancer and senescent cells through CD47 Receptor.

1. Exchanging amino acids on the N and C terminals from L form to D form increased the stability of the 4N1Ks peptide.
2. 4N1Ks peptide significantly reduced the emergent clones from CIS model of both MCF7 and LS174t and migratory ability of the SASP.
3. It also reduced the proliferative capacity of both cancer cell lines and reduced the metabolic activity of senescent cells.
4. Boyden chamber assay on SASP from cells treated with peptide, proved that 4N1Ks affect the production of SASP factors.
5. Those results can be attributed to autophagy induction in cells treated with 4N1Ks, as 4N1Ks reduced the expression of the light chain of LC3B and p62. In addition, 4N1Ks treatment resulted in mTOR downregulation proved by p-S6 reduced expression.
6. B-galactosidase induction by 4N1Ks treatment can be also explained by promoting autophagy program.

Based on all above 4N1Ks represent an attractive candidate for Senotherapy in order to enhance the health-span and lifespan of cancer patients who have received chemotherapies and prevent cancer relapse. Of course, further experiments are needed to demonstrate its true therapeutic potential like in vivo studies. It would be also interesting to study the effect of 4N1Ks peptide on other cellular senescence models like oncogene-induced senescence or in age-related diseases animal models.

Chapter 2: Senolytic and Senostatic Sphingomyelin based Nanosystems.

Part 1: SNs-Ks nanosystems.

1. 4N1Ks peptide was chemically modified with PEG-C18 to facilitate its incorporation to the surface of the nanoemulsion. MTT and CFA studies on MCF7 cells proved that this chemical modification did not alter its therapeutic efficacy.

2. We successfully prepared SNs with the modified peptide C18-PEG-Ks (SNs-Ks). Those nanosystems were around 100 nm in size and have strong surface positive charge.

3. The modified peptide C18-PEG-Ks possesses amphiphilic properties (surfactant like), which was proved by its ability to form nanosystems with VitE only (V-Ks formulations). In addition, the positive surface charge of SNs-Ks and V-Ks provide evidence regarding the peptide surfactant properties and its disposition onto the nanosystems surface, available to interact with senescent cells receptors.

4. DLS, NTA, and MADLS results on dialyzed SNs-Ks verified that the purification method did not compromise the integrity of the nanosystems.

5. SNs-Ks (1:0.1:0.1) nanosystems had high association efficiency (AE% of 87.2 ± 6.9 %), which correlates with a loading capacity (LC%) of 7.3%. In addition, SNs-Ks nanosystems were stable in several biological media such as plasma.

6. SNs-Ks showed a good hemocompatibility profile and demonstrated a higher internalization by cancer cells in comparison to the blank nanosystems. In addition, SNs improved the 4N1Ks senolytic activity by lowering its effective dose to impair cancer and senescent cancer cells' capacity to proliferate and form colonies.

Part 2: SNs-ABT nanosystems.

1. SNs-ABT nanosystems were successfully prepared, with an EE% of 87.86 ± 4.24, and shown to be stable after purification by dialysis, as proved by NTA, MADLS and AFM characterization.

2. SNs-ABT were also stable upon incubation in different biological medias, such as plasma and RPMI.

3. SNs improved the hemocompatibility of ABT as SNs-ABT (1:0.1:0.01) in the range of concentrations tested.

4. SNs-ABT possessed senolytic activity by reducing the emergent clones by 72%.

Part 3: SNs-Ole Nanosystems.

1. SNs-Ole prepared nanosystems were around 100 nm in size, had negative zeta potential, and were stable after purification by dialysis, according to NTA, MADLS, AFM, and DLS measurements.

2. MADLS and AFM results proved that the dialysis process did not alter nanosystems size nor affected its stability.

3. SNs-Ole were stable in different biological medias and did not induce any haemolytic activity in the range of concentration used.

4. Due to covid-19 situation we could not do any further experiments to assess its possible senolytic effect.

Further experiments are also needed to proof those nanosystems therapeutic potential such as *in vivo* studies. It is very tempting to investigate the therapeutic efficacy of the prepared nanosystems on another cellular senescence or load SNs-Ks with another senolytic/ senostatic drug that target different molecular pathway in the senescent cells. Also, it would be highly interesting to associate diagnostic probes for detecting senescent cell.

Titre : **Nouvelles stratégies thérapeutiques qui interfèrent avec l'échappement à la sénescence pour le traitement de la résistance aux médicaments dans le cancer colorectal et du sein**

Mots clés : échappement de la sénescence, peptide 4N1Ks, sénolytiques, nanosystèmes à base de sphingomyéline SN.

Résumé : Les agents chimiothérapeutiques et anticancéreux ont la capacité d'induire l'entrée en sénescence des cellules en croissance mais aussi les cellules cancéreuses. Ces cellules cancéreuses sénescentes présentent des caractéristiques proches de cellules quiescentes. Plusieurs études ont montré que ces cellules sont capables de recommencer à proliférer et qu'elles possèdent des propriétés d'agressivités plus marquées que les cellules parentales, pouvant conduire chez les patients à une rechute. Les cellules sénescentes secrètent un ensemble de molécules appelé SASP, qui favorisent l'inflammation et contribue à long terme à plusieurs maladies liées à l'âge. Par conséquent, l'utilisation d'agents sénolytiques et sénostatiques ciblant les cellules sénescentes peut prévenir les rechutes du cancer, réduire les effets secondaires à court et à long terme attribués aux agents anticancéreux et améliorer la qualité de la santé avec l'âge et éventuellement la durée de vie. Dans ce travail, nous avons montré que le peptide 4N1Ks, dérivé du domaine C-terminal de la protéine TSP1, inhibe l'échappement à la sénescence dans un modèle de sénescence induite par chimiothérapie des cellules tumorales mammaires MCF7 et colorectales LS174T.
Ce peptide réduit aussi les propriétés du SAPS produit par ces cellules et notamment la capacité migratoire de cellules tumorales.Nous avons également montré que 4N1Ks réduit l'activité métabolique des cellules sénescentes. L'ensemble de ces résultats nous a permis de montrer que ce peptide est capable d'induire l'autophagie de cellules tumorales sénescentes. Nous avons incorporé 4N1Ks à la surface de nanosystèmes à base de sphingomyéline après modification chimique avec du PEG-C18 afin de faciliter son association à la surface de ces nanosystèmes. Les nanosystèmes préparés par SNs-Ks ont démontré des caractéristiques appropriées en termes de taille (~ 100 nm), d'efficacité d'association (87,2 ± 6,9 %) et de stabilité dans différents milieux biopertinents. Les SNs-Ks ont montré un profil de toxicité plus élevé par rapport aux peptides modifiés et aux 4N1Ks. De plus, les SNs-Ks possédaient un bon profil d'hémocompatibilité et un taux d'internalisation cellulaire plus élevé que les nanosystèmes vierges. Les SNs-Ks ont amélioré l'activité sénolytique du peptide 4N1Ks et réduit le nombre de clones émergents dans les expériences d'échappement de la sénescence de cellules MCF7 à une dose 10 fois inférieure à celle du peptide modifié. Ces nanosystèmes représentent une approche intéressante pour réduire le nombre de cellules sénescentes accumulées après des traitements anticancéreux.

Title : **Novel Therapeutic strategies that interfere with senescence escape for the treatment of drug resistance in colorectal and breast cancer**

Keywords : Senescence escape, 4N1Ks peptide, Senolytics, sphingomyelin based nanosystems SN.

Abstract: Chemotherapeutic and anti-cancer agents have the ability to induce cellular senescence in proliferative and cancer cells. Cancer cells turning to senescent have similar characteristics to tumour dormancy. Several studies have indicated that those cells have the capacity to escape senescence state and emerge as a more aggressive form of cancer leading to cancer relapse. In addition, those accumulated senescent cells with their secretory phenotype promote local and systemic inflammation and on the long term contribute to several age-related diseases. Therefore, using senolytic and senostatic agents targeting senescent cells and their SASP can prevent cancer relapse, reduce the short- and long-term side effects attributed to anti-cancer agents, and improve the health quality over age and possibly life span. In this work, 4N1Ks peptide derived from the C-terminal domain of TSP1 protein prevented senescence escape in chemotherapy-induced senescence CIS model of MCF7 and LS174t cells. In addition, it reduced the migratory ability of the SASP and its production as well. Moreover, 4N1Ks treatment reduced the metabolic activity of senescent cells. Those results were explained by autophagy program induction triggered by 4N1Ks peptide.
Later we incorporated 4N1Ks to the surface of sphingomyelin based nanosystems after chemical modification with PEG-C18 in order to facilitate its association to the surface of those nanosystems. SNs-Ks prepared nanosystems demonstrated suitable features in terms of size (~ 100 nm), association efficiency (87.2± 6.9%) and stability in different biorelevant media. SNs-Ks showed higher toxicity profile compared to both modified peptide and 4N1Ks, proved by colony forming assay on MCF7 cells. In addition, SNs-Ks possessed good hemocompatibility profile, and had higher cell internalisation rate compared to blank nanosystems. Lastly and most importantly, SNs-Ks improved the senolytic activity of 4N1Ks peptide and reduced the number of emergent clones in senescence escape experiments of CIS model of MCF7 cells at a dose 10 times smaller compared to the modified peptide. These nanosystems represent an interesting approach for reducing the burden of accumulated senescent cells caused due to anticancer treatments as chemotherapeutics, and therefore make a step forward in the management of this disease.